CURE RATE AND DESTRUCTIVE CURE RATE MODELS UNDER PROPORTIONAL HAZARDS LIFETIME DISTRIBUTIONS

CURE RATE AND DESTRUCTIVE CURE RATE MODELS UNDER PROPORTIONAL HAZARDS LIFETIME DISTRIBUTIONS

By

SANDIP BARUI, B.Sc., M.Sc.

A Thesis

Submitted to the School of Graduate Studies

in Partial Fulfillment of the Requirements

for the Degree of

Doctor of Philosophy

McMaster University

DOCTOR OF PHILOSOPHY (2017) McMaster University

(Mathematics) Hamilton, Ontario

TITLE: CURE RATE AND DESTRUCTIVE CURE RATE MODELS UNDER PROPORTIONAL HAZARDS LIFETIME DISTRIBUTIONS

AUTHOR: SANDIP BARUI, B.Sc. (University of Calcutta)

M.Sc. (Indian Institute of Technology, Bombay)

SUPERVISOR: Professor N. Balakrishnan

NUMBER OF PAGES: xxi , 196

Abstract

Cure rate models are widely used to model time-to-event data in the presence of long-term survivors. Cure rate models, since introduced by Boag (1949), have gained significance over time due to remarkable advancements in the drug industry resulting in cures for a number of diseases. In this thesis, cure rate models are considered under a competing risk scenario wherein the initial number of competing causes is described by a Conway-Maxwell (COM) Poisson distribution, under the assumption of proportional hazards (PH) lifetime for the susceptibles. This provides a natural extension of the work of Balakrishnan & Pal (2013) who had considered independently and identically distributed (i.i.d.) lifetimes in this setup. By linking covariates to the lifetime through PH assumption, we obtain a flexible cure rate model. First, the baseline hazard is assumed to be of the Weibull form. Parameter estimation is carried out using EM algorithm and the standard errors are estimated using Louis' method. The performance of estimation is assessed through a simulation study. A model discrimination study is performed using Likelihood-based and Information-based criteria since the COM-Poisson model includes geometric, Poisson and Bernoulli as special cases. The details are covered in Chapter 2. As a natural extension of this work, we next approximate the baseline hazard with a piecewise linear function (PLA) and estimated it non-parametrically for the COM-Poisson cure rate model under PH setup. The corresponding simulation study and model discrimination results are presented in Chapter 3. Lastly, we consider a destructive cure rate model, introduced by Rodrigues et. al (2011), and study it under the PH assumption for the lifetimes of susceptibles. In this, the initial number of competing causes are modeled by a weighted Poisson distribution. We then focus mainly on three special cases, *viz.*, destructive exponentially weighted Poisson, destructive length-biased Poisson and destructive negative binomial cure rate models, and all corresponding results are presented in Chapter 4.

KEY WORDS: COM-Poisson distribution; Proportional hazards model; Weighted Poisson distribution; EM algorithm; Weibull distribution; Maximum likelihood estimation; Akaike Information Criterion (AIC); Bayesian Information Criterion (BIC); Cutaneous melanoma data; Mixture chi-square.

Acknowledgements

I believe that the path to attain a doctoral degree often leads to self discovery. It enables us to recognize our strengths and weaknesses and instills us with some great virtues like perseverance and humility. My journey is dedicated to all those individuals whose motivation and guidance are my northern star.

I would like to take this opportunity to express my gratitude primarily to my Ph.D. supervisor, Dr. N. Balakrishnan who introduced me to the topic of my thesis. Being an encyclopedia in statistics, his enormous knowledge, guidance and support have made my journey much effortless and safe. His constant inspiration, influence and faith in me have helped me go through this rigorous process for the last four years. I look forward to remain in close association with him in years to come.

I am indebted to my supervisory committee members Dr. B. Bolker and Dr. A. Childs whose suggestions, technical supports (especially using R) and constructive criticisms have provided me with opportunities to improve my works. I would like to thank Dr. S. Pal and Dr. F. Milienos for their invaluable input and suggestions toward my thesis.

An attempt to acknowledge the contributions of my parents Reba Barui and Jayanta Kumar Barui would be infantile. I would just mention that they are my strongest inspirations and unconditional supporters. I express my deepest gratitude to my wife Manipa for her sustained faith in me. I thank my brother Sourav, my dear friends Sankha, Avra, Sasanka, Keya, Shahriar, Sumit, Mayukh, Suvra, Kavitha, Henry and all other friends who have influenced or helped me at different stages of life. Lastly, I am grateful to God that He has offered me some of the best things in this ever-changing life.

Publications from the thesis

- Balakrishnan, N., Barui, S., & Milienos, F. S. (2017). Proportional hazards under Conway-Maxwell-Poisson cure rate model and associated inference. *Statistical Methods in Medical Research*, DOI: 10.1177/ 0962280217708683.
- Balakrishnan, N., Barui, S. & Milienos, F. (2016). Piecewise linear approximations of baseline under proportional hazards and COM-Poisson cure rate models. (Submitted for publication, under review).
- Balakrishnan, N. & Barui, S. Destructive cure rate models under proportional hazards lifetime. (Under Peer review).

Contents

List of Tables

List of Figures

Chapter 1

Introduction

1.1 Introduction

In cancer studies, a cure is defined as the state when the hazard rate of the affected group carrying the disease equals to the same level as that of the general population (Lambert et al., 2007). This is often measured in terms of disease-free survival time after 5 or 10 years of the treatment, however, it depends on the type of cancer. In Statistics, modeling of time-to-event data is typically done by assuming that every individual in the study cohort encounters the event of interest (death, relapse etc.) in the long run. However, for example, due to the remarkable advancements in bio-medical and drug development industry in past few decades, it is not only possible but quite likely for a proportion of patients in the cohort to get cured completely and never face recurrences. These individuals are called *cured* or non-susceptible or long-term survivors or immunes and the population under study could be considered as a mixture of immunes and susceptible. This prominent characteristic of data, having a proportion of disease free individuals, gives rise to a whole new branch of modeling techniques under the nomenclature of cure rate models. The estimation of cure rate is of particular importance to the investigators and patients, as it represents a measure of efficacy of the treatment and helps in analysis of survival trends. The application of cure rate models is not limited to the area of clinical trials but can effectively be extended to industrial reliability. In industrial reliability, cure occurs in the form of components of a manufacturing process working indefinitely without failure. For example, while testing failure of circuit boards when exposed to various levels of stress factors, a proportion of boards may not fail at all. Again, in computer manufacturing industry, computers with failed motherboards are sent to the dealers/company technicians for repair. However, there exists a certain proportion of computers in which motherboards continue to work even after many years of being manufactured. Under such circumstances, a cure rate model may be appropriate to analyze data and estimate chances of long-term functioning. It is to be noted that the occurrences of failure may involve more than one risk factor, e.g., damages in computer motherboards may occur due to improper handling, voltage fluctuation, excessive heat, electrical problems such as short or a static discharge etc. This gives rise to a competing cause scenario (Cox and Oakes, 1984). Cure rate model also finds application in finance (business failure, strategy failure), criminology (recidivism) etc. (e.g. Maller and Zhou, 1996).

The origin of cure rate models can be traced back at least to the works of Boag (1949) and Berkson and Gage (1952), where the importance of the existence of a cured proportion is discussed from a clinician's point of view. Thus, considering an indicator random variable I where $I = 0$ if the individual is cured and $I = 1$ if the individual is susceptible, the population or long-term survival function of the time-to-event T could be given by

$$S_p(t) = P(T > t) = p_0 + (1 - p_0)S_u(t), \tag{1.1.1}$$

where $p_0 = P(I = 0)$ and $S_u(t) = P(T > t|I = 1)$ is the survival function of susceptible. It is to be noted that if $S_u(t)$ is a proper survival function then $S_p(t)$ is not, since $\lim_{t\to\infty} S_p(t) = p_0$. The modeling of $S_u(t)$ with survival function of many well known distributions are known throughout literature.

Let us now discuss about a well studied competing cause scenario. Assume that M is an unobservable (latent) random variable denoting the number of competing causes related to the occurrence of an event of interest where $P(M = 0)$ denotes cured proportion p_0. Also, let $W_1, \ldots, W_M$ be random variables where W_j denotes the lifetime corresponding to the j-th competing cause; furthermore, W_j's are assumed independent of M with common cumulative distribution function (c.d.f.) $F(w) = 1 - S(w)$, where $S(.)$ is the survival function. Then, the overall population time-to-event Y is given by

$$Y = \min\{W_0, W_1, \ldots, W_M\}$$

with $P(W_0 = \infty) = 1$ and therefore,

$$\begin{aligned} S_p(y) = P(Y > y) = P(Y > y \mid M = 0)P(M = 0) \qquad\qquad \\ + \sum_{m=1}^{\infty} P(Y > y \mid M = m)P(M = m) \\ = P(W_0 = \infty)p_0 + \sum_{m=1}^{\infty} P\left[\min\{W_1, \ldots, W_m\} > y\right] P(M = m) \end{aligned} \tag{1.1.2}$$

$$= p_0 + \sum_{m=1}^{\infty} [S(y)]^m \, P(M = m) = E[S(y)^M] = G_M(S(y)),$$

where G_M is the probability generating function of M at $S(y)$ (e.g.,Tsodikov et al., 2003). It is to be noted that the mixture model in (1.1.1) is a special case of the above competing cause scenario, in which the number of competing causes M is a Bernoulli random variable with $p_0 = P(M = 0)$ and $1 - p_0 = P(M = 1)$. For more details on model (1.1.2), the interested reader may be referred to Tsodikov et al. (2003) or the monographs by Ibrahim et al. (2005) and Maller and Zhou (1996).

A more realistic approach to the cure rate models called destructive cure rate models was introduced by Rodrigues et al. (2011) which assumes the initial number of competing causes undergoing a process of destruction in a competing risk scenario. In cancer studies, often the event of interest is patient's death which can be caused by one or more number of malignant metastasis-component (see Yakovlev and Tsodikov, 1996) tumor cells. After a chemotherapy or radiation, only a portion of initial metastasis-component cells remain active and undamaged, thereby reducing the initial number of competing causes. Given $M = m$, we may consider X_g as a Bernoulli r.v. distributed independently of M. X_g takes 1 if the g-th competing cause is still active (i.e. if g-th malignant tumor cell remains undamaged after the treatment) with probability $p \in (0, 1)$ or 0 otherwise. Thus, if we define

$$D = \begin{cases} X_1 + \ldots + X_M, & \text{if } M > 0 \\ 0, & \text{if } M = 0 \end{cases} \tag{1.1.3}$$

then, D represents the number of initial competing causes which are not destroyed. Obviously, $D \leq M$; the conditional distribution of D given $M = m$ is known as the damaged distribution which is distributed binomially with parameters m and p if $m > 0$ and $P(D = 0|M = 0) = 1$. The cure rate is defined as $P(D = 0)$ in this case. As stated by Yang and Chen (1991), an alternative way of thinking involves X_g to be the number of living malignant cells that are descendants of g-th initiated malignant cells within a time frame, where initial competing causes are some primary initiated malignant cells. This destructive mechanism often provides realistic interpretations for occurrence of events related to an underlying biological activity.

1.2 A brief literature review

As stated earlier, one of the earliest evidences of cure rate model can be found in the works of Boag (1949) where he introduced the cure rate model emphasizing on the information loss in conventional five year survival rate from a clinician's view point. Berkson and Gage (1952) estimated the cured fraction using a least squared method while considering a mixture cure rate model. Their work was followed by Haybittle (1965), who estimated the proportion of treated cancer patient surviving to a specific time with respect to the normal population. Henceforth, several parametric, semi-parametric and non-parametric assumptions have been made about the distribution of the lifetime of the non-cured individuals. Farewell (1982) assumed a Weibull distribution for the lifetime of the susceptible, incorporating the covariates into the model through a logistic-link for p_0 and log-link for the scale parameter of the lifetime distribution; the estimation of the model parameters was carried out by employing the maximum likelihood (ML) method. Kuk and Chen (1992) generalized the previous parametric model using a semi-parametric Cox proportional hazard model for the lifetime of the susceptible; the baseline hazard function was treated as nuisance parameter, and a marginal likelihood estimation method was followed. Chen et al. (1999) however, considered a promotion time cure rate model instead of mixture and established a proportional hazard structure to it. Sy and Taylor (2000) also considered Cox proportional hazard model (see also Sy and Taylor, 2001) using a Breslow-type estimator for the baseline hazard function; similar assumptions and estimation method were also adopted by Peng and Dear (2000). A similar Bayesian approach to Chen et al. (1999) was mentioned in Ibrahim et al. (2001) for a new class of semi-parametric cure rate model with a smoothing parameter maintaining the degree of parametricity. Tsodikov et al. (2003) in their paper described the advantage of using bounded cumulative hazard model in estimating cured proportion as an alternative to conventional mixture model and inferences were drawn considering both semi-parametric and Bayesian methods.

Cox proportional hazard cure rate model was also discussed in Fang et al. (2005) where the existence, consistency and asymptotic normality of the maximum likelihood estimators (MLE) were studied. Lu (2008) used a nonparametric approach for estimating the parameters of the same model. In Zhao et al. (2014), a Bayesian approach was developed for estimating the parameters of the Cox proportional hazard cure rate model where a threshold in the regression coefficient was considered (see also

Liu et al. (2006)). A class of semi-parametric transformation models, including both the proportional hazard and the proportional odds cure rate model as special cases, was studied by Zeng et al. (2006); a recursive algorithm for computing the MLEs was also introduced while the estimators of the regression coefficients were shown to be consistent and asymptotically normal. A similar approach on Cox proportional hazard cure rate model with expectation-maximization (EM) based ML estimation was developed for interval mapping of quantitative trait loci for time-to-event data by Liu et al. (2006); the study of Cox proportional hazard cure rate model was also the subject of Larson and Dinse (1985) (under a competing cause scenario and a piecewise constant assumption for the baseline hazard function) and Lo et al. (1993) (with a piecewise linear assumption for the baseline hazard function).

A more recent work on cure rate model was suggested by Rodrigues et al. (2009) who introduced a flexible Conway-Maxwell (COM) Poisson cure rate model under a competing risk scenario. Shortly after, it was explored vastly by Balakrishnan and Pal (2012), Balakrishnan and Pal (2013b) and Balakrishnan and Pal (2014) considering different parametric distributions (e.g. exponential, Weibull, log-normal and generalized gamma) as the lifetime distributions of the susceptible. Balakrishnan et al. (2015) in their work extended the idea by approximating hazard function of the susceptible by a piecewise linear function.

In their paper, Rodrigues et al. (2011) discussed the destructive cure rate model considering the distribution of M as weighted Poisson. Gallardo et al. (2016) developed an EM algorithm based technique for the same model to estimate the parameters under three special cases, *viz.*, destructive exponentially weighted Poisson, destructive length-biased Poisson, and destructive negative binomial cure rate models. The lifetime distributions of the susceptible were taken to be generalized gamma, Birnbaum-Saunders, Gamma, log-normal and Weibull. A similar model was described by Borges et al. (2012) by creating a correlation structure between the initiated cells using generalized power series distribution. A Bayesian method of inference was further proposed in the context of destructive weighted Poisson cure rate model by Rodrigues et al. (2012). Further references can be found in the works of Cancho et al. (2013), Pal and Balakrishnan (2015), Pal and Balakrishnan (2017) and Pal and Balakrishnan (2016).

1.3 COM-Poisson cure rate models

The COM-Poisson distribution was introduced by Conway and Maxwell (1961). This distribution accommodates and generalizes some well known discrete distributions; it is a flexible family of distributions since it can be over-dispersed or under-dispersed depending on the value of the dispersion parameter (see also Shmueli et al., 2005 and Kadane et al., 2006). The COM-Poisson distribution has already been used for modeling the number of competing causes in (1.1.2); see Rodrigues et al. (2009) and Balakrishnan and Pal (2012, 2013b, 2014). Thus, if the number of competing causes M follow a COM-Poisson distribution, its probability mass function is given by

$$P(M = m; \eta, \phi) = \frac{1}{Z(\eta, \phi)} \frac{\eta^m}{(m!)^\phi}, \quad m = 0, 1, \ldots \tag{1.3.1}$$

where

$$Z(\eta, \phi) = \sum_{j=0}^{\infty} \frac{\eta^j}{(j!)^\phi}, \tag{1.3.2}$$

with $\phi \geq 0$ and $\eta > 0$. If $\phi = 1$, M is an equi-dispersed Poisson random variable (r.v.) with $E(M) = \eta$ while if $\phi \to \infty$, M becomes an under-dispersed Bernoulli r.v. with parameter $\frac{1}{1+\eta}$. Furthermore, if $\phi = 0$ and $\eta < 1$, then M is an over-dispersed geometric r.v. with parameter $1 - \eta$. Thus, according to the value of ϕ, we can have over-dispersed ($\phi < 1$), equi-dispersed ($\phi = 1$) or under-dispersed ($\phi > 1$) distribution.

The cure rate is given by

$$p_0 = P(M = 0; \eta, \phi) = Z(\eta, \phi)^{-1}, \tag{1.3.3}$$

since $\lim_{y\to\infty} Z(\eta S(y); \phi) = 1$, while (1.1.2) becomes

$$S_p(y) = \frac{Z(\eta S(y); \phi)}{Z(\eta; \phi)}, \tag{1.3.4}$$

with the corresponding improper density function being given by

$$f_p(y) = -\frac{\partial S_p(y)}{\partial y} = \frac{1}{Z(\eta; \phi)} \frac{f(y)}{S(y)} \sum_{j=1}^{\infty} \frac{j\{\eta S(y)\}^j}{(j!)^\phi}. \tag{1.3.5}$$

The long-term population survival function, improper population density function and cure fraction (p_0) for the special cases of the COM-Poisson cure rate model are presented in Table 1.1.

Table 1.1: Population survival function, density function and cured proportion for the three special cases of COM-Poisson cure rate model.

Model	$S_p(y)$	$f_p(y)$	p_0
Geometric ($\phi = 0$)	$\frac{1-\eta}{1-\eta S(y)}$	$\frac{\eta(1-\eta)}{(1-\eta S(y))^2} f(y)$	$1-\eta$
Poisson ($\phi = 1$)	$e^{-\eta(1-S(y))}$	$\eta e^{-\eta(1-S(y))} f(y)$	$e^{-\eta}$
Bernoulli ($\phi \to \infty$)	$\frac{1+\eta S(y)}{1+\eta}$	$\frac{\eta}{1+\eta} f(y)$	$\frac{1}{1+\eta}$

1.4 Destructive weighted Poisson cure rate models

The probability mass function (p.m.f) of M following a weighted Poisson distribution is given by

$$P(M = m; \eta, \phi) = \begin{cases} \frac{\Omega(m;\phi)}{\mathbb{E}_\eta[\Omega(M;\phi)]} p^*(m;\eta), & m = 0, 1, 2, \ldots \\ 0, & \text{o.w.} \end{cases} \tag{1.4.1}$$

where $\Omega(.;\phi)$ is a non-negative weight function characterized by ϕ with $\phi \in \mathbb{R}$, $p^*(.;\eta)$ is the p.m.f of a Poisson distribution with parameter $\eta > 0$ and $\mathbb{E}_\eta[.]$ is the expectation taken with respect to a Poisson p.m.f. (see Rodrigues et al., 2011). Given $M = m > 0$, the conditional distribution of D is Binomial with parameters m and $p = P(X_g = 1)$ as obtained from equation (1.1.3), while $D = 0$ if $M = 0$. The initial number of competing causes M is assumed to follow a weighted Poisson distribution, with weight functions as $e^{\phi m}$, m, and $\Gamma(m + \phi^{-1})$, undergoing a damaging process as discussed earlier. The corresponding models on considering these weight functions are known as destructive exponentially weighted Poisson (DEWP), destructive length-biased Poisson (DLBP), and destructive negative binomial (DNB) cure rate models respectively. By choosing $\Omega(m;\phi) = (m!)^{1-\phi}$, we obtain a COM-Poisson distribution as defined in equation (1.3.1). The corresponding model is called destructive COM-Poisson cure rate model. However, this model is not discussed in the thesis.

1.4.1 Destructive exponentially weighted Poisson cure rate model

Under this model, we assume $\Omega(m;\phi) = e^{\phi m}$ as the weight function which gives the p.m.f of M as

$$P(M = m; \eta, \phi) = \begin{cases} e^{-\eta e^{\phi}} \frac{(\eta e^{\phi})^m}{m!}, & m = 0, 1, 2, \ldots \\ 0, & \text{otherwise} \end{cases} \tag{1.4.2}$$

which is a Poisson distribution with rate parameter ηe^{ϕ}. The unconditional distribution of the undamaged number of initial competing causes D is expressed through

$$\begin{aligned} P(D = d; \eta, \phi, p) &= \sum_{m=d}^{\infty} P(D = d|M = m)P(M = m) \\ &= \sum_{m=d}^{\infty} \frac{m!}{(m-d)!d!} p^d (1-p)^{m-d} e^{-\eta e^{\phi}} \frac{(\eta e^{\phi})^m}{m!} \\ &= e^{-\eta p e^{\phi}} \frac{(\eta p e^{\phi})^d}{d!}, \ d = 0, 1, 2, ... \end{aligned} \tag{1.4.3}$$

which is again a Poisson r.v. with expectation $\mathbb{E}(D) = \eta p e^{\phi}$. The cure rate, population survival function and population density function are derived as

$$p_0 = e^{-\eta p e^{\phi}}, \tag{1.4.4}$$

$$S_p(y) = e^{-\eta p e^{\phi} F(y)} \tag{1.4.5}$$

and

$$f_p(y) = \eta p e^{\phi} S_p(y) f(y) \tag{1.4.6}$$

respectively. Note that the model gets reduced to a destructive Poisson cure rate model if $\phi = 0$. Furthermore, taking $p = 1$ gives Poisson cure rate model.

1.4.2 Destructive length-biased Poisson cure rate model

Assuming $\Omega(m; \phi) = m$, the p.m.f. of M is expressed as

$$P(M = m; \eta, \phi) = \begin{cases} \frac{e^{-\eta}\eta^{m-1}}{(m-1)!}, & m = 1, 2, \ldots \\ 0, & \text{o.w.} \end{cases} \tag{1.4.7}$$

which is a truncated Poisson distribution with truncation point being $m = 0$. Since $(D|M = m) \sim$ Bernoulli$(m,\ p)$, the unconditional p.m.f of D, i.e., the number of active competing causes is given by

$$\begin{aligned} P(D=d;\eta,\phi,p) &= \sum_{m=d}^{\infty} P(D=d|M=m)P(M=m) \\ &= \sum_{m=d}^{\infty} \frac{m!}{(m-d)!d!} p^d (1-p)^{m-d} \frac{e^{-\eta}\eta^{m-1}}{(m-1)!} \\ &= \frac{e^{-\eta p}(\eta p)^d}{d!}\left[1-p+\frac{d}{\eta}\right],\ d=0,1,2,... \end{aligned} \tag{1.4.8}$$

The expression for the cure rate is, therefore, given as

$$p_0 = P(D=0) = e^{-\eta p}(1-p) \tag{1.4.9}$$

while the population survival function and the population density function is given by

$$S_p(y) = P(Y>y) = e^{-\eta p F(y)}[1-pF(y)] \tag{1.4.10}$$

and

$$f_p(y) = P(Y>y) = \eta p f(y) e^{-\eta p F(y)}\left[1-pF(y)-\frac{pf(y)}{\eta}\right] \tag{1.4.11}$$

where $f(.)$ is the probability density function (p.d.f.) of W_j for all $j=1,2,\ldots,d$.

1.4.3 Destructive negative binomial cure rate model

Let us consider

$$P(M=m;\eta,\phi) = \begin{cases} \frac{\Gamma(m+\phi^{-1})}{\Gamma\phi^{-1}m!}\left(\frac{\phi\eta}{1+\phi\eta}\right)^m (1+\phi\eta)^{-\phi^{-1}}, & m=0,1,2,\ldots \\ 0, & \text{o.w.} \end{cases} \tag{1.4.12}$$

where M is a negative binomial r.v. denoting number of failures before ϕ^{-1} successes and probability of each success being $\frac{\phi\eta}{1+\phi\eta}$. This is a weighted Poisson distribution with parameter $\frac{\phi\eta}{1+\phi\eta}$ and $\Omega(m;\phi) = \Gamma(m+\phi^{-1})$, where $\phi > 0$. The expression for the p.m.f of D is given by

$$\begin{aligned}
P(D=d;\eta,\phi,p) =& \sum_{m=d}^{\infty} P(D=d|M=m)P(M=m) \\
=& \frac{p^d}{d!}\left(\frac{\phi\eta}{1+\phi\eta}\right)^d (1+\phi\eta)^{-\phi^{-1}} \sum_{m=d}^{\infty} \frac{\Gamma(m+\phi^{-1})}{(m-d)!\Gamma(\phi^{-1})}\left[\frac{(1-p)\phi\eta}{1+\phi\eta}\right]^{m-d} \\
=& \frac{\Gamma(d+\phi^{-1})}{\Gamma\phi^{-1}d!}\left(\frac{p\phi\eta}{1+p\phi\eta}\right)^d (1+p\phi\eta)^{-\phi^{-1}},\ d=0,1,2,...
\end{aligned} \tag{1.4.13}$$

The number of active competing causes is also distributed with a negative binomial distribution with parameters ϕ^{-1} and $\frac{p\phi\eta}{1+p\phi\eta}$. The cure rate, population survival function and population density function are given by the following expressions:

$$p_0 = (1+p\eta\phi)^{-\phi^{-1}}, \tag{1.4.14}$$

$$S_p(y) = (1+p\eta\phi F(y))^{-\phi^{-1}}, \tag{1.4.15}$$

and

$$f_p(y) = p\eta(1+p\eta\phi F(y))^{-1}S_p(y)f(y) \tag{1.4.16}$$

respectively. Note that, destructive negative binomial cure rate model includes destructive geometric ($\phi = 1$), negative binomial ($p = 1$) and geometric ($\phi = 1, p = 1$) cure rate models as special cases.

1.5 Proportional hazards model for lifetime data

In lifetime data, time-to-event is often affected by observable factors like age, sex, severity of disease, smoking status, results of blood tests, other laboratory data, hospital unit facilities, expertise of medical practitioners etc. These factors are called covariates and it is important to include these into the model for analysis. One possible way to include covariates is by using regression through hazard function $h(w) = \lim_{\delta \to 0} P(w < W \leq w + \delta \mid W > w)$. To be more specific, the hazard function of $W_j; j = 1, \ldots, M$ is taken as

$$h(w; \boldsymbol{x}, \boldsymbol{\gamma}) = h_0(w) e^{\boldsymbol{x}'\boldsymbol{\gamma}}, \tag{1.5.1}$$

where $\boldsymbol{x} = (x_1, \ldots, x_p)'$ is a vector of p covariates, $\boldsymbol{\gamma} = (\gamma_1, \ldots, \gamma_p)'$ is the vector of regression coefficients, $h_0(w)$ is the baseline hazard function independent of covariate vector $\boldsymbol{x}$. Note that, for any two covariate vectors $\boldsymbol{x}_1$ and $\boldsymbol{x}_2$,

$$\frac{h(w; \boldsymbol{x}_1, \boldsymbol{\gamma})}{h(w; \boldsymbol{x}_2, \boldsymbol{\gamma})} = \frac{h_0(w) e^{\boldsymbol{x}_1'\boldsymbol{\gamma}}}{h_0(w) e^{\boldsymbol{x}_2'\boldsymbol{\gamma}}} = e^{(\boldsymbol{x}_1 - \boldsymbol{x}_2)'\boldsymbol{\gamma}},$$

i.e. the hazard ratio is independent of observed time w. This implies that the ratio of hazards between two individuals or groups remains constant with respect to time. The model defined in equation (1.5.1) is thus known as proportional hazards model. The baseline hazard function $h(w)$ represents the amount of hazard present in all individuals inherently even if no covariate is involved and may be estimated parametrically i.e. by assuming a distribution or non-parametrically without any distributional assumption. A Weibull distribution is often used to model lifetime data, so the corresponding hazard function is used to define the baseline hazard function as given in equation (1.5.1). Alternatively, we approximate the baseline hazard non-parametrically using a piecewise linear function (PLA), thereby, the resultant model in equation (1.5.1) follows a Cox proportional hazards model. The proportional hazards model allows us to link covariates to the lifetime distribution of susceptible through hazard function. This assumption provides more flexibility to the overall cure rate model since the lifetimes of the non-cured individuals vary according to the covariates and acts as an extension to cure rate models with independently and identically distributed (i.i.d.) lifetimes (see Balakrishnan and Pal, 2014).

1.5.1 Weibull distribution to model baseline hazard

A continuous random variable W follows a two-parameter Weibull distribution if the probability density function is of the form

$$f(w; \gamma_0, \gamma_1) = \frac{\gamma_0}{\gamma_1}\left(\frac{w}{\gamma_1}\right)^{\gamma_0 - 1} e^{-\left(\frac{w}{\gamma_1}\right)^{\gamma_0 - 1}}, \tag{1.5.2}$$

where $w > 0$, $\gamma_0 > 0$ denotes the shape parameter and $\gamma_1 > 0$ denotes the scale parameter. The survival function and the hazard function of W are given as

$$S(w; \gamma_0, \gamma_1) = e^{-\left(\frac{w}{\gamma_1}\right)^{\gamma_0 - 1}} \tag{1.5.3}$$

and

$$h(w; \gamma_0, \gamma_1) = \frac{\gamma_0}{\gamma_1}\left(\frac{w}{\gamma_1}\right)^{\gamma_0 - 1} \tag{1.5.4}$$

respectively. A Weibull distribution is closed under proportional hazards family when the shape parameter is kept fixed. Moreover, a two parameter Weibull provides a great degree of flexibility to the lifetime of the susceptible since it represents cases of decreasing hazard ($\gamma_0 < 1$), constant hazard (γ_0=1 i.e. exponential distribution) and increasing hazard ($\gamma_0 > 1$). Cure rate models taking a Weibull distribution as the lifetime of the susceptible are prevalent in literature e.g. Farewell (1982), Tsodikov et al. (2003), Chen et al. (1999) and Balakrishnan and Pal (2014).

Now, let us assume the baseline hazard function in (1.5.1) to be that of a Weibull distribution, then, the hazard function of W_j is given by

$$h(w;\boldsymbol{x},\boldsymbol{\gamma}) = \frac{\gamma_0}{\gamma_1}\left(\frac{w}{\gamma_1}\right)^{\gamma_0-1} e^{\boldsymbol{x}'\boldsymbol{\gamma}_2}; \tag{1.5.5}$$

clearly, W_i still follows a Weibull distribution with shape parameter γ_0 and scale parameter $\gamma_1 \exp(-\boldsymbol{x}'\boldsymbol{\gamma}_2/\gamma_0)$, where $\boldsymbol{\gamma} = (\gamma_0, \gamma_1, \boldsymbol{\gamma}')'$. By assuming a proportional hazard model, we allow the lifetime distribution of the susceptible to vary according to the covariate categories, thereby adding a greater flexibility to the model. It should be noted that this model reduces to the parametric Weibull lifetime cure rate model (Balakrishnan and Pal, 2014) if we set $\boldsymbol{\gamma}_2 = \mathbf{0}$. This would therefore facilitate us to test the hypothesis of uniformity among the covariate groups by testing $\boldsymbol{\gamma}_2 = \mathbf{0}$ and if significant evidence is found against this hypothesis it would then suggest the suitability of this model over the parametric Weibull lifetime cure rate model with i.i.d. lifetimes.

1.5.2 A piecewise linear approximation to model baseline hazard

For the piecewise linear approximation (PLA) of the baseline hazard function $h_0(w)$, we consider a set of cut points $\{\tau_0, \ldots, \tau_N\}$ on the time axis, with $\tau_0 < \tau_1, \cdots < \tau_N$ and N being the number of line segments. Further, it is assumed that the PLA is a continuous function at cut points. Under these assumptions, the PLA to the baseline hazard in the interval $[\tau_0, \tau_N]$ is given by

$$h_0(w) = \sum_{l=1}^{N} (a_l + b_l w) I_{[\tau_{l-1}, \tau_l]}(w) \tag{1.5.6}$$

where a_l and b_l are the intercept and slope of the l-th line segment with

$$I_{[\tau_{l-1}, \tau_l]}(w) = \begin{cases} 1, & \tau_{l-1} \leq w \leq \tau_l \\ 0, & \text{otherwise.} \end{cases} \tag{1.5.7}$$

Additionally, letting $\psi_l \geq 0$ denote the values of the PLA at the l-th cut point τ_l, $l = 0, \ldots, N$ we have

$$b_l = \frac{\psi_l - \psi_{l-1}}{\tau_l - \tau_{l-1}}, \; a_l = \psi_l - b_l \tau_l$$

for $l = 1, \ldots, N$. Thus, considering $\boldsymbol{\psi} = (\psi_0, \ldots, \psi_N)'$ equation (1.5.6) can be rewritten as

$$h_0(w) = h_0(w; \boldsymbol{\psi}) = \sum_{l=1}^{N} \left[\psi_l + \frac{\psi_l - \psi_{l-1}}{\tau_l - \tau_{l-1}} (w - \tau_l) \right] I_{[\tau_{l-1}, \tau_l]}(w) \tag{1.5.8}$$

with $\lim_{w \to \tau_l} h_0(w; \boldsymbol{\psi}) = \psi_l$, for $l = 0, \ldots, N$. The cumulative baseline hazard function under the PLA is given by

$$\begin{aligned} H_0(w; \boldsymbol{\psi}) &= \sum_{l=1}^{N} \psi_l (\min(w, \tau_l) - \tau_{l-1}) I_{[\tau_{l-1}, \infty)}(w) \\ &+ \sum_{l=1}^{N} \left[\left(\frac{\psi_l - \psi_{l-1}}{\tau_l - \tau_{l-1}} \right) \frac{\min(w, \tau_l)^2 - \tau_{l-1}^2}{2} - \tau_l (\min(w, \tau_l) - \tau_{l-1}) \right] I_{[\tau_{l-1}, \infty)}(w). \end{aligned} \tag{1.5.9}$$

It is to be noted that although the PLA provides an approximation in the interval $[\tau_0, \tau_N]$, it could also be extended to $[0, \tau_0] \cup [\tau_N, \infty)$ in many ways, such as, taking $\tau_0 = 0$ and extending $a_N + b_N w$ to $[\tau_N, \infty)$. This model follows a Cox proportional hazards model since the baseline is approximated non-parametrically.

1.6 Form of the data and the likelihood function

In survival analysis or reliability theory, the existence of right censored data is quite common mainly due to the limitations imposed by the duration of the study. Therefore, assuming that our data are subject to non-informative right censoring, the censored group may include not only cured individuals but also susceptibles who met the event of interest after censoring time. To be more specific, let us denote by C_i the censoring time and Y_i the actual lifetime for the i-th individual, for $i = 1, \ldots, n$. Thus, the observed lifetime T_i is defined as

$$T_i = \min\{Y_i, C_i\}$$

while $\delta_i = I(Y_i \leq C_i)$ indicates whether the i-th individual is censored ($\delta_i = 0$) or not ($\delta_i = 1$), for $i = 1, \ldots, n$. Additionally, let us also define the sets Δ_1 and Δ_0, with $\Delta_1 = \{i : \delta_i = 1\}$ and $\Delta_0 = \{i : \delta_i = 0\}$. $\boldsymbol{x}_i$ denotes the vector of covariates corresponding to the i-th individual for $i = 1, \ldots, n$. Therefore, the observed data are of the form $(t_i, \delta_i, \boldsymbol{x}_i)$, for $i = 1, \ldots, n$ and the likelihood function can be expressed as

$$L(\boldsymbol{\theta}; \boldsymbol{t}, \boldsymbol{x}, \boldsymbol{\delta}) \propto \prod_{i=1}^{n} f_p(t_i, \boldsymbol{x}_i; \boldsymbol{\theta})^{\delta_i} S_p(t_i, \boldsymbol{x}_i; \boldsymbol{\theta})^{1-\delta_i} = \prod_{i \in \Delta_1} f_p(t_i, \boldsymbol{x}_i; \boldsymbol{\theta}) \prod_{i \in \Delta_0} S_p(t_i, \boldsymbol{x}_i; \boldsymbol{\theta}), \tag{1.6.1}$$

where $\boldsymbol{\theta}$ denotes the vector of parameters involved, $\boldsymbol{t} = (t_1, \ldots, t_n)'$, $\boldsymbol{x} = (\boldsymbol{x}'_1, \ldots, \boldsymbol{x}'_n)'$ and $\boldsymbol{\delta} = (\delta_1, \ldots, \delta_n)'$. $S_p(t_i, \boldsymbol{x}_i; \boldsymbol{\theta})$ and $f_p(t_i, \boldsymbol{x}_i; \boldsymbol{\theta})$ denote population survival and density functions respectively. Here, $\boldsymbol{x}_i$ is generally linked to parameters associated to cure rate and also to the lifetimes $W_j; j = 1, \ldots, M$ as defined by the proportional hazards model in equation (1.5.1). The likelihood described in equation (1.6.1) is an observed likelihood function. For all $i \in \Delta_1$, we observe the lifetime $T_i = Y_i$. So all such $i \in \Delta_1$ contribute to the likelihood function through the population density function. For all $i \in \Delta_0$, we just observe $T_i = C_i < Y_i$ i.e. the actual lifetime is greater than some censoring value. Thus, for these individuals, contribution to the likelihood occurs through the population survival function.

1.7 Likelihood inference

The likelihood function is a function of parameter which denotes the probability of obtaining a parameter value when data is already observed. The likelihood principle suggests that all information relevant to the model parameters contained in a sample are present in the likelihood function. Maximizing the likelihood function with respect to the unknown parameter helps us to estimate the parameter and this technique is commonly referred to as maximum likelihood estimation (MLE). Thus, the ML estimator $\hat{\boldsymbol{\theta}}$ is obtained as

$$\hat{\boldsymbol{\theta}}_{\text{mle}} = \arg\max_{\theta \in \Theta} \hat{L}(\boldsymbol{\theta}\,; \boldsymbol{t}, \boldsymbol{x}, \boldsymbol{\delta}),$$

where $\boldsymbol{\Theta}$ denotes the parameter space. Since, the parameters we are interested in are continuous in nature, estimates of the parameters can be obtained by finding the critical points of the likelihood function using the first derivative test. ML estimators possess some statistically desirable properties like consistency, asymptotic normality, asymptotic efficiency and unbiasedness. However, the ML estimators are not always found in explicit forms, and in some cases, may not even exist. In survival analysis, we often encounter censored data which leads to observing only partial data. This is referred to as incomplete data. Under this scenario, an EM algorithm (Dempster et al., 1977) is often applied to find the ML estimates using iterative methods.

1.7.1 EM algorithm

The incomplete data is introduced through a random variable $I_i; i = 1, \ldots, n$, where $I_i = 0$ if the i-th individual is cured or $I_i = 1$ otherwise. It is to be noted that I_i is unobserved if $i \in \Delta_0$ since we just observe the censoring time for these individuals and no information about their cure status is known. On the other hand, $I_i = 1$ for all $i \in \Delta_1$. This incomplete data provides an opportunity to implement EM algorithm.

We implement EM algorithm (McLachlan and Krishnan, 2007) to estimate $\boldsymbol{\theta}^*$ except the parameter ϕ which is estimated using profile likelihood method. $\boldsymbol{\theta}^*$ denotes the vector of parameters without ϕ.

The complete data are denoted by $\{(t_i, \delta_i, \boldsymbol{x}_i, I_i)'; i = 1, \ldots, n\}$. The complete data likelihood function is expressed as

$$\begin{aligned} &L_c(\boldsymbol{\theta}; \boldsymbol{t}, \boldsymbol{x}, \boldsymbol{\delta}, \boldsymbol{I}) \\ &\propto \prod_{i \in \Delta_1} f_p(t_i, \boldsymbol{x}_i; \boldsymbol{\theta}) \prod_{i \in \Delta_0} p_0(\boldsymbol{\theta}^{**}, \boldsymbol{x}_i)^{1-I_i} \{(1 - p_0(\boldsymbol{\theta}^{**}, \boldsymbol{x}_i)) S_u(t_i, \boldsymbol{x}_i; \boldsymbol{\theta})\}^{I_i} \end{aligned} \tag{1.7.1}$$

and the complete data log-likelihood function is given by

$$\begin{aligned} l_c(\boldsymbol{\theta}; \boldsymbol{t}, \boldsymbol{x}, \boldsymbol{\delta}, \boldsymbol{I}) = \quad & \text{constant} + \sum_{i \in \Delta_1} \log f_p(t_i, \boldsymbol{x}_i; \boldsymbol{\theta}) + \sum_{i \in \Delta_0} (1 - I_i) \log p_0(\boldsymbol{\theta}^{**}, \boldsymbol{x}_i) \\ & + \sum_{i \in \Delta_0} I_i \log(1 - p_0(\boldsymbol{\theta}^{**}, \boldsymbol{x}_i)) + \sum_{i \in \Delta_0} I_i \log S_u(t_i, \boldsymbol{x}_i; \boldsymbol{\theta}), \end{aligned} \tag{1.7.2}$$

where $\boldsymbol{I} = (I_1, \ldots, I_n)'$ and $S_u(t_i, \boldsymbol{x}_i; \boldsymbol{\theta})$ is obtained using equation (1.1.1) as $S_u(t_i, \boldsymbol{x}_i; \boldsymbol{\theta}) = \frac{S_p(t_i, \boldsymbol{x}_i; \boldsymbol{\theta}) - p_0(\boldsymbol{\theta}^{**}, \boldsymbol{x}_i)}{1 - p_0(\boldsymbol{\theta}^{**}, \boldsymbol{x}_i)}$. Note that $\boldsymbol{\theta}^{**}$ is a subset of the set of parameters in the vector $\boldsymbol{\theta}$ since in all cases of our study, the cure rate p_0 is linked to $\boldsymbol{\theta}^{**}$ through some link function. More specifically, $\boldsymbol{\theta}^{**}$ generally does not involve any lifetime parameters in our studied cure rate models. In equation 1.7.1, the likelihood is split into the product of two components, *viz.*, corresponding to cured and non-cured individuals for all $i \in \Delta_0$. The contribution to the complete data likelihood function occurs through $p_0(\boldsymbol{\theta}^{**}, \boldsymbol{x}_i)$ if $I_i = 0$ and $(1 - p_0(\boldsymbol{\theta}^{**}, \boldsymbol{x}_i))S_u(t_i, \boldsymbol{x}_i; \boldsymbol{\theta})$ if $I_i = 1$.

E-step: For a fixed value ϕ_0 of ϕ and $(a+1)$-th iteration of EM algorithm, we compute the expected value of $l_c(\boldsymbol{\theta}; \boldsymbol{t}, \boldsymbol{x}, \boldsymbol{\delta}, \boldsymbol{I})$, given the observed data $\boldsymbol{O} = \{(t_i, \delta_i, \boldsymbol{x}_i, I_{i'}) : i = 1, \ldots, n; i' \in \Delta_1\}$ and the current parameter estimates $\boldsymbol{\theta}^{*(a)}$ obtained from the a-th iteration. Therefore, from Equation (1.7.2) we have

$$\begin{aligned}
&\mathbb{E}(l_c(\boldsymbol{\theta}; \boldsymbol{t}, \boldsymbol{x}, \boldsymbol{\delta}, \boldsymbol{I})|\boldsymbol{\theta}^{*(a)}, \boldsymbol{O}) \\
= \quad & \text{constant} + \sum_{i \in \Delta_1} \log f_p(t_i, \boldsymbol{x}_i; \boldsymbol{\theta}) + \sum_{i \in \Delta_0} (1 - \pi_i^{(a)}) \log p_0(\boldsymbol{\theta}^{**}, \boldsymbol{x}_i) \\
+ & \sum_{i \in \Delta_0} \pi_i^{(a)} \log(1 - p_0(\boldsymbol{\theta}^{**}, \boldsymbol{x}_i)) + \sum_{i \in \Delta_0} \pi_i^{(a)} \log S_u(t_i, \boldsymbol{x}_i; \boldsymbol{\theta}),
\end{aligned} \tag{1.7.3}$$

where

$$\pi_i^{(a)} = \mathbb{E}[I_i|\boldsymbol{O}, \boldsymbol{\theta}^{*(a)}] = \left. \frac{(1 - p_0(\boldsymbol{\theta}^{**}, \boldsymbol{x}_i))S_u(t_i, \boldsymbol{x}_i, \boldsymbol{z}_i; \boldsymbol{\theta})}{S_p(t_i, \boldsymbol{x}_i; \boldsymbol{\theta})} \right|_{\boldsymbol{\theta}^* = \boldsymbol{\theta}^{*(a)}}.$$

We define $Q = Q(\boldsymbol{\theta}^*, \boldsymbol{\pi}^{(a)}) = \mathbb{E}(l_c(\boldsymbol{\theta}; \boldsymbol{t}, \boldsymbol{x}, \boldsymbol{z}, \boldsymbol{\delta}, \boldsymbol{I})|\boldsymbol{\theta}^{*(a)}, \boldsymbol{O})$ where $\boldsymbol{\pi}^{(a)} = (\pi_i^{(a)} : i \in \Delta_0)$.

M-step: In the maximization step, we maximize $Q(\boldsymbol{\theta}^*, \boldsymbol{\pi}^{(a)})$ with respect to $\boldsymbol{\theta}^*$ to find the estimate $\boldsymbol{\theta}^{*(a+1)}$ of $\boldsymbol{\theta}^*$. The numerical maximization is carried out using Nelder-Mead method for fixed ϕ_0. The iteration process is considered to converge if $\max_{1 \le k' \le p} \left| \frac{\hat{\theta}^*_{k'} - \theta^*_{k'}}{\theta^*_{k'}} \right| < \epsilon$, for some small ϵ and p denotes the number of parameters. The explicit expressions for the Q-function is provided in Appendices A.1, B.1 and C.1 for various cure rate models we have studied.

In case of a COM-Poisson cure rate model, ϕ is a dispersion parameter whereas for a weighted Poisson cure rate model, ϕ is a parameter in the weight function. In both cases, it is observed that the likelihood function is very flat with respect to ϕ. As a result, the algorithm for finding ML estimates encounters frequent convergence problem unless the initial parameter estimates are very close to the true values. Even if the algorithm converges, the estimate of ϕ often has a high standard error which seems to affect the precision of the estimates of other parameters as well. Consequently, ϕ is kept fixed in the objective function while maximizing with respect to other parameters. However, this process is repeated for a discrete range of values of ϕ, thereby, considering the one, which produces the highest value of log-likelihood function. In other words, the *E-step* and *M-step* are repeated for all $\phi \in \Phi$ where Φ denotes the admissible range of ϕ. The value of $\phi \in \Phi$ which provides the maximum value of the observed likelihood function is taken to be the ML estimate $\hat{\phi}$ of ϕ.

1.7.2 Estimation of standard errors

For finding the standard error of the parameter estimates, we applied Louis' principle for computing the observed information matrix (see Louis, 1982); that is,

$$\begin{aligned} I(\boldsymbol{\theta}^*) = \quad & \mathbb{E}[B(\boldsymbol{\theta}^*; \boldsymbol{t}, \boldsymbol{x}, \boldsymbol{\delta}, \boldsymbol{I})] - \mathbb{E}[S(\boldsymbol{\theta}^*; \boldsymbol{t}, \boldsymbol{x}, \boldsymbol{\delta}, \boldsymbol{I}) S^T(\boldsymbol{\theta}^*; \boldsymbol{t}, \boldsymbol{x}, \boldsymbol{\delta}, \boldsymbol{I})] \\ & + \mathbb{E}[S(\boldsymbol{\theta}^*; \boldsymbol{t}, \boldsymbol{x}, \boldsymbol{\delta}, \boldsymbol{I})] \mathbb{E}[S^T(\boldsymbol{\theta}^*; \boldsymbol{t}, \boldsymbol{x}, \boldsymbol{\delta}, \boldsymbol{I})], \end{aligned} \tag{1.7.4}$$

where $I(\boldsymbol{\theta}^*)$ is the information on $\boldsymbol{\theta}^*$, $B(\boldsymbol{\theta}^*; \boldsymbol{t}, \boldsymbol{x}, \boldsymbol{\delta}, \boldsymbol{I})$ and $S(\boldsymbol{\theta}^*; \boldsymbol{t}, \boldsymbol{x}, \boldsymbol{\delta}, \boldsymbol{I})$ denote the negative of the matrix of second derivatives and the gradient vector of $l_c(\boldsymbol{\theta}; \boldsymbol{t}, \boldsymbol{x}, \boldsymbol{\delta}, \boldsymbol{I})$ (score function). The standard errors of the parameter estimates were then calculated by taking the square-root of the corresponding variances which are nothing more than the diagonal elements of the variance-covariance matrix $I^{-1}(\boldsymbol{\theta}^*)$. By using the asymptotic normality of the MLEs, 95% confidence intervals (CI) of the parameters were obtained. The normality of the parameter estimates obtained from 1000 simulated data were validated graphically using QQ plot and also using bootstrap method. The pertinent details of the first-order and second-order derivatives of the complete data log-likelihood for obtaining the information matrix are presented in Appendices A.2, B.2 and C.2. Asymptotic normality of the MLEs can also be used to estimate the cure rate and is given by $\hat{p}_0 = p_0(\hat{\boldsymbol{\theta}^{**}}, \boldsymbol{x}_i)$. The standard error of the cure rate is obtained using multivariate delta method since $p_0(\boldsymbol{\theta}^{**}, \boldsymbol{x}_i) = g(\boldsymbol{\theta}^{**}) : \mathbb{R}^{(p+1)} \to \mathbb{R}$ is a continuous function.

It can be observed that Equation 1.7.2 and 1.7.3 differ only with respect to I_i. For the latter, I_i is replaced by $\pi_i^{(a)}$, where at a-th step $\pi_i^{(a)}$ is a fixed quantity independent of $\boldsymbol{\theta}^*$. Thus, taking derivatives on both equations with respect to $\boldsymbol{\theta}^*$ lead to the same expressions. As such, the expressions for first-order and second-order derivatives of $l_c(\boldsymbol{\theta}; \boldsymbol{t}, \boldsymbol{x}, \boldsymbol{z}, \boldsymbol{\delta}, \boldsymbol{I})$ required for calculating the observed information matrix are not presented separately and can be obtained from Appendices A.1-C.1 and A.2-C.2.

1.8 Simulation study and real data analysis

The robustness of the models and accuracy of the estimation technique are studied and validated using detailed Monte Carlo simulations. The effects of different sample sizes, cure rates, censoring proportions and lifetime parameters on the estimation are investigated thoroughly. Parameter estimates, asymptotic standard errors, biases, root mean squared errors and coverage probabilities at 95% nominal level are presented under different model settings. Coverage probabilities are obtained based on assuming the asymptotic normality of the ML estimators. The results are based on the average of R replications of simulated data for each scenario and all calculations are done in software R-3.1.3. R varies according to the computational load and complexity of the model under study. The Shared Hierarchical Academic Research Computing Network (SHARCNET) is used to compile all the R-codes to reduce overall computational time.

All studies are supported by model discrimination. This is accomplished by generating samples from a true model and analyzing the effect of fitting some candidate models on the parameter estimates and other measures. Likelihood-based criterion, i.e., likelihood ratio test (LRT) and information-based criteria, i.e., Akaike information criterion (AIC) and Bayesian information criterion (BIC) are used to find rejection and selection rates of various candidate models. AIC and BIC are defined as:

$$AIC = -2\hat{l} + 2p \qquad \text{and} \qquad BIC = -2\hat{l} + (\log n)p,$$

where $\hat{l}$ denotes the maximized log-likelihood value, p denotes the number of parameters estimated and n is the sample size. Models with minimum AIC or BIC are chosen. For the COM-Poisson cure rate model, we are interested in testing $H_0 : \phi = 0$, $H_0 : \phi = 1$ and $H_0 : \phi \to \infty$. For testing purpose, LRT statistic is defined as $\Lambda = -2(\hat{l}_0 - \hat{l})$ where $\hat{l}_0$ and $\hat{l}$ denote the restricted and unrestricted maximized log-likelihood function values, respectively. The rejection rates are obtained by the number of times H_0 is getting rejected for some specified level of significance. The null distribution of Λ asymptotically follows χ^2- distribution with one degree of freedom (d.f.) for testing $H_0 : \phi = 1$. However, when we test $H_0 : \phi = 0$ or $H_0 : \phi \to \infty$ i.e. when ϕ is on the boundaries of the parameter space, the asymptotic distribution of

Λ is such that $P(\Lambda \leq \lambda) = \frac{1}{2} + \frac{1}{2}P(\chi^2 \leq \lambda)$. In case of destructive weighted Poisson cure rate model, the necessity of a model discrimination is justified by studying the biases and mean squared errors of the cured proportion under model mis-specification and developing measures like total relative bias (TRB) and total relative efficiency (TRE). The details can be found in Chapter 4.

We implement our proposed models on a malignant melanoma data. This data provides detail of a historically prospective clinical study on 225 skin cancer patients, who were operated in the period 1962-77 and followed up till 1977. Andersen et al. (2012) studied this data set where *time since operation* was considered to be the response of the study with several risk factors like *age at operation*, *sex*, *tumor thickness*, *width*, *location*, *types of malignant cells*, *ulceration status* etc. Among these patients, 20 were not included for analysis since they did not permit a histological evaluation. Later, this data set was the topic of analysis for many studies, e.g., Rodrigues et al. (2011), Pal and Balakrishnan (2016), Pal and Balakrishnan (2017) etc. Out of these 205 patients, 57 patients died from melanoma, 14 died from other causes and are considered censored at death. The remaining 134 patients were alive as on January 1, 1978 and are also considered to be right censored. Thus, the study has a high rate of censored observations (i.e. 72%). This dataset is also available in the 'timereg' package in R.

1.9 Scope of the thesis

Further details of the link functions used, EM algorithm, simulation study results and real data analysis results, specific to each model, can be found in the following chapters. In Chapter 2, by assuming a COM-Poisson distribution under a competing cause scenario a defined in Section 1.3, we study a flexible cure rate model in which the lifetimes of non-cured individuals are described by a proportional hazard model with a Weibull hazard as the baseline function as discussed in Section 1.5.1. A logistic-link is used to associate covariates $\boldsymbol{x}$ to the rate parameter η of the COM-Poisson distribution and to the cure rate using $p_0 = \frac{1}{z(\eta,\phi)}$ in this case. The performance of the models are presented based on five candidate models, namely, geometric ($\phi = 0$), Poisson ($\phi = 1$), Bernoulli ($\phi \to \infty$), COM-Poisson with $\phi = 0.5$ and COM-Poisson with $\phi = 2$. In Chapter 3, we consider a COM-Poisson cure rate model under a competing cause scenario with the unobserved lifetime distribution of the non-cured individual following a Cox proportional hazard model; the baseline hazard is estimated by piecewise linear functions as discussed in Section 1.5.2 with covariates being linked to the cure rate using a logistic-link function. In our analysis, we consider the number of lines (N) approximating the baseline hazard function to be $1, 2, \ldots, 5$. The candidate models for the COM-Poisson family are taken to be the same as mentioned for Chapter 2. In Chapter 4, we investigate a destructive cure rate model where the initial number of competing causes is assumed to follow one of the three special cases of a weighted Poisson distribution as discussed in Section 1.4, *viz.*, exponentially weighted Poisson, length-biased Poisson and negative binomial. The novelty of the work, however, is introduced by assuming the unobserved lifetime distribution of the non-cured subjects to be defined by a proportional hazards model with a Weibull hazard as the baseline function. A log-linear link function and a logistic-link function are used to link the rate parameter η of the weighted Poisson distribution and the parameter p representing the proportion of initial causes that remains active respectively.

For all these models, the estimation of the parameters are carried out using ML method by implementing the EM algorithm, except for the dispersion parameter, which is estimated by a profile likelihood approach. The performance of the model is tested under various settings of censoring rates, sample sizes, cure rates and mean lifetimes and model discrimination is performed. For illustrative purposes, analysis of the cutaneous melanoma data, as mentioned before, is also carried out. The detailed expressions for the $Q-$functions and the first- and second- derivatives of the $Q-$ functions, corresponding to the models discussed in each chapters, can be found in Appendices A.1-C.1 and Appendices A.2-C.2 respectively. It is to be noted that notations may slightly vary from one chapter to another for better comprehensibility of a specific model.

Chapter 2

COM-Poisson Cure Rate Model under Proportional Hazards Lifetime

2.1 Introduction

We assume a proportional hazards model for the distribution of $W_j; j = 1, \ldots, M$, with a parametric assumption on the baseline hazard function. To be more specific, the hazard function of W_j is taken as

$$h(w; \boldsymbol{x}_c, \boldsymbol{\gamma}) = h_0(w; \gamma_0, \gamma_1) e^{\boldsymbol{x}_c' \boldsymbol{\gamma}_2}, \tag{2.1.1}$$

where $\boldsymbol{x}_c = (x_1, \ldots, x_p)'$ is a vector of p covariates, $\boldsymbol{\gamma}_2 = (\gamma_{21}, \ldots, \gamma_{2p})'$ is the vector of proportional hazards regression coefficients, $h_0(w; \gamma_0, \gamma_1)$ is the hazard function of a two-parameter (γ_0 and γ_1) Weibull distribution and $\boldsymbol{\gamma} = (\gamma_0, \gamma_1, \boldsymbol{\gamma}_2')'$. The number of competing causes M is assumed to have a COM-Poisson distribution; under this assumption, more flexibility is achieved since we can deal with under- and over-dispersed data (see Balakrishnan and Pal, 2013a and Rodrigues et al., 2009).

The form of the available data and the likelihood function are given in Section 2.2. In Section 2.3, the steps of the EM algorithm and the estimation of the asymptotic covariance matrix of the MLEs are provided. An extensive simulation study under various scenarios on cure rates, censoring proportions, sample sizes and lifetime parameters is carried out in Section 2.4. In Section 2.5, we study the model discrimination using likelihood-based and information-based methods. In Section 2.6, we use the proposed model for the analysis of a real data set on cutaneous melanoma.

2.2 Form of the data and the likelihood function

In lifetime data analysis, right censoring in data is quite common mainly due to the limitations imposed by duration of the study. Therefore, we assume that our data are subject to non-informative right censoring. The censored group includes susceptibles who have their lifetimes to be larger than the censoring time, and also all the cured individuals. To be more specific, let us denote by C_i the censoring time and Y_i the actual lifetime for the ith individual. Then, T_i is defined as

$$T_i = \min\{Y_i, C_i\}$$

while $\delta_i = I(Y_i \leq C_i)$ indicates whether the ith individual is censored ($\delta_i = 0$) or not ($\delta_i = 1$), for $i = 1, \ldots, n$; let us also define the sets Δ_1 and Δ_0 and $\Delta_1 = \{i : \delta_i = 1\}$ and $\Delta_0 = \{i : \delta_i = 0\}$. It is to be noted that $Z(\eta, \phi) = \frac{1}{p_0} = H_\phi(\eta)$ is only a function of η, for a fixed value of ϕ and is monotone in η with $\lim_{\eta \to 0} H_\phi(\eta) = 1$ and

$\lim_{\eta\to\infty} H_\phi(\eta) = \infty$. Hence, it would be appropriate to link the covariates $x_1, \ldots, x_p$ to the cured proportion using a logistic regression model i.e.

$$p_{0i} = p_0(\boldsymbol{\beta}, \boldsymbol{x}_i) = \frac{1}{1 + e^{\boldsymbol{x}_i'\boldsymbol{\beta}}},$$

where p_{0i} is the cured proportion, $\boldsymbol{x}_i = (1, x_{i1}, \ldots, x_{ip})' = (1, \boldsymbol{x}_{ic}')'$ and $\boldsymbol{\beta} = (\beta_0, \ldots, \beta_p)'$ is the vector of the regression coefficients for the ith individual. This link implies $\eta = H_\phi^{-1}(1 + \exp(\boldsymbol{x}'\boldsymbol{\beta}))$ where $H_\phi^{-1}(.)$ is an inverse function of $H_\phi(.)$ and cannot be calculated analytically for general COM-Poisson distribution. Consequently, the observed data is of the form $(t_i, \delta_i, \boldsymbol{x}_i)$, $i = 1, \ldots, n$, and the likelihood function is given by

$$L(\boldsymbol{\theta}; \boldsymbol{t}, \boldsymbol{x}, \boldsymbol{\delta}) \propto \prod_{i\in\Delta_1} f_p(t_i, \boldsymbol{x}_i; \boldsymbol{\theta}) \prod_{i\in\Delta_0} S_p(t_i, \boldsymbol{x}_i; \boldsymbol{\theta}),$$

where $\boldsymbol{\theta} = (\phi, \boldsymbol{\beta}', \boldsymbol{\gamma}')'$, $\boldsymbol{t} = (t_1, \ldots, t_n)'$, $\boldsymbol{x} = (\boldsymbol{x}_1', \ldots, \boldsymbol{x}_n')'$ and $\boldsymbol{\delta} = (\delta_1, \ldots, \delta_n)'$. Now, let us assume the baseline hazard function in (2.1.1) to be that of a Weibull distribution, i.e.,

$$h_0(w; \gamma_0, \gamma_1) = \frac{\gamma_0}{\gamma_1}\left(\frac{w}{\gamma_1}\right)^{\gamma_0 - 1},$$

where $\gamma_0 > 0$ (the shape parameter) and $\gamma_1 > 0$ (the scale parameter). Then, the hazard function of W_i is given by

$$h(w; \boldsymbol{x}_c, \boldsymbol{\gamma}) = \frac{\gamma_0}{\gamma_1}\left(\frac{w}{\gamma_1}\right)^{\gamma_0 - 1} e^{\boldsymbol{x}_c'\boldsymbol{\gamma}_2}; \qquad (2.2.1)$$

clearly, W_i still follows a Weibull distribution with shape parameter γ_0 and scale parameter $\gamma_1 \exp(-\boldsymbol{x}_c{}'\boldsymbol{\gamma}_2/\gamma_0)$.

In the recent work of Balakrishnan and Pal (2014) on COM-Poisson cure rate model, the lifetime distribution was assumed to be the same and not change with the covariates. In the present work, by assuming a proportional hazard model, we allow the lifetime distribution of the susceptible to vary according to the covariate categories, thereby adding a greater flexibility to the model. It should be noted that this model reduces to the parametric Weibull lifetime COM-Poisson cure rate model studied in detail by Balakrishnan and Pal (2014) if we set $\boldsymbol{\gamma}_2 = \mathbf{0}$. This would therefore facilitate us to test the hypothesis of uniformity among the covariate groups by testing $\boldsymbol{\gamma}_2 = \mathbf{0}$ and if significant evidence is found against this hypothesis it would then suggest the suitability of this model over the parametric Weibull lifetime cure rate model.

2.3 Estimation of parameters and standard errors

The estimation of the model parameters is carried out by using the EM algorithm (see McLachlan and Krishnan, 2007, for details) and a profile likelihood approach for the dispersion parameter ϕ. The complete data are given by $\{(t_i, \boldsymbol{x}_i, \delta_i, I_i) : i = 1, \ldots, n\}$, where I_is are observed for $i \in \Delta_1$ and unobserved for $i \in \Delta_0$ (recall that $I_i = 0$ if and only if the ith individual is cured and 1 otherwise). The complete data likelihood and log-likelihood functions are, respectively, given by

$$L_c(\boldsymbol{\theta}; \boldsymbol{t}, \boldsymbol{x}, \boldsymbol{\delta}, \boldsymbol{I}) \propto \prod_{i \in \Delta_1} f_p(t_i, \boldsymbol{x}_i; \boldsymbol{\theta}) \prod_{i \in \Delta_0} p_0(\boldsymbol{\beta}, \boldsymbol{x}_i)^{1-I_i} \{(1 - p_0(\boldsymbol{\beta}, \boldsymbol{x}_i)) S_u(t_i, \boldsymbol{x}_{ic}; \boldsymbol{\theta})\}^{I_i}$$

and

$$\begin{aligned} l_c(\boldsymbol{\theta}; \boldsymbol{t}, \boldsymbol{x}, \boldsymbol{\delta}, \boldsymbol{I}) = \quad & \text{constant} + \sum_{i \in \Delta_1} \log f_p(t_i, \boldsymbol{x}_i; \boldsymbol{\theta}) + \sum_{i \in \Delta_0} (1 - I_i) \log p_0(\boldsymbol{\beta}, \boldsymbol{x}_i) \\ & + \sum_{i \in \Delta_0} I_i \log(1 - p_0(\boldsymbol{\beta}, \boldsymbol{x}_i)) + \sum_{i \in \Delta_0} I_i \log S_u(t_i, \boldsymbol{x}_{ic}; \boldsymbol{\theta}), \end{aligned} \tag{2.3.1}$$

where $\boldsymbol{I} = (I_1, \ldots, I_n)'$, $\boldsymbol{x}_{ic} = (x_{i1}, \ldots, x_{ip})'$ and $\boldsymbol{x}_i = (1, \boldsymbol{x}'_{ic})'$. For a fixed value of the dispersion parameter ϕ, and at the $(k+1)$th iteration of the EM algorithm, we have to compute the expected value of $l_c(\boldsymbol{\theta}; \boldsymbol{t}, \boldsymbol{x}, \boldsymbol{\delta}, \boldsymbol{I})$, given the observed data $\boldsymbol{O} = \{I_i, i \in \Delta_1, \boldsymbol{t}, \boldsymbol{x}, \boldsymbol{\delta}\}$ and the current estimates obtained from the kth iteration, denoted by $\boldsymbol{\theta}^{(k)} = (\phi, \boldsymbol{\beta}'^{(k)}, \boldsymbol{\gamma}'^{(k)})'$. Therefore, for $i \in \Delta_0$, we have

$$\pi_i^{(k+1)} = \mathbb{E}[I_i | \boldsymbol{O}, \boldsymbol{\theta}^{(k)}] = \frac{(1 - p_0(\boldsymbol{\beta}^{(k)}, \boldsymbol{x}_i)) S_u(t_i, \boldsymbol{x}_{ic}; \boldsymbol{\theta}^{(k)})}{S_p(t_i, \boldsymbol{x}_i; \boldsymbol{\theta}^{(k)})},$$

and so, $Q^{(k+1)} = Q(\boldsymbol{\theta}, \boldsymbol{\pi}^{(k)}) = E[l_c(\boldsymbol{\theta}; \boldsymbol{t}, \boldsymbol{x}, \boldsymbol{\delta}, \boldsymbol{I}) | \boldsymbol{O}, \boldsymbol{\theta}^{(k)}]$ must be maximized with respect to $(\boldsymbol{\beta}', \boldsymbol{\gamma}')'$ (since ϕ is assumed to be fixed), with $\boldsymbol{\pi}^{(k)} = (\pi_i^{(k)} : i \in \Delta_0)$. The numerical maximization is carried out by using the single-step Newton-Raphson or Quasi-Newton method. Explicit expressions for $Q(\boldsymbol{\theta}, \boldsymbol{\pi}^{(k)})$ and the first-order and second-order partial derivatives of $Q(\boldsymbol{\theta}, \boldsymbol{\pi}^{(k)})$ are presented in Appendix A.1 and A.2, respectively. We considered a specific range of values for ϕ with fixed increment; for each choice of ϕ, we found the MLEs of $(\boldsymbol{\beta}', \boldsymbol{\gamma}')'$ and then the final estimate was taken by the choice of ϕ which yielded the maximum likelihood value. We set $\phi \in \{0.0, 0.1, \ldots, 2.0\}$ when data are generated from true $\phi \leq 1$ and $\phi \in \{0.0, 0.1, \ldots, 4.0\}$ when data are generated from true $\phi > 1$.

For finding the standard error of the parameter estimates, we applied Louis' principle for computing the observed information matrix (see Louis, 1982); that is,

$$\begin{aligned} I(\boldsymbol{\theta}^*) = \quad & \mathbb{E}[B(\boldsymbol{\theta}^*; \boldsymbol{t}, \boldsymbol{x}, \boldsymbol{\delta}, \boldsymbol{I})] - \mathbb{E}[S(\boldsymbol{\theta}^*; \boldsymbol{t}, \boldsymbol{x}, \boldsymbol{\delta}, \boldsymbol{I}) S^T(\boldsymbol{\theta}^*; \boldsymbol{t}, \boldsymbol{x}, \boldsymbol{\delta}, \boldsymbol{I})] \\ & + \mathbb{E}[S(\boldsymbol{\theta}^*; \boldsymbol{t}, \boldsymbol{x}, \boldsymbol{\delta}, \boldsymbol{I})] \mathbb{E}[S^T(\boldsymbol{\theta}^*; \boldsymbol{t}, \boldsymbol{x}, \boldsymbol{\delta}, \boldsymbol{I})], \end{aligned} \tag{2.3.2}$$

where $I(\boldsymbol{\theta}^*)$ is the information on $\boldsymbol{\theta}^*$, $B(\boldsymbol{\theta}^*; \boldsymbol{t}, \boldsymbol{x}, \boldsymbol{\delta}, \boldsymbol{I})$ and $S(\boldsymbol{\theta}^*; \boldsymbol{t}, \boldsymbol{x}, \boldsymbol{\delta}, \boldsymbol{I})$ denote the negative of the matrix of second derivatives and the gradient vector of $l_c(\boldsymbol{\theta}; \boldsymbol{t}, \boldsymbol{x}, \boldsymbol{\delta}, \boldsymbol{I})$

(score function). The standard errors of the parameter estimates were then calculated by taking the square-root of the corresponding variances which are nothing more than the diagonal elements of the variance-covariance matrix $I^{-1}(\boldsymbol{\theta}^*)$. By using the asymptotic normality of the MLEs, 95% confidence intervals (CI) of the parameters were obtained. To examine the accuracy of the interval estimation, the coverage probabilities were found at 95% nominal level. The pertinent details of the first-order and second-order derivatives of the complete data log-likelihood for obtaining the information matrix are presented in Appendix A.2. Asymptotic normality of the MLEs can also be used to estimate the standard error of the cure rates with the use of multivariate delta method since $p_0 = g(\boldsymbol{\beta}) : \mathbb{R}^{(p+1)} \to \mathbb{R}$ is a continuous function.

2.4 Simulation study

In our simulation study, we studied the effects of different sample sizes, cure rates, censoring proportions and lifetime parameters in order to examine the performance and robustness of the proposed model. Motivated by the real data, we considered a single categorical covariate x, affecting the lifetimes of the susceptible, having four possible values, namely, $x = 1, 2, 3, 4$. Two different sample sizes were taken into account, distributed among the four covariate groups, viz., $n = 200$ $(50, 42, 53, 55)$ and $n = 400$ $(95, 102, 97, 106)$. The choices of the regression parameters were made by utilizing the monotone behavior of the logit link function. By fixing the true cure rates for $x = 1$ and $x = 4$ as (0.60, 0.25) and (0.40, 0.20) representing the "high" and "low" cure rate scenarios and solving

$$\frac{1}{1 + e^{\beta_0 + \beta_1}} = 0.60(0.40), \frac{1}{1 + e^{\beta_0 + 4\beta_1}} = 0.25(0.20),$$

the true values of (β_0, β_1) were obtained as $(-0.906, 0.501)$ and $(0.078, 0.326)$, respectively. Furthermore, the performance of the model was tested under "heavy" and "light" censored data. Specifically, the censoring proportions considered for the groups $x = 1, 2, 3, 4$ were (0.80, 0.64, 0.50, 0.38) ("heavy" censoring) and (0.70, 0.57, 0.45, 0.35) ("light" censoring) for the "high" cure rate and (0.60, 0.49, 0.40, 0.33) ("heavy" censoring) and (0.50, 0.42, 0.35, 0.30) ("light" censoring) for the "low" cure rate, respectively. It was assumed that the censoring time follow an exponential distribution with rate $\lambda_x, x = 1, 2, 3, 4$. For determining this λ_x, we equated the probability of getting censored for susceptible to the difference between the censoring and cured proportion, and solved them numerically, i.e.

$$P[Y \geq C_x \cap M \geq 1 | X = x] = c_x - p_{0x},$$

for the xth covariate group. Upon considering $C_x \sim$ exponential(λ_x), we therefore solved for λ_x from the equation

$$\lambda_x \int_0^\infty \exp\left[-\left(\frac{c_x}{\gamma_1}\right)^{\gamma_0} e^{\gamma_2 x} + \lambda_x c_x\right] dc_x - \frac{H_\phi^{-1}(c_x/p_{0x})}{H_\phi^{-1}(1/p_{0x})} = 0,$$

by numerical methods. We also took two choices for $(\gamma_0, \gamma_1, \gamma_2)$ as (1.75, 3.25, 0.10) and (3.25, 5.50, 0.20) corresponding to lower and higher lifetimes, respectively, to study its effect on the model.

Here, we discuss the techniques of simulation for different cure rate models, but focusing only on a single covariate group x. For the Bernoulli cure rate model, we generated a random sample M_x of desired size from a Bernoulli distribution ($\phi \to \infty$) having success ($I = 0$) probability to be p_{0x}. If $M_x = 0$, then C_x (censoring time variable) was generated from an exponential distribution with rate λ_x and T_x (observed lifetime) was assigned as C_x with δ_x (censoring indicator) = 0. On the other hand, if $M_x = 1$, C_x was generated from an exponential (λ_x) and Y_x (actual lifetime) from a Weibull with shape γ_0 and scale $\gamma_1 e^{-\frac{\gamma_2 x}{\gamma_0}}$. T_x was calculated as $\min\{Y_x, C_x\}$; $\delta_x = 1$ when $T_x = Y_x$ and $\delta_x = 0$, otherwise. For the Poisson cure rate model, we generated M_x from a Poisson distribution ($\phi = 1$) with mean $H_\phi^{-1}(1 + e^{\beta_0+\beta_1 x}) = -\log p_{0x}$. The procedure remains the same if $M_x = 0$ as in the Bernoulli case. For $M_x = m$ where $m \geq 1$, we generated $W_1, \ldots, W_m$ lifetimes from a Weibull distribution with shape and scale as discussed before and took $Y_x = \min\{W_1, \ldots, W_m\}$. We simultaneously generated C_x from exponential with rate λ_x and took $T_x = \min\{Y_x, C_x\}$. The censoring indicators were generated as $\delta_x = 0$ for $M_x = 0$ and $M_x \geq 1$ with $T_x = C_x$, but $\delta_x = 1$ if $M_x \geq 1$ with $T_x = Y_x$. For the geometric and COM-Poisson cure rate models, the technique remained the same as of the Poisson, except that M_x was generated from a geometric distribution with parameter $1 - p_{0x}$ and a COM-Poisson distribution with parameter $\eta_x = H_\phi^{-1}(1 + e^{\beta_0+\beta_1 x})$ for a fixed ϕ, respectively. η_x was found numerically for the choices of β_0 and β_1. The number of iterations in each scenario was fixed to be at most 500 and the computations were performed on R-software (R-3.1.1). The estimates (Est), i.e., the average over all replications were calculated using Monte Carlo method along with empirical bias, root mean square error (RMSE) and coverage probabilities (CP) to assess the accuracy of our estimates.

For the simulation study, a 15% variability on both sides of the real values, i.e., a random number from the interval $(0.85\boldsymbol{\theta}^*, 1.15\boldsymbol{\theta}^*)$, was taken as the initial parameter guess. As discussed before, the MLE of $(\boldsymbol{\beta}', \boldsymbol{\gamma}')$ was obtained for that ϕ which yielded the maximum log-likelihood value. Thus, $\hat{\phi}$ was obtained by a profile-likelihood and s.e. of the MLE $\boldsymbol{\theta}^*$ by Louis' method by considering $\phi = \hat{\phi}$.

In Tables 2.1 to 2.8, we can see that the estimation of the model parameters is quite accurate for all different scenarios (due to space limitations, the results for the case $\phi = 2$ are not presented). The standard errors and RMSE are found to decrease as the sample size increases. The same is observed when the cure rate or the censoring proportion decreases. The standard error of β_0 is almost always larger than the standard error of any other parameter, except the standard error of γ_1 which is comparatively high; it is to be noted that the lifetime of Y itself is quite sensitive with respect to the scale γ_1. The standard error for γ_0 is greater when the true lifetime parameters are large. However, the effect is quite opposite for the other parameters since the standard errors get reduced. The estimates of ϕ has a relatively high bias since it has been estimated by profile likelihood method. This large bias can also be attributed to the fact that the precision is affected by gap present in the interval consideration of ϕ. In most of the cases, we observed an under-estimated value for $\hat{\phi}$ when data generated from $\phi = 0.5$, which became less apparent for higher true lifetime values.

In most of the cases, the CPs are quite close to the nominal level. The CPs reach the nominal level as the censoring proportion decreases or as the sample size increases. The under-coverage is most apparent in the case of geometric cure rate model, especially, when the censoring proportion is high and lifetime parameters take small values; the CP for the Bernoulli cure rate model is quite close to the nominal level in all cases. The coverage of γ_0 is consistently lower than the nominal level when data is generated from $\phi = 0.5$. Table 2.9 and 2.10 presents the estimates of the cure rate, bias, RMSE and 95% CI for $n = 200$ and $n = 400$ with heavy censoring and higher lifetime; note that the Bernoulli cure rate model has the least bias and

RMSE. It is also worth mentioning that the profile likelihood approach seems to cause bias and larger standard errors which reduce as the grid search for ϕ is performed on intervals with more refined increments (a similar remark can be found in Balakrishnan and Pal, 2014). Overall, more sample observations, less censoring, low cure rate, high lifetime and $\phi > 1$ results in better accuracy of the estimates.

2.5 Model discrimination

The motivation for model discrimination comes from the fact that a COM-Poisson distribution encompasses many well known discrete distributions. So, by choosing the parameter ϕ suitably, we can adequately fit an appropriate model to a data characterized by a cured proportion since it provides access to a wide range of distributions for the number of competing cause. It enables us to observe how often a model different than the true model gets selected or rejected, thereby, utilizing the generality of a COM-Poisson distribution to model a data.

We generated 500 random samples from a specific ϕ (here, $\phi = 0$ (geometric) , 0.5, 1 (Poisson), 2 and ∞ (Bernoulli)), and then fitted the three special cases of a COM-Poisson cure rate model to the generated data. For each replication, we tested whether the geometric ($H_0 : \phi = 0$) or Poisson ($H_0 : \phi = 1$) or Bernoulli ($H_0 : \phi \to \infty$) model could be assumed as an appropriate model for our data, against the alternative that a model described by a COM-Poisson distribution where $\phi \notin H_0$ provided a better fit. The number of times the correct model was rejected (i.e., H_0 is incorrectly rejected, providing the observed level of significance) and that the incorrect models were rejected (i.e., H_0 is correctly rejected, providing the observed power of the test), were computed. Two kinds of selection criteria were examined here, namely, likelihood-based approach and information-based criteria. We took into account the following scenarios: Setting 1: $n = 400$ and "light" censoring; Setting 2: $n = 400$ and "heavy" censoring; Setting 3: $n = 600$ and "light" censoring; Setting 4: $n = 600$ and "heavy" censoring; the censoring proportion exceeded the cured proportion by 0.1, for each covariate group in each of these cases.

2.5.1 Likelihood-based method

Let us denote by $\hat{l}_0$ and $\hat{l}$ the maximized log-likelihood value under the null and alternative hypothesis, respectively; it is known that the asymptotic distribution of the test statistic $\Lambda = -2(\hat{l}_0 - \hat{l})$ (Wilks' likelihood ratio test; LRT), under the null hypothesis, is a Chi-squared distribution with one degrees of freedom (d.f.). However, the cases $\phi = 0$ and $\phi \to \infty$ are on the boundaries of the parametric space and so the asymptotic distribution of Λ is a mixture Chi-squared distribution such that $P(\Lambda \leq \lambda) = \frac{1}{2} + \frac{1}{2}P(\chi_1^2 \leq \lambda)$, where χ_1^2 is a random variable having χ^2-distribution with 1 d.f. (see Self and Liang, 1987). From Table 2.11, we see that the observed level of significance for the geometric model is quite close to the nominal level 0.05. For the Bernoulli cure rate model, the observed level of significance is close to 0.10 in most of the cases, while for the Poisson cure rate model it varies greatly from 0.06 to 0.20. This could be attributed to the fact that the mixture Chi-squared distribution provides good approximation to the asymptotic distribution of Λ (as in case of geometric and Bernoulli), whereas the Chi-squared distribution does not (as in case of the Poisson distribution). Besides, we note that the observed level of significance improves as the sample size increases or/and the cure rate decreases. In case when the data are generated from a true geometric cure rate model, the rejection rate of Bernoulli model was significantly higher than of other models, taking values from 0.597 to 0.830. For the true Poisson model, the rejection rate of the Bernoulli model is greater than the geometric model, though not as much as observed in the true geometric case. For the true Bernoulli cure rate model, the rejection rate of a geometric model ranges from 0.418 to 0.670, whereas that of the Poisson model is in the range of 0.046 and 0.252. For $\phi = 0.5$, it is more likely to reject the Bernoulli model while for $\phi = 2$, the rejection rates of geometric and Bernoulli models are almost similar. Note also that in most of the cases the power increases as sample size increases or/and if the cure rate decreases.

2.5.2 Information-based method

The second method of model selection is based on the Akaike's information criterion (AIC) and Bayesian information criterion (BIC); AIC is defined as $-2\hat{l} + 2p$, where $\hat{l}$ is the maximized likelihood value and p is the number of model parameters to be estimated and BIC is given by $-2\hat{l} + p \log N$, where N is the sample size. Clearly, the model which takes the minimum value for AIC (or BIC) is the model which best fits the data; it is necessary to mention that in our simulation study, the AIC and BIC always selected the same model as the models that are compared have the same number of parameters. From Table 2.12, it can be seen that the selection rate for the geometric model decreases as ϕ increases while that of Bernoulli model increases as ϕ increases; clearly, both of these features are quite reasonable. Based on AIC, the selection rates of the correct model are from 67.0% to 73.2% if the true distribution is geometric, from 39.2% to 49.4% if the true distribution is Poisson, and from 71.2% to 76.0% if the true distribution is Bernoulli. Similar selection rates are also found for the cases $\phi = 0.5$ and $\phi = 2$. It can therefore be stated that if $\phi < 1$, the geometric model is more likely to be selected than the Bernoulli model whilst if $\phi > 1$, the

Bernoulli model is more likely to be selected than the geometric. Note that the selection rates for the correct models increase as the sample size increases, while it decreases as censoring rate increases, as expected.

2.6 Analysis of cutaneous melanoma data

The proposed model is illustrated with a data set on cancer recurrence taken from Ibrahim et al. (2005); the data is part of a study on cutaneous melanoma (a type of malignant cancer) for the evaluation of postoperative treatment performance with a high dose of interferon alpha-2b as a drug to prevent recurrence. There were originally 427 patients in the study divided into four nodule categories based on tumor thickness and this will be the only covariate ($x = 1, 2, 3, 4$) in our analysis; 10 patients were excluded from our analysis due to missing values of tumor thickness information. The patients have been observed for the period 1991-1995 and followed until 1998. The overall percentage of censored observations is 56%. What was observed was either the exact lifetimes (time till patient's death) or the censoring times, in years; the observed lifetimes had mean and standard deviation as 3.18 and 1.69, respectively. The sample sizes for the four nodule categories are n_1= 111, n_2= 137, n_3= 87 and n_4= 82.

To provide the initial values of the regression parameters β_0 and β_1, we considered the observed censoring proportion of each group to be its cure rate (overestimated); for the parameter $\boldsymbol{\gamma}$, we used a multiple linear regression model of $\log\{-\log[S(t;\boldsymbol{\gamma})]\}$ values over $\log(t)$; note that $\log\{-\log[S(t;\boldsymbol{\gamma})]\} = \gamma_0 \log t + \gamma_2 x - \gamma_0 \log \gamma_1$, wherein $S(t;\boldsymbol{\gamma})$ was estimated by the Kaplan-Meier estimator. We used a profile likelihood approach for estimating the parameter ϕ over $[0, 5]$ with increment of 0.1 and then

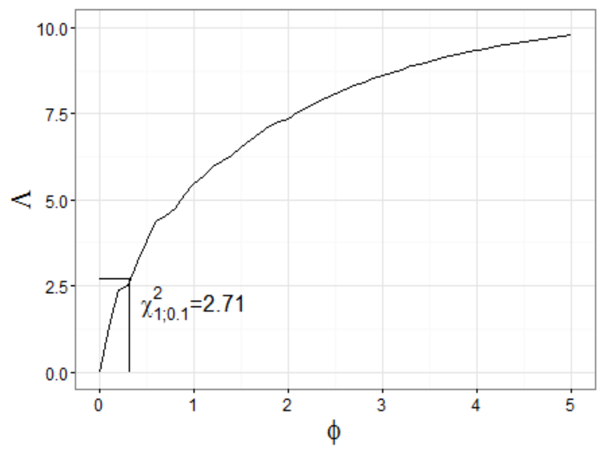

Figure 2.1: The plot of $\Lambda = -2(\hat{l} - \hat{l}_0)$ vs ϕ, for cutaneous melanoma data.

evaluating the log-likelihood value for each ϕ. It was observed that the maximum log-likelihood was achieved at $\phi = 0$, with corresponding log-likelihood value -509.338; hence, the geometric model is found to be most suitable for our data. In order to test the hypothesis $H_0 : \phi = 0$ against $H_1 : \phi > 0$, we follow the same procedure as described in Section 2.5; we find $\Lambda = -2(\hat{l}_0 - \hat{l}) \approx 0$, with p-value equal to 0.50. On the other hand, if we test for the Poisson and Bernoulli cure rate models, we obtain p-values of 0.019 and 0.001, respectively, thus not supporting these models.

The models are also compared on the basis of AIC and BIC. From Table 2.13, it can be seen that AIC and BIC are increasing functions with respect to ϕ. Based on this observation, we used the values of Λ against ϕ (Figure 2.1) with $\phi \in [0, 5]$ and 10% level of significance; hence, $\Lambda = 2.71$ ($\chi^2_{1,0.9}$) and the null hypothesis $H_0 : \phi = 0$ does not get supported if Λ is greater than 2.71. This means that $\phi \in [0, 0.285)$, implying that the geometric model adequately fits the data.Furthermore, we test $H_0 : \gamma_2 = 0$ vs. $H_1 : \gamma_2 \neq 0$ using the likelihood ratio test; note that if $\gamma_2 = 0$, then the lifetime of susceptible follows a Weibull distribution with shape γ_0 and shape γ_1 and the covariates would not have any effect on the lifetime. The maximized log-likelihood values for the geometric, COM-Poisson with $\phi = 0.5$, Poisson, COM-Poisson with $\phi = 2$, and Bernoulli cure rate models are -509.419, -512.194, -513.394, -514.896 and -517.591, respectively. The corresponding Λ values (p-values) are 0.161 (0.687), 1.920 (0.165), 2.627 (0.105), 3.748 (0.052) and 6.234 (0.012), respectively. It can be seen that the p-values decrease as ϕ increases which indicates that for under-dispersed cure rate models, considering proportional-hazards with Weibull baseline is clearly better than considering a constant Weibull lifetime over the four nodule categories. In Table 2.14, we present the estimates for the cure rate proportions, their standard errors and 95% confidence intervals stratified by nodule category, for the geometric cure rate model; the parameters estimates are $\hat{\beta}_0 = -1.076$ (0.292), $\hat{\beta}_1 = 0.456$ (0.109), $\hat{\gamma}_0 = 1.887$ (0.118), $\hat{\gamma}_1 = 3.286$ (0.586) and $\hat{\gamma}_2 = 0.078$ (0.115). Note that the confidence intervals of cure rates for the first and fourth nodule categories are non-overlapping and we can therefore conclude that cure rates of the nodule category 1 is significantly greater than that of nodule category 4.

One more measure of importance is the probability an individual to be cured, given that he/she has survived up to a specific time t, i.e., $P(I = 0|T > t)$. The estimate of this probability is given by

$$\hat{P}(I = 0|T > t) = \left(1 + e^{\hat{\beta}_0 + \hat{\beta}_1 x} \exp\left[-\left(\frac{t}{\hat{\gamma}_1}\right)^{\hat{\gamma}_0} e^{x\hat{\gamma}_2}\right]\right)^{-1}.$$

A plot of this probability for the four nodule categories along with its 95% CI are presented in Figure 2.2 from which the difference between the four groups can clearly be seen. The cure probability for nodule category 1 is the highest, whereas that of nodule category 4 is the lowest.

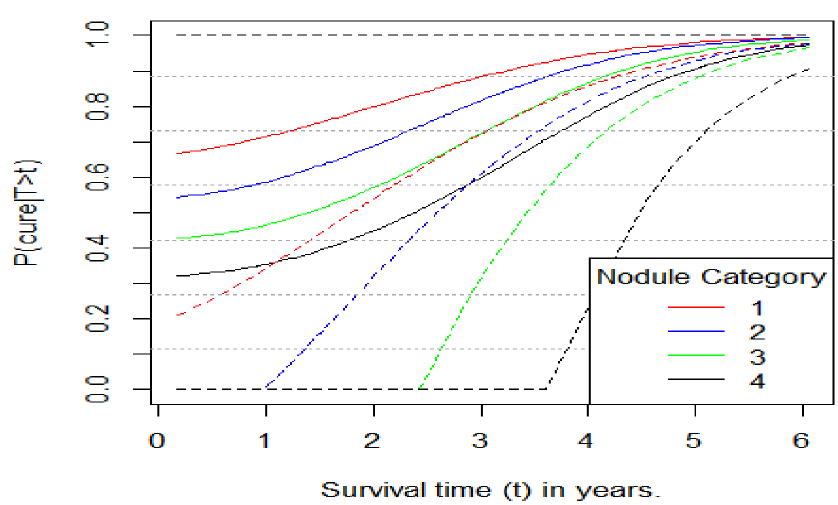

Figure 2.2: Plots representing cure rate given an individual has survived up to a specific time t (solid line), and its 95%CI (dotted line) over four covariate groups.

Table 2.1: Estimates, bias, RMSE and CP for the Bernoulli cure rate model with heavy censoring.

n	p_0	Par	True	Est (s.e.)	Bias	RMSE	CP (95%)
200 (50, 42, 53, 55)	High	β_0	-0.906	-0.921 (0.519)	-0.014	0.517	0.953
		β_1	0.501	0.510 (0.182)	0.009	0.185	0.949
		γ_0	1.750	1.780 (0.147)	0.030	0.153	0.959
		γ_1	3.250	3.366 (0.760)	0.116	0.785	0.938
		γ_2	0.100	0.105 (0.123)	0.005	0.128	0.950
	Low	β_0	0.078	0.077 (0.483)	-0.001	0.482	0.960
		β_1	0.326	0.331 (0.176)	0.004	0.182	0.967
		γ_0	1.750	1.770 (0.130)	0.020	0.136	0.952
		γ_1	3.250	3.304 (0.549)	0.054	0.532	0.944
		γ_2	0.100	0.104 (0.096)	0.004	0.094	0.956
400 (95, 102, 97, 106)	High	β_0	-0.906	-0.934 (0.369)	-0.028	0.380	0.953
		β_1	0.501	0.510 (0.129)	0.009	0.133	0.947
		γ_0	1.750	1.766 (0.105)	0.016	0.113	0.936
		γ_1	3.250	3.262 (0.528)	0.012	0.531	0.940
		γ_2	0.100	0.095 (0.088)	-0.004	0.091	0.945
	Low	β_0	0.078	0.089 (0.334)	0.011	0.338	0.949
		β_1	0.326	0.325 (0.125)	-0.001	0.122	0.957
		γ_0	1.750	1.763 (0.092)	0.013	0.102	0.926
		γ_1	3.250	3.292 (0.380)	0.042	0.394	0.953
		γ_2	0.100	0.103 (0.068)	0.003	0.069	0.947
200 (50, 42, 53, 55)	High	β_0	-0.906	-0.909 (0.493)	-0.002	0.536	0.946
		β_1	0.501	0.500 (0.173)	-0.001	0.183	0.956
		γ_0	3.250	3.329 (0.272)	0.079	0.302	0.930
		γ_1	5.500	5.545 (0.605)	0.045	0.623	0.930
		γ_2	0.200	0.207 (0.115)	0.007	0.124	0.924
	Low	β_0	0.078	0.078 (0.447)	0.000	0.517	0.947
		β_1	0.326	0.328 (0.167)	0.001	0.185	0.953
		γ_0	3.250	3.316 (0.236)	0.066	0.153	0.953
		γ_1	5.500	5.513 (0.440)	0.013	0.785	0.949
		γ_2	0.200	0.204 (0.090)	0.004	0.128	0.935
400 (95, 102, 97, 106)	High	β_0	-0.906	-0.932 (0.352)	-0.025	0.340	0.955
		β_1	0.501	0.511 (0.125)	0.010	0.122	0.959
		γ_0	3.250	3.289 (0.194)	0.039	0.210	0.941
		γ_1	5.500	5.515 (0.433)	0.015	0.429	0.945
		γ_2	0.200	0.201 (0.082)	0.001	0.083	0.943
	Low	β_0	0.078	0.082 (0.312)	0.004	0.380	0.957
		β_1	0.326	0.328 (0.117)	0.001	0.133	0.967
		γ_0	3.250	3.272 (0.166)	0.022	0.113	0.957
		γ_1	5.500	5.482 (0.312)	-0.017	0.531	0.955
		γ_2	0.200	0.197 (0.063)	-0.002	0.091	0.947

Table 2.2: Estimates, bias, RMSE and CP for the Poisson cure rate model with heavy censoring.

n	p_0	Par	True	Est (s.e.)	Bias	RMSE	CP (95%)
200 (50, 42, 53, 55)	High	β_0	-0.906	-0.862 (0.566)	0.044	0.616	0.935
		β_1	0.501	0.494 (0.195)	-0.006	0.202	0.946
		γ_0	1.750	1.797 (0.155)	0.047	0.164	0.938
		γ_1	3.250	3.492 (0.995)	0.242	1.189	0.916
		γ_2	0.100	0.116 (0.157)	0.016	0.170	0.935
	Low	β_0	0.078	0.062 (0.508)	-0.016	0.550	0.933
		β_1	0.326	0.345 (0.192)	0.018	0.212	0.935
		γ_0	1.750	1.776 (0.135)	0.026	0.134	0.945
		γ_1	3.250	3.319 (0.725)	0.069	0.848	0.916
		γ_2	0.100	0.092 (0.133)	-0.007	0.154	0.910
400 (95, 102, 97, 106)	High	β_0	-0.906	-0.923 (0.389)	-0.017	0.415	0.940
		β_1	0.501	0.507 (0.136)	0.006	0.148	0.940
		γ_0	1.750	1.771 (0.109)	0.021	0.111	0.956
		γ_1	3.250	3.316 (0.658)	0.066	0.717	0.934
		γ_2	0.100	0.101 (0.111)	0.001	0.118	0.923
	Low	β_0	0.078	0.094 (0.365)	0.016	0.372	0.946
		β_1	0.326	0.328 (0.136)	0.001	0.137	0.954
		γ_0	1.750	1.768 (0.097)	0.018	0.094	0.960
		γ_1	3.250	3.328 (0.522)	0.078	0.582	0.938
		γ_2	0.100	0.105 (0.095)	0.005	0.102	0.934
200 (50, 42, 53, 55)	High	β_0	-0.906	-0.911 (0.528)	-0.005	0.544	0.943
		β_1	0.501	0.504 (0.188)	0.003	0.194	0.943
		γ_0	3.250	3.304 (0.282)	0.054	0.279	0.952
		γ_1	5.500	5.537 (0.750)	0.037	0.714	0.946
		γ_2	0.200	0.205 (0.147)	0.005	0.144	0.958
	Low	β_0	0.078	0.085 (0.457)	0.006	0.481	0.934
		β_1	0.326	0.326 (0.173)	0.000	0.180	0.946
		γ_0	3.250	3.308 (0.237)	0.058	0.254	0.946
		γ_1	5.500	5.536 (0.556)	0.036	0.578	0.944
		γ_2	0.200	0.212 (0.118)	0.012	0.126	0.938
400 (95, 102, 97, 106)	High	β_0	-0.906	-0.880 (0.362)	0.026	0.370	0.940
		β_1	0.501	0.494 (0.128)	-0.007	0.131	0.944
		γ_0	3.250	3.281 (0.194)	0.031	0.187	0.959
		γ_1	5.500	5.523 (0.509)	0.023	0.518	0.946
		γ_2	0.200	0.204 (0.099)	0.004	0.103	0.940
	Low	β_0	0.078	0.123 (0.345)	0.045	0.342	0.947
		β_1	0.326	0.316 (0.128)	-0.010	0.126	0.955
		γ_0	3.250	3.283 (0.175)	0.033	0.181	0.945
		γ_1	5.500	5.559 (0.421)	0.171	0.413	0.963
		γ_2	0.200	0.208 (0.087)	0.007	0.083	0.963

Table 2.3: Estimates, bias, RMSE and CP for the geometric cure rate model with heavy censoring.

n	p_0	Par	True	Est (s.e.)	Bias	RMSE	CP (95%)
200 (50, 42, 53, 55)	High	β_0	-0.906	-0.893 (0.541)	0.013	0.681	0.888
		β_1	0.501	0.496 (0.188)	-0.004	0.238	0.884
		γ_0	1.750	1.810 (0.160)	0.060	0.172	0.948
		γ_1	3.250	3.676 (1.244)	0.426	2.041	0.859
		γ_2	0.100	0.118 (0.198)	0.018	0.269	0.859
	Low	β_0	0.078	0.023 (0.502)	-0.055	0.636	0.879
		β_1	0.326	0.354 (0.189)	0.027	0.244	0.886
		γ_0	1.750	1.793 (0.144)	0.043	0.169	0.907
		γ_1	3.250	3.416 (1.032)	0.166	1.484	0.855
		γ_2	0.100	0.083 (0.192)	-0.016	0.255	0.866
400 (95, 102, 97, 106)	High	β_0	-0.906	-0.900 (0.388)	0.006	0.470	0.899
		β_1	0.501	0.496 (0.137)	-0.004	0.166	0.895
		γ_0	1.750	1.773 (0.115)	0.023	0.134	0.907
		γ_1	3.250	3.435 (0.837)	0.185	1.160	0.866
		γ_2	0.100	0.110 (0.144)	0.010	0.190	0.862
	Low	β_0	0.078	0.089 (0.355)	0.010	0.426	0.896
		β_1	0.326	0.321 (0.131)	-0.005	0.160	0.887
		γ_0	1.750	1.766 (0.101)	0.016	0.107	0.937
		γ_1	3.250	3.426 (0.732)	0.176	0.989	0.898
		γ_2	0.100	0.109 (0.133)	0.009	0.173	0.876
200 (50, 42, 53, 55)	High	β_0	-0.906	-0.944 (0.530)	-0.037	0.566	0.943
		β_1	0.501	0.512 (0.186)	0.011	0.203	0.938
		γ_0	3.250	3.329 (0.292)	0.079	0.305	0.952
		γ_1	5.500	5.537 (0.913)	0.037	1.033	0.922
		γ_2	0.200	0.198 (0.189)	-0.001	0.218	0.913
	Low	β_0	0.078	0.085 (0.503)	0.006	0.556	0.920
		β_1	0.326	0.331 (0.185)	0.004	0.210	0.922
		γ_0	3.250	3.345 (0.268)	0.095	0.282	0.960
		γ_1	5.500	5.545 (0.836)	0.045	0.939	0.918
		γ_2	0.200	0.198 (0.183)	-0.001	0.210	0.912
400 (95, 102, 97, 106)	High	β_0	-0.906	-0.918 (0.373)	-0.012	0.419	0.918
		β_1	0.501	0.509 (0.133)	0.008	0.150	0.912
		γ_0	3.250	3.326 (0.208)	0.076	0.238	0.920
		γ_1	5.500	5.567 (0.642)	0.067	0.690	0.932
		γ_2	0.200	0.209 (0.134)	0.009	0.149	0.930
	Low	β_0	0.078	0.078 (0.357)	-0.000	0.376	0.932
		β_1	0.326	0.330 (0.133)	0.003	0.144	0.928
		γ_0	3.250	3.320 (0.189)	0.070	0.216	0.928
		γ_1	5.500	5.515 (0.589)	0.015	0.656	0.919
		γ_2	0.200	0.203 (0.131)	0.003	0.152	0.915

Table 2.4: Estimates, bias, RMSE and CP for the COM-Poisson cure rate model with $\phi = 0.5$ and heavy censoring.

n	p_0	Par	True	Est (s.e.)	Bias	RMSE	CP (95%)
200 (50, 42, 53, 55)	High	β_0	-0.906	-0.935 (0.557)	-0.028	0.588	0.933
		β_1	0.501	0.509 (0.192)	0.008	0.204	0.926
		γ_0	1.750	1.909 (0.171)	0.159	0.250	0.840
		γ_1	3.250	3.274 (1.000)	0.024	1.152	0.920
		γ_2	0.100	0.032 (0.191)	-0.067	0.229	0.920
		ϕ	0.500	0.247 (-)	-0.252	0.578	-
	Low	β_0	0.078	0.067 (0.504)	-0.010	0.508	0.955
		β_1	0.326	0.333 (0.184)	0.006	0.183	0.955
		γ_0	1.750	1.897 (0.152)	0.147	0.228	0.816
		γ_1	3.250	3.474 (0.908)	0.224	1.003	0.955
		γ_2	0.100	0.058 (0.172)	-0.041	0.187	0.948
		ϕ	0.500	0.240 (-)	-0.260	0.588	-
400 (95, 102, 97, 106)	High	β_0	-0.906	-0.885 (0.392)	0.021	0.372	0.954
		β_1	0.501	0.482 (0.136)	-0.019	0.128	0.954
		γ_0	1.750	1.855 (0.118)	0.105	0.181	0.812
		γ_1	3.250	3.293 (0.724)	0.043	0.820	0.935
		γ_2	0.100	0.055 (0.135)	-0.044	0.165	0.890
		ϕ	0.500	0.279 (-)	-0.220	0.609	-
	Low	β_0	0.078	0.064 (0.358)	-0.014	0.424	0.903
		β_1	0.326	0.324 (0.131)	-0.002	0.160	0.903
		γ_0	1.750	1.873 (0.107)	0.123	0.186	0.696
		γ_1	3.250	3.476 (0.658)	0.226	0.888	0.872
		γ_2	0.100	0.053 (0.125)	-0.046	0.166	0.866
		ϕ	0.500	0.209 (-)	-0.290	0.562	-
200 (50, 42, 53, 55)	High	β_0	-0.906	-0.891 (0.540)	0.015	0.504	0.960
		β_1	0.501	0.500 (0.186)	-0.001	0.178	0.973
		γ_0	3.250	3.543 (0.309)	0.293	0.466	0.814
		γ_1	5.500	5.619 (0.841)	0.119	0.859	0.933
		γ_2	0.200	0.190 (0.76)	-0.009	0.185	0.947
		ϕ	0.500	0.345 (-)	-0.154	0.629	-
	Low	β_0	0.078	0.061 (0.496)	-0.017	0.470	0.975
		β_1	0.326	0.328 (0.181)	0.002	0.179	0.950
		γ_0	3.250	3.506 (0.277)	0.257	0.431	0.808
		γ_1	5.500	5.562 (0.713)	0.062	0.811	0.913
		γ_2	0.200	0.167 (0.161)	-0.032	0.188	0.895
		ϕ	0.500	0.401 (-)	-0.098	0.663	-
400 (95, 102, 97, 106)	High	β_0	-0.906	-0.912 (0.376)	-0.005	0.371	0.957
		β_1	0.501	0.499 (0.132)	-0.001	0.132	0.944
		γ_0	3.250	3.413 (0.211)	0.163	0.333	0.822
		γ_1	5.500	5.535 (0.581)	0.035	0.591	0.926
		γ_2	0.200	0.179 (0.121)	-0.020	0.140	0.901
		ϕ	0.500	0.380 (-)	-0.119	0.607	-
	Low	β_0	0.078	0.080 (0.347)	0.002	0.382	0.946
		β_1	0.326	0.314 (0.127)	-0.012	0.136	0.928
		γ_0	3.250	3.494 (0.194)	0.244	0.342	0.724
		γ_1	5.500	5.598 (0.511)	0.098	0.578	0.898
		γ_2	0.200	0.176 (0.115)	-0.023	0.126	0.934
		ϕ	0.500	0.289 (-)	-0.211	0.614	-

Table 2.5: Estimates, bias, RMSE and CP for the Bernoulli cure rate model with light censoring.

n	p_0	Par	True	Est (s.e.)	Bias	RMSE	CP (95%)
200 (50, 42, 53, 55)	High	β_0	-0.906	-0.961 (0.410)	-0.054	0.424	0.945
		β_1	0.501	0.524 (0.155)	0.023	0.161	0.947
		γ_0	1.750	1.781 (0.138)	0.031	0.135	0.956
		γ_1	3.250	3.303 (0.573)	0.053	0.614	0.935
		γ_2	0.100	0.101 (0.102)	0.001	0.108	0.933
	Low	β_0	0.078	0.066 (0.394)	-0.011	0.433	0.941
		β_1	0.326	0.338 (0.153)	0.011	0.167	0.931
		γ_0	1.750	1.772 (0.119)	0.022	0.119	0.962
		γ_1	3.250	3.263 (0.437)	0.013	0.402	0.952
		γ_2	0.100	0.102 (0.082)	0.002	0.076	0.970
400 (95, 102, 97, 106)	High	β_0	-0.906	-0.931 (0.294)	-0.024	0.288	0.948
		β_1	0.501	0.512 (0.108)	0.011	0.104	0.969
		γ_0	1.750	1.760 (0.098)	0.010	0.102	0.942
		γ_1	3.250	3.290 (0.412)	0.040	0.391	0.965
		γ_2	0.100	0.104 (0.071)	0.004	0.071	0.959
	Low	β_0	0.078	0.054 (0.289)	-0.024	0.300	0.938
		β_1	0.326	0.337 (0.112)	0.010	0.114	0.944
		γ_0	1.750	1.770 (0.087)	0.020	0.094	0.957
		γ_1	3.250	3.267 (0.322)	0.017	0.306	0.969
		γ_2	0.100	0.102 (0.060)	0.002	0.059	0.970
200 (50, 42, 53, 55)	High	β_0	-0.906	-0.908 (0.405)	-0.001	0.375	0.973
		β_1	0.501	0.504 (0.150)	0.003	0.139	0.975
		γ_0	3.250	3.299 (0.249)	0.049	0.262	0.955
		γ_1	5.500	5.507 (0.490)	0.007	0.478	0.948
		γ_2	0.200	0.200 (0.097)	0.000	0.098	0.951
	Low	β_0	0.078	0.058 (0.392)	-0.019	0.401	0.945
		β_1	0.326	0.336 (0.150)	0.009	0.156	0.953
		γ_0	3.250	3.293 (0.221)	0.043	0.222	0.947
		γ_1	5.500	5.528 (0.393)	0.028	0.382	0.953
		γ_2	0.200	0.206 (0.081)	0.006	0.079	0.965
400 (95, 102, 97, 106)	High	β_0	-0.906	-0.914 (0.290)	-0.007	0.288	0.945
		β_1	0.501	0.504 (0.108)	-0.003	0.110	0.943
		γ_0	3.250	3.287 (0.180)	0.037	0.173	0.961
		γ_1	5.500	5.511 (0.352)	0.011	0.365	0.957
		γ_2	0.200	0.203 (0.070)	0.003	0.072	0.951
	Low	β_0	0.078	0.075 (0.282)	-0.002	0.296	0.955
		β_1	0.326	0.335 (0.108)	0.008	0.111	0.957
		γ_0	3.250	3.278 (0.156)	0.028	0.160	0.953
		γ_1	5.500	5.479 (0.279)	-0.021	0.278	0.949
		γ_2	0.200	0.195 (0.058)	-0.004	0.057	0.965

Table 2.6: Estimates, bias, RMSE and CP for the Poisson cure rate model with light censoring.

n	p_0	Par	True	Est (s.e.)	Bias	RMSE	CP (95%)
200 (50, 42, 53, 55)	High	β_0	-0.906	-0.943 (0.432)	-0.036	0.427	0.956
		β_1	0.501	0.516 (0.163)	0.014	0.164	0.956
		γ_0	1.750	1.782 (0.142)	0.032	0.154	0.926
		γ_1	3.250	3.280 (0.685)	0.030	0.729	0.928
		γ_2	0.100	0.094 (0.127)	-0.005	0.142	0.934
	Low	β_0	0.078	0.092 (0.431)	0.013	0.443	0.966
		β_1	0.326	0.324 (0.163)	-0.002	0.170	0.949
		γ_0	1.750	1.788 (0.125)	0.038	0.135	0.945
		γ_1	3.250	3.308 (0.586)	0.058	0.634	0.922
		γ_2	0.100	0.103 (0.003)	0.003	0.123	0.934
400 (95, 102, 97, 106)	High	β_0	-0.923	-0.931 (0.303)	-0.016	0.288	0.934
		β_1	0.501	0.507 (0.113)	0.006	0.100	0.942
		γ_0	1.750	1.772 (0.099)	0.022	0.102	0.940
		γ_1	3.250	3.285 (0.482)	0.035	0.391	0.932
		γ_2	0.100	0.103 (0.089)	0.003	0.071	0.934
	Low	β_0	0.078	0.071 (0.298)	-0.007	0.314	0.953
		β_1	0.326	0.335 (0.117)	0.008	0.115	0.940
		γ_0	1.750	1.766 (0.088)	0.016	0.104	0.942
		γ_1	3.250	3.256 (0.404)	0.006	0.501	0.922
		γ_2	0.100	0.095 (0.080)	-0.004	0.094	0.928
200 (95, 102, 97, 106)	High	β_0	-0.906	-0.914 (0.411)	-0.007	0.431	0.938
		β_1	0.501	0.509 (0.153)	0.007	0.159	0.954
		γ_0	3.250	3.332 (0.256)	0.082	0.268	0.935
		γ_1	5.500	5.537 (0.560)	0.037	0.586	0.944
		γ_2	0.200	0.211 (0.117)	0.011	0.124	0.944
	Low	β_0	0.078	0.0411 (0.402)	-0.037	0.413	0.944
		β_1	0.326	0.347 (0.155)	0.020	0.166	0.946
		γ_0	3.250	3.299 (0.224)	0.049	0.223	0.963
		γ_1	5.500	5.499 (0.479)	-0.001	0.510	0.934
		γ_2	0.200	0.198 (0.105)	-0.002	0.112	0.932
400 (50, 42, 53, 55)	High	β_0	-0.906	-0.905 (0.295)	0.001	0.295	0.957
		β_1	0.501	0.505 (0.111)	0.004	0.115	0.933
		γ_0	3.250	3.282 (0.179)	0.032	0.179	0.959
		γ_1	5.500	5.497 (0.402)	-0.002	0.401	0.955
		γ_2	0.200	0.199 (0.084)	-0.001	0.088	0.941
	Low	β_0	0.078	0.075 (0.300)	-0.003	0.294	0.961
		β_1	0.326	0.329 (0.115)	0.003	0.114	0.971
		γ_0	3.250	3.265 (0.162)	0.015	0.164	0.947
		γ_1	5.500	5.504 (0.360)	0.004	0.367	0.941
		γ_2	0.200	0.198 (0.078)	-0.001	0.080	0.943

Table 2.7: Estimates, bias, RMSE and CP for the geometric cure rate model with light censoring.

n	p_0	Par	True	Est (s.e.)	Bias	RMSE	CP (95%)
200 (50, 42, 53, 55)	High	β_0	-0.906	-0.898 (0.439)	0.008	0.479	0.933
		β_1	0.501	0.505 (0.162)	0.003	0.178	0.922
		γ_0	1.750	1.805 (0.143)	0.055	0.156	0.947
		γ_1	3.250	3.405 (0.869)	0.155	0.979	0.939
		γ_2	0.100	0.111 (0.167)	0.011	0.184	0.933
	Low	β_0	0.078	0.089 (0.414)	0.011	0.446	0.947
		β_1	0.326	0.324 (0.161)	-0.002	0.176	0.928
		γ_0	1.750	1.800 (0.130)	0.050	0.142	0.930
		γ_1	3.250	3.332 (0.775)	0.082	0.877	0.907
		γ_2	0.100	0.103 (0.160)	0.003	0.181	0.920
400 (95, 102, 97, 106)	High	β_0	-0.906	-0.894 (0.306)	0.008	0.314	0.944
		β_1	0.501	0.498 (0.114)	-0.002	0.122	0.944
		γ_0	1.750	1.781 (0.103)	0.031	0.106	0.950
		γ_1	3.250	3.325 (0.592)	0.075	0.636	0.938
		γ_2	0.100	0.110 (0.117)	0.010	0.132	0.931
	Low	β_0	0.078	0.094 (0.299)	0.015	0.329	0.931
		β_1	0.326	0.319 (0.115)	-0.007	0.129	0.937
		γ_0	1.750	1.777 (0.092)	0.027	0.098	0.942
		γ_1	3.250	3.301 (0.557)	0.051	0.615	0.929
		γ_2	0.100	0.105 (0.115)	0.005	0.134	0.906
200 (50, 42, 53, 55)	High	β_0	-0.906	-0.924 (0.430)	-0.017	0.429	0.953
		β_1	0.501	0.513 (0.162)	0.011	0.163	0.955
		γ_0	3.250	3.326 (0.267)	0.076	0.269	0.949
		γ_1	5.500	5.580 (0.712)	0.080	0.735	0.939
		γ_2	0.200	0.217 (0.161)	0.017	0.171	0.936
	Low	β_0	0.078	0.048 (0.430)	-0.030	0.448	0.949
		β_1	0.326	0.337 (0.164)	0.010	0.177	0.945
		γ_0	3.250	3.323 (0.243)	0.073	0.262	0.943
		γ_1	5.500	5.478 (0.682)	-0.021	0.746	0.924
		γ_2	0.200	0.193 (0.159)	-0.006	0.180	0.914
400 (95, 102, 97, 106)	High	β_0	-0.906	-0.906 (0.302)	0.000	0.305	0.948
		β_1	0.501	0.503 (0.114)	0.002	0.113	0.955
		γ_0	3.250	3.285 (0.189)	0.035	0.183	0.967
		γ_1	5.500	5.482 (0.494)	-0.017	0.503	0.942
		γ_2	0.200	0.192 (0.112)	-0.007	0.121	0.936
	Low	β_0	0.078	0.092 (0.299)	0.013	0.326	0.932
		β_1	0.326	0.320 (0.115)	-0.006	0.131	0.922
		γ_0	3.250	3.303 (0.171)	0.053	0.172	0.959
		γ_1	5.500	5.557 (0.479)	0.057	0.546	0.910
		γ_2	0.200	0.211 (0.111)	0.011	0.129	0.910

Table 2.8: Estimates, bias, RMSE and CP for the COM-Poisson cure rate model with $\phi = 0.5$ and light censoring.

n	p_0	Par	True	Est (s.e.)	Bias	RMSE	CP (95%)
200 (50, 42, 53, 55)	High	β_0	-0.906	-0.865 (0.443)	0.041	0.492	0.932
		β_1	0.501	0.502 (0.161)	0.001	0.184	0.906
		γ_0	1.750	1.893 (0.154)	0.143	0.231	0.859
		γ_1	3.250	3.436 (0.794)	0.186	0.824	0.953
		γ_2	0.100	0.070 (0.154)	-0.029	0.177	0.892
		ϕ	0.500	0.253 (-)	-0.246	0.578	-
	Low	β_0	0.078	0.174 (0.435)	0.095	0.479	0.943
		β_1	0.326	0.304 (0.164)	-0.022	0.186	0.943
		γ_0	1.750	1.903 (0.139)	0.153	0.231	0.765
		γ_1	3.250	3.441 (0.731)	0.191	0.780	0.943
		γ_2	0.100	0.059 (0.149)	-0.040	0.183	0.905
		ϕ	0.500	0.274 (-)	-0.225	0.603	-
400 (95, 102, 97, 106)	High	β_0	-0.906	-0.886 (0.309)	0.020	0.285	0.930
		β_1	0.501	0.494 (0.114)	-0.006	0.103	0.962
		γ_0	1.750	1.872 (0.108)	0.122	0.181	0.746
		γ_1	3.250	3.203 (0.518)	-0.046	0.584	0.905
		γ_2	0.100	0.037 (0.109)	-0.062	0.136	0.898
		ϕ	0.500	0.203 (-)	-0.296	0.548	-
	Low	β_0	0.078	0.083 (0.306)	0.004	0.329	0.933
		β_1	0.326	0.328 (0.117)	0.001	0.127	0.927
		γ_0	1.750	1.890 (0.098)	0.140	0.197	0.618
		γ_1	3.250	3.348 (0.503)	0.098	0.629	0.903
		γ_2	0.100	0.054 (0.107)	-0.045	0.131	0.909
		ϕ	0.500	0.295 (-)	-0.204	0.629	-
200 (50, 42, 53, 55)	High	β_0	-0.906	-0.928 (0.436)	-0.022	0.484	0.941
		β_1	0.501	0.521 (0.159)	0.020	0.180	0.922
		γ_0	3.250	3.423 (0.274)	0.173	0.364	0.896
		γ_1	5.500	5.469 (0.644)	-0.030	0.613	0.954
		γ_2	0.200	0.162 (0.144)	-0.037	0.159	0.935
		ϕ	0.500	0.427 (-)	-0.072	0.656	-
	Low	β_0	0.078	0.122 (0.427)	0.044	0.428	0.947
		β_1	0.326	0.311 (0.161)	-0.015	0.163	0.927
		γ_0	3.250	3.473 (0.252)	0.223	0.380	0.801
		γ_1	5.500	5.566 (0.602)	0.066	0.588	0.947
		γ_2	0.200	0.173 (0.141)	-0.026	0.143	0.960
		ϕ	0.500	0.412 (-)	-0.087	0.671	-
400 (95, 102, 97, 106)	High	β_0	-0.906	-0.894 (0.305)	0.012	0.322	0.931
		β_1	0.501	0.493 (0.112)	-0.007	0.116	0.931
		γ_0	3.250	3.415 (0.194)	0.165	0.308	0.788
		γ_1	5.500	5.514 (0.452)	0.014	0.481	0.925
		γ_2	0.200	0.173 (0.102)	-0.026	0.118	0.902
		ϕ	0.500	0.394 (-)	-0.105	0.637	-
	Low	β_0	0.078	0.127 (0.301)	0.049	0.281	0.976
		β_1	0.326	0.306 (0.114)	-0.020	0.108	0.953
		γ_0	3.250	3.482 (0.178)	0.232	0.344	0.619
		γ_1	5.500	5.603 (0.428)	0.103	0.487	0.919
		γ_2	0.200	0.177 (0.101)	-0.022	0.116	0.895
		ϕ	0.500	0.319 (-)	-0.180	0.634	-

Table 2.9: Estimates of cure rates, bias and RMSE for Geometric and Poisson cure rate models with heavy censoring and $\boldsymbol{\gamma} = (1.750, 3.500, 0.100)$.

n	p_0	True	Est	Bias	RMSE	95% CI
Geometric						
200 (50, 42, 53, 55)	p_{01}	0.400	0.410	0.010	0.124	(0.168, 0.652)
	p_{02}	0.324	0.327	0.002	0.073	(0.184, 0.470)
	p_{03}	0.257	0.255	-0.002	0.067	(0.124, 0.386)
	p_{04}	0.200	0.200	0.000	0.087	(0.029, 0.371)
	p_{01}	0.600	0.602	0.012	0.122	(0.364, 0.840)
	p_{02}	0.476	0.480	0.004	0.080	(0.323, 0.637)
	p_{03}	0.354	0.357	0.003	0.067	(0.226, 0.488)
	p_{04}	0.250	0.253	0.003	0.085	(0.087, 0.419)
400 (95, 102, 97, 106)	p_{01}	0.400	0.400	0.000	0.088	(0.228, 0.572)
	p_{02}	0.324	0.326	0.002	0.052	(0.224, 0.428)
	p_{03}	0.257	0.260	0.003	0.047	(0.168, 0.352)
	p_{04}	0.200	0.206	0.006	0.062	(0.085, 0.327)
	p_{01}	0.600	0.598	-0.002	0.090	(0.422, 0.774)
	p_{02}	0.476	0.475	-0.001	0.060	(0.357, 0.593)
	p_{03}	0.354	0.353	-0.001	0.051	(0.253, 0.453)
	p_{04}	0.250	0.249	-0.001	0.064	(0.124, 0.374)
Poisson						
200 (50, 42, 53, 55)	p_{01}	0.400	0.402	0.002	0.115	(0.177, 0.627)
	p_{02}	0.324	0.322	-0.002	0.068	(0.189, 0.455)
	p_{03}	0.257	0.252	-0.004	0.062	(0.131, 0.373)
	p_{04}	0.200	0.198	-0.001	0.080	(0.041, 0.355)
	p_{01}	0.600	0.587	-0.012	0.136	(0.321, 0.853)
	p_{02}	0.476	0.468	-0.007	0.090	(0.292, 0.644)
	p_{03}	0.354	0.350	-0.004	0.068	(0.217, 0.483)
	p_{04}	0.250	0.251	0.001	0.083	(0.088, 0.414)
400 (95, 102, 97, 106)	p_{01}	0.400	0.397	-0.003	0.082	(0.236, 0.558)
	p_{02}	0.324	0.321	-0.003	0.049	(0.225, 0.417)
	p_{03}	0.257	0.254	-0.003	0.044	(0.168, 0.340)
	p_{04}	0.200	0.199	-0.001	0.057	(0.087, 0.311)
	p_{01}	0.600	0.600	0.000	0.091	(0.422, 0.778)
	p_{02}	0.476	0.477	0.001	0.060	(0.359, 0.595)
	p_{03}	0.354	0.355	0.001	0.050	(0.257, 0.453)
	p_{04}	0.250	0.251	0.001	0.064	(0.126, 0.376)

Table 2.10: Estimates of cure rates, bias and RMSE for Bernoulli and COM-Poisson ($\phi = 0.5$) cure rate models with heavy censoring and $\boldsymbol{\gamma} = (1.750, 3.500, 0.100)$.

n	p_0	True	Est	Bias	RMSE	95% CI
Bernoulli						
200 (50, 42, 53, 55)	p_{01}	0.400	0.401	0.001	0.108	(0.189, 0.613)
	p_{02}	0.324	0.324	0.000	0.065	(0.197, 0.451)
	p_{03}	0.257	0.257	0.000	0.057	(0.145, 0.369)
	p_{04}	0.200	0.202	0.002	0.073	(0.059, 0.345)
	p_{01}	0.600	0.598	-0.001	0.117	(0.369, 0.827)
	p_{02}	0.476	0.475	-0.001	0.077	(0.324, 0.626)
	p_{03}	0.354	0.353	-0.001	0.065	(0.226, 0.480)
	p_{04}	0.250	0.250	0.000	0.081	(0.091, 0.409)
400 (95, 102, 97, 106)	p_{01}	0.400	0.399	-0.001	0.076	(0.250, 0.548)
	p_{02}	0.324	0.323	-0.001	0.045	(0.235, 0.411)
	p_{03}	0.257	0.257	0.000	0.040	(0.179, 0.335)
	p_{04}	0.200	0.201	0.001	0.052	(0.099, 0.303)
	p_{01}	0.600	0.602	0.002	0.086	(0.433, 0.771)
	p_{02}	0.476	0.478	0.002	0.056	(0.368, 0.588)
	p_{03}	0.354	0.355	0.001	0.050	(0.257, 0.453)
	p_{04}	0.250	0.250	0.000	0.058	(0.136, 0.364)
COM-Poisson ($\phi = 0.5$)						
200 (50, 42, 53, 55)	p_{01}	0.400	0.401	0.001	0.088	(0.229, 0.573)
	p_{02}	0.324	0.325	0.001	0.062	(0.203, 0.446)
	p_{03}	0.257	0.256	-0.001	0.059	(0.141, 0.371)
	p_{04}	0.200	0.198	-0.002	0.067	(0.067, 0.329)
	p_{01}	0.600	0.605	0.005	0.090	(0.429, 0.781)
	p_{02}	0.476	0.479	0.003	0.053	(0.375, 0.583)
	p_{03}	0.354	0.356	0.002	0.035	(0.287, 0.425)
	p_{04}	0.250	0.250	0.000	0.051	(0.149, 0.350)
400 (95, 102, 97, 106)	p_{01}	0.400	0.404	0.004	0.062	(0.283, 0.525)
	p_{02}	0.324	0.329	0.005	0.043	(0.246, 0.413)
	p_{03}	0.257	0.262	0.005	0.040	(0.183, 0.341)
	p_{04}	0.200	0.204	0.004	0.047	(0.112, 0.296)
	p_{01}	0.600	0.599	-0.001	0.083	(0.438, 0.761)
	p_{02}	0.476	0.480	0.004	0.087	(0.311, 0.650)
	p_{03}	0.354	0.363	0.009	0.093	(0.183, 0.544)
	p_{04}	0.250	0.261	0.011	0.094	(0.078, 0.443)

Table 2.11: Powers and observed levels (in bold) of LRT under different settings.

Fitted Model	True COM-Poisson Model				
	$\phi = 0$	$\phi = 0.5$	$\phi = 1$	$\phi = 2$	$\phi \to \infty$
Setting 1					
Geometric ($\phi = 0$)	**0.055**	0.080	0.164	0.140	0.510
Poisson ($\phi = 1$)	0.345	0.085	**0.202**	0.015	0.088
Bernoulli ($\phi \to \infty$)	0.745	0.365	0.452	0.210	**0.120**
Setting 2					
Geometric ($\phi = 0$)	**0.063**	0.075	0.130	0.235	0.418
Poisson ($\phi = 1$)	0.210	0.095	**0.106**	0.040	0.046
Bernoulli ($\phi \to \infty$)	0.597	0.555	0.378	0.265	**0.120**
Setting 3					
Geometric ($\phi = 0$)	**0.037**	0.110	0.164	0.255	0.670
Poisson ($\phi = 1$)	0.540	0.130	**0.122**	0.015	0.252
Bernoulli ($\phi \to \infty$)	0.830	0.385	0.520	0.225	**0.116**
Setting 4					
Geometric ($\phi = 0$)	**0.043**	0.120	0.158	0.270	0.542
Poisson ($\phi = 1$)	0.353	0.185	**0.062**	0.085	0.110
Bernoulli ($\phi \to \infty$)	0.740	0.520	0.470	0.345	**0.108**

Table 2.12: Selection rates based on Akaike's information criterion under different settings.

Fitted Model	True COM-Poisson Model				
	$\phi = 0$	$\phi = 0.5$	$\phi = 1$	$\phi = 2$	$\phi \to \infty$
Setting 1					
Geometric ($\phi = 0$)	0.685	0.372	0.290	0.176	0.049
Poisson ($\phi = 1$)	0.229	0.400	0.392	0.362	0.214
Bernoulli ($\phi \to \infty$)	0.086	0.228	0.318	0.462	0.737
Setting 2					
Geometric ($\phi = 0$)	0.674	0.470	0.304	0.225	0.085
Poisson ($\phi = 1$)	0.230	0.280	0.402	0.313	0.202
Bernoulli ($\phi \to \infty$)	0.096	0.250	0.294	0.462	0.713
Setting 3					
Geometric ($\phi = 0$)	0.732	0.386	0.219	0.131	0.017
Poisson ($\phi = 1$)	0.226	0.464	0.494	0.400	0.223
Bernoulli ($\phi \to \infty$)	0.042	0.150	0.287	0.469	0.760
Setting 4					
Geometric ($\phi = 0$)	0.670	0.398	0.270	0.168	0.056
Poisson ($\phi = 1$)	0.257	0.392	0.428	0.353	0.232
Bernoulli ($\phi \to \infty$)	0.073	0.210	0.302	0.479	0.712

Table 2.13: AIC, BIC and maximized log-likelihood (l) values for candidate COM-Poisson cure rate models.

COM-Poisson Model	AIC	BIC	$\hat{l}$
Geometric ($\phi = 0$)	**1028.677**	**1048.842**	**-509.3383**
$\phi = 0.5$	1032.468	1052.633	-511.2338
Poisson ($\phi = 0$)	1034.161	1054.326	-512.0803
$\phi = 2$	1036.043	1056.209	-513.0217
Bernoulli ($\phi = \infty$)	1038.948	1059.114	-514.4741

Table 2.14: Estimates, standard errors and 95% C.I. for the cure rates stratified by nodule category, for the geometric cure rate model.

Nod Cat (X)	$\hat{p_0}$	s.e.	95% C.I.
1	0.650	0.044	(0.562, 0.737)
2	0.540	0.031	(0.478, 0.602)
3	0.426	0.032	(0.363, 0.490)
4	0.320	0.045	(0.231, 0.409)

Chapter 3

Piecewise linear approximations of baseline under proportional hazard and COM-Poisson cure rate models

3.1 Introduction

Under the competing cause scenario as defined in Section 1.1, we assume that the common hazard function $h(w)$ of W_j follows a Cox proportional hazard structure, i.e.

$$h(w) = h(w, \boldsymbol{x}; \boldsymbol{\psi}, \boldsymbol{\gamma}) = h_0(w; \boldsymbol{\psi})e^{\boldsymbol{x}'\boldsymbol{\gamma}} \tag{3.1.1}$$

where $h_0(w; \boldsymbol{\psi})$ (baseline hazard function) is approximated by a piecewise linear function characterized by a parameter $\boldsymbol{\psi}$ and $\boldsymbol{x} = (x_1, \ldots, x_p)'$ is a vector of p covariates with corresponding regression coefficients $\boldsymbol{\gamma} = (\gamma_1, ..., \gamma_p)'$. Therefore, the idea is to create finite partitions $\tau_0, \tau_1, \ldots, \tau_N$ on the time axis and approximate the baseline hazard with N lines, one for each interval $[\tau_{l-1}, \tau_l]; l = 1, \ldots, N$. The number of competing causes M follows a COM-Poisson distribution; under this assumption, more flexibility in our model will be added since we can deal with under- and over-dispersed data (e.g. Rodrigues et al., 2009; Balakrishnan and Pal, 2014).

The form of the available data and the likelihood function are given in Section 3.2. In Section 3.3, the steps for the EM algorithm and the estimation of the asymptotic variance and covariance matrix of the MLEs using Louis' principle are provided. An extensive simulation study under various N (number of linear functions), censoring proportions, sample sizes and lifetime parameters is presented in Section 3.4. In Section 3.5, we study model discrimination using likelihood-based and information criteria based methods, for the model selection. In Section 3.6, for illustrative purpose, the proposed model is applied to a real life cutaneous melanoma data set.

3.2 Form of the data and the likelihood function

In survival analysis or reliability theory, the existence of right censored data is quite common due to the limitations imposed by the duration of the study. Therefore, assuming that our data are subject to non-informative right censoring, the censored group may include not only cured individuals but also susceptible who met the event of interest after censoring time. To be more specific, let us denote by C_i the censoring time and Y_i the actual lifetime for the i-th individual, for $i = 1, \dots, n$. Thus, the observed lifetime T_i is defined as

$$T_i = \min\{Y_i, C_i\}$$

while $\delta_i = I(Y_i \leq C_i)$ indicates whether the i-th individual is censored ($\delta_i = 0$) or not ($\delta_i = 1$), for $i = 1, \ldots, n$. Additionally, let us also define the sets Δ_1 and Δ_0, with $\Delta_1 = \{i : \delta_i = 1\}$ and $\Delta_0 = \{i : \delta_i = 0\}$. It is to be noted that $Z(\eta, \phi) = \frac{1}{p_0} = H^*_\phi(\eta)$ is only a function of η, given a specific value of ϕ and is monotone in η with $\lim_{\eta\to 0} H^*_\phi(\eta) = 1$ and $\lim_{\eta\to\infty} H^*_\phi(\eta) = \infty$. Hence, it would be appropriate to link the covariates $x_1, \ldots, x_p$ to the cured proportion using a logistic regression model i.e.

$$p_{0i} = p_0(\boldsymbol{\beta}, \boldsymbol{x}_i) = \frac{1}{1 + e^{\boldsymbol{\beta}'\boldsymbol{x}^*_i}},$$

where p_{0i} is the cured proportion for the i-th individual, $\boldsymbol{x}^*_i = (1, x_{i1}, \ldots, x_{ip})' = (1, \boldsymbol{x}'_i)'$ and $\boldsymbol{\beta} = (\beta_0, \ldots, \beta_p)'$ is the vector of the regression coefficients with $i = 1, \ldots, n$. Therefore, the observed data are of the form $(t_i, \delta_i, \boldsymbol{x}_i)$, for $i = 1, \ldots, n$ and the likelihood function can be expressed as

$$L(\boldsymbol{\theta}; \boldsymbol{t}, \boldsymbol{x}, \boldsymbol{\delta}) \propto \prod_{i=1}^{n} f_p(t_i, \boldsymbol{x}_i; \boldsymbol{\theta})^{\delta_i} S_p(t_i, \boldsymbol{x}_i; \boldsymbol{\theta})^{1-\delta_i} = \prod_{i\in\Delta_1} f_p(t_i, \boldsymbol{x}_i; \boldsymbol{\theta}) \prod_{i\in\Delta_0} S_p(t_i, \boldsymbol{x}_i; \boldsymbol{\theta}),$$

where $\boldsymbol{\theta} = (\phi, \boldsymbol{\beta}', \boldsymbol{\psi}', \boldsymbol{\gamma}')$, $\boldsymbol{t} = (t_1, \ldots, t_n)'$, $\boldsymbol{x} = (\boldsymbol{x}'_1, \ldots, \boldsymbol{x}'_n)'$ and $\boldsymbol{\delta} = (\delta_1, \ldots, \delta_n)'$. Moreover, we have

$$S_p(t_i, \boldsymbol{x}_i; \boldsymbol{\theta}) = \frac{1}{(1 + e^{\boldsymbol{\beta}'\boldsymbol{x}^*_i})} \sum_{j=0}^{\infty} \frac{\{H^{*-1}_\phi(1 + e^{\boldsymbol{\beta}'\boldsymbol{x}^*_i}) S(t_i; \boldsymbol{x}, \boldsymbol{\psi}, \boldsymbol{\gamma})\}^j}{(j!)^\phi}$$

$$f_p(t_i, \boldsymbol{x}_i; \boldsymbol{\theta}) = \frac{h_0(t_i; \boldsymbol{\psi}) e^{\boldsymbol{x}'_i\boldsymbol{\gamma}}}{(1 + e^{\boldsymbol{\beta}'\boldsymbol{x}^*_i})} \sum_{j=1}^{\infty} \frac{j\{H^{*-1}_\phi(1 + e^{\boldsymbol{\beta}'\boldsymbol{x}^*_i}) S(t_i; \boldsymbol{x}, \boldsymbol{\psi}, \boldsymbol{\gamma})\}^j}{(j!)^\phi} \tag{3.2.1}$$

where $h_0(t_i; \boldsymbol{\psi})$ given through the PLA and $S(t_i, \boldsymbol{x}; \boldsymbol{\psi}, \boldsymbol{\gamma})$ as defined in Section 1.5.2.

3.3 Estimation of parameters and standard errors

The estimation of the model parameters is carried out by using the EM algorithm along with a profile likelihood approach for parameter ϕ. The complete data are given by $\{(t_i, \boldsymbol{x}_i, \delta_i, I_i) : i = 1, \ldots, n\}$ where I_is are observed for $i \in \Delta_1$ and unobserved for $i \in \Delta_0$ (recall that: $I_i = 0$ if and only if the i-th individual is cured and $I_i = 1$, otherwise).

The complete data likelihood and log-likelihood functions are respectively given by

$$L_c(\boldsymbol{\theta}; \boldsymbol{t}, \boldsymbol{x}, \boldsymbol{\delta}, \boldsymbol{I}) \propto \prod_{i \in \Delta_1} f_p(t_i, \boldsymbol{x}_i; \boldsymbol{\theta}) \prod_{i \in \Delta_0} p_0(\boldsymbol{\beta}, \boldsymbol{x}_i)^{1-I_i} \{(1 - p_0(\boldsymbol{\beta}, \boldsymbol{x}_i)) S_u(t_i, \boldsymbol{x}_i; \boldsymbol{\theta})\}^{I_i}$$

and

$$\begin{aligned} l_c(\boldsymbol{\theta}; \boldsymbol{t}, \boldsymbol{x}, \boldsymbol{\delta}, \boldsymbol{I}) = \quad & \text{constant} + \sum_{i \in \Delta_1} \log f_p(t_i, \boldsymbol{x}_i; \boldsymbol{\theta}) + \sum_{i \in \Delta_0} (1 - I_i) \log p_0(\boldsymbol{\beta}, \boldsymbol{x}_i) \\ & + \sum_{i \in \Delta_0} I_i \log(1 - p_0(\boldsymbol{\beta}, \boldsymbol{x}_i)) + \sum_{i \in \Delta_0} I_i \log S_u(t_i, \boldsymbol{x}_i; \boldsymbol{\theta}), \end{aligned} \tag{3.3.1}$$

where $\boldsymbol{I} = (I_1, \ldots, I_n)'$, $f_p(t_i, \boldsymbol{x}_i; \boldsymbol{\theta})$ as in (3.2.1) and

$$S_u(t_i, \boldsymbol{x}_i; \boldsymbol{\theta}) = e^{-\boldsymbol{\beta}' \boldsymbol{x}_i^*} \sum_{j=1}^{\infty} \frac{\{H_\phi^{*-1}(1 + e^{\boldsymbol{\beta}' \boldsymbol{x}_i^*}) S(t_i; \boldsymbol{x}, \boldsymbol{\psi}, \boldsymbol{\gamma})\}^j}{(j!)^\phi}.$$

For a fixed ϕ and $i \in \Delta_0$, at the $(k+1)$-th iteration, we define

$$\pi_i^{(k+1)} = \mathbb{E}[I_i | \boldsymbol{O}, \boldsymbol{\theta}^{(k)}] = \frac{(1 - p_0(\boldsymbol{\beta}^{(k)}, \boldsymbol{x}_i)) S_u(t_i, \boldsymbol{x}_i; \boldsymbol{\theta}^{(k)})}{S_p(t_i, \boldsymbol{x}_i; \boldsymbol{\theta}^{(k)})},$$

where $\boldsymbol{\theta}^{(k)} = (\phi, \boldsymbol{\beta}'^{(k)}, \boldsymbol{\psi}'^{(k)}, \boldsymbol{\gamma}'^{(k)})$ is the parameter estimate at k-th iteration and $\boldsymbol{O} = \{I_i, \boldsymbol{t}, \boldsymbol{x}, \boldsymbol{\delta}\}$ are the observed data (note that, $\pi_i^{(k+1)} = \mathbb{E}[I_i|\boldsymbol{O}, \boldsymbol{\theta}^{(k)}] = 1$, for each uncensored item). The quantity $Q^{(k)} = Q(\boldsymbol{\theta}, \boldsymbol{\pi}^{(k)}) = \mathbb{E}[l_c(\boldsymbol{\theta}; \boldsymbol{t}, \boldsymbol{x}, \boldsymbol{\delta}, \boldsymbol{I})|\boldsymbol{O}, \boldsymbol{\theta}^{(k)}]$ is then maximized to obtain the next estimate as

$$\boldsymbol{\theta}^{(k+1)} = \arg\max_{\theta \in \boldsymbol{\Theta}} Q(\boldsymbol{\theta}, \boldsymbol{\pi}^{(k)})$$

considering $\boldsymbol{\Theta}$ to be the parametric space with fixed ϕ and $\boldsymbol{\pi}^{(k)} = (\pi_1^{(k)}, \ldots, \pi_n^{(k)})'$. The numerical maximization is carried out using the Nelder-Mead algorithms. The explicit expressions for $Q(\boldsymbol{\theta}, \boldsymbol{\pi}^{(k)})$ and the first-order and second-order partial derivatives of $Q(\boldsymbol{\theta}, \boldsymbol{\pi}^{(k)})$ are given in Appendix B.1 and B.2, respectively. We consider a specific range of values for ϕ with fixed increment; for each choice of ϕ, we find the MLEs for $(\boldsymbol{\beta}', \boldsymbol{\psi}, \boldsymbol{\gamma}')'$ and our final estimation (i.e. $\hat{\phi}$) is given by the choice of ϕ which yields the maximum log-likelihood. The range of ϕ considered for this profile likelihood method is $\{0.0, 0.1, \ldots, 2.0\} \cup \{\infty\}$.

For finding the standard error of the parameter estimates, we apply Louis' principle, that is,

$$\begin{aligned} I(\boldsymbol{\theta}) = \quad & \mathbb{E}[B(\boldsymbol{\theta}; \boldsymbol{t}, \boldsymbol{x}, \boldsymbol{\delta}, \boldsymbol{I})] - \mathbb{E}[S(\boldsymbol{\theta}; \boldsymbol{t}, \boldsymbol{x}, \boldsymbol{\delta}, \boldsymbol{I}) S^T(\boldsymbol{\theta}; \boldsymbol{t}, \boldsymbol{x}, \boldsymbol{\delta}, \boldsymbol{I})] \\ & + S^*(\boldsymbol{\theta}; \boldsymbol{t}, \boldsymbol{x}, \boldsymbol{\delta}) S^{*T}(\boldsymbol{\theta}; \boldsymbol{t}, \boldsymbol{x}, \boldsymbol{\delta}) \end{aligned} \tag{3.3.2}$$

where $I(\boldsymbol{\theta})$ is the information on $\boldsymbol{\theta}$, $B(\boldsymbol{\theta}; \boldsymbol{t}, \boldsymbol{x}, \boldsymbol{\delta}, \boldsymbol{I})$ and $S(\boldsymbol{\theta}; \boldsymbol{t}, \boldsymbol{x}, \boldsymbol{\delta}, \boldsymbol{I})$ denotes the negative of the matrix of second derivatives and the gradient vector of $l_c(\boldsymbol{\theta}; \boldsymbol{t}, \boldsymbol{x}, \boldsymbol{\delta}, \boldsymbol{I})$ respectively, and $S^*(\boldsymbol{\theta}; \boldsymbol{t}, \boldsymbol{x}, \boldsymbol{\delta}, \boldsymbol{I})$ is the expected gradient vector of $l_c(\boldsymbol{\theta}; \boldsymbol{t}, \boldsymbol{x}, \boldsymbol{\delta}, \boldsymbol{I})$. Relying on the asymptotic normality of the MLEs, 95% confidence intervals (C.I.) of the parameters can be easily calculated. Asymptotic normality of the MLEs can also be used to estimate the standard error of the cure rates applying multivariate delta method since $p_0 = g(\boldsymbol{\beta})$ with $g(.)$ being a continuous function with $g : \mathbb{R}^{(p+1)} \to \mathbb{R}$. The form of the first-order and second-order derivatives of the complete data log-likelihood are given in Appendix B.2.

3.4 Simulation study

A detailed Monte Carlo simulation study was carried out to assess the performance of the proposed cure rate model and inferential method. Motivated by the real-life dataset on cutaneous melanoma data (Section 3.6), we considered a single covariate x with four possible values (categories/groups), i.e., $x = 1, 2, 3, 4$. To analyse the effect of censoring on the estimation, we introduced two sets of cure rates for $x = 1$ and $x = 4$ namely $(0.600, 0.250)$ and $(0.400, 0.150)$. It may be noted that by fixing the cure rates of the first and the fourth group, we can easily determine the cure rates for $x = 2$ and $x = 3$ using the solutions of the system

$$\frac{1}{1 + e^{\beta_0+\beta_1}} = 0.600, \frac{1}{1 + e^{\beta_0+3\beta_1}} = 0.250.$$

Thus, we obtained the pre-specified cure rates for four groups to be $(0.600, 0.470, 0.350, 0.250)$ and $(0.400, 0.290, 0.210, 0.150)$, respectively. We further assume that the probability a susceptible to be censored is 0.10 greater than the cured rate of each group. Therefore the censoring proportions become $(0.700, 0.570, 0.450, 0.350)$ and $(0.500, 0.390, 0.310, 0.250)$ to reflect the "heavy" and "light" censoring scenarios. Thus, the corresponding true values of (β_0, β_1) are respectively $(-0.907, 0.501)$ and $(-0.038, 0.443)$. The lifetime distribution for W_j was assumed to be Weibull with hazard function $\frac{\gamma_0}{\gamma_1}\left(\frac{w}{\gamma_1}\right)^{\gamma_0-1} e^{\gamma x}$, where γ_0 and γ_1 are the shape and scale parameter respectively, of the baseline hazard function (which is also a Weibull), while γ is the regression parameter. To evaluate the accuracy of the estimates for different lifetime parameters, two choices of expected lifetime values were made for the baseline distribution, viz., 1.000 and 2.000 for "low" and "high" lifetime scenarios, respectively; a unit variance was assumed in both cases. Hence the respective true values of (γ_0, γ_1) were $(1.000, 1.000)$ and $(2.101, 2.258)$ with $\gamma = 0.200$. Furthermore, the effects of large and small sample sizes on the accuracy of our estimates were assessed by taking n, viz., $n = 600(150, 150, 150, 150)$ and $n = 400(100, 100, 100, 100)$, respectively. All the true values were selected in order to closely resemble the real-life dataset.

The censoring time was assumed to follow an exponential distribution with rate $\lambda_x, x = 1, 2, 3, 4$, while λ_x was determined by solving

$$P[Y \geq C_x \cap M \geq 1 | X = x] = c_x - p_{0x}$$

for the x-th group; c_x and p_{0x} denote the pre-specified censoring and cured proportion respectively. Proceeding mathematically, with $C_x \sim$ exponential(λ_x), λ_x were obtained by solving,

$$\lambda_x \int_0^\infty \exp\left[-\left(\frac{c_x}{\gamma_1}\right)^{\gamma_0} e^{\gamma x} + \lambda_x c_x\right] dc_x - \frac{H_\phi^{*-1}(c_x/p_{0x})}{H_\phi^{*-1}(1/p_{0x})} = 0.$$

Let us now clarify the basics steps followed for generating our data. For the Bernoulli cure rate model ($\phi \to \infty$), M was generated from a Bernoulli distribution with success $(I = 0)$ probability p_{0x}. If $M = 0$, then C (censoring time variable) was generated from an exponential with rate λ_x, and we set $T = C$ and $\delta = 0$. Otherwise, if $M = 1$, then Y was generated from a Weibull distribution with shape γ_0 and scale $\gamma_1 e^{-\frac{\gamma x}{\gamma_0}}$ and $T = \min\{Y, C\}$ (C is also generated by an exponential distribution with parameter λ_x), with $\delta = 1$ for $T = Y$, whereas $\delta = 0$ for $T = C$. For the Poisson cure rate model, we generated M from a Poisson distribution ($\phi = 1$) with mean $\eta_x = -\log p_{0x}$. The procedure remained the same for $M = 0$, as in the Bernoulli case. However, for $M = m$, where $m \geq 1$, we generated $W_1, W_2, ..., W_m$ lifetimes from a Weibull distribution with shape and scale as discussed before, and we set $Y = \min\{W_1, W_2, ..., W_m\}$ and $T = \min\{Y, C\}$, with C being an exponential(λ_x) variable. Furthermore, we had $\delta = 0$ for $M = 0$ or $M \geq 1$, $T = C$ and $\delta = 1$, if $M \geq 1$ and $T = Y$. For the geometric cure rate model, we generated M from a geometric distribution with parameter $1 - p_{0x}$ and the rest of the procedure remained as above. This is also the case for every COM-Poisson cure rate model in which M was generated from a COM-Poisson distribution with parameter $\eta_x = H_\phi^{-1}(1 + e^{\beta_0 + \beta_1 x})$ for a fixed ϕ where η_x was found numerically for the choices of β_0 and β_1.

Due to heavy computational load, our numerical study was based on $r = 100$ replications (using R-software), for each of the five COM-Poisson models: $\phi = 0$ (geometric), $0.5, 1$ (Poisson), 2 and ∞ (Bernoulli). The cut points were taken to be the sample quantiles of the lifetimes of the uncensored data with $\tau_0 = \min\{Y_i\}$ and $\tau_N = \max\{Y_i\}$. An alternative choice could have been to select $\tau_N = \max\{T_i\}$, however, was often very far from τ_{N-1} resulting in high degree of bias and variability in the estimation. Henceforth, the line (i.e. $a_N + b_N t$) in $[\tau_{N-1}, \tau_N]$ is used to approximate the hazard function in $[\tau_{N-1}, \infty)$. A 15% variability on both sides of the real values were taken as the initial parameter guess for $(\beta_0, \beta_1, \gamma)$ and a 20% variability on both sides of the baseline Weibull hazard function, at the cut points as an initial estimate for $(\psi_0, \ldots, \psi_N)$. As mentioned before, the estimates were found using ML estimation with EM algorithm except that of ϕ, for which a profile likelihood approach was employed. In Table 3.1 to 3.20, we present the simulation results for all the settings. Results for the low lifetime cases are not provided for $\phi = 0.5$ and 2 due to space limitation. Estimated parameter values (Est) and cure rates, standard errors (s.e.), root mean squared errors (RMSE), coverage probabilities with 95% nominal level (95% C.P.) of the cure rates and root integrated squared errors (RISE) for the four groups are provided. RMSE for the parameter α is calculated as $\sqrt{(r-1)^{-1}\sum_{q=1}^{r}(\hat{\alpha}_q-\alpha)^2}$, where $\hat{\alpha}_q$ is the estimate for the q-th iteration, α is the true parameter value. RISE for the x-th covariate group is given by

$$RISE_x = \sqrt{\frac{1}{r-1}\sum_{q=1}^{r}\int_{\tau_0}^{\tau_N}[S_p(w,x;\hat{\boldsymbol{\theta}}_q) - S_p(w,x;\boldsymbol{\theta})]^2 dw},$$

for $x = 1, 2, 3, 4$ and $\hat{\boldsymbol{\theta}}_q$ is the estimate of $\boldsymbol{\theta}$ for q-th replication. Since we are estimating the baseline hazard function using piecewise linear functions, RISE provides a measure of deviance of the estimated long-term survival function and the true long-term survival function. RMSE of the lifetime parameters, in this case, could be vague to interpret and is often large for ψ_N.

The following observations were made from the simulation study. The estimates of the regression parameters (β_0, β_1), and hence, the cure rate over all settings were found to be quite precise (i.e. close to the true values). As a result, s.e. and RMSE of the estimates were relatively low given the complexity of the model. Bias of the estimates corresponding to the geometric cure rate model was observed to be larger than the other models. The RISE for all the scenarios were also quite small, thereby suggesting that the approximation of Weibull baseline hazard by PLA provides good fit. In both of high mean (i.e. $\gamma_0 = 2.101$, $\gamma_1 = 2.258$; increasing hazard function) and low mean (i.e. $\gamma_0 = 1.000$, $\gamma_1 = 1.000$; constant hazard function) lifetimes, the estimates of the hazards $\psi_0, \ldots, \psi_N$ were quite consistent with the true hazards, except, at τ_N. The estimates of ψ_N were observed to be highly affected by the distribution of the censoring time and were relatively far from τ_{N-1}, resulting in large standard deviation. In general, adding more lines (i.e., on increasing N) for approximating the baseline hazard seemed not to highly affect the precision of the estimates, although, there are some indications for a negative effect. For the high mean lifetime case, RISE were generally lowest for $N = 1$ reflecting that this model provided the best fit since the true hazard is almost linearly increasing. However, for the low mean lifetime case, RISE for $N = 1$ were mostly the highest (owing to the true constant hazard function). RISE did not seem to show any observable increasing or decreasing pattern with respect to N, otherwise. The Cox proportional hazard regression parameter (γ) was over-estimated in most of the settings, except when the true model is $\phi = 0.5$ or 2. The results corresponding to the low mean ($\gamma_0 = 1.000$, $\gamma_1 = 1.000$) cases are not provided in the thesis, however, can be retrieved from the author on request.

Tables 3.1 to 3.20 further revealed that decrease in the censoring proportion resulted in lower s.e. and RMSE of the estimates and higher RISE for the corresponding covariate groups. As a consequence, the coverage probabilities of the true cure rates also decreased. An observation of decreased s.e., RMSE of the estimates and 95% CP of the true cure rates were also made when the sample size was increased, while RISE also decreased, though slightly. It was also noted that s.e. and RMSE were comparatively less if data were generated from high mean lifetime Weibull distribution; however, no such effect was evident for 95% CP. The CPs for the cure rates were seen to be close to 95% nominal value when the true model were geometric, Poisson or Bernoulli. With light censoring and larger sample size, the CPs became more stable around the nominal level. But the true cure rates encountered a significant under-coverage (varying around 80%) when the true model was COM-Poisson with $\phi = 0.5$ or 2. This is because we have estimated ϕ using the profile likelihood method since the likelihood surface is very flat w.r.t ϕ, thereby, ignoring the component of variability of $\hat{\phi}$ in the variance-covariance matrix. This resulted in smaller standard error of the parameter estimates, hence, giving rise to the under-coverage. A relatively large bias was involved in the estimation of ϕ, which could arise due to presence of gaps in the search interval $[0, 2]$. The accuracy of the estimation of ϕ were seen to increase with N when the true model is $\phi = 2$, but decreases with N when the true model is $\phi = 0.5$. In all of the settings, the PLA models are compared to the correct parametric model with Weibull baseline hazard. In most of the cases, the performance of the two models were quite similar.

3.5 Model discrimination

We already have mentioned that a COM-Poisson distribution encompasses many well known discrete distributions. Thus, it is of practical interest to study how frequently a true model gets selected and others get rejected depending on some pre-specified criteria. This was carried out using two different criteria, viz., likelihood-based criterion and information-based criterion. We generated 100 samples where the true competing cause distributions were: geometric ($\phi = 0$), COM-Poisson with $\phi = 0.5$, Poisson ($\phi = 1$), COM-Poisson with $\phi = 2$ and Bernoulli ($\phi \to \infty$). The three special cases, i.e., geometric, Poisson and Bernoulli were fitted to the simulated data and the number of times each model was selected or rejected based on the criterion, was studied. The hazard function was considered to follow a proportional hazards model with baseline hazard function from a Weibull distribution with shape and scale γ_0 and γ_1 respectively. Four different settings were considered with $\gamma_0 = 2.101$, $\gamma_1 = 2.258$ and $\gamma = 0.200$, viz., Setting 1: n=400 and 'light' censoring (censoring proportions: 0.500, 0.390, 0.310, 0.250), Setting 2: n=400 and 'heavy' censoring (censoring proportions: 0.700, 0.570, 0.450, 0.350), Setting 3: n=600 and 'light' censoring, Setting 4: n=600 and 'heavy' censoring to this end, where γ is a regression parameter.

3.5.1 Likelihood-based method

Here using the likelihood ratio test (LRT), we tested for $H_0 : \phi = 0$ vs. $H_1 : \phi > 0$, $H_0 : \phi = 1$ vs. $H_1 : \phi \neq 1$ and $H_0 : \phi = \infty$ vs. $H_1 : \phi < \infty$, at 5% significance level. The number of times H_0 got rejected gave us the rejection rates of the candidate models. Let $\hat{l}_0$ and $\hat{l}$ be the maximized log-likelihood value under the null (H_0) and alternative (H_1) hypothesis, respectively. The asymptotic distribution of the test statistic $\Lambda = -2(\hat{l}_0 - \hat{l})$ (Wilk's LRT statistic), under the H_0 is known to follow a Chi-squared (χ^2) distribution with one degrees of freedom (d.f.). However, this does not provide a good approximation when we are dealing with cases when the values that are being tested are on the boundaries of the parametric space, e.g., the cases $\phi = 0$ and $\phi = \infty$. Hence, the asymptotic distribution of Λ considered, is a mixture χ^2 distribution i.e., $P(\Lambda \leq \lambda) = \frac{1}{2} + \frac{1}{2}P(\chi_1^2 \leq \lambda)$, where χ_1^2 is a random variable having χ^2-distribution with 1 d.f.

Table 3.21 provides us with model discrimination results based on LRT. The observed power and level of significance (given in bold) of the tests are presented in the table corresponding to four settings and $N = 1, \ldots, 5$. It can be noticed that the observed level of significance decreases, in case $\phi = 0$, as the number of lines (N) increases; no observable pattern was found for $\phi = \infty$. On an average, the observed level is high when the true model is geometric varying greatly between 0-62 %, however, the levels are between 0-20% for the Poisson and 0-33% for the Bernoulli case. This could be attributed to imprecise estimation of ϕ with profile likelihood method since it was noted that $\phi = 0.5$ were rejected less number of times than geometric when the true model was geometric. As one would expect, the observed level of significance were more pronounced when the sample size was small, censoring was heavy and N is less. For light censored data, the observed level changed drastically (0-33%) for the geometric, which was not very obvious for the other two cases. $N = 3$ provided observed levels close to the nominal level (5%) consistently. Rejection rates for the fitted geometric model gradually increased as true ϕ increased. The power on fitting Poisson gradually increased as the true ϕ moved far from 1. Similarly, power on fitting the Benoulli decreased with true ϕ. Power of the tests were seen to increase with lightly censored data and higher sample size. The number of lines used to approximate the baseline Weibull hazard seemed insignificant with respect to the power of the test. It was seen that setting 3 with $N = 5$ provided the most consistent results while setting 2 with $N = 1$ provided the least. A graphical representation to facilitate the understanding of the readers about the behavior of LRT across the true model and fitted model for all N is given in Figure 3.4.

3.5.2 Information-based method

The very well known Akaike's information criterion (AIC) and Bayesian information criterion (BIC) were incorporated to set the criteria of selection in order to discriminate among the candidate models. AIC is defined as $-2\hat{l}+2p$, where $\hat{l}$ is the unrestricted maximized log-likelihood value and p is the number of parameters and BIC is defined as $-2\hat{l}+p\log N_0$, where N_0 is the sample size. For each true ϕ, we fitted the three special cases of COM-Poisson and calculated the corresponding AIC and BIC values; the one with minimum AIC/BIC was selected. It is to be noted that AIC and BIC provided us with the same model since we always compared models with the same number of parameters.

Table 3.22 presents the selection rates of the candidate models when data were generated from different ϕ (i.e., 0, 0.5, 1, 2, ∞). Overall, the selection rate of the proper candidate models were quite reasonable, i.e., the probability of selecting the correct models were high and incorrect models were low in most of the cases. Chances of selecting the geometric cure rate model decreased while that of the Bernoulli increased when samples were generated from higher true ϕ values. The selection rates by fitting of a Poisson model, when the true model is indeed Poisson, were relatively low for every N and all settings, when compared to the respective rates of geometric or Bernoulli models. This could be accounted to the large bias in the estimation of ϕ which leads to select $\phi = 0.5$ or 2 when indeed the true model is Poisson. The selection rates of the true models were consistently high for $N = 1$, indicating, that a single linear approximation provided the best fit for the baseline hazard function (a finding consistent with our results in Section 3.4). Beyond this remark, the effect of fitting more lines seemed very little with no discernable patterns in the choice of the models. In general, Bernoulli provided the highest selection rates, which varied between 0.578 to 0.975. The selection rates of correct geometric model varied from 0.342 to 0.725, while that for the correct Poisson model from 0.200 to 0.694. For the other true models (viz., $\phi = 0.5$, 2), the probability of selecting the fitted candidate models were comparatively low. A decrease in the true censoring proportion affected the correct selection rates to be increased significantly in most of the scenarios. An increase in the sample size from 400 to 600 also resulted in a greater selection of the correct models. Thus, Setting 3 provided us with the best selection rates while Setting 2 provided the worst indicating similar trends as found for the results based on LRT. A graph representing the power study with respect to AIC/BIC can be found in Figure 3.5.

3.6 Analysis of cutaneous melanoma data

To further evaluate the performance and appropriateness of the proposed model, we considered a real-life data set on cancer recurrence. The data is part of a study by Eastern Cooperative Oncology Group (ECOG) on cutaneous melanoma (a type of malignant cancer) for the evaluation of postoperative treatment performance with a high dose of interferon alpha-2b as a drug to prevent recurrence as provided in Ibrahim et al. (2005). The study cohort contained 427 patients randomized into four nodule categories (1-4); nodule category is considered to be the only covariate in our analysis. 10 patients were excluded from our analysis due to missing information on tumor thickness. The sample sizes for the four nodule categories were 1:n_1= 111, 2:n_2= 137, 3:n_3= 87 and 4:n_4= 82, respectively. The patients were observed for the period 1991-1995 and were followed until 1998. The overall percentage of censored observations was 56%. As explained before, the observations were either the exact lifetimes (time till patient's death) or the censoring times, in years; the observed lifetimes had mean and standard deviation as 3.180 and 1.690, respectively. Thus, the available data contain: censoring time or exact lifetime (t), censoring indicator (δ) and covariate group (x) to which the individual belongs to.

An overestimated initial guess to the regression parameters β_0 (-1.215) and β_1 (0.482) were provided based on the observed censoring proportions 0.676 and 0.329 of groups with nodule category 1 and 4, respectively. Following the results from approximating the baseline hazard with a Weibull distribution in a proportional hazards lifetime and COM-Poisson cure rate set-up, we used an estimate of 0.072 for Cox regression coefficient γ. For the set of PLA parameters $(\psi_0, \ldots, \psi_N)$, we solved $N+1$ non-linear equations each of the form $S(t; \psi_0, \ldots, \psi_N, \gamma) = \exp\left[-H_0(t; \psi_0, \ldots, \psi_N)e^{\gamma x}\right]$ for $N+1$ time points from the data; $S(t; \psi_0, \ldots, \psi_N, \gamma)$ is approximated using Kaplan-Meier estimates. For $N = 5$, the initial baseline hazard estimates at the cut points (quantile-based) was $(\hat{\psi}_0, \hat{\psi}_1, \hat{\psi}_2, \hat{\psi}_3, \hat{\psi}_4, \hat{\psi}_5) = (0.010, 0.150, 0.250, 0.200, 0.030, 0.100)$. The choices of cut points on the time axis were considered in two different ways and their effects were compared on the estimates in case of this real-life data. The first set of cut points is quantile based i.e. suitable quantiles of the observed lifetimes were taken to be $\tau_0, \tau_1, ..., \tau_{N-1}$ whereas τ_N was taken as the maximum of both censoring and exact lifetimes so as to cover the whole time range. A second approach to choose the cut points based on the curvature of the baseline hazard function was also studied. In this case, a kernel-based hazard estimates were obtained by taking only the susceptible lifetimes (using `muhaz` function in R) and approximate hazard values at various time points were noted. The first- and second-order approximate numerical derivatives of these hazards were calculated at every time point. This is done by dividing the difference in hazards at two time points with difference in the time points, considering the time points to be close enough. These values are then checked for their nearness to zero; thus, implying approximate extremas. The same technique is carried out using the first derivative values derived numerically and points of inflections were obtained, thereby, indicating curvatures. Now, more suitable among those points were chosen as the cut points τ_1, ..., τ_{N-1} depending on N whereas τ_0 and τ_N were still the same as considered in the previous approach. The number of lines were set from $N = 1$ to $N = 5$, while the profile likelihood method was performed on the interval [0, 2] with increment 0.1.

For the quantile-based selection of cut points, the geometric cure rate model with $N = 5$ provided the maximum value of the log-likelihood function (-499.996) and minimum value of AIC (1017.992). The minimum value of BIC (1044.662) was obtained also for the geometric cure rate model with $N = 2$. For the curvature-based selection of cut points, maximum log-likelihood value was found to be -504.190 with $N = 5$, minimum AIC (1024.892) with $N = 2$ and minimum BIC with $N = 1$ all for the geometric cure rate model. Summing up together, it can be safely said that the geometric cure rate model with baseline hazard being approximated by five lines under proportional hazards assumption and quantile-based selection of cut points provided the best fit to the cutaneous melanoma data. The quantile based cut points consistently provided a better fit than the curvature, however, both show similar kind of trend with respect to the selection criteria. Also, AIC and BIC were observed to be steadily increasing with ϕ. The details are provided in Table 3.23.

The appropriateness of the geometric cure rate model over Poisson and Bernoulli was established further by testing for the hypotheses: $H_{0G} : \phi = 0$ vs $H_{1G} : \phi > 0$, $H_{0P} : \phi = 1$ vs $H_{1P} : \phi \neq 1$ and $H_{0B} : \phi = \infty$ vs $H_{1B} : \phi < \infty$ as described in Section 3.5. This resulted in the corresponding likelihood ratio test statistic values $\Lambda_G = -2(\hat{l}_{0G} - \hat{l}) = 0$, $\Lambda_P = -2(\hat{l}_{0P} - \hat{l}) = 3.538$ and $\Lambda_B = -2(\hat{l}_{0B} - \hat{l}) = 4.540$ with p-values being 0.500, 0.059 and 0.017 respectively for $N = 5$ (quantile-based); thereby rejecting both Bernoulli and Poisson cure rate model at 10% level of significance. The graph of Λ (i.e., $-2(\hat{l}_0 - \hat{l}_\phi)$) vs. ϕ is presented in Figure 3.1 taking $N = 5$ which is found to be steadily increasing with some noises. It should be noted that $\hat{l}_0$ is the value of log-likelihood function under H_0 when the log-likelihood is maximized with respect to other parameters for a fixed ϕ. The value of $\hat{l}_0$ changes according to the ϕ under H_0. On doing so, we actually kept the cut points to be fixed for estimating all $\hat{l}_0$. Thus, the maximization is not true in the sense that we need to choose the cut points according to the value of ϕ we are using. If one does so, we predict the noise to be much less in the plot. For the same model, i.e., PLA of the baseline hazard with $N = 5$, the test for $H_0 : \gamma = 0$ vs. $H_1 : \gamma \neq 0$ was also performed for the geometric, $\phi = 0.5$, Poisson, $\phi = 2$ and Bernoulli cure rates. The test statistic (i.e., $\Lambda = -2(\hat{l}_0 - \hat{l}) \sim \chi^2_1$ under H_0) values and the p-values were 1.338, 3.889, 4.882, 6.131, 10.679 and 0.247, 0.048, 0.027, 0.013, 0.001 respectively. This indicates that the homogeneity of individual lifetimes among the nodule categories were not rejected at 5% level if geometric provided the best fit to the data. A similar observation was made when the baseline hazard was considered from a parametric Weibull distribution under proportional hazard.

The estimate, standard error and 95% CI of the parameters and cure rates are presented in Table 3.24 for the geormetric cure rate model with piecewise linear approximation of the baseline hazard for $N = 1, \ldots, 5$. It was observed that the estimated cure rates decreased with N for both ways of selecting the cut points. The estimated cure rates were further lowered in case of the curvature-based selection of cut-points. The s.e. of the estimated cure rates were seen to be comparatively less for $N = 1$ in both cases. It can also be reported that for all choices of N, 95% CI for the cure rate estimates for $x = 1$ and $x = 4$ were mostly non-overlapping, thereby, signifying a marked distinction in the chances of getting cured between them.

Figure 3.1: The plot of Λ vs ϕ, for cutaneous melanoma data using PLA with $N = 5$.

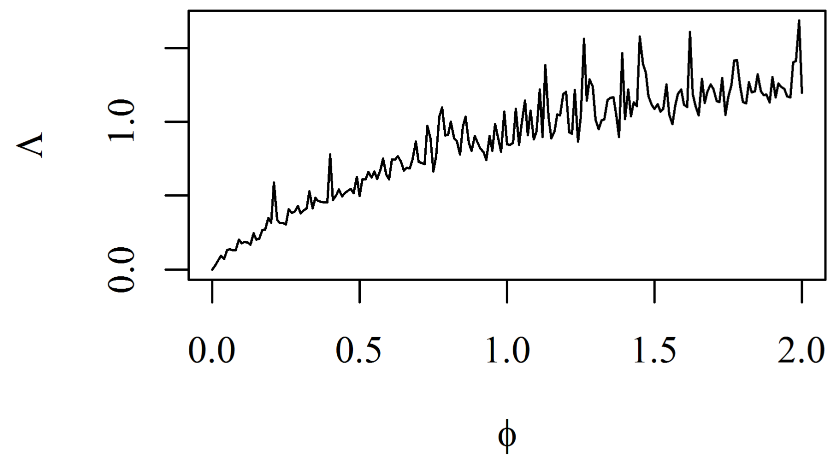

These results were quite similar to the results obtained by using Weibull baseline hazard in proportional hazard set-up. When the lifetime distribution of the non-cured individuals was assumed to be Weibull, the cure rate estimates were (0.664, 0.546, 0.422, 309) and when the lifetime distribution of Weibull was assumed along with the proportional hazards assumption, then the estimated cure rates were (0.650, 0.540, 0.426, 0.320) which are very close to the results obtained on taking $N = 1$. The s.e of the estimated hazards were found to be increasing as the value of the cut points increased. Apart from the above mentioned analysis, the cure probability given that an individual has not met the event of interest till t was also estimated for $x = 1, 2, 3, 4$ by

$$\hat{P}(I = 0|T > t) = \left(1 + \exp\left[\hat{\beta}_0 + \hat{\beta}_1 x - H_0(t; \psi_0, \psi_1, ..., \psi_N)e^{\gamma x}\right]\right)^{-1}$$

Figure 3.2: The probability to be cured (solid line), given that an individual has survived up to a specific time t and their 95% CI (dotted line).

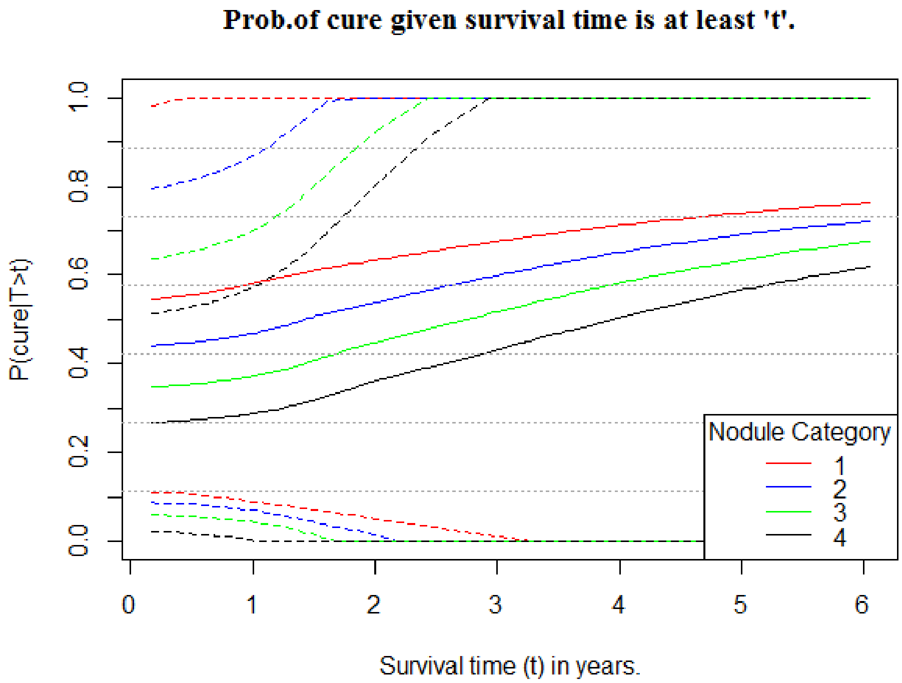

and presented along with 95% CI in Figure 3.2 using PLA with $N = 5$. So, an individual has 60% chance of getting cured provided he/she survives up to 1.430, 3.010, 4.180 and 5.350 years, if he/she belongs to nodule category $1, 2, 3$ and 4 respectively. Similar to the parametric inference, the four nodule categories was observed to be asymptotically converging with increasing trends.

The model was also tested on the same dataset with a different set of covariates, namely, treatment group (OBS:0, INF:1), gender (male:0, female:1) and age which is a continuous variable. The average age of the study cohort is 47.892 years years while 62% was male and 50% belonged to the OBS group. Table 3.25 includes parameter estimates while the cut-points were chosen to be suitable quantiles of τ_i. It was observed that geometric cure rate model provided the best fits for $N = 1, 2, 3$, Poisson cure rate model for $N = 4$ whereas Bernoulli cure rate model for $N = 5$ in terms of AIC and BIC (see Table 3.26). Approximating the baseline hazard with two lines ($N = 2$) was found to have least AIC or BIC for all candidate models. For $N = 2$, on testing $H_0 : \phi = 0$, the LRT statistic $\Lambda \approx 0$ with p-value 0.5. On verifying whether a Poisson or Bernoulli cure rate models are suitable for the data, Λ was found to be 0.090 and 0.958, resulting in p-values as 0.764 and 0.164, respectively. Thus, none of the candidate cure rate models were found to be unsuitable for the data using three covariates at 10% level of significance. The mean (median) estimated cure rate for females receiving OBS is the highest e.g. 0.657 (0.658), for males with OBS is 0.571 (0.573), for females with INF is 0.561 (0.574) and for males receiving INF is 0.474 (0.478). The overall estimated cured probability combining all individuals has mean equal to 0.554 (s.e.= 0.084), while the median is 0.554. The graph of estimated cure rates versus age for all the four categories is presented in Figure 3.3. It can also observed from Table 3.26 that the maximum value of the log-likelihood function was obtained on using $N = 4$ for the Poisson cure rate model, implying that this model could also be effective for fitting of the data.

Figure 3.3: The graph presents estimated cure rates ($\hat{p}_0$) by age for four categories: Female+OBS, Male+OBS, Female+INF and Male+INF.

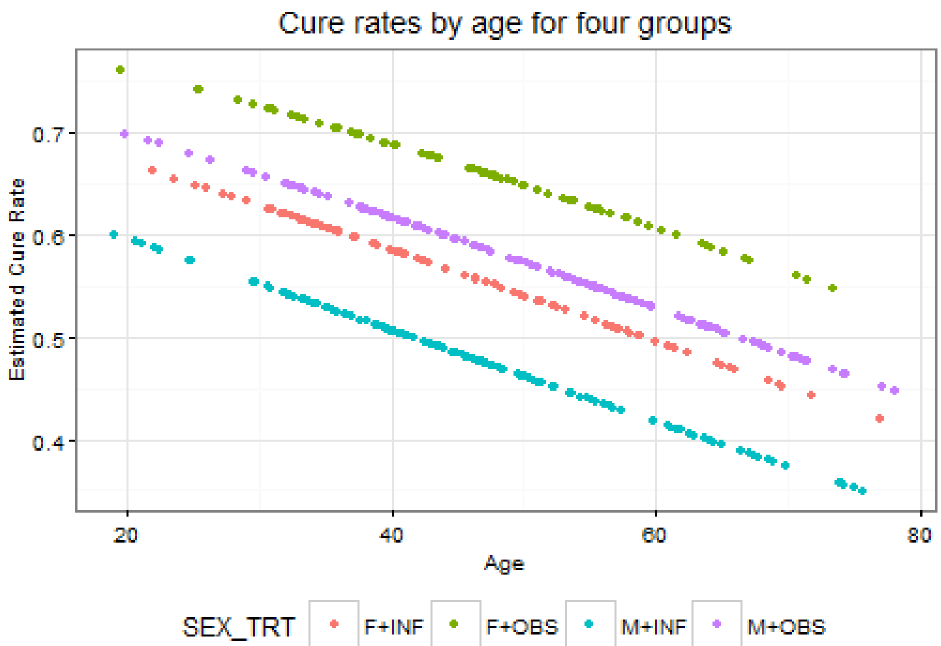

[0]N:W represents the case of baseline Weibull hazard model.

Figure 3.4: A power study based on LRT corresponding to table 3.21.

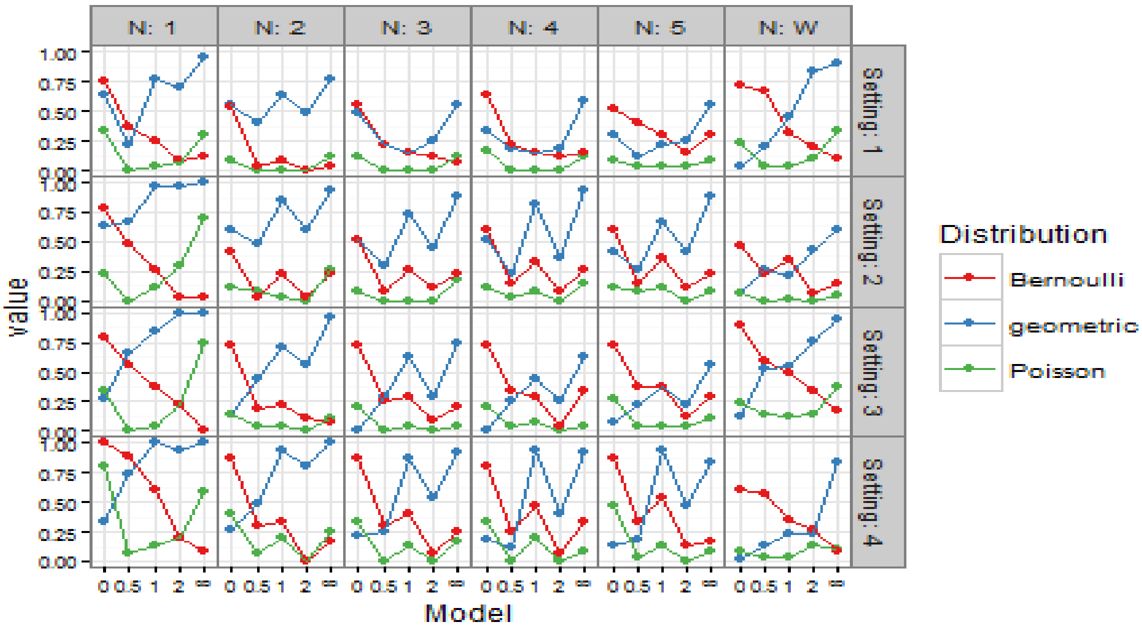

Figure 3.5: A power study based on AIC corresponding to table 3.22.

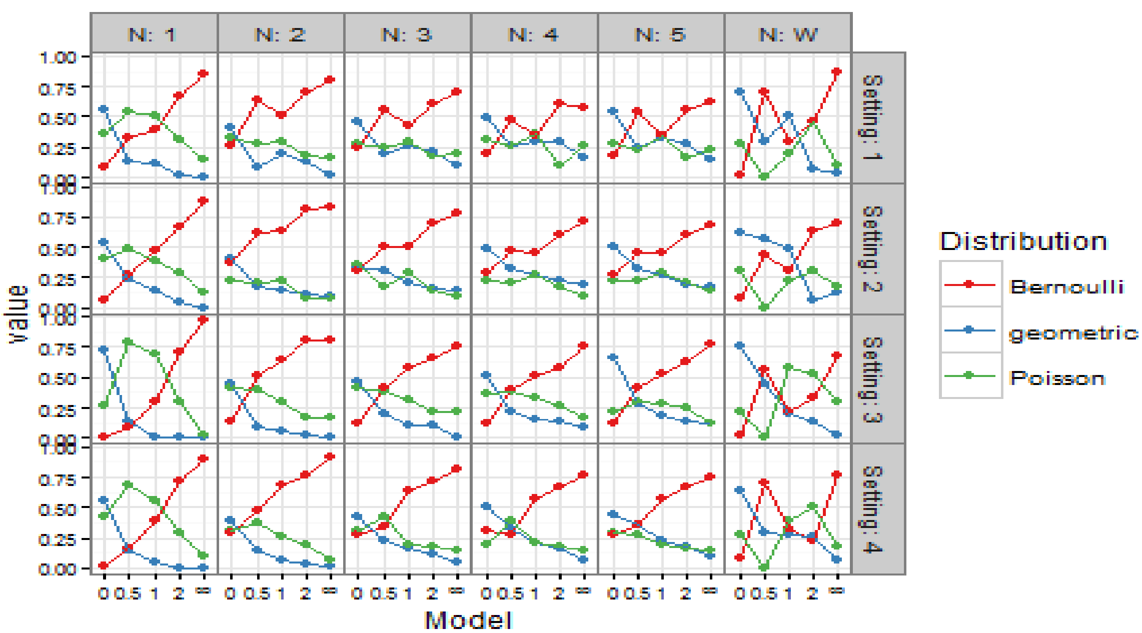

Table 3.1: Simulation results for geometric cure rate model having high lifetime $(\gamma_0 = 2.101, \gamma_1 = 2.258)$ with heavy censoring for small sample size.

Measure						$(\tau_i, \hat{\psi}_i)$					
	N	$(\hat{\beta}_0, \hat{\beta}_1, \hat{\gamma})$	$\hat{p}_0$	$\hat{l}$	AIC	$i=0$	$i=1$	$i=2$	$i=3$	$i=4$	$i=5$
$n = 400$ (100, 100, 100, 100)		(-0.907, 0.501, 0.200)	(0.600, 0.470, 0.350, 0.250)								
Est	1	(-0.792, 0.477, 0.375)	(0.577, 0.460, 0.346, 0.249)	-350.441	710.884	(0.066, 0.090)	(3.520, 1.223)				
	2	(-0.689, 0.451, 0.376)	(0.560, 0.448, 0.341, 0.249)	-349.913	709.828	(0.066, 0.061)	(0.881, 0.415)	(3.520, 0.705)			
	3	(-0.706, 0.456, 0.371)	(0.561, 0.449, 0.341, 0.249)	-349.634	709.270	(0.066, 0.059)	(0.529, 0.277)	(0.881, 0.411)	(3.520, 0.747)		
	4	(-0.720, 0.461, 0.367)	(0.561, 0.449, 0.341, 0.248)	-349.061	708.120	(0.066, 0.064)	(0.321, 0.175)	(0.529, 0.292)	(0.881, 0.414)	(3.520, 0.766)	
	5	(-0.737, 0.466, 0.362)	(0.565, 0.450, 0.340, 0.247)	-348.957	707.916	(0.066, 0.064)	(0.321, 0.183)	(0.737, 0.376)	(0.881, 0.399)	(1.365, 0.524)	(3.520, 0.654)
	*	(-1.068, 0.557, 0.229)	(0.624, 0.488, 0.354, 0.240)	-353.017	716.034			(2.060, 2.216)			
s.e.	1	(0.355, 0.132, 0.091)	(0.058, 0.038, 0.035, 0.045)			(0.035, 0.041)	(0.481, 0.355)				
	2	(0.498, 0.160, 0.114)	(0.084, 0.055, 0.041, 0.047)			(0.035, 0.038)	(0.058, 0.152)	(0.481, 0.548)			
	3	(0.478, 0.157, 0.113)	(0.081, 0.054, 0.040, 0.047)			(0.035, 0.038)	(0.039, 0.111)	(0.058, 0.149)	(0.481, 0.545)		
	4	(0.487, 0.160, 0.115)	(0.082, 0.054, 0.040, 0.047)			(0.035, 0.045)	(0.035, 0.080)	(0.039, 0.124)	(0.058, 0.152)	(0.481, 0.563)	
	5	(0.532, 0.170, 0.129)	(0.089, 0.060, 0.043, 0.047)			(0.035, 0.048)	(0.035, 0.087)	(0.053, 0.173)	(0.058, 0.195)	(0.078, 0.238)	(0.481, 0.725)
	*	(0.311, 0.118, 0.111)	(0.624, 0.488, 0.354, 0.240)					(0.124, 0.330)			
RMSE	1	(0.349, 0.124, 0.201)	(0.062, 0.039, 0.035, 0.045)								
	2	(0.438, 0.147, 0.202)	(0.093, 0.059, 0.042, 0.047)								
	3	(0.424, 0.142, 0.198)	(0.090, 0.058, 0.041, 0.047)								
	4	(0.407, 0.138, 0.193)	(0.091, 0.058, 0.041, 0.047)								
	5	(0.389, 0.133, 0.188)	(0.096, 0.063, 0.044, 0.047)								
	*	(0.335, 0.120, 0.154)	(0.055, 0.037, 0.035, 0.043)								
95% C.P.	1		(0.980, 0.970, 0.980, 0.990)								
	2		(0.980, 0.980, 0.990, 0.980)								
	3		(0.970, 0.970, 0.980, 0.970)								
	4		(0.970, 0.970, 0.980, 0.970)								
	5		(0.950, 0.940, 0.950, 0.950)								
	*		(0.898, 0.933, 0.945, 0.923)								
			(Gr-1, Gr-2, Gr-3, Gr-4)								
RISE	1		(0.090, 0.123, 0.182, 0.251)								
	2		(0.092, 0.127, 0.187, 0.256)								
	3		(0.093, 0.128, 0.188, 0.257)								
	4		(0.095, 0.129, 0.189, 0.258)								
	5		(0.095, 0.130, 0.189, 0.256)								
	*		(0.076, 0.082, 0.077, 0.075)								

Table 3.2: Simulation results for geometric cure rate model having high lifetime $(\gamma_0 = 2.101, \gamma_1 = 2.258)$ with heavy censoring for large sample size.

Measure						$(\tau_i, \hat{\psi}_i)$					
	N	$(\hat{\beta}_0, \hat{\beta}_1, \hat{\gamma})$	$\hat{p}_0$	$\hat{l}$	AIC	$i=0$	$i=1$	$i=2$	$i=3$	$i=4$	$i=5$
$n = 600$ (150, 150, 150, 150)		(-0.907, 0.501, 0.200)	(0.600, 0.470, 0.350, 0.250)								
Est	1	(-0.706, 0.456, 0.371)	(0.583, 0.464, 0.349, 0.250)	-475.297	960.594	(0.049, 0.067)	(3.680, 1.323)				
	2	(-0.821, 0.482, 0.384)	(0.571, 0.456, 0.345, 0.250)	-473.596	957.194	(0.049, 0.046)	(0.887, 0.418)	(3.680, 0.789)			
	3	(-0.760, 0.468, 0.373)	(0.572, 0.456, 0.345, 0.249)	-472.709	955.418	(0.049, 0.044)	(0.537, 0.273)	(0.887, 0.417)	(3.680, 0.816)		
	4	(-0.765, 0.469, 0.372)	(0.573, 0.457, 0.345, 0.249)	-472.019	954.038	(0.049, 0.048)	(0.319, 0.165)	(0.537, 0.284)	(0.887, 0.416)	(3.680, 0.831)	
	5	(-0.769, 0.471, 0.369)	(0.574, 0.457, 0.345, 0.249)	-470.816	951.632	(0.049, 0.047)	(0.319, 0.170)	(0.737, 0.371)	(0.887, 0.403)	(1.356, 0.520)	(3.680, 0.762)
	*	(-1.048, 0.559, 0.215)	(0.619, 0.482, 0.348, 0.235)	-480.043	970.086			(2.072, 2.210)			
s.e.	1	(0.279, 0.104, 0.072)	(0.046, 0.003, 0.028, 0.036)			(0.021, 0.028)	(0.443, 0.295)				
	2	(0.335, 0.116, 0.082)	(0.057, 0.037, 0.030, 0.037)			(0.021, 0.025)	(0.047, 0.107)	(0.443, 0.395)			
	3	(0.334, 0.116, 0.082)	(0.056, 0.037, 0.030, 0.037)			(0.021, 0.026)	(0.038, 0.080)	(0.047, 0.109)	(0.443, 0.428)		
	4	(0.332, 0.116, 0.083)	(0.056, 0.037, 0.030, 0.037)			(0.021, 0.030)	(0.029, 0.056)	(0.038, 0.089)	(0.047, 0.110)	(0.443, 0.431)	
	5	(0.384, 0.127, 0.094)	(0.065, 0.043, 0.032, 0.037)			(0.021, 0.031)	(0.029, 0.062)	(0.042, 0.124)	(0.047, 0.147)	(0.061, 0.165)	(0.443, 0.692)
	*	(0.280, 0.105, 0.101)	(0.044, 0.031, 0.029, 0.035)					(0.103, 0.293)			
RMSE	1	(0.259, 0.099, 0.196)	(0.049, 0.031, 0.028, 0.036)								
	2	(0.304, 0.111, 0.190)	(0.064, 0.040, 0.030, 0.037)								
	3	(0.296, 0.109, 0.187)	(0.063, 0.040, 0.039, 0.037)								
	4	(0.284, 0.104, 0.185)	(0.062, 0.039, 0.030, 0.037)								
	5	(0.293, 0.107, 0.183)	(0.070, 0.045, 0.032, 0.037)								
	*	(0.250, 0.106, 0.114)	(0.048, 0.032, 0.030, 0.038)								
95% C.P.	1		(0.990, 0.990, 0.980, 0.970)								
	2		(0.990, 0.980, 0.980, 0.970)								
	3		(0.990, 0.990, 0.990, 0.980)								
	4		(0.990, 0.980, 0.990, 0.960)								
	5		(0.990, 0.970, 0.970, 0.950)								
	*		(0.930, 0.950, 0.970, 0.980)								
			(Gr-1, Gr-2, Gr-3, Gr-4)								
RISE	1		(0.076, 0.117, 0.182, 0.254)								
	2		(0.079, 0.121, 0.187, 0.260)								
	3		(0.079, 0.121, 0.188, 0.259)								
	4		(0.079, 0.122, 0.188, 0.260)								
	5		(0.080, 0.123, 0.188, 0.259)								
	*		(0.083, 0.085, 0.087, 0.089)								

Table 3.3: Simulation results for geometric cure rate model having high lifetime ($\gamma_0 = 2.101, \gamma_1 = 2.258$) with light censoring for small sample size.

Measure						$(\tau_i, \hat{\psi}_i)$					
	N	$(\hat{\beta}_0, \hat{\beta}_1, \hat{\gamma})$	$\hat{p}_0$	$\hat{l}$	AIC	$i=0$	$i=1$	$i=2$	$i=3$	$i=4$	$i=5$
$n = 400$ (100, 100, 100, 100)		(-0.038, 0.443, 0.200)	(0.400, 0.290, 0.210, 0.150)								
Est	1	(0.008, 0.444, 0.392)	(0.390, 0.291, 0.209, 0.148)	-315.586	641.174	(0.049, 0.129)	(3.566, 1.483)				
	2	(0.259, 0.376, 0.404)	(0.346, 0.267, 0.202, 0.152)	-314.956	639.914	(0.049, 0.070)	(0.738, 0.473)	(3.566, 0.588)			
	3	(0.219, 0.389, 0.397)	(0.353, 0.270, 0.203, 0.150)	-314.159	638.318	(0.049, 0.062)	(0.437, 0.327)	(0.738, 0.460)	(3.566, 0.672)		
	4	(0.205, 0.395, 0.393)	(0.354, 0.270, 0.202, 0.149)	-313.167	636.336	(0.049, 0.067)	(0.258, 0.205)	(0.437, 0.336)	(0.738, 0.465)	(3.566, 0.692)	
	5	(0.201, 0.396, 0.395)	(0.357, 0.272, 0.202, 0.148)	-313.329	636.658	(0.049, 0.065)	(0.258, 0.208)	(0.610, 0.421)	(0.738, 0.426)	(1.179, 0.545)	(3.566, 0.515)
	*	(-0.829, 0.503, 0.231)	(0.583, 0.457, 0.335, 0.234)	-318.347	646.696			(0.962, 1.048)			
s.e.	1	(0.366, 0.149, 0.076)	(0.057, 0.033, 0.032, 0.038)			(0.026, 0.047)	(0.518, 0.344)				
	2	(0.660, 0.207, 0.102)	(0.095, 0.056, 0.038, 0.041)			(0.026, 0.039)	(0.042, 0.149)	(0.518, 0.532)			
	3	(0.635, 0.204, 0.102)	(0.092, 0.054, 0.038, 0.041)			(0.026, 0.038)	(0.032, 0.118)	(0.042, 0.144)	(0.518, 0.567)		
	4	(0.625, 0.204, 0.100)	(0.089, 0.052, 0.037, 0.041)			(0.026, 0.046)	(0.026, 0.080)	(0.032, 0.124)	(0.042, 0.141)	(0.518, 0.533)	
	5	(0.676, 0.216, 0.109)	(0.109, 0.063, 0.041, 0.042)			(0.026, 0.044)	(0.026, 0.086)	(0.035, 0.161)	(0.042, 0.173)	(0.067, 0.207)	(0.518, 0.701)
	*	(0.37, 0.142, 0.152)	(0.583, 0.457, 0.335, 0.234)					(0.063, 0.494)			
RMSE	1	(0.300, 0.132, 0.214)	(0.218, 0.182, 0.145, 0.109)								
	2	(0.438, 0.158, 0.222)	(0.271, 0.211, 0.153, 0.106)								
	3	(0.398, 0.148, 0.215)	(0.264, 0.207, 0.152, 0.108)								
	4	(0.395, 0.146, 0.212)	(0.262, 0.207, 0.153, 0.109)								
	5	(0.371, 0.139, 0.211)	(0.266, 0.208, 0.154, 0.110)								
	*	(0.362, 0.131, 0.151)	(0.061, 0.045, 0.045, 0.052)								
95% C.P.	1		(0.980, 0.960, 0.940, 0.950)								
	2		(0.900, 0.890, 0.890, 0.880)								
	3		(0.920, 0.910, 0.900, 0.900)								
	4		(0.890, 0.880, 0.870, 0.870)								
	5		(0.860, 0.860, 0.850, 0.850)								
	*		(0.913, 0.957, 0.933, 0.913)								
			(Gr-1, Gr-2, Gr-3, Gr-4)								
RISE	1		(0.155, 0.232, 0.316, 0.390)								
	2		(0.160, 0.234, 0.316, 0.388)								
	3		(0.159, 0.233, 0.315, 0.388)								
	4		(0.156, 0.233, 0.317, 0.390)								
	5		(0.154, 0.228, 0.307, 0.379)								
	*		(0.534, 0.517, 0.506, 0.500)								

Table 3.4: Simulation results for geometric cure rate model having high lifetime ($\gamma_0 = 2.101, \gamma_1 = 2.258$) with light censoring for large sample size.

Measure						$(\tau_i, \hat{\psi}_i)$					
	N	$(\hat{\beta}_0, \hat{\beta}_1, \hat{\gamma})$	$\hat{p}_0$	$\hat{l}$	AIC	$i=0$	$i=1$	$i=2$	$i=3$	$i=4$	$i=5$
n = 600 (150, 150, 150, 150)		(-0.038, 0.443, 0.200)	(0.400, 0.290, 0.210, 0.150)								
Est	1	(0.219, 0.389, 0.397)	(0.391, 0.293, 0.211, 0.149)	-38.514	87.030	(0.038, 0.108)	(3.703, 1.605)				
	2	(0.013, 0.437, 0.393)	(0.359, 0.275, 0.205, 0.151)	-38.329	86.660	(0.038, 0.059)	(0.742, 0.484)	(3.703, 0.697)			
	3	(0.181, 0.392, 0.389)	(0.363, 0.277, 0.205, 0.150)	-37.985	85.972	(0.038, 0.052)	(0.444, 0.329)	(0.742, 0.472)	(3.703, 0.758)		
	4	(0.159, 0.398, 0.385)	(0.366, 0.278, 0.205, 0.149)	-35.109	80.220	(0.038, 0.052)	(0.257, 0.204)	(0.444, 0.335)	(0.742, 0.475)	(3.703, 0.783)	
	5	(0.153, 0.402, 0.384)	(0.365, 0.277, 0.204, 0.149)	-33.999	78.000	(0.038, 0.052)	(0.257, 0.207)	(0.613, 0.435)	(0.742, 0.455)	(1.188, 0.551)	(3.703, 0.718)
	*	(-0.945, 0.515, 0.206)	(0.604, 0.477, 0.354, 0.248)	-32.848	75.698			(0.986, 0.992)			
s.e.	1	(0.292, 0.119, 0.061)	(0.045, 0.027, 0.026, 0.031)			(0.018, 0.035)	(0.488, 0.290)				
	2	(0.452, 0.153, 0.076)	(0.070, 0.040, 0.029, 0.033)			(0.018, 0.028)	(0.036, 0.110)	(0.488, 0.427)			
	3	(0.437, 0.150, 0.074)	(0.066, 0.038, 0.029, 0.033)			(0.018, 0.028)	(0.028, 0.086)	(0.036, 0.106)	(0.488, 0.463)		
	4	(0.416, 0.147, 0.073)	(0.064, 0.037, 0.029, 0.032)			(0.018, 0.031)	(0.024, 0.059)	(0.028, 0.093)	(0.036, 0.104)	(0.488, 0.445)	
	5	(0.516, 0.169, 0.085)	(0.078, 0.045, 0.031, 0.033)			(0.018, 0.032)	(0.024, 0.068)	(0.033, 0.129)	(0.036, 0.146)	(0.058, 0.154)	(0.488, 0.722)
	*	(0.303, 0.116, 0.134)	(0.048, 0.033, 0.033, 0.042)					(0.053, 0.363)			
RMSE	1	(0.287, 0.122, 0.205)	(0.214, 0.179, 0.141, 0.106)								
	2	(0.407, 0.148, 0.204)	(0.251, 0.199, 0.148, 0.104)								
	3	(0.383, 0.142, 0.200)	(0.246, 0.197, 0.148, 0.105)								
	4	(0.368, 0.137, 0.196)	(0.243, 0.196, 0.148, 0.106)								
	5	(0.368, 0.140, 0.196)	(0.248, 0.198, 0.149, 0.106)								
	*	(0.169, 0.069, 0.099)	(0.048, 0.033, 0.033, 0.042)								
95% C.P.	1		(0.970, 0.960, 0.970, 0.939)								
	2		(0.929, 0.929, 0.919, 0.899)								
	3		(0.929, 0.919, 0.929, 0.889)								
	4		(0.939, 0.929, 0.939, 0.899)								
	5		(0.919, 0.919, 0.929, 0.889)								
	*		(0.910, 0.950, 0.930, 0.933)								
			(Gr-1, Gr-2, Gr-3, Gr-4)								
RISE	1		(0.152, 0.226, 0.305, 0.376)								
	2		(0.156, 0.233, 0.314, 0.385)								
	3		(0.157, 0.232, 0.313, 0.385)								
	4		(0.157, 0.233, 0.314, 0.385)								
	5		(0.158, 0.234, 0.315, 0.385)								
	*		(0.022, 0.025, 0.028, 0.029)								

Table 3.5: Simulation results for Poisson cure rate model having high lifetime ($\gamma_0 = 2.101, \gamma_1 = 2.258$) with heavy censoring for small sample size.

Measure						$(\tau_i, \hat{\psi}_i)$					
	N	$(\hat{\beta}_0, \hat{\beta}_1, \hat{\gamma})$	$\hat{p}_0$	$\hat{l}$	AIC	$i=0$	$i=1$	$i=2$	$i=3$	$i=4$	$i=5$
$n = 400$ (100, 100, 100, 100)		(-0.907, 0.501, 0.200)	(0.600, 0.470, 0.350, 0.250)								
Est	1	(-0.909, 0.517, 0.209)	(0.596, 0.469, 0.346, 0.241)	-375.4026	760.805	(0.123, 0.048)	(4.036, 1.489)				
	2	(-0.907, 0.516, 0.214)	(0.596, 0.469, 0.346, 0.241)	-373.4371	758.874	(0.123, 0.050)	(1.385, 0.497)	(4.036, 1.633)			
	3	(-0.903, 0.515, 0.214)	(0.595, 0.468, 0.345, 0.241)	-370.2826	754.565	(0.123, 0.058)	(0.904, 0.299)	(1.385, 0.543)	(4.036, 1.512)		
	4	(-0.901, 0.515, 0.213)	(0.595, 0.468, 0.345, 0.241)	-370.0934	756.187	(0.123, 0.063)	(0.557, 0.183)	(0.904, 0.318)	(1.385, 0.539)	(4.036, 1.535)	
	5	(-0.896, 0.515, 0.213)	(0.594, 0.467, 0.344, 0.240)	-368.7355	755.471	(0.123, 0.064)	(0.557, 0.179)	(1.190, 0.446)	(1.385, 0.519)	(1.928, 0.783)	(4.036, 1.402)
	*	(-0.723, 0.434, 0.188)	(0.576, 0.466, 0.359, 0.265)	-375.1799	760.360			(2.195, 2.242)			
s.e.	1	(0.317, 0.117, 0.086)	(0.051, 0.034, 0.031, 0.039)			(0.058, 0.027)	(0.506, 0.404)				
	2	(0.319, 0.117, 0.085)	(0.052, 0.035, 0.032, 0.039)			(0.058, 0.029)	(0.080, 0.136)	(0.506, 0.603)			
	3	(0.322, 0.118, 0.086)	(0.052, 0.035, 0.032, 0.039)			(0.058, 0.035)	(0.062, 0.093)	(0.080, 0.160)	(0.506, 0.628)		
	4	(0.321, 0.117, 0.086)	(0.052, 0.035, 0.032, 0.039)			(0.058, 0.041)	(0.059, 0.066)	(0.062, 0.109)	(0.080, 0.160)	(0.506, 0.636)	
	5	(0.332, 0.119, 0.090)	(0.055, 0.037, 0.033, 0.040)			(0.058, 0.042)	(0.059, 0.065)	(0.073, 0.146)	(0.080, 0.190)	(0.086, 0.251)	(0.506, 0.984)
	*	(0.138, 0.053, 0.047)	(0.023, 0.018, 0.019, 0.023)					(0.121, 0.172)			
RMSE	1	(0.270, 0.104, 0.061)	(0.051, 0.034, 0.031, 0.040)								
	2	(0.265, 0.103, 0.063)	(0.052, 0.035, 0.032, 0.040)								
	3	(0.266, 0.103, 0.064)	(0.052, 0.035, 0.032, 0.040)								
	4	(0.260, 0.101, 0.063)	(0.052, 0.035, 0.032, 0.040)								
	5	(0.258, 0.100, 0.062)	(0.055, 0.037, 0.034, 0.041)								
	*	(0.229, 0.086, 0.048)	(0.033, 0.021, 0.019, 0.028)								
95% C.P.	1		(0.980, 0.960, 0.930, 0.920)								
	2		(0.980, 0.970, 0.930, 0.920)								
	3		(0.970, 0.960, 0.950, 0.920)								
	4		(0.980, 0.970, 0.930, 0.930)								
	5		(0.970, 0.970, 0.940, 0.930)								
	*		(0.400, 0.600, 0.650, 0.500)								
			(Gr-1, Gr-2, Gr-3, Gr-4)								
RISE	1		(0.064, 0.050, 0.050, 0.065)								
	2		(0.065, 0.051, 0.052, 0.067)								
	3		(0.065, 0.052, 0.053, 0.067)								
	4		(0.064, 0.051, 0.052, 0.067)								
	5		(0.063, 0.051, 0.053, 0.068)								
	*		(0.089, 0.092, 0.094, 0.096)								

Table 3.6: Simulation results for Poisson cure rate model having high lifetime ($\gamma_0 = 2.101, \gamma_1 = 2.258$) with heavy censoring for large sample size.

Measure						$(\tau_i, \hat{\psi}_i)$					
	N	$(\hat{\beta}_0, \hat{\beta}_1, \hat{\gamma})$	$\hat{p}_0$	$\hat{l}$	AIC	$i=0$	$i=1$	$i=2$	$i=3$	$i=4$	$i=5$
$n = 600$ (150, 150, 150, 150)		(-0.907, 0.501, 0.200)	(0.600, 0.470, 0.350, 0.250)								
Est	1	(-0.903, 0.515, 0.214)	(0.596, 0.474, 0.354, 0.251)	-543.617	1097.233	(0.095, 0.035)	(4.206, 1.614)				
	2	(-0.888, 0.497, 0.202)	(0.595, 0.473, 0.353, 0.251)	-542.810	1097.620	(0.095, 0.036)	(1.376, 0.513)	(4.206, 1.718)			
	3	(-0.881, 0.496, 0.206)	(0.595, 0.473, 0.353, 0.251)	-540.706	1095.412	(0.095, 0.040)	(0.895, 0.318)	(1.376, 0.544)	(4.206, 1.634)		
	4	(-0.884, 0.497, 0.205)	(0.595, 0.472, 0.353, 0.250)	-540.682	1097.363	(0.095, 0.046)	(0.555, 0.186)	(0.895, 0.341)	(1.376, 0.539)	(4.206, 1.658)	
	5	(-0.881, 0.496, 0.203)	(0.595, 0.472, 0.353, 0.250)	-540.099	1098.197	(0.095, 0.046)	(0.555, 0.188)	(1.183, 0.462)	(1.376, 0.536)	(1.941, 0.784)	(4.206, 1.597)
	*	(-0.860, 0.480, 0.201)	(0.592, 0.476, 0.362, 0.263)	-544.662	1099.325			(2.161, 2.288)			
s.e.	1	(0.252, 0.093, 0.067)	(0.041, 0.027, 0.025, 0.032)			(0.047, 0.020)	(0.441, 0.338)				
	2	(0.253, 0.093, 0.067)	(0.041, 0.028, 0.025, 0.032)			(0.047, 0.021)	(0.057, 0.110)	(0.441, 0.492)			
	3	(0.254, 0.093, 0.067)	(0.041, 0.028, 0.025, 0.032)			(0.047, 0.024)	(0.046, 0.076)	(0.057, 0.126)	(0.441, 0.516)		
	4	(0.254, 0.093, 0.067)	(0.041, 0.028, 0.025, 0.032)			(0.047, 0.029)	(0.049, 0.053)	(0.046, 0.090)	(0.057, 0.126)	(0.441, 0.519)	
	5	(0.257, 0.094, 0.068)	(0.042, 0.028, 0.026, 0.032)			(0.047, 0.029)	(0.049, 0.052)	(0.050, 0.116)	(0.057, 0.151)	(0.073, 0.191)	(0.441, 0.815)
	*	(0.100, 0.039, 0.038)	(0.018, 0.016, 0.017, 0.019)					(0.102, 0.152)			
RMSE	1	(0.217, 0.082, 0.057)	(0.041, 0.027, 0.025, 0.032)								
	2	(0.215, 0.082, 0.058)	(0.041, 0.028, 0.025, 0.032)								
	3	(0.216, 0.082, 0.058)	(0.041, 0.028, 0.025, 0.032)								
	4	(0.212, 0.081, 0.058)	(0.041, 0.028, 0.025, 0.032)								
	5	(0.213, 0.081, 0.057)	(0.042, 0.028, 0.026, 0.032)								
	*	(0.110, 0.044, 0.038)	(0.020, 0.016, 0.018, 0.023)								
95% C.P.	1		(0.970, 0.980, 0.960, 0.970)								
	2		(0.980, 0.980, 0.950, 0.960)								
	3		(0.980, 0.990, 0.950, 0.970)								
	4		(0.970, 0.970, 0.950, 0.960)								
	5		(0.980, 0.970, 0.950, 0.970)								
	*		(0.480, 0.600, 0.680, 0.640)								
			(Gr-1, Gr-2, Gr-3, Gr-4)								
RISE	1		(0.050, 0.039, 0.040, 0.054)								
	2		(0.051, 0.039, 0.040, 0.055)								
	3		(0.051, 0.039, 0.041, 0.055)								
	4		(0.050, 0.039, 0.041, 0.055)								
	5		(0.051, 0.040, 0.041, 0.055)								
	*		(0.092, 0.095, 0.098, 0.100)								

Table 3.7: Simulation results for Poisson cure rate model having high lifetime ($\gamma_0 = 2.101, \gamma_1 = 2.258$) with light censoring for small sample size.

Measure						$(\tau_i, \hat{\psi}_i)$					
	N	$(\hat{\beta}_0, \hat{\beta}_1, \hat{\gamma})$	$\hat{p}_0$	$\hat{l}$	AIC	$i=0$	$i=1$	$i=2$	$i=3$	$i=4$	$i=5$
$n = 400$ (100, 100, 100, 100)		(-0.038, 0.443, 0.200)	(0.400, 0.290, 0.210, 0.150)								
	1	(0.011, 0.434, 0.213)	(0.392, 0.295, 0.214, 0.152)	-383.139	776.277	(0.107, 0.040)	(4.233, 1.565)				
	2	(0.004, 0.435, 0.216)	(0.394, 0.296, 0.214, 0.152)	-382.089	776.178	(0.107, 0.042)	(1.415, 0.508)	(4.233, 1.690)			
Est	3	(0.013, 0.433, 0.218)	(0.391, 0.294, 0.213, 0.151)	-381.848	777.696	(0.107, 0.046)	(0.924, 0.312)	(1.415, 0.541)	(4.233, 1.594)		
	4	(0.012, 0.434, 0.218)	(0.392, 0.295, 0.214, 0.152)	-381.629	779.257	(0.107, 0.050)	(0.568, 0.184)	(0.924, 0.331)	(1.415, 0.535)	(4.233, 1.612)	
	5	(0.011, 0.434, 0.216)	(0.392, 0.294, 0.213, 0.151)	-381.614	781.228	(0.107, 0.051)	(0.568, 0.185)	(1.220, 0.453)	(1.415, 0.532)	(1.990, 0.771)	(4.233, 1.588)
	*	(-0.064, 0.469, 0.193)	(0.395, 0.295, 0.212, 0.148)	-384.320	778.640			(2.087, 2.247)			
	1	(0.318, 0.125, 0.067)	(0.050, 0.029, 0.027, 0.032)			(0.054, 0.022)	(0.447, 0.317)				
	2	(0.320, 0.124, 0.067)	(0.050, 0.030, 0.027, 0.032)			(0.054, 0.023)	(0.056, 0.107)	(0.447, 0.487)			
s.e.	3	(0.327, 0.126, 0.068)	(0.051, 0.030, 0.027, 0.032)			(0.054, 0.027)	(0.054, 0.074)	(0.056, 0.125)	(0.447, 0.511)		
	4	(0.326, 0.126, 0.068)	(0.051, 0.030, 0.027, 0.032)			(0.054, 0.032)	(0.052, 0.054)	(0.054, 0.089)	(0.056, 0.125)	(0.447, 0.515)	
	5	(0.341, 0.128, 0.071)	(0.054, 0.032, 0.027, 0.032)			(0.054, 0.032)	(0.052, 0.053)	(0.055, 0.116)	(0.056, 0.154)	(0.066, 0.193)	(0.447, 0.834)
	*	(0.094, 0.048, 0.039)	(0.407, 0.302, 0.214, 0.148)					(0.098, 0.170)			
	1	(0.318, 0.122, 0.057)	(0.214, 0.177, 0.139, 0.103)								
	2	(0.313, 0.120, 0.059)	(0.212, 0.177, 0.139, 0.103)								
RMSE	3	(0.317, 0.120, 0.060)	(0.215, 0.179, 0.140, 0.104)								
	4	(0.312, 0.120, 0.060)	(0.214, 0.178, 0.139, 0.103)								
	5	(0.313, 0.120, 0.059)	(0.215, 0.179, 0.140, 0.104)								
	*	(0.103, 0.052, 0.040)	(0.018, 0.015, 0.015, 0.016)								
	1		(0.960, 0.950, 0.950, 0.970)								
	2		(0.960, 0.940, 0.960, 0.960)								
95% C.P.	3		(0.960, 0.950, 0.960, 0.960)								
	4		(0.970, 0.960, 0.970, 0.970)								
	5		(0.970, 0.950, 0.970, 0.970)								
	*		(0.480, 0.630, 0.565, 0.655)								
			(Gr-1, Gr-2, Gr-3, Gr-4)								
	1		(0.070, 0.043, 0.044, 0.062)								
	2		(0.071, 0.044, 0.045, 0.062)								
RISE	3		(0.071, 0.044, 0.044, 0.062)								
	4		(0.071, 0.045, 0.046, 0.063)								
	5		(0.071, 0.045, 0.046, 0.063)								
	*		(0.248, 0.266, 0.278, 0.285)								

Table 3.8: Simulation results for Poisson cure rate model having high lifetime ($\gamma_0 = 2.101, \gamma_1 = 2.258$) with light censoring for large sample size.

Measure						$(\tau_i, \hat{\psi}_i)$					
	N	$(\hat{\beta}_0, \hat{\beta}_1, \hat{\gamma})$	$\hat{p}_0$	$\hat{l}$	AIC	$i=0$	$i=1$	$i=2$	$i=3$	$i=4$	$i=5$
$n = 600$ (150, 150, 150, 150)		(-0.038, 0.443, 0.200)	(0.400, 0.290, 0.210, 0.150)								
Est	1	(0.013, 0.433, 0.218)	(0.392, 0.294, 0.212, 0.150)	-590.814	1191.628	(0.090, 0.031)	(4.398, 1.653)				
	2	(0.005, 0.437, 0.215)	(0.392, 0.294, 0.212, 0.150)	-590.389	1192.778	(0.090, 0.032)	(1.401, 0.511)	(4.398, 1.768)			
	3	(0.007, 0.437, 0.220)	(0.392, 0.294, 0.212, 0.149)	-588.790	1191.579	(0.090, 0.038)	(0.919, 0.312)	(1.401, 0.550)	(4.398, 1.653)		
	4	(0.006, 0.437, 0.219)	(0.392, 0.294, 0.212, 0.149)	-586.561	1189.121	(0.090, 0.043)	(0.567, 0.183)	(0.919, 0.332)	(1.401, 0.545)	(4.398, 1.675)	
	5	(0.004, 0.438, 0.217)	(0.392, 0.294, 0.212, 0.149)	-585.601	1189.201	(0.090, 0.044)	(0.567, 0.184)	(1.207, 0.461)	(1.401, 0.540)	(1.970, 0.782)	(4.398, 1.601)
	*	(-0.079, 0.463, 0.191)	(0.407, 0.302, 0.214, 0.148)	-593.680	1197.360			(2.147, 2.209)			
s.e.	1	(0.254, 0.100, 0.052)	(0.040, 0.023, 0.022, 0.025)			(0.046, 0.016)	(0.442, 0.261)				
	2	(0.255, 0.100, 0.053)	(0.040, 0.023, 0.022, 0.025)			(0.046, 0.017)	(0.048, 0.085)	(0.442, 0.397)			
	3	(0.257, 0.101, 0.053)	(0.040, 0.024, 0.022, 0.025)			(0.046, 0.020)	(0.046, 0.059)	(0.048, 0.101)	(0.442, 0.419)		
	4	(0.257, 0.101, 0.053)	(0.040, 0.024, 0.022, 0.025)			(0.046, 0.024)	(0.046, 0.042)	(0.046, 0.071)	(0.048, 0.101)	(0.442, 0.421)	
	5	(0.260, 0.101, 0.054)	(0.041, 0.024, 0.022, 0.025)			(0.046, 0.024)	(0.046, 0.042)	(0.047, 0.091)	(0.048, 0.122)	(0.059, 0.151)	(0.442, 0.667)
	*	(0.094, 0.048, 0.039)	(0.017, 0.015, 0.015, 0.016)					(0.087, 0.139)			
RMSE	1	(0.273, 0.103, 0.049)	(0.212, 0.177, 0.140, 0.103)								
	2	(0.275, 0.103, 0.050)	(0.212, 0.177, 0.140, 0.103)								
	3	(0.277, 0.104, 0.050)	(0.212, 0.178, 0.140, 0.104)								
	4	(0.273, 0.103, 0.050)	(0.212, 0.178, 0.140, 0.104)								
	5	(0.268, 0.101, 0.048)	(0.212, 0.178, 0.140, 0.104)								
	*	(0.103, 0.052, 0.040)	(0.018, 0.019, 0.016, 0.016)								
95% C.P.	1		(0.910, 0.910, 0.930, 0.960)								
	2		(0.920, 0.930, 0.920, 0.960)								
	3		(0.920, 0.920, 0.920, 0.950)								
	4		(0.920, 0.930, 0.930, 0.960)								
	5		(0.930, 0.930, 0.920, 0.940)								
	*		(0.480, 0.630, 0.565, 0.655)								
			(Gr-1, Gr-2, Gr-3, Gr-4)								
RISE	1		(0.063, 0.039, 0.040, 0.054)								
	2		(0.063, 0.040, 0.041, 0.054)								
	3		(0.064, 0.040, 0.041, 0.055)								
	4		(0.063, 0.040, 0.041, 0.054)								
	5		(0.063, 0.040, 0.041, 0.054)								
	*		(0.248, 0.266, 0.278, 0.285)								

Table 3.9: Simulation results for Bernoulli cure rate model having high lifetime ($\gamma_0 = 2.101, \gamma_1 = 2.258$) with heavy censoring for small sample size.

Measure						$(\tau_i, \hat{\psi}_i)$					
	N	$(\hat{\beta}_0, \hat{\beta}_1, \hat{\gamma})$	$\hat{p}_0$	$\hat{l}$	AIC	$i=0$	$i=1$	$i=2$	$i=3$	$i=4$	$i=5$
$n = 400$ (100, 100, 100, 100)		(-0.907, 0.501, 0.200)	(0.600, 0.470, 0.350, 0.250)								
Est	1	(-0.909, 0.517, 0.209)	(0.596, 0.469, 0.346, 0.241)	-426.014	862.028	(0.123, 0.048)	(4.036, 1.489)				
	2	(-0.907, 0.516, 0.214)	(0.596, 0.469, 0.346, 0.241)	-425.802	863.603	(0.123, 0.050)	(1.385, 0.497)	(4.036, 1.633)			
	3	(-0.903, 0.515, 0.214)	(0.595, 0.468, 0.345, 0.241)	-423.608	861.217	(0.123, 0.058)	(0.904, 0.299)	(1.385, 0.543)	(4.036, 1.512)		
	4	(-0.901, 0.515, 0.213)	(0.595, 0.468, 0.345, 0.241)	-421.060	858.119	(0.123, 0.063)	(0.557, 0.183)	(0.904, 0.318)	(1.385, 0.539)	(4.036, 1.535)	
	5	(-0.896, 0.515, 0.213)	(0.594, 0.467, 0.344, 0.240)	-418.575	855.149	(0.123, 0.064)	(0.557, 0.179)	(1.190, 0.446)	(1.385, 0.519)	(1.928, 0.783)	(4.036, 1.402)
	*	(-0.925, 0.505, 0.157)	(0.603, 0.476, 0.352, 0.246)	-428.086	866.172			(2.237, 2.300)			
s.e.	1	(0.317, 0.117, 0.086)	(0.051, 0.034, 0.031, 0.039)			(0.058, 0.027)	(0.506, 0.404)				
	2	(0.319, 0.117, 0.085)	(0.052, 0.035, 0.032, 0.039)			(0.058, 0.029)	(0.080, 0.136)	(0.506, 0.603)			
	3	(0.322, 0.118, 0.086)	(0.052, 0.035, 0.032, 0.039)			(0.058, 0.035)	(0.062, 0.093)	(0.080, 0.160)	(0.506, 0.628)		
	4	(0.321, 0.117, 0.086)	(0.052, 0.035, 0.032, 0.039)			(0.058, 0.041)	(0.059, 0.066)	(0.062, 0.109)	(0.080, 0.160)	(0.506, 0.636)	
	5	(0.332, 0.119, 0.090)	(0.055, 0.037, 0.033, 0.040)			(0.058, 0.042)	(0.059, 0.065)	(0.073, 0.146)	(0.080, 0.190)	(0.086, 0.251)	(0.506, 0.984)
	*	(0.239, 0.091, 0.061)	(0.038, 0.028, 0.027, 0.033)					(0.124, 0.208)			
RMSE	1	(0.270, 0.104, 0.061)	(0.051, 0.034, 0.031, 0.040)								
	2	(0.265, 0.103, 0.063)	(0.052, 0.035, 0.032, 0.040)								
	3	(0.266, 0.103, 0.064)	(0.052, 0.035, 0.032, 0.040)								
	4	(0.260, 0.101, 0.063)	(0.052, 0.035, 0.032, 0.040)								
	5	(0.258, 0.100, 0.062)	(0.055, 0.037, 0.034, 0.041)								
	*	(0.240, 0.091, 0.074)	(0.038, 0.029, 0.027, 0.033)								
95% C.P.	1		(0.980, 0.960, 0.930, 0.920)								
	2		(0.980, 0.970, 0.930, 0.920)								
	3		(0.970, 0.960, 0.950, 0.920)								
	4		(0.980, 0.970, 0.930, 0.930)								
	5		(0.970, 0.970, 0.940, 0.930)								
	*		(0.750, 0.850, 0.875, 0.850)								
			(Gr-1, Gr-2, Gr-3, Gr-4)								
RISE	1		(0.064, 0.050, 0.050, 0.065)								
	2		(0.065, 0.051, 0.052, 0.067)								
	3		(0.065, 0.052, 0.053, 0.067)								
	4		(0.064, 0.051, 0.052, 0.067)								
	5		(0.063, 0.051, 0.053, 0.068)								
	*		(0.005, 0.006, 0.006, 0.009)								

Table 3.10: Simulation results for Bernoulli cure rate model having high lifetime $(\gamma_0 = 2.101, \gamma_1 = 2.258)$ with heavy censoring for large sample size.

Measure						$(\tau_i, \hat{\psi}_i)$					
	N	$(\hat{\beta}_0, \hat{\beta}_1, \hat{\gamma})$	$\hat{p}_0$	$\hat{l}$	AIC	$i=0$	$i=1$	$i=2$	$i=3$	$i=4$	$i=5$
$n = 600$ (150, 150, 150, 150)		(-0.907, 0.501, 0.200)	(0.600, 0.470, 0.350, 0.250)								
	1	(-0.903, 0.515, 0.214)	(0.596, 0.474, 0.354, 0.251)	-624.773	1259.546	(0.095, 0.035)	(4.206, 1.614)				
	2	(-0.888, 0.497, 0.202)	(0.595, 0.473, 0.353, 0.251)	-624.570	1261.141	(0.095, 0.036)	(1.376, 0.513)	(4.206, 1.718)			
Est	3	(-0.881, 0.496, 0.206)	(0.595, 0.473, 0.353, 0.251)	-621.393	1256.787	(0.095, 0.040)	(0.895, 0.318)	(1.376, 0.544)	(4.206, 1.634)		
	4	(-0.884, 0.497, 0.205)	(0.595, 0.472, 0.353, 0.250)	-620.764	1257.527	(0.095, 0.046)	(0.555, 0.186)	(0.895, 0.341)	(1.376, 0.539)	(4.206, 1.658)	
	5	(-0.881, 0.496, 0.203)	(0.595, 0.472, 0.353, 0.250)	-620.305	1258.611	(0.095, 0.046)	(0.555, 0.188)	(1.183, 0.462)	(1.376, 0.536)	(1.941, 0.784)	(4.206, 1.597)
	*	(-0.915, 0.514, 0.154)	(0.591, 0.466, 0.344, 0.241)	-624.440	1258.879			(2.217, 2.258)			
	1	(0.252, 0.093, 0.067)	(0.041, 0.027, 0.025, 0.032)			(0.047, 0.020)	(0.441, 0.338)				
	2	(0.253, 0.093, 0.067)	(0.041, 0.028, 0.025, 0.032)			(0.047, 0.021)	(0.057, 0.110)	(0.441, 0.492)			
s.e.	3	(0.254, 0.093, 0.067)	(0.041, 0.028, 0.025, 0.032)			(0.047, 0.024)	(0.046, 0.076)	(0.057, 0.126)	(0.441, 0.516)		
	4	(0.254, 0.093, 0.067)	(0.041, 0.028, 0.025, 0.032)			(0.047, 0.029)	(0.049, 0.053)	(0.046, 0.090)	(0.057, 0.126)	(0.441, 0.519)	
	5	(0.257, 0.094, 0.068)	(0.042, 0.028, 0.026, 0.032)			(0.047, 0.029)	(0.049, 0.052)	(0.050, 0.116)	(0.057, 0.151)	(0.073, 0.191)	(0.441, 0.815)
	*	(0.181, 0.069, 0.046)	(0.029, 0.021, 0.021, 0.025)					(0.098, 0.158)			
	1	(0.217, 0.082, 0.057)	(0.041, 0.027, 0.025, 0.032)								
	2	(0.215, 0.082, 0.058)	(0.041, 0.028, 0.025, 0.032)								
RMSE	3	(0.216, 0.082, 0.058)	(0.041, 0.028, 0.025, 0.032)								
	4	(0.212, 0.081, 0.058)	(0.041, 0.028, 0.025, 0.032)								
	5	(0.213, 0.081, 0.057)	(0.042, 0.028, 0.026, 0.032)								
	*	(0.181, 0.071, 0.064)	(0.030, 0.021, 0.021, 0.027)								
	1		(0.970, 0.980, 0.960, 0.970)								
	2		(0.980, 0.980, 0.950, 0.960)								
95% C.P.	3		(0.980, 0.990, 0.950, 0.970)								
	4		(0.970, 0.970, 0.950, 0.960)								
	5		(0.980, 0.970, 0.950, 0.970)								
	*		(0.750, 0.775, 0.800, 0.725)								
			(Gr-1, Gr-2, Gr-3, Gr-4)								
	1		(0.050, 0.039, 0.040, 0.054)								
	2		(0.051, 0.039, 0.040, 0.055)								
RISE	3		(0.051, 0.039, 0.041, 0.055)								
	4		(0.050, 0.039, 0.041, 0.055)								
	5		(0.051, 0.040, 0.041, 0.055)								
	*		(0.008, 0.007, 0.007, 0.010)								

Table 3.11: Simulation results for Bernoulli cure rate model having high lifetime $(\gamma_0 = 2.101, \gamma_1 = 2.258)$ with light censoring for small sample size.

Measure						$(\tau_i, \hat{\psi}_i)$					
	N	$(\hat{\beta}_0, \hat{\beta}_1, \hat{\gamma})$	$\hat{p}_0$	$\hat{l}$	AIC	$i=0$	$i=1$	$i=2$	$i=3$	$i=4$	$i=5$
$n = 400$ (100, 100, 100, 100)		(-0.038, 0.443, 0.200)	(0.400, 0.290, 0.210, 0.150)								
Est	1	(0.011, 0.434, 0.213)	(0.392, 0.295, 0.214, 0.152)	-459.403	928.806	(0.107, 0.040)	(4.233, 1.565)				
	2	(0.004, 0.435, 0.216)	(0.394, 0.296, 0.214, 0.152)	-458.678	929.357	(0.107, 0.042)	(1.415, 0.508)	(4.233, 1.690)			
	3	(0.013, 0.433, 0.218)	(0.391, 0.294, 0.213, 0.151)	-457.098	928.195	(0.107, 0.046)	(0.924, 0.312)	(1.415, 0.541)	(4.233, 1.594)		
	4	(0.012, 0.434, 0.218)	(0.392, 0.295, 0.214, 0.152)	-456.883	929.767	(0.107, 0.050)	(0.568, 0.184)	(0.924, 0.331)	(1.415, 0.535)	(4.233, 1.612)	
	5	(0.011, 0.434, 0.216)	(0.392, 0.294, 0.213, 0.151)	-456.837	931.674	(0.107, 0.051)	(0.568, 0.185)	(1.220, 0.453)	(1.415, 0.532)	(1.990, 0.771)	(4.233, 1.588)
	*	(-0.002, 0.432, 0.185)	(0.391, 0.296, 0.217, 0.155)	-460.967	931.934			(2.211, 2.388)			
s.e.	1	(0.318, 0.125, 0.067)	(0.050, 0.029, 0.027, 0.032)			(0.054, 0.022)	(0.447, 0.317)				
	2	(0.320, 0.124, 0.067)	(0.050, 0.030, 0.027, 0.032)			(0.054, 0.023)	(0.056, 0.107)	(0.447, 0.487)			
	3	(0.327, 0.126, 0.068)	(0.051, 0.030, 0.027, 0.032)			(0.054, 0.027)	(0.054, 0.074)	(0.056, 0.125)	(0.447, 0.511)		
	4	(0.326, 0.126, 0.068)	(0.051, 0.030, 0.027, 0.032)			(0.054, 0.032)	(0.052, 0.054)	(0.054, 0.089)	(0.056, 0.125)	(0.447, 0.515)	
	5	(0.341, 0.128, 0.071)	(0.054, 0.032, 0.027, 0.032)			(0.054, 0.032)	(0.052, 0.053)	(0.055, 0.116)	(0.056, 0.154)	(0.066, 0.193)	(0.447, 0.834)
	*	(0.247, 0.101, 0.053)	(0.039, 0.024, 0.023, 0.027)					(0.109, 0.176)			
RMSE	1	(0.318, 0.122, 0.057)	(0.214, 0.177, 0.139, 0.103)								
	2	(0.313, 0.120, 0.059)	(0.212, 0.177, 0.139, 0.103)								
	3	(0.317, 0.120, 0.060)	(0.215, 0.179, 0.140, 0.104)								
	4	(0.312, 0.120, 0.060)	(0.214, 0.178, 0.139, 0.103)								
	5	(0.313, 0.120, 0.059)	(0.215, 0.179, 0.140, 0.104)								
	*	(0.249, 0.101, 0.055)	(0.040, 0.025, 0.024, 0.027)								
95% C.P.	1		(0.960, 0.950, 0.950, 0.970)								
	2		(0.960, 0.940, 0.960, 0.960)								
	3		(0.960, 0.950, 0.960, 0.960)								
	4		(0.970, 0.960, 0.970, 0.970)								
	5		(0.970, 0.950, 0.970, 0.970)								
	*		(0.775, 0.900, 0.900, 0.825)								
			(Gr-1, Gr-2, Gr-3, Gr-4)								
RISE	1		(0.070, 0.043, 0.044, 0.062)								
	2		(0.071, 0.044, 0.045, 0.062)								
	3		(0.071, 0.044, 0.044, 0.062)								
	4		(0.071, 0.045, 0.046, 0.063)								
	5		(0.071, 0.045, 0.046, 0.063)								
	*		(0.004, 0.005, 0.006, 0.007)								

Table 3.12: Simulation results for Bernoulli cure rate model having high lifetime $(\gamma_0 = 2.101, \gamma_1 = 2.258)$ with light censoring for large sample size.

Measure						$(\tau_i, \hat{\psi}_i)$					
	N	$(\hat{\beta}_0, \hat{\beta}_1, \hat{\gamma})$	$\hat{p}_0$	$\hat{l}$	AIC	$i=0$	$i=1$	$i=2$	$i=3$	$i=4$	$i=5$
$n = 600$ (150, 150, 150, 150)		(-0.038, 0.443, 0.200)	(0.400, 0.290, 0.210, 0.150)								
Est	1	(0.013, 0.433, 0.218)	(0.392, 0.294, 0.212, 0.150)	-713.902	1437.804	(0.090, 0.031)	(4.398, 1.653)				
	2	(0.005, 0.437, 0.215)	(0.392, 0.294, 0.212, 0.150)	-713.857	1439.714	(0.090, 0.032)	(1.401, 0.511)	(4.398, 1.768)			
	3	(0.007, 0.437, 0.220)	(0.392, 0.294, 0.212, 0.149)	-712.695	1439.391	(0.090, 0.038)	(0.919, 0.312)	(1.401, 0.550)	(4.398, 1.653)		
	4	(0.006, 0.437, 0.219)	(0.392, 0.294, 0.212, 0.149)	-712.665	1441.331	(0.090, 0.043)	(0.567, 0.183)	(0.919, 0.332)	(1.401, 0.545)	(4.398, 1.675)	
	5	(0.004, 0.438, 0.217)	(0.392, 0.294, 0.212, 0.149)	-711.258	1440.517	(0.090, 0.044)	(0.567, 0.184)	(1.207, 0.461)	(1.401, 0.540)	(1.970, 0.782)	(4.398, 1.601)
	*	(-0.036, 0.445, 0.176)	(0.397, 0.297, 0.214, 0.151)	-713.482	1436.965			(2.188, 2.315)			
s.e.	1	(0.254, 0.100, 0.052)	(0.040, 0.023, 0.022, 0.025)			(0.046, 0.016)	(0.442, 0.261)				
	2	(0.255, 0.100, 0.053)	(0.040, 0.023, 0.022, 0.025)			(0.046, 0.017)	(0.048, 0.085)	(0.442, 0.397)			
	3	(0.257, 0.101, 0.053)	(0.040, 0.024, 0.022, 0.025)			(0.046, 0.020)	(0.046, 0.059)	(0.048, 0.101)	(0.442, 0.419)		
	4	(0.257, 0.101, 0.053)	(0.040, 0.024, 0.022, 0.025)			(0.046, 0.024)	(0.046, 0.042)	(0.046, 0.071)	(0.048, 0.101)	(0.442, 0.421)	
	5	(0.260, 0.101, 0.054)	(0.041, 0.024, 0.022, 0.025)			(0.046, 0.024)	(0.046, 0.042)	(0.047, 0.091)	(0.048, 0.122)	(0.059, 0.151)	(0.442, 0.667)
	*	(0.203, 0.084, 0.048)	(0.032, 0.021, 0.019, 0.023)					(0.086, 0.150)			
RMSE	1	(0.275, 0.103, 0.048)	(0.212, 0.177, 0.140, 0.103)								
	2	(0.274, 0.103, 0.050)	(0.212, 0.177, 0.140, 0.103)								
	3	(0.277, 0.104, 0.050)	(0.212, 0.178, 0.140, 0.104)								
	4	(0.273, 0.103, 0.050)	(0.212, 0.178, 0.140, 0.104)								
	5	(0.268, 0.101, 0.048)	(0.212, 0.178, 0.140, 0.104)								
	*	(0.203, 0.084, 0.053)	(0.033, 0.022, 0.020, 0.023)								
95% C.P.	1		(0.910, 0.910, 0.930, 0.960)								
	2		(0.920, 0.930, 0.920, 0.960)								
	3		(0.920, 0.920, 0.920, 0.950)								
	4		(0.920, 0.930, 0.930, 0.960)								
	5		(0.930, 0.930, 0.920, 0.940)								
	*		(0.775, 0.900, 0.900, 0.850)								
			(Gr-1, Gr-2, Gr-3, Gr-4)								
RISE	1		(0.063, 0.039, 0.040, 0.054)								
	2		(0.063, 0.040, 0.041, 0.054)								
	3		(0.064, 0.040, 0.041, 0.055)								
	4		(0.063, 0.040, 0.041, 0.054)								
	5		(0.063, 0.040, 0.041, 0.054)								
	*		(0.006, 0.008, 0.008, 0.008)								

Table 3.13: Simulation results for COM-Poisson cure rate model ($\phi = 0.5$) having high lifetime ($\gamma_0 = 2.101, \gamma_1 = 2.258$) with heavy censoring for small sample size.

Measure						$(\tau_i, \hat{\psi}_i)$					
	N	$(\hat{\beta}_0, \hat{\beta}_1, \hat{\gamma}, \hat{\phi})$	$\hat{p}_0$	$\hat{l}$	AIC	$i=0$	$i=1$	$i=2$	$i=3$	$i=4$	$i=5$
$n = 400$ (100, 100, 100, 100)		(-0.907, 0.501, 0.200, 0.500)	(0.600, 0.470, 0.370, 0.250)								
Est	1	(-0.792, 0.466, 0.156, 0.701)	(0.581, 0.465, 0.353, 0.255)	-367.509	737.017	(0.080, 0.039)	(3.649, 1.623)				
	2	(-0.751, 0.456, 0.193, 0.560)	(0.573, 0.460, 0.350, 0.255)	-368.254	740.508	(0.080, 0.042)	(1.012, 0.502)	(3.649, 1.340)			
	3	(-0.757, 0.458, 0.174, 0.590)	(0.574, 0.460, 0.351, 0.255)	-368.084	742.169	(0.080, 0.042)	(0.634, 0.290)	(1.012, 0.515)	(3.649, 1.412)		
	4	(-0.770, 0.462, 0.166, 0.613)	(0.576, 0.462, 0.351, 0.254)	-368.074	744.148	(0.080, 0.050)	(0.386, 0.161)	(0.634, 0.319)	(1.012, 0.510)	(3.649, 1.472)	
	5	(-0.768, 0.462, 0.171, 0.761)	(0.576, 0.461, 0.350, 0.253)	-367.202	744.404	(0.080, 0.049)	(0.386, 0.164)	(0.859, 0.431)	(1.012, 0.491)	(1.498, 0.725)	(3.649, 1.317)
	*	(-1.015, 0.553, 0.179, -)	(0.601, 0.469, 0.340, 0.231)	-368.709	739.419			(2.108, 2.178)			
s.e.	1	(0.359, 0.137, 0.141, 0.807)	(0.057, 0.037, 0.036, 0.047)			(0.038, 0.027)	(0.298, 0.604)				
	2	(0.361, 0.132, 0.128, 0.745)	(0.061, 0.041, 0.038, 0.048)			(0.038, 0.032)	(0.060, 0.182)	(0.298, 0.815)			
	3	(0.371, 0.138, 0.141, 0.794)	(0.060, 0.040, 0.037, 0.047)			(0.038, 0.033)	(0.053, 0.146)	(0.060, 0.237)	(0.298, 0.851)		
	4	(0.371, 0.138, 0.138, 0.606)	(0.060, 0.040, 0.037, 0.047)			(0.038, 0.039)	(0.033, 0.085)	(0.053, 0.157)	(0.060, 0.225)	(0.298, 0.849)	
	5	(0.392, 0.141, 0.138, 0.654)	(0.064, 0.043, 0.038, 0.047)			(0.038, 0.038)	(0.033, 0.080)	(0.053, 0.198)	(0.060, 0.244)	(0.072, 0.314)	(0.298, 1.143)
	*	(0.116, 0.047, 0.044, -)	(0.601, 0.469, 0.340, 0.231)					(0.147, 0.219)			
RMSE	1	(0.295, 0.100, 0.119, 0.832)	(0.060, 0.037, 0.036, 0.047)								
	2	(0.352, 0.109, 0.111, 0.748)	(0.067, 0.042, 0.038, 0.048)								
	3	(0.353, 0.110, 0.135, 0.799)	(0.065, 0.041, 0.037, 0.047)								
	4	(0.325, 0.102, 0.133, 0.616)	(0.065, 0.041, 0.037, 0.047)								
	5	(0.333, 0.102, 0.131, 0.705)	(0.068, 0.044, 0.038, 0.047)								
	*	(0.159, 0.070, 0.049, -)	(0.023, 0.024, 0.028, 0.031)								
95% C.P.	1		(0.933, 0.933, 0.967, 0.967)								
	2		(0.967, 0.933, 0.933, 0.967)								
	3		(0.933, 0.900, 0.933, 0.967)								
	4		(0.933, 0.900, 0.900, 0.933)								
	5		(0.900, 0.867, 0.900, 0.900)								
	*		(0.400, 0.600, 0.600, 0.533)								
			(Gr-1, Gr-2, Gr-3, Gr-4)								
RISE	1		(0.085, 0.065, 0.062, 0.091)								
	2		(0.099, 0.099, 0.109, 0.130)								
	3		(0.096, 0.092, 0.103, 0.130)								
	4		(0.092, 0.090, 0.102, 0.129)								
	5		(0.094, 0.093, 0.106, 0.134)								
	*		(0.355, 0.251, 0.123, 0.097)								

Table 3.14: Simulation results for COM-Poisson cure rate model ($\phi = 0.5$) having high lifetime ($\gamma_0 = 2.101, \gamma_1 = 2.258$) with heavy censoring for large sample size.

Measure						$(\tau_i, \hat{\psi}_i)$					
	N	$(\hat{\beta}_0, \hat{\beta}_1, \hat{\gamma}, \hat{\phi})$	$\hat{p}_0$	$\hat{l}$	AIC	$i = 0$	$i = 1$	$i = 2$	$i = 3$	$i = 4$	$i = 5$
$n = 600$ (150, 150, 150, 150)		(-0.907, 0.501, 0.200, 0.500)	(0.600, 0.470, 0.370, 0.250)								
Est	1	(-0.902, 0.495, 0.235, 0.740)	(0.600, 0.478, 0.358, 0.254)	-537.613	1077.226	(0.073, 0.035)	(1.126, 1.427)				
	2	(-0.888, 0.493, 0.264, 0.763)	(0.597, 0.476, 0.357, 0.253)	-536.492	1076.985	(0.073, 0.040)	(0.658, 0.434)	(1.679, 1.268)			
	3	(-0.894, 0.493, 0.247, 0.818)	(0.598, 0.477, 0.358, 0.254)	-536.489	1078.978	(0.073, 0.039)	(0.638, 0.251)	(1.022, 0.423)	(3.715, 1.300)		
	4	(-0.897, 0.495, 0.244, 1.192)	(0.599, 0.477, 0.357, 0.253)	-536.476	1080.952	(0.073, 0.037)	(0.374, 0.152)	(0.638, 0.253)	(1.022, 0.421)	(3.715, 1.313)	
	5	(-0.889, 0.491, 0.242, 1.059)	(0.598, 0.477, 0.358, 0.255)	-536.835	1083.669	(0.073, 0.038)	(0.374, 0.148)	(0.859, 0.337)	(1.022, 0.412)	(1.495, 0.601)	(3.715, 1.243)
	*	(-0.987, 0.530, 0.192, -)	(0.614, 0.482, 0.352, 0.241)	-540.329	1082.658			(2.099, 2.262)			
s.e.	1	(0.275, 0.101, 0.104, 0.802)	(0.045, 0.030, 0.028, 0.036)			(0.023, 0.027)	(0.356, 0.372)				
	2	(0.292, 0.106, 0.090, 0.722)	(0.048, 0.031, 0.028, 0.037)			(0.023, 0.025)	(0.036, 0.113)	(0.356, 0.490)			
	3	(0.289, 0.104, 0.187, 0.831)	(0.047, 0.032, 0.028, 0.036)			(0.023, 0.037)	(0.044, 0.155)	(0.036, 0.205)	(0.356, 0.779)		
	4	(0.293, 0.106, 0.097, 0.820)	(0.047, 0.031, 0.028, 0.036)			(0.023, 0.030)	(0.038, 0.056)	(0.044, 0.085)	(0.036, 0.125)	(0.356, 0.529)	
	5	(0.299, 0.107, 0.103, 0.653)	(0.050, 0.033, 0.029, 0.036)			(0.023, 0.030)	(0.038, 0.057)	(0.051, 0.117)	(0.036, 0.148)	(0.062, 0.172)	(0.356, 0.763)
	*	(0.162, 0.062, 0.052, -)	(0.027, 0.022, 0.020, 0.024)					(0.099, 0.189)			
RMSE	1	(0.275, 0.084, 0.087, 0.838)	(0.045, 0.031, 0.029, 0.036)								
	2	(0.290, 0.087, 0.112, 0.768)	(0.048, 0.032, 0.029, 0.037)								
	3	(0.280, 0.085, 0.107, 0.889)	(0.047, 0.033, 0.029, 0.036)								
	4	(0.285, 0.087, 0.103, 1.073)	(0.047, 0.032, 0.029, 0.036)								
	5	(0.281, 0.084, 0.102, 0.860)	(0.050, 0.034, 0.030, 0.036)								
	*	(0.181, 0.068, 0.053, -)	(0.030, 0.023, 0.020, 0.026)								
95% C.P.	1		(0.900, 0.933, 0.967, 0.967)								
	2		(0.767, 0.800, 0.833, 0.833)								
	3		(0.900, 0.933, 0.967, 0.967)								
	4		(0.800, 0.833, 0.833, 0.833)								
	5		(0.900, 0.900, 0.933, 0.933)								
	*		(0.733, 0.833, 0.833, 0.800)								
			(Gr-1, Gr-2, Gr-3, Gr-4)								
RISE	1		(0.061, 0.051, 0.052, 0.070)								
	2		(0.067, 0.074, 0.102, 0.139)								
	3		(0.063, 0.066, 0.092, 0.129)								
	4		(0.066, 0.070, 0.095, 0.132)								
	5		(0.065, 0.069, 0.092, 0.127)								
	*		(0.259, 0.168, 0.085, 0.112)								

Table 3.15: Simulation results for COM-Poisson cure rate model ($\phi = 0.5$) having high lifetime ($\gamma_0 = 2.101, \gamma_1 = 2.258$) with light censoring for small sample size.

Measure						$(\tau_i, \hat{\psi}_i)$					
	N	$(\hat{\beta}_0, \hat{\beta}_1, \hat{\gamma}, \hat{\phi})$	$\hat{p}_0$	$\hat{l}$	AIC	$i=0$	$i=1$	$i=2$	$i=3$	$i=4$	$i=5$
$n = 400$ (100, 100, 100, 100)		(-0.038, 0.443, 0.200, 0.500)	(0.400, 0.290, 0.210, 0.150)								
Est	1	(0.015, 0.471, 0.202, 0.517)	(0.381, 0.278, 0.194, 0.132)	-347.393	696.786	(0.054, 0.028)	(3.999, 1.461)				
	2	(0.022, 0.470, 0.204, 0.610)	(0.380, 0.277, 0.193, 0.131)	-345.652	695.304	(0.054, 0.034)	(0.957, 0.406)	(3.999, 1.410)			
	3	(0.014, 0.474, 0.196, 0.465)	(0.381, 0.277, 0.193, 0.130)	-345.079	696.158	(0.054, 0.033)	(0.591, 0.232)	(0.957, 0.395)	(3.999, 1.436)		
	4	(-0.01, 0.482, 0.168, 0.430)	(0.384, 0.278, 0.193, 0.129)	-345.067	698.134	(0.054, 0.032)	(0.352, 0.123)	(0.591, 0.222)	(0.957, 0.371)	(3.999, 1.554)	
	5	(0.004, 0.478, 0.176, 1.010)	(0.382, 0.277, 0.193, 0.130)	-345.108	700.216	(0.054, 0.033)	(0.352, 0.127)	(0.807, 0.310)	(0.957, 0.386)	(1.463, 0.564)	(3.999, 1.563)
	*	(-1.015, 0.553, 0.179, -)	(0.601, 0.469, 0.340, 0.231)	-349.304	700.608			(2.108, 2.178)			
s.e.	1	(0.377, 0.153, 0.121, 0.689)	(0.056, 0.033, 0.031, 0.035)			(0.023, 0.022)	(0.680, 0.501)				
	2	(0.395, 0.160, 0.123, 0.783)	(0.061, 0.035, 0.031, 0.035)			(0.023, 0.023)	(0.045, 0.128)	(0.680, 0.648)			
	3	(0.391, 0.159, 0.118, 0.626)	(0.060, 0.035, 0.031, 0.035)			(0.023, 0.024)	(0.031, 0.080)	(0.045, 0.134)	(0.680, 0.681)		
	4	(0.383, 0.158, 0.140, 0.624)	(0.062, 0.035, 0.032, 0.036)			(0.023, 0.027)	(0.030, 0.067)	(0.031, 0.110)	(0.045, 0.160)	(0.680, 0.737)	
	5	(0.398, 0.162, 0.147, 0.780)	(0.061, 0.036, 0.032, 0.035)			(0.023, 0.025)	(0.030, 0.055)	(0.039, 0.123)	(0.045, 0.162)	(0.061, 0.202)	(0.680, 1.230)
	*	(0.116, 0.047, 0.044, -)	(0.601, 0.469, 0.340, 0.231)					(0.147, 0.219)			
RMSE	1	(0.297, 0.139, 0.095, 0.690)	(0.226, 0.195, 0.159, 0.123)								
	2	(0.334, 0.151, 0.127, 0.791)	(0.228, 0.196, 0.160, 0.124)								
	3	(0.322, 0.150, 0.134, 0.627)	(0.227, 0.196, 0.160, 0.125)								
	4	(0.292, 0.139, 0.135, 0.628)	(0.225, 0.195, 0.160, 0.126)								
	5	(0.311, 0.144, 0.134, 0.932)	(0.226, 0.196, 0.160, 0.125)								
	*	(0.159, 0.070, 0.049, -)	(0.023, 0.024, 0.028, 0.031)								
95% C.P.	1		(0.967, 0.933, 0.933, 0.933)								
	2		(0.933, 0.933, 0.933, 0.933)								
	3		(0.867, 0.867, 0.867, 0.867)								
	4		(0.833, 0.833, 0.833, 0.833)								
	5		(0.967, 0.933, 0.933, 0.933)								
	*		(0.400, 0.600, 0.600, 0.533)								
			(Gr-1, Gr-2, Gr-3, Gr-4)								
RISE	1		(0.070, 0.078, 0.093, 0.112)								
	2		(0.105, 0.125, 0.156, 0.189)								
	3		(0.095, 0.117, 0.146, 0.173)								
	4		(0.089, 0.103, 0.124, 0.144)								
	5		(0.085, 0.101, 0.127, 0.152)								
	*		(0.355, 0.251, 0.123, 0.097)								

Table 3.16: Simulation results for COM-Poisson cure rate model ($\phi = 0.5$) having high lifetime ($\gamma_0 = 2.101, \gamma_1 = 2.258$) with light censoring for large sample size.

Measure						$(\tau_i, \hat{\psi}_i)$					
	N	$(\hat{\beta}_0, \hat{\beta}_1, \hat{\gamma}, \hat{\phi})$	$\hat{p}_0$	$\hat{l}$	AIC	$i=0$	$i=1$	$i=2$	$i=3$	$i=4$	$i=5$
$n = 600$ (150, 150, 150, 150)		(-0.038, 0.443, 0.200, 0.500)	(0.400, 0.290, 0.210, 0.150)								
Est	1	(0.140, 0.370, 0.238, 0.738)	(0.376, 0.294, 0.223, 0.166)	-528.923	1059.845	(0.063, 0.026)	(3.916, 1.413)				
	2	(0.170, 0.365, 0.228, 0.835)	(0.370, 0.289, 0.221, 0.164)	-528.161	1060.322	(0.063, 0.024)	(0.950, 0.349)	(3.916, 1.450)			
	3	(0.163, 0.368, 0.235, 0.839)	(0.371, 0.290, 0.220, 0.164)	-526.593	1059.187	(0.063, 0.025)	(0.579, 0.225)	(0.950, 0.361)	(3.916, 1.448)		
	4	(0.155, 0.370, 0.230, 0.747)	(0.372, 0.290, 0.221, 0.164)	-525.186	1058.372	(0.063, 0.029)	(0.355, 0.123)	(0.579, 0.238)	(0.950, 0.352)	(3.916, 1.494)	
	5	(0.168, 0.365, 0.224, 0.771)	(0.370, 0.290, 0.221, 0.164)	-525.317	1060.634	(0.063, 0.026)	(0.355, 0.117)	(0.793, 0.296)	(0.950, 0.328)	(1.435, 0.551)	(3.916, 1.231)
	*	(-0.987, 0.530, 0.192, -)	(0.614, 0.482, 0.352, 0.241)	-527.206	1056.412			(2.099, 2.262)			
s.e.	1	(0.261, 0.104, 0.089, 0.824)	(0.041, 0.025, 0.025, 0.030)			(0.033, 0.016)	(0.397, 0.359)				
	2	(0.386, 0.148, 0.112, 0.773)	(0.055, 0.029, 0.027, 0.038)			(0.033, 0.013)	(0.032, 0.091)	(0.397, 0.557)			
	3	(0.317, 0.119, 0.084, 0.826)	(0.047, 0.027, 0.025, 0.031)			(0.033, 0.018)	(0.026, 0.090)	(0.032, 0.122)	(0.397, 0.476)		
	4	(0.316, 0.120, 0.085, 0.723)	(0.046, 0.027, 0.025, 0.031)			(0.033, 0.020)	(0.028, 0.061)	(0.026, 0.106)	(0.032, 0.130)	(0.397, 0.497)	
	5	(0.325, 0.121, 0.098, 0.505)	(0.049, 0.029, 0.026, 0.032)			(0.033, 0.017)	(0.028, 0.054)	(0.033, 0.116)	(0.032, 0.137)	(0.033, 0.180)	(0.397, 0.643)
	*	(0.162, 0.062, 0.052, -)	(0.027, 0.022, 0.020, 0.024)					(0.099, 0.189)			
RMSE	1	(0.300, 0.107, 0.085, 0.858)	(0.228, 0.178, 0.129, 0.089)								
	2	(0.299, 0.108, 0.102, 0.842)	(0.236, 0.183, 0.132, 0.094)								
	3	(0.300, 0.107, 0.094, 0.893)	(0.234, 0.182, 0.132, 0.091)								
	4	(0.287, 0.103, 0.094, 0.764)	(0.233, 0.182, 0.131, 0.091)								
	5	(0.296, 0.107, 0.097, 0.573)	(0.235, 0.182, 0.132, 0.092)								
	*	(0.181, 0.068, 0.053, -)	(0.030, 0.023, 0.020, 0.026)								
95% C.P.	1		(0.733, 0.867, 0.900, 0.867)								
	2		(0.833, 0.867, 0.900, 0.900)								
	3		(0.767, 0.767, 0.800, 0.800)								
	4		(0.867, 0.867, 0.900, 0.867)								
	5		(0.867, 0.900, 0.933, 0.933)								
	*		(0.733, 0.833, 0.833, 0.800)								
			(Gr-1, Gr-2, Gr-3, Gr-4)								
RISE	1		(0.077, 0.063, 0.065, 0.084)								
	2		(0.087, 0.091, 0.114, 0.142)								
	3		(0.095, 0.098, 0.118, 0.144)								
	4		(0.093, 0.099, 0.120, 0.147)								
	5		(0.089, 0.094, 0.119, 0.148)								
	*		(0.259, 0.168, 0.085, 0.112)								

Table 3.17: Simulation results for COM-Poisson cure rate model ($\phi = 2$) having high lifetime ($\gamma_0 = 2.101, \gamma_1 = 2.258$) with heavy censoring for small sample size.

Measure						$(\tau_i, \hat{\psi}_i)$					
	N	$(\hat{\beta}_0, \hat{\beta}_1, \hat{\gamma}, \hat{\phi})$	$\hat{p}_0$	$\hat{l}$	AIC	$i=0$	$i=1$	$i=2$	$i=3$	$i=4$	$i=5$
$n = 400$ (100, 100, 100, 100)		(-0.907, 0.501, 0.200, 0.500)	(0.600, 0.470, 0.370, 0.250)								
Est	1	(-0.993, 0.543, 0.212, 1.106)	(0.610, 0.476, 0.346, 0.235)	-570.374	1150.749	(0.117, 0.058)	(4.025, 1.463)				
	2	(-0.987, 0.544, 0.195, 1.113)	(0.609, 0.475, 0.344, 0.234)	-569.371	1150.742	(0.117, 0.056)	(1.218, 0.449)	(4.025, 1.639)			
	3	(-0.987, 0.547, 0.168, 1.103)	(0.608, 0.473, 0.342, 0.231)	-569.250	1152.499	(0.117, 0.057)	(0.780, 0.267)	(1.218, 0.467)	(4.025, 1.695)		
	4	(-0.970, 0.541, 0.164, 1.185)	(0.605, 0.472, 0.342, 0.232)	-568.853	1153.706	(0.117, 0.061)	(0.486, 0.148)	(0.780, 0.275)	(1.218, 0.446)	(4.025, 1.729)	
	5	(-0.975, 0.543, 0.163, 1.687)	(0.606, 0.472, 0.342, 0.232)	-568.203	1154.407	(0.117, 0.061)	(0.486, 0.145)	(1.063, 0.375)	(1.218, 0.436)	(1.795, 0.725)	(4.025, 1.552)
	*	(-0.864, 0.470, 0.184, -)	(0.598, 0.482, 0.482, 0.267)	-570.646	1151.292			(2.228, 2.369)			
s.e.	1	(0.329, 0.122, 0.111, 0.862)	(0.052, 0.035, 0.033, 0.018)			(0.045, 0.034)	(0.303, 0.441)				
	2	(0.331, 0.123, 0.112, 0.915)	(0.053, 0.036, 0.033, 0.018)			(0.045, 0.033)	(0.079, 0.138)	(0.303, 0.714)			
	3	(0.323, 0.120, 0.104, 0.948)	(0.052, 0.036, 0.033, 0.040)			(0.045, 0.036)	(0.048, 0.100)	(0.079, 0.158)	(0.303, 0.719)		
	4	(0.319, 0.127, 0.122, 0.828)	(0.052, 0.036, 0.033, 0.019)			(0.045, 0.043)	(0.034, 0.064)	(0.048, 0.113)	(0.079, 0.160)	(0.303, 0.788)	
	5	(0.342, 0.126, 0.118, 0.586)	(0.055, 0.037, 0.033, 0.018)			(0.045, 0.046)	(0.034, 0.072)	(0.067, 0.169)	(0.079, 0.193)	(0.103, 0.274)	(0.303, 1.199)
	*	(0.120, 0.045, 0.037, -)	(0.021, 0.017, 0.017, 0.019)					(0.097, 0.149)			
RMSE	1	(0.258, 0.102, 0.090, 1.243)	(0.053, 0.036, 0.033, 0.043)								
	2	(0.271, 0.103, 0.103, 1.274)	(0.053, 0.036, 0.033, 0.044)								
	3	(0.270, 0.105, 0.133, 1.305)	(0.052, 0.036, 0.032, 0.044)								
	4	(0.254, 0.101, 0.135, 1.019)	(0.054, 0.036, 0.032, 0.044)								
	5	(0.261, 0.100, 0.117, 0.664)	(0.055, 0.037, 0.034, 0.044)								
	*	(0.127, 0.055, 0.040, -)	(0.021, 0.018, 0.021, 0.025)								
95% C.P.	1		(0.867, 0.900, 0.933, 0.833)								
	2		(0.800, 0.867, 0.900, 0.800)								
	3		(0.867, 0.900, 0.867, 0.833)								
	4		(0.833, 0.900, 0.867, 0.833)								
	5		(0.867, 0.900, 0.900, 0.800)								
	*		(0.700, 0.633, 0.600, 0.600)								
			(Gr-1, Gr-2, Gr-3, Gr-4)								
RISE	1		(0.059, 0.048, 0.073, 0.117)								
	2		(0.067, 0.065, 0.086, 0.125)								
	3		(0.066, 0.072, 0.107, 0.157)								
	4		(0.066, 0.071, 0.106, 0.154)								
	5		(0.060, 0.063, 0.101, 0.148)								
	*		(0.193, 0.244, 0.277, 0.298)								

Table 3.18: Simulation results for COM-Poisson cure rate model ($\phi = 2$) having high lifetime ($\gamma_0 = 2.101, \gamma_1 = 2.258$) with heavy censoring for large sample size.

Measure						$(\tau_i, \hat{\psi}_i)$					
	N	$(\hat{\beta}_0, \hat{\beta}_1, \hat{\gamma}, \hat{\phi})$	$\hat{p}_0$	$\hat{l}$	AIC	$i=0$	$i=1$	$i=2$	$i=3$	$i=4$	$i=5$
$n = 600$ (150, 150, 150, 150)		(-0.907, 0.501, 0.200, 0.500)	(0.600, 0.470, 0.370, 0.250)								
Est	1	(-0.987, 0.547, 0.168, 1.103)	(0.588, 0.465, 0.346, 0.244)	-398.690	807.380	(0.074, 0.034)	(4.327, 1.684)				
	2	(-0.853, 0.496, 0.211, 1.384)	(0.588, 0.464, 0.345, 0.243)	-398.562	809.124	(0.074, 0.032)	(1.253, 0.474)	(4.327, 1.840)			
	3	(-0.853, 0.497, 0.184, 1.337)	(0.588, 0.465, 0.346, 0.243)	-398.073	810.147	(0.074, 0.036)	(0.801, 0.266)	(1.253, 0.501)	(4.327, 1.783)		
	4	(-0.860, 0.500, 0.189, 1.608)	(0.589, 0.465, 0.345, 0.242)	-397.944	811.887	(0.074, 0.038)	(0.481, 0.175)	(0.801, 0.276)	(1.253, 0.508)	(4.327, 1.761)	
	5	(-0.848, 0.497, 0.177, 1.858)	(0.587, 0.463, 0.344, 0.242)	-397.307	812.613	(0.074, 0.037)	(0.481, 0.169)	(1.069, 0.390)	(1.253, 0.501)	(1.789, 0.779)	(4.327, 1.729)
	*	(-0.925, 0.505, 0.209, -)	(0.601, 0.476, 0.476, 0.251)	-399.410	808.819			(2.116, 2.335)			
s.e.	1	(0.255, 0.096, 0.071, 0.790)	(0.226, 0.171, 0.126, 0.095)			(0.018, 0.020)	(0.586, 0.380)				
	2	(0.253, 0.095, 0.067, 0.858)	(0.160, 0.120, 0.090, 0.071)			(0.018, 0.021)	(0.033, 0.117)	(0.586, 0.544)			
	3	(0.254, 0.095, 0.072, 0.815)	(0.226, 0.171, 0.126, 0.095)			(0.018, 0.024)	(0.042, 0.076)	(0.033, 0.135)	(0.586, 0.589)		
	4	(0.254, 0.095, 0.072, 0.635)	(0.225, 0.170, 0.126, 0.095)			(0.018, 0.027)	(0.046, 0.056)	(0.042, 0.089)	(0.033, 0.136)	(0.586, 0.594)	
	5	(0.264, 0.098, 0.070, 0.355)	(0.226, 0.170, 0.125, 0.094)			(0.018, 0.027)	(0.046, 0.054)	(0.039, 0.117)	(0.033, 0.162)	(0.059, 0.208)	(0.586, 0.933)
	*	(0.195, 0.075, 0.056, -)	(0.033, 0.024, 0.024, 0.028)					(0.117, 0.213)			
RMSE	1	(0.186, 0.074, 0.056, 1.002)	(0.226, 0.171, 0.126, 0.095)								
	2	(0.180, 0.074, 0.065, 1.104)	(0.161, 0.121, 0.090, 0.071)								
	3	(0.174, 0.071, 0.070, 1.050)	(0.226, 0.171, 0.126, 0.095)								
	4	(0.176, 0.072, 0.069, 0.746)	(0.226, 0.170, 0.126, 0.095)								
	5	(0.182, 0.073, 0.074, 0.382)	(0.227, 0.171, 0.125, 0.094)								
	*	(0.196, 0.075, 0.057, -)	(0.033, 0.024, 0.024, 0.028)								
95% C.P.	1		(0.967, 0.967, 0.933, 0.933)								
	2		(0.933, 0.933, 0.900, 0.900)								
	3		(0.933, 0.933, 0.900, 0.900)								
	4		(0.933, 0.933, 0.833, 0.900)								
	5		(0.900, 0.900, 0.833, 0.867)								
	*		(0.633, 0.700, 0.700, 0.600)								
			(Gr-1, Gr-2, Gr-3, Gr-4)								
RISE	1		(0.063, 0.055, 0.062, 0.080)								
	2		(0.062, 0.055, 0.062, 0.082)								
	3		(0.064, 0.061, 0.076, 0.105)								
	4		(0.064, 0.061, 0.076, 0.106)								
	5		(0.063, 0.062, 0.080, 0.112)								
	*		(0.095, 0.086, 0.084, 0.084)								

Table 3.19: Simulation results for COM-Poisson cure rate model ($\phi = 2$) having high lifetime ($\gamma_0 = 2.101, \gamma_1 = 2.258$) with light censoring for small sample size.

Measure						$(\tau_i, \hat{\psi}_i)$					
	N	$(\hat{\beta}_0, \hat{\beta}_1, \hat{\gamma}, \hat{\phi})$	$\hat{p}_0$	$\hat{l}$	AIC	$i=0$	$i=1$	$i=2$	$i=3$	$i=4$	$i=5$
$n = 400$ (100, 100, 100, 100)		(-0.038, 0.443, 0.200, 0.500)	(0.400, 0.290, 0.210, 0.150)								
Est	1	(0.031, 0.448, 0.217, 0.988)	(0.382, 0.284, 0.202, 0.139)	-619.873	1249.745	(0.095, 0.044)	(4.010, 1.486)				
	2	(0.041, 0.446, 0.160, 0.967)	(0.381, 0.282, 0.201, 0.139)	-619.841	1251.681	(0.095, 0.029)	(1.237, 0.388)	(4.010, 1.747)			
	3	(0.038, 0.447, 0.126, 1.041)	(0.381, 0.282, 0.201, 0.139)	-619.841	1253.681	(0.095, 0.028)	(0.784, 0.182)	(1.237, 0.355)	(4.010, 1.737)		
	4	(0.036, 0.448, 0.115, 1.298)	(0.381, 0.283, 0.201, 0.139)	-619.626	1255.251	(0.095, 0.032)	(0.491, 0.100)	(0.784, 0.194)	(1.237, 0.344)	(4.010, 1.789)	
	5	(0.013, 0.454, 0.093, 1.722)	(0.385, 0.285, 0.202, 0.139)	-618.941	1255.881	(0.095, 0.031)	(0.491, 0.095)	(1.045, 0.261)	(1.237, 0.338)	(1.771, 0.625)	(4.010, 1.893)
	*	(-0.055, 0.435, 0.191, -)	(0.410, 0.310, 0.310, 0.160)	-625.229	1260.459			(2.201, 2.334)			
s.e.	1	(0.405, 0.157, 0.084, 0.928)	(0.063, 0.034, 0.028, 0.035)			(0.035, 0.025)	(0.185, 0.396)				
	2	(0.317, 0.125, 0.094, 0.940)	(0.048, 0.030, 0.028, 0.030)			(0.035, 0.021)	(0.077, 0.107)	(0.185, 0.600)			
	3	(0.376, 0.156, 0.201, 0.948)	(0.055, 0.031, 0.031, 0.036)			(0.035, 0.024)	(0.078, 0.071)	(0.077, 0.128)	(0.185, 1.075)		
	4	(0.342, 0.137, 0.132, 0.868)	(0.054, 0.031, 0.029, 0.033)			(0.035, 0.024)	(0.057, 0.048)	(0.078, 0.085)	(0.077, 0.128)	(0.185, 0.701)	
	5	(0.334, 0.135, 0.138, 0.423)	(0.053, 0.031, 0.029, 0.033)			(0.035, 0.026)	(0.057, 0.049)	(0.081, 0.111)	(0.077, 0.149)	(0.102, 0.227)	(0.185, 1.135)
	*	(0.113, 0.052, 0.037, -)	(0.018, 0.014, 0.014, 0.015)					(0.085, 0.132)			
RMSE	1	(0.260, 0.077, 0.079, 1.373)	(0.227, 0.190, 0.151, 0.116)								
	2	(0.265, 0.078, 0.144, 1.396)	(0.225, 0.190, 0.151, 0.115)								
	3	(0.272, 0.084, 0.145, 1.348)	(0.226, 0.190, 0.152, 0.117)								
	4	(0.276, 0.081, 0.148, 1.116)	(0.225, 0.190, 0.152, 0.116)								
	5	(0.268, 0.082, 0.142, 0.506)	(0.221, 0.188, 0.151, 0.116)								
	*	(0.115, 0.053, 0.038, -)	(0.021, 0.024, 0.021, 0.018)								
95% C.P.	1		(0.933, 0.867, 0.967, 0.967)								
	2		(0.900, 0.867, 0.900, 0.900)								
	3		(0.900, 0.900, 0.967, 0.967)								
	4		(0.900, 0.867, 0.967, 0.967)								
	5		(0.933, 0.867, 0.900, 0.900)								
	*		(0.533, 0.566, 0.566, 0.583)								
			(Gr-1, Gr-2, Gr-3, Gr-4)								
RISE	1		(0.083, 0.073, 0.068, 0.070)								
	2		(0.110, 0.135, 0.171, 0.210)								
	3		(0.120, 0.154, 0.197, 0.240)								
	4		(0.128, 0.158, 0.195, 0.230)								
	5		(0.129, 0.160, 0.194, 0.224)								
	*		(0.135, 0.156, 0.219, 0.232)								

Table 3.20: Simulation results for COM-Poisson cure rate model ($\phi = 2$) having high lifetime ($\gamma_0 = 2.101, \gamma_1 = 2.258$) with light censoring for large sample size.

Measure						$(\tau_i, \hat{\psi}_i)$					
	N	$(\hat{\beta}_0, \hat{\beta}_1, \hat{\gamma}, \hat{\phi})$	$\hat{p}_0$	$\hat{l}$	AIC	$i=0$	$i=1$	$i=2$	$i=3$	$i=4$	$i=5$
$n = 600$ (150, 150, 150, 150)		(-0.038, 0.443, 0.200, 0.500)	(0.400, 0.290, 0.210, 0.150)								
Est	1	(0.038, 0.447, 0.126, 1.041)	(0.415, 0.302, 0.209, 0.140)	-419.388	848.776	(0.073, 0.035)	(3.982, 1.635)				
	2	(-0.149, 0.493, 0.198, 1.480)	(0.412, 0.300, 0.208, 0.140)	-419.173	850.345	(0.073, 0.039)	(1.180, 0.528)	(3.982, 1.474)			
	3	(-0.147, 0.495, 0.166, 1.443)	(0.414, 0.301, 0.208, 0.139)	-417.729	849.457	(0.073, 0.036)	(0.768, 0.272)	(1.180, 0.502)	(3.982, 1.590)		
	4	(-0.145, 0.493, 0.139, 1.806)	(0.414, 0.301, 0.209, 0.140)	-416.459	848.918	(0.073, 0.034)	(0.455, 0.137)	(0.768, 0.250)	(1.180, 0.460)	(3.982, 1.702)	
	5	(-0.154, 0.497, 0.152, 1.833)	(0.415, 0.301, 0.208, 0.139)	-415.767	849.534	(0.073, 0.039)	(0.455, 0.149)	(1.015, 0.389)	(1.180, 0.497)	(1.713, 0.709)	(3.982, 1.684)
	*	(-0.081, 0.453, 0.202, -)	(0.414, 0.307, 0.307, 0.149)	-418.638	847.277			(2.139, 2.294)			
s.e.	1	(0.264, 0.107, 0.067, 0.808)	(0.042, 0.025, 0.023, 0.026)			(0.026, 0.019)	(0.398, 0.325)				
	2	(0.269, 0.108, 0.069, 0.893)	(0.043, 0.025, 0.023, 0.026)			(0.026, 0.021)	(0.017, 0.115)	(0.398, 0.451)			
	3	(0.268, 0.108, 0.085, 0.769)	(0.043, 0.025, 0.023, 0.026)			(0.026, 0.023)	(0.038, 0.098)	(0.017, 0.164)	(0.398, 0.507)		
	4	(0.271, 0.110, 0.115, 0.510)	(0.043, 0.025, 0.024, 0.027)			(0.026, 0.024)	(0.019, 0.061)	(0.038, 0.107)	(0.017, 0.175)	(0.398, 0.575)	
	5	(0.275, 0.110, 0.125, 0.343)	(0.044, 0.026, 0.024, 0.027)			(0.026, 0.025)	(0.019, 0.066)	(0.024, 0.148)	(0.017, 0.188)	(0.038, 0.211)	(0.398, 0.975)
	*	(0.164, 0.069, 0.057, -)	(0.028, 0.021, 0.019, 0.019)					(0.092, 0.192)			
RMSE	1	(0.264, 0.121, 0.054, 0.961)	(0.191, 0.170, 0.143, 0.113)								
	2	(0.261, 0.121, 0.062, 1.171)	(0.193, 0.172, 0.144, 0.113)								
	3	(0.276, 0.127, 0.107, 0.949)	(0.191, 0.171, 0.144, 0.114)								
	4	(0.279, 0.128, 0.109, 0.546)	(0.191, 0.171, 0.143, 0.113)								
	5	(0.272, 0.125, 0.104, 0.382)	(0.190, 0.171, 0.144, 0.115)								
	*	(0.170, 0.070, 0.057, -)	(0.031, 0.027, 0.020, 0.019)								
95% C.P.	1		(0.800, 0.867, 0.933, 0.867)								
	2		(0.800, 0.867, 0.933, 0.867)								
	3		(0.867, 0.933, 0.933, 0.933)								
	4		(0.800, 0.867, 0.933, 0.867)								
	5		(0.800, 0.867, 0.933, 0.867)								
	*		(0.567, 0.716, 0.766, 0.700)								
			(Gr-1, Gr-2, Gr-3, Gr-4)								
RISE	1		(0.051, 0.049, 0.072, 0.094)								
	2		(0.067, 0.078, 0.104, 0.128)								
	3		(0.068, 0.087, 0.119, 0.148)								
	4		(0.085, 0.109, 0.142, 0.169)								
	5		(0.076, 0.093, 0.125, 0.154)								
	*		(0.359, 0.352, 0.389, 0.407)								

Table 3.21: Model rejection rates based on Likelihood-Ratio Test Criterion (LRT).

True COM - Poisson Model		Fitted Model																	
		N=1			N=2			N=3			N=4			N=5			Weibull Baseline		
Setting	Model	Geometric	Poisson	Bernoulli	Geometric	Poisson	Bernoulli	Geometric	Poisson	Bernoulli	Geometric	Poisson	Bernoulli	Geometric	Poisson	Bernoulli	Geometric	Poisson	Bernoulli
1	$\phi=0$	**0.630**	0.333	0.750	**0.556**	0.083	0.542	**0.481**	0.125	0.556	**0.333**	0.167	0.630	**0.296**	0.083	0.519	**0.040**	0.240	0.720
	$\phi=0.5$	0.222	0.000	0.375	0.407	0.000	0.042	0.222	0.000	0.222	0.185	0.000	0.222	0.111	0.042	0.407	0.200	0.030	0.667
	$\phi=1$	0.778	**0.037**	0.250	0.630	0.000	0.083	0.148	0.000	0.148	0.148	0.000	0.148	0.222	**0.042**	0.296	0.460	**0.040**	0.320
	$\phi=2$	0.704	0.074	0.083	0.481	0.000	0.000	0.259	0.000	0.111	0.185	0.000	0.111	0.259	0.042	0.148	0.833	0.100	0.200
	$\phi\to\infty$	0.963	0.296	**0.125**	0.778	0.125	**0.042**	0.556	0.125	**0.074**	0.593	0.125	**0.148**	0.556	0.083	**0.296**	0.900	0.340	**0.100**
2	$\phi=0$	**0.630**	0.222	0.778	**0.593**	0.111	0.407	**0.519**	0.074	0.519	**0.519**	0.111	0.593	**0.407**	0.111	0.593	**0.060**	0.060	0.460
	$\phi=0.5$	0.667	0.000	0.481	0.481	0.074	0.037	0.296	0.000	0.074	0.222	0.037	0.148	0.259	0.074	0.148	0.266	0.000	0.233
	$\phi=1$	0.963	**0.111**	0.259	0.852	**0.037**	0.222	0.741	0.000	0.259	0.815	**0.074**	0.333	0.667	**0.111**	0.370	0.220	**0.020**	0.340
	$\phi=2$	0.963	0.296	0.037	0.593	0.000	0.037	0.444	0.000	0.111	0.370	0.000	0.074	0.407	0.000	0.111	0.433	0.000	0.066
	$\phi\to\infty$	1.000	0.704	**0.037**	0.926	0.259	**0.222**	0.889	0.185	**0.222**	0.926	0.148	**0.259**	0.889	0.074	**0.222**	0.600	0.040	**0.140**
3	$\phi=0$	**0.267**	0.333	0.800	**0.133**	0.133	0.733	0.000	0.200	0.733	0.000	0.200	0.733	**0.067**	0.267	0.733	**0.120**	0.240	0.900
	$\phi=0.5$	0.667	0.000	0.556	0.444	0.037	0.185	0.296	0.000	0.250	0.259	0.037	0.333	0.222	0.037	0.375	0.533	0.133	0.600
	$\phi=1$	0.852	**0.037**	0.370	0.704	**0.037**	0.222	0.630	**0.037**	0.292	0.444	**0.074**	0.292	0.370	**0.037**	0.375	0.540	**0.120**	0.500
	$\phi=2$	1.000	0.222	0.222	0.556	0.000	0.111	0.296	0.000	0.083	0.259	0.000	0.042	0.222	0.037	0.125	0.767	0.133	0.333
	$\phi\to\infty$	1.000	0.741	0.000	0.963	0.111	**0.074**	0.741	0.037	**0.208**	0.630	0.037	**0.333**	0.556	0.111	**0.292**	0.940	0.380	**0.180**
4	$\phi=0$	**0.333**	0.800	1.000	**0.267**	0.400	0.867	**0.222**	0.333	0.867	**0.185**	0.333	0.800	**0.133**	0.467	0.867	**0.020**	0.080	0.600
	$\phi=0.5$	0.741	0.074	0.889	0.481	0.074	0.296	0.259	0.000	0.296	0.111	0.000	0.259	0.185	0.037	0.333	0.133	0.033	0.566
	$\phi=1$	1.000	**0.133**	0.600	0.933	**0.200**	0.333	0.867	**0.133**	0.400	0.933	**0.200**	0.467	0.933	**0.133**	0.533	0.240	**0.040**	0.360
	$\phi=2$	0.933	0.200	0.200	0.800	0.000	0.000	0.533	0.000	0.067	0.400	0.000	0.067	0.467	0.000	0.133	0.233	0.133	0.266
	$\phi\to\infty$	1.000	0.583	**0.083**	1.000	0.250	**0.167**	0.917	0.167	**0.250**	0.917	0.083	**0.333**	0.833	0.083	**0.167**	0.840	0.100	**0.080**

Table 3.22: Model selection rates based on Akaike's Information Criterion (AIC).

True COM - Poisson Model		Fitted Model																	
		N=1			N=2			N=3			N=4			N=5			Weibull Baseline		
Setting	Model	Geometric	Poisson	Bernoulli	Geometric	Poisson	Bernoulli	Geometric	Poisson	Bernoulli	Geometric	Poisson	Bernoulli	Geometric	Poisson	Bernoulli	Geometric	Poisson	Bernoulli
1	$\phi=0$	**0.549**	0.363	0.088	**0.407**	0.330	0.264	**0.462**	0.286	0.253	**0.484**	0.319	0.198	**0.538**	0.286	0.176	**0.700**	0.280	0.020
	$\phi=0.5$	0.125	0.545	0.330	0.080	0.284	0.636	0.193	0.250	0.557	0.261	0.261	0.477	0.239	0.227	0.534	0.300	0.000	0.700
	$\phi=1$	0.108	**0.506**	0.386	0.193	**0.301**	0.506	0.265	**0.301**	0.434	0.301	**0.361**	0.337	0.325	**0.337**	0.337	0.500	**0.200**	0.300
	$\phi=2$	0.011	0.315	0.674	0.124	0.180	0.697	0.213	0.180	0.607	0.292	0.101	0.607	0.281	0.157	0.562	0.066	0.466	0.467
	$\phi\to\infty$	0.000	0.145	**0.855**	0.024	0.169	**0.807**	0.096	0.205	**0.699**	0.157	0.265	**0.578**	0.145	0.229	**0.627**	0.040	0.100	**0.860**
2	$\phi=0$	**0.539**	0.408	0.053	**0.408**	0.224	0.368	**0.342**	0.355	0.303	**0.487**	0.224	0.289	**0.500**	0.224	0.276	**0.620**	0.300	0.080
	$\phi=0.5$	0.241	0.482	0.277	0.181	0.205	0.614	0.313	0.181	0.506	0.325	0.205	0.470	0.325	0.229	0.446	0.566	0.000	0.444
	$\phi=1$	0.135	**0.392**	0.473	0.135	**0.230**	0.635	0.203	**0.297**	0.500	0.270	**0.270**	0.459	0.270	**0.284**	0.446	0.480	**0.220**	0.300
	$\phi=2$	0.049	0.284	0.667	0.111	0.074	0.815	0.160	0.148	0.691	0.222	0.173	0.605	0.185	0.210	0.605	0.066	0.300	0.633
	$\phi\to\infty$	0.000	0.127	**0.873**	0.089	0.076	**0.835**	0.139	0.089	**0.772**	0.190	0.101	**0.709**	0.177	0.139	**0.684**	0.120	0.180	**0.700**
3	$\phi=0$	**0.726**	0.274	0.000	**0.452**	0.419	0.129	**0.468**	0.419	0.113	**0.516**	0.371	0.113	**0.661**	0.226	0.113	**0.760**	0.220	0.020
	$\phi=0.5$	0.129	0.786	0.086	0.086	0.400	0.514	0.200	0.386	0.414	0.214	0.386	0.400	0.286	0.300	0.414	0.440	0.000	0.560
	$\phi=1$	0.000	**0.694**	0.306	0.059	**0.294**	0.647	0.106	**0.318**	0.576	0.153	**0.329**	0.518	0.188	**0.282**	0.529	0.200	**0.580**	0.220
	$\phi=2$	0.000	0.298	0.702	0.024	0.167	0.810	0.107	0.226	0.667	0.143	0.274	0.583	0.131	0.250	0.619	0.133	0.533	0.333
	$\phi\to\infty$	0.000	0.025	**0.975**	0.013	0.175	**0.813**	0.013	0.225	**0.763**	0.088	0.163	**0.750**	0.113	0.113	**0.775**	0.020	0.300	**0.680**
4	$\phi=0$	**0.563**	0.417	0.021	**0.396**	0.313	0.292	**0.417**	0.313	0.271	**0.500**	0.188	0.313	**0.438**	0.292	0.271	**0.640**	0.280	0.080
	$\phi=0.5$	0.148	0.689	0.164	0.148	0.377	0.475	0.230	0.426	0.344	0.328	0.393	0.279	0.361	0.279	0.361	0.300	0.000	0.700
	$\phi=1$	0.043	**0.557**	0.400	0.057	**0.257**	0.686	0.171	**0.200**	0.629	0.214	**0.214**	0.571	0.229	**0.200**	0.571	0.280	**0.400**	0.320
	$\phi=2$	0.000	0.288	0.713	0.038	0.188	0.775	0.113	0.175	0.713	0.163	0.175	0.663	0.175	0.163	0.663	0.267	0.500	0.233
	$\phi\to\infty$	0.000	0.099	**0.901**	0.014	0.070	**0.915**	0.042	0.141	**0.817**	0.070	0.155	**0.775**	0.099	0.155	**0.746**	0.060	0.180	**0.760**

Table 3.23: AIC, BIC and maximized log-likelihood (l) values for candidate COM-Poisson cure rate models for different numbers of cut points.

COM-Poisson	Quantile-based			Curvature-based		
Model	AIC	BIC	$\hat{l}$	AIC	BIC	$\hat{l}$
	N=1					
Geometric ($\phi = 0$)	1027.039	1047.205	-508.520	1027.039	**1047.205**	-508.520
ϕ=0.5	1030.456	1050.621	-510.228	1030.456	1050.621	-510.228
Poisson ($\phi = 1$)	1032.354	1052.520	-511.177	1032.354	1052.520	-511.177
ϕ=2.0	1034.756	1054.921	-512.378	1034.756	1054.921	-512.378
Bernoulli ($\phi \to \infty$)	1038.062	1058.227	-514.031	1038.062	1058.227	-514.031
	N=2					
Geometric ($\phi = 0$)	1020.463	**1044.662**	-504.232	**1024.892**	1049.091	-506.446
ϕ=0.5	1021.391	1045.590	-504.696	1025.452	1049.650	-506.726
Poisson ($\phi = 1$)	1021.148	1045.346	-504.574	1025.026	1049.225	-506.513
ϕ=2.0	1021.981	1046.180	-504.991	1025.531	1049.730	-506.766
Bernoulli ($\phi \to \infty$)	1022.922	1047.121	-505.461	1026.125	1050.323	-507.062
	N=3					
Geometric ($\phi = 0$)	1022.107	1050.338	-504.053	1026.965	1055.196	-506.482
ϕ=0.5	1024.087	1052.318	-505.043	1027.193	1055.425	-506.597
Poisson ($\phi = 1$)	1024.180	1052.411	-505.090	1026.614	1054.845	-506.307
ϕ=2.0	1025.625	1053.856	-505.812	1026.920	1055.152	-506.460
Bernoulli ($\phi \to \infty$)	1026.197	1054.428	-506.098	1026.588	1054.819	-506.294
	N=4					
Geometric ($\phi = 0$)	1018.922	1051.187	-501.461	1025.262	1057.527	-504.631
ϕ=0.5	1020.226	1052.491	-502.113	1026.164	1058.429	-505.082
Poisson ($\phi = 1$)	1019.621	1051.886	-501.811	1025.876	1058.141	-504.938
ϕ=2.0	1020.027	1052.291	-502.013	1026.678	1058.943	-505.339
Bernoulli ($\phi \to \infty$)	1020.486	1052.751	-502.243	1026.834	1059.099	-505.417
	N=5					
Geometric ($\phi = 0$)	**1017.992**	1054.290	**-499.996**	1026.380	1062.678	**-504.190**
ϕ=0.5	1022.587	1058.885	-502.294	1030.868	1067.166	-506.434
Poisson ($\phi = 1$)	1021.530	1057.828	-501.765	1030.003	1066.301	-506.002
ϕ=2.0	1022.913	1059.211	-502.457	1032.372	1068.669	-507.186
Bernoulli ($\phi \to \infty$)	1022.532	1058.830	-502.266	1030.916	1067.214	-506.458

COM-Poisson	Parametric Weibull PH model		
Model	AIC	BIC	$\hat{l}$
Geometric ($\phi = 0$)	**1028.677**	**1048.842**	**-509.3383**
$\phi = 0.5$	1032.468	1052.633	-511.2338
Poisson ($\phi = 1$)	1034.161	1054.326	-512.0803
$\phi = 2.0$	1036.043	1056.209	-513.0217
Bernoulli ($\phi \to \infty$)	1038.948	1059.114	-514.4741

Table 3.24: Estimates (Est.), standard errors (s.e.), lower confidence limits (LCL) and upper confidence limits (UCL) for the geometric cure rate model.

Quantile-based cut points									
				$(\tau_i, \hat{\psi}_i)$					
Measure	N	$(\hat{\beta}_0, \hat{\beta}_1, \hat{\gamma})$	$\hat{p}_0$	$i=0$	$i=1$	$i=2$	$i=3$	$i=4$	$i=5$
Est	1	(-1.095, 0.463, 0.072)	(0.653, 0.542, 0.427)	(0.148, 0.049)	(7.012, 1.285)				
	2	(-0.637, 0.361, 0.195)	(0.569, 0.479, 0.390)	(0.148, 0.021)	(1.599, 0.208)	(7.012, 0.153)			
	3	(-0.520, 0.338, 0.231)	(0.545, 0.461, 0.379)	(0.148, 0.020)	(0.956, 0.104)	(2.223, 0.202)	(7.012, 0.073)		
	4	(-0.621, 0.362, 0.201)	(0.565, 0.474, 0.386)	(0.148, 0.026)	(0.956, 0.105)	(1.599, 0.231)	(2.223, 0.186)	(7.012, 0.157)	
	5	(-0.527, 0.385, 0.162)	(0.536, 0.440, 0.349)	(0.148, 0.026)	(0.956, 0.099)	(1.599, 0.214)	(2.223, 0.155)	(3.307, 0.155)	(7.012, 0.081)
s.e.	1	(0.296, 0.111, 0.119)	(0.045, 0.033, 0.034)	(-, 0.026)	(-, 0.467)				
	2	(1.185, 0.288, 0.350)	(0.223, 0.162, 0.100)	(-, 0.029)	(-, 0.298)	(-, 0.521)			
	3	(0.621, 0.172, 0.194)	(0.118, 0.089, 0.069)	(-, 0.017)	(-, 0.069)	(-, 0.160)	(-, 0.143)		
	4	(1.056, 0.253, 0.296)	(0.202, 0.149, 0.098)	(-, 0.033)	(-, 0.127)	(-, 0.289)	(-, 0.270)	(-, 0.447)	
	5	(1.022, 0.220, 0.253)	(0.214, 0.18, 0.147)	(-, 0.030)	(-, 0.107)	(-, 0.246)	(-, 0.214)	(-, 0.249)	(-, 0.223)
Lower C.L. (95%)	1	(-1.676, 0.246, -0.161)	(0.564, 0.479, 0.362)	(-, 0.000)	(-, 0.368)				
	2	(-2.960, -0.203, -0.491)	(0.131, 0.162, 0.194)	(-, 0.000)	(-, 0.000)	(-, 0.000)			
	3	(-1.738, 0.002, -0.148)	(0.314, 0.287, 0.244)	(-, 0.000)	(-, 0.000)	(-, 0.000)	(-, 0.000)		
	4	(-2.690, -0.133, -0.379)	(0.169, 0.182, 0.194)	(-, 0.000)	(-, 0.000)	(-, 0.000)	(-, 0.000)	(-, 0.000)	
	5	(-2.531, -0.046, -0.335)	(0.116, 0.088, 0.06)	(-, 0.000)	(-, 0.000)	(-, 0.000)	(-, 0.000)	(-, 0.000)	(-, 0.000)
Upper C.L. (95%)	1	(-0.514, 0.681, 0.306)	(0.742, 0.606, 0.493)	(-, 0.100)	(-, 2.201)				
	2	(1.686, 0.926, 0.882)	(1.006, 0.796, 0.586)	(-, 0.078)	(-, 0.793)	(-, 1.175)			
	3	(0.697, 0.675, 0.611)	(0.777, 0.635, 0.514)	(-, 0.055)	(-, 0.239)	(-, 0.516)	(-, 0.354)		
	4	(1.448, 0.857, 0.781)	(0.960, 0.767, 0.578)	(-, 0.091)	(-, 0.353)	(-, 0.798)	(-, 0.716)	(-, 1.034)	
	5	(1.476, 0.816, 0.658)	(0.955, 0.792, 0.637)	(-, 0.085)	(-, 0.309)	(-, 0.697)	(-, 0.575)	(-, 0.644)	(-, 0.518)
Curvature-based cut points									
				$(\tau_i, \hat{\psi}_i)$					
Measure	N	$(\hat{\beta}_0, \hat{\beta}_1, \hat{\gamma})$	$\hat{p}_0$	$i=0$	$i=1$	$i=2$	$i=3$	$i=4$	$i=5$
Est	1	(-1.095, 0.463, 0.072)	(0.653, 0.542, 0.427)	(0.148, 0.049)	(7.012, 1.285)				
	2	(-0.623, 0.348, 0.234)	(0.569, 0.482, 0.396)	(0.148, 0.030)	(3.000, 0.282)	(7.012, 0.088)			
	3	(-0.469, 0.347, 0.208)	(0.531, 0.444, 0.361)	(0.148, 0.019)	(0.700, 0.087)	(3.000, 0.201)	(7.012, 0.049)		
	4	(-0.350, 0.349, 0.194)	(0.501, 0.414, 0.333)	(0.148, 0.018)	(1.300, 0.128)	(3.200, 0.156)	(3.900, 0.060)	(7.012, 0.137)	
	5	(-0.401, 0.348, 0.204)	(0.513, 0.427, 0.345)	(0.148, 0.022)	(0.700, 0.066)	(1.300, 0.139)	(3.200, 0.162)	(3.900, 0.068)	(7.012, 0.148)
s.e.	1	(0.296, 0.111, 0.119)	(0.045, 0.033, 0.034)	(-, 0.026)	(-, 0.467)				
	2	(0.400, 0.131, 0.142)	(0.071, 0.051, 0.045)	(-, 0.017)	(-, 0.135)	(-, 0.163)			
	3	(0.611, 0.156, 0.184)	(0.130, 0.116, 0.108)	(-, 0.016)	(-, 0.047)	(-, 0.172)	(-, 0.129)		
	4	(1.223, 0.250, 0.281)	(0.090, 0.062, 0.043)	(-, 0.024)	(-, 0.163)	(-, 0.276)	(-, 0.123)	(-, 0.324)	
	5	(0.926, 0.215, 0.244)	(0.191, 0.157, 0.129)	(-, 0.023)	(-, 0.065)	(-, 0.137)	(-, 0.216)	(-, 0.112)	(-, 0.277)
Lower C.L. (95%)	1	(-1.676, 0.246, -0.161)	(0.564, 0.479, 0.362)	(-, 0.000)	(-, 0.368)				
	2	(-2.960, -0.203, -0.491)	(0.429, 0.381, 0.309)	(-, 0.000)	(-, 0.000)	(-, 0.000)			
	3	(-1.738, 0.002, -0.148)	(0.275, 0.216, 0.149)	(-, 0.000)	(-, 0.000)	(-, 0.000)	(-, 0.000)		
	4	(-2.690, -0.133, -0.379)	(0.451, 0.405, 0.338)	(-, 0.000)	(-, 0.000)	(-, 0.000)	(-, 0.000)	(-, 0.000)	
	5	(-2.531, -0.046, -0.335)	(0.138, 0.120, 0.093)	(-, 0.000)	(-, 0.000)	(-, 0.000)	(-, 0.000)	(-, 0.000)	(-, 0.000)
Upper C.L. (95%)	1	(-0.514, 0.681, 0.306)	(0.742, 0.606, 0.493)	(-, 0.100)	(-, 2.201)				
	2	(1.686, 0.926, 0.882)	(0.708, 0.583, 0.484)	(-, 0.078)	(-, 0.793)	(-, 1.175)			
	3	(0.697, 0.675, 0.611)	(0.786, 0.672, 0.573)	(-, 0.055)	(-, 0.239)	(-, 0.516)	(-, 0.354)		
	4	(1.448, 0.857, 0.781)	(0.802, 0.646, 0.507)	(-, 0.091)	(-, 0.353)	(-, 0.798)	(-, 0.716)	(-, 1.034)	
	5	(1.476, 0.816, 0.658)	(0.889, 0.734, 0.597)	(-, 0.085)	(-, 0.309)	(-, 0.697)	(-, 0.575)	(-, 0.644)	(-, 0.518)

Table 3.25: Estimates (Est.), standard errors (s.e.), lower confidence limits (LCL) and upper confidence limits (UCL) for some candidate COM-Poisson cure rate models using three covariates.

		$N=1$		$N=2$		$N=3$		$N=4$		$N=5$	
par	ϕ	Est. (s.e.)	(LCL, UCL)	Est. (s.e.)	(LCL, UCL)	Est. (s.e.)	(LCL, UCL)	Est. (s.e.)	(LCL, UCL)	Est. (s.e.)	(LCL, UCL)
β_0	0	-1.044 (0.592)	(-2.204, 0.117)	-1.204 (1.789)	(-4.710, 2.302)	-0.978 (0.882)	(-2.707, 0.752)	-1.035 (1.139)	(-3.269, 1.198)	-0.916 (1.295)	(-3.453, 1.622)
	1	-0.900 (0.581)	(-2.039, 0.240)	-1.193 (0.984)	(-3.121, 0.735)	-0.776 (0.774)	(-2.293, 0.740)	-0.944 (0.885)	(-2.679, 0.791)	-0.907 (1.202)	(-3.264, 1.450)
	∞	-0.904 (0.594)	(-2.067, 0.260)	-0.885 (0.827)	(-2.506, 0.737)	-0.950 (0.848)	(-2.612, 0.711)	-0.915 (0.793)	(-2.469, 0.638)	-0.922 (0.901)	(-2.689, 0.844)
β_{11}	0	0.296 (0.250)	(-0.194, 0.787)	0.449 (0.631)	(-0.788, 1.686)	0.364 (0.406)	(-0.433, 1.160)	0.374 (0.441)	(-0.489, 1.238)	0.388 (0.475)	(-0.542, 1.318)
	1	0.264 (0.242)	(-0.210, 0.739)	0.508 (0.484)	(-0.440, 1.456)	0.372 (0.431)	(-0.473, 1.216)	0.369 (0.390)	(-0.395, 1.132)	0.330 (0.402)	(-0.457, 1.117)
	∞	0.322 (0.256)	(-0.181, 0.824)	0.431 (0.418)	(-0.389, 1.251)	0.432 (0.535)	(-0.617, 1.482)	0.393 (0.418)	(-0.426, 1.212)	0.388 (0.462)	(-0.517, 1.293)
β_{12}	0	0.015 (0.009)	(-0.003, 0.033)	0.018 (0.026)	(-0.033, 0.070)	0.014 (0.014)	(-0.012, 0.041)	0.015 (0.017)	(-0.018, 0.049)	0.013 (0.019)	(-0.024, 0.051)
	1	0.013 (0.009)	(-0.004, 0.031)	0.017 (0.015)	(-0.014, 0.047)	0.011 (0.013)	(-0.014, 0.036)	0.013 (0.014)	(-0.013, 0.040)	0.013 (0.018)	(-0.021, 0.048)
	∞	0.012 (0.009)	(-0.006, 0.030)	0.012 (0.013)	(-0.014, 0.037)	0.014 (0.014)	(-0.014, 0.041)	0.013 (0.013)	(-0.012, 0.037)	0.013 (0.014)	(-0.015, 0.041)
β_{13}	0	-0.225 (0.250)	(-0.714, 0.264)	-0.319 (0.376)	(-1.055, 0.418)	-0.261 (0.324)	(-0.897, 0.374)	-0.278 (0.324)	(-0.913, 0.358)	-0.306 (0.347)	(-0.987, 0.375)
	1	-0.242 (0.244)	(-0.720, 0.237)	-0.328 (0.369)	(-1.050, 0.395)	-0.256 (0.350)	(-0.942, 0.430)	-0.27 (0.318)	(-0.893, 0.352)	-0.255 (0.308)	(-0.858, 0.347)
	∞	-0.248 (0.248)	(-0.735, 0.239)	-0.277 (0.342)	(-0.947, 0.394)	-0.295 (0.419)	(-1.117, 0.527)	-0.269 (0.337)	(-0.929, 0.391)	-0.255 (0.337)	(-0.916, 0.406)
γ_{21}	0	-0.559 (0.280)	(-1.106, -0.011)	-0.715 (0.814)	(-2.309, 0.880)	-0.649 (0.491)	(-1.610, 0.312)	-0.643 (0.546)	(-1.714, 0.427)	-0.650 (0.601)	(-1.828, 0.527)
	1	-0.396 (0.220)	(-0.828, 0.036)	-0.602 (0.430)	(-1.444, 0.241)	-0.453 (0.379)	(-1.196, 0.291)	-0.474 (0.373)	(-1.205, 0.258)	-0.444 (0.463)	(-1.352, 0.463)
	∞	-0.360 (0.200)	(-0.752, 0.031)	-0.405 (0.301)	(-0.995, 0.186)	-0.365 (0.313)	(-0.979, 0.250)	-0.375 (0.285)	(-0.933, 0.183)	-0.370 (0.325)	(-1.006, 0.267)
γ_{22}	0	-0.003 (0.010)	(-0.023, 0.017)	-0.007 (0.037)	(-0.079, 0.065)	-0.004 (0.018)	(-0.039, 0.031)	-0.004 (0.023)	(-0.049, 0.041)	-0.002 (0.027)	(-0.055, 0.051)
	1	0.003 (0.008)	(-0.012, 0.019)	-0.001 (0.017)	(-0.034, 0.031)	0.005 (0.013)	(-0.021, 0.030)	0.002 (0.015)	(-0.028, 0.032)	0.002 (0.023)	(-0.044, 0.048)
	∞	0.007 (0.007)	(-0.007, 0.020)	0.006 (0.012)	(-0.018, 0.029)	0.005 (0.012)	(-0.018, 0.027)	0.005 (0.011)	(-0.017, 0.028)	0.005 (0.015)	(-0.024, 0.034)
γ_{23}	0	0.201 (0.299)	(-0.385, 0.788)	0.321 (0.483)	(-0.626, 1.268)	0.241 (0.417)	(-0.577, 1.058)	0.264 (0.410)	(-0.539, 1.068)	0.295 (0.440)	(-0.568, 1.158)
	1	0.146 (0.251)	(-0.346, 0.638)	0.221 (0.369)	(-0.502, 0.943)	0.148 (0.369)	(-0.576, 0.872)	0.164 (0.330)	(-0.482, 0.811)	0.143 (0.330)	(-0.504, 0.789)
	∞	0.099 (0.227)	(-0.347, 0.544)	0.080 (0.297)	(-0.503, 0.664)	0.110 (0.331)	(-0.538, 0.759)	0.090 (0.286)	(-0.471, 0.652)	0.071 (0.290)	(-0.497, 0.640)
ψ_0	0	0.181 (0.132)	(-0.078, 0.439)	0.157 (0.409)	(0.000, 0.958)	0.137 (0.172)	(0.000, 0.474)	0.154 (0.246)	(0.000, 0.636)	0.141 (0.271)	(0.000, 0.672)
	1	0.206 (0.119)	(0.000, 0.439)	0.182 (0.209)	(0.000, 0.591)	0.103 (0.094)	(0.000, 0.288)	0.159 (0.168)	(0.000, 0.488)	0.146 (0.250)	(0.000, 0.636)
	∞	0.295 (0.149)	(0.003, 0.587)	0.166 (0.141)	(-0.110, 0.443)	0.133 (0.109)	(0.000, 0.347)	0.191 (0.146)	(0.000, 0.476)	0.170 (0.184)	(0.000, 0.530)
ψ_1	0	3.268 (1.847)	(0.000, 6.888)	1.228 (3.097)	(0.000 7.299)	0.639 (0.735)	(0.000, 2.079)	1.410 (1.655)	(0.000, 4.654)	0.506 (0.941)	(0.000, 2.351)
	1	2.161 (0.951)	(0.297, 4.026)	1.085 (1.149)	(0.000, 3.336)	0.465 (0.359)	(0.000, 1.169)	1.050 (0.820)	(0.000, 2.657)	0.488 (0.820)	(0.000, 2.097)
	∞	1.696 (0.672)	(0.379, 3.013)	0.794 (0.600)	(0.000, 1.970)	0.590 (0.396)	(0.000, 1.366)	0.901 (0.549)	(0.000, 1.977)	0.524 (0.528)	(0.000, 1.560)
ψ_2	0			1.020 (2.485)	(0.000, 5.891)	1.181 (1.317)	(0.000, 3.764)	1.088 (1.931)	(0.000, 3.654)	1.063 (1.989)	(0.000, 4.961)
	1			0.503 (0.864)	(0.000, 2.196)	0.665 (0.520)	(0.000, 1.684)	0.711 (1.005)	(0.000, 2.010)	0.964 (1.631)	(0.000, 4.161)
	∞			0.223 (0.408)	(0.000, 1.022)	0.675 (0.451)	(0.000, 1.560)	0.621 (0.615)	(0.000, 1.370)	0.965 (0.986)	(0.000, 2.897)
ψ_3	0					0.952 (1.402)	(0.000, 3.699)	0.875 (1.461)	(0.000, 1.869)	0.798 (1.520)	(0.000, 3.778)
	1					0.346 (0.608)	(0.000, 1.537)	0.502 (0.877)	(0.000, 1.110)	0.658 (1.146)	(0.000, 2.904)
	∞					0.243 (0.520)	(0.000, 1.262)	0.416 (0.582)	(0.000, 0.778)	0.590 (0.643)	(0.000, 1.850)
ψ_4	0							1.031 (2.389)	(0.000, 1.167)	0.956 (1.894)	(0.000, 4.668)
	1							0.846 (1.903)	(0.000, 0.890)	0.771 (1.422)	(0.000, 3.558)
	∞							0.600 (1.084)	(0.000, 0.552)	0.616 (0.813)	(0.000, 2.210)
ψ_5	0									1.105 (2.883)	(0.000, 6.757)
	1									0.920 (2.383)	(0.000, 5.592)
	∞									0.584 (1.356)	(0.000, 3.241)

Table 3.26: Maximized log-likelihood, AIC & BIC for the E1690 dataset using three covariates.

	Geometric			Poisson			Bernoulli			$\hat{\phi}$		
N	$\hat{l}$	AIC	BIC	$\hat{l}$	AIC	BIC	$\hat{l}$	AIC	BIC	$\hat{l}$	AIC	BIC
1 ($\hat{\phi}$=0)	-536.118	1090.236	1126.725	-537.479	1092.959	1129.449	-539.151	1096.302	1132.792	-536.118	1090.236	1126.725
2 ($\hat{\phi}$=0)	-532.561	**1085.123**	**1125.667**	-532.606	**1085.212**	**1125.757**	-533.040	**1086.080**	**1126.624**	-532.561	**1085.123**	**1125.667**
3 ($\hat{\phi}$=0)	-534.175	1090.349	1134.948	-534.614	1091.227	1135.826	-534.743	1091.485	1136.084	-534.175	1090.349	1134.948
4 ($\hat{\phi} \to \infty$)	-532.121	1088.241	1136.895	-531.739	1087.479	1136.133	-531.824	1087.648	1136.301	-531.739	1087.479	1136.133
5 ($\hat{\phi} \to \infty$)	-532.180	1090.360	1143.068	-532.102	1090.203	1142.911	-531.854	1089.708	1142.415	-531.854	1089.708	1142.415

Chapter 4

Destructive cure rate models under proportional hazards lifetime

4.1 Introduction

We propose the initial number of competing causes M to follow a weighted Poisson distribution, with weight functions as $e^{\phi m}$, m, and $\Gamma(m+\phi^{-1})$, undergoing a damaging process as discussed earlier in Section 1.4. The corresponding models are known as destructive exponentially weighted Poisson (DEWP), destructive length-biased Poisson (DLBP), and destructive negative binomial (DNB) cure rate models respectively. The hazard function $h(.)$ of W_j is defined by a proportional hazards model and is given by

$$h(w) = -\frac{\partial \log S(w)}{\partial w} = h_0(w) e^{\boldsymbol{\gamma}' \boldsymbol{x}}, \tag{4.1.1}$$

for all $j = 1, \ldots, D$, where $h_0(.)$ is the baseline hazard function and $\boldsymbol{x}$ is a vector of covariates with corresponding parameter $\boldsymbol{\gamma}$ of same dimension. The baseline hazard is considered to be a two-parameter Weibull hazard function.

The form of the data and the likelihood function are discussed in detail in Section 4.2. The method of estimation of model parameters using EM algorithm and computation of asymptotic standard errors are provided in Section 4.3. In Section 4.4, an analysis of a real-life data on cutaneous melanoma is presented. In Section 4.5, an extensive simulation study is carried out with various parameter settings and sample sizes to examine the performance of the estimation method. A model discrimination is performed among three candidate models based on information criteria and the results are provided in Section 4.6.

4.2 Form of the data and the likelihood function

In survival analysis, occurrence of right censored data is a common phenomenon which may take place due to patient's discontinuation, duration of study or lost to follow-up. Due to this, we assume a non-informative right censored data for our analysis. In general, if we consider Y_i to be the actual lifetime and C_i to be the censoring time for the i-th individual, then time to event T_i is defined as

$$T_i = \min\{Y_i, C_i\}.$$

T_i denotes the observed lifetime of the i-th individual . The censoring indicator is given by $\delta_i = I(T_i \leq C_i)$ which takes 1 when the actual lifetime is the observed lifetime or 0 when only the censoring time is observed for a subject.

Two sets of covariates $\boldsymbol{x}$ and $\boldsymbol{z}$ are linked to the parameters p and η such that $\eta_i = e^{\boldsymbol{\alpha}'\boldsymbol{z}_i}$ is linked using a log-linear function whereas $p_i = \frac{e^{\boldsymbol{\beta}'\boldsymbol{x}_i}}{1+e^{\boldsymbol{\beta}'\boldsymbol{x}_i}}$ is linked using a logit function where $\boldsymbol{\alpha} = (\alpha_1, \ldots, \alpha_{q_2})'$ and $\boldsymbol{\beta} = (\beta_0, \beta_1, \ldots, \beta_{q_1})'$. To circumvent the issue of non-identifiability of parameters in DEWP, DLBP or DNB cure rate models, $\boldsymbol{\alpha}$ is assumed without an intercept term and covariate $\boldsymbol{x}_i$ is assumed to be disjoint of $\boldsymbol{z}_i$ in the sense that they have no common element (see Li et al., 2001). The observed data for n individuals is of the form $(t_i, \delta_i, \boldsymbol{x}_i, \boldsymbol{z}_i)'; i = 1, \ldots, n$. Hence, the observed data likelihood function can be expressed as

$$L(\boldsymbol{\theta}; \boldsymbol{t}, \boldsymbol{\delta}, \boldsymbol{X}, \boldsymbol{Z}) \propto \prod_{i=1}^{n} f_p(t_i, \boldsymbol{x}_i, \boldsymbol{z}_i; \boldsymbol{\theta})^{\delta_i} S_p(t_i, \boldsymbol{x}_i, \boldsymbol{z}_i; \boldsymbol{\theta})^{1-\delta_i} \tag{4.2.1}$$

where $\boldsymbol{\theta} = (\boldsymbol{\alpha}', \boldsymbol{\beta}', \boldsymbol{\gamma}', \phi)'$, $\boldsymbol{\alpha} = (\alpha_1, \ldots, \alpha_{q_2})'$, $\boldsymbol{\beta} = (\beta_1, \ldots, \beta_{q_1})'$,$\boldsymbol{\gamma} = (\gamma_0, \gamma_1, \boldsymbol{\gamma}_2', \boldsymbol{\gamma}_3')'$, $\boldsymbol{\gamma}_2 = (\gamma_{21}, \ldots, \gamma_{2q_1})'$, $\boldsymbol{\gamma}_3 = (\gamma_{31}, \ldots, \gamma_{3q_2})'$, $\boldsymbol{t} = (t_1, \ldots, t_n)'$, $\boldsymbol{\delta} = (\delta_1, \ldots, \delta_n)'$, $\boldsymbol{X} = (\boldsymbol{x}_1, \ldots, \boldsymbol{x}_n)$ and $\boldsymbol{Z} = (\boldsymbol{z}_1, \ldots, \boldsymbol{z}_n)$. The expressions for $S(w) = S(w, \boldsymbol{x}, \boldsymbol{z}; \boldsymbol{\gamma})$ and $f(w) = f(w, \boldsymbol{x}, \boldsymbol{z}; \boldsymbol{\gamma})$ can be obtained from Equation (4.3.1) using $S(w, \boldsymbol{x}, \boldsymbol{z}; \boldsymbol{\gamma}) = e^{-\int_0^w h(w^*, \boldsymbol{x}, \boldsymbol{z}; \boldsymbol{\gamma}) dw^*}$ and $f(w) = f(w, \boldsymbol{x}, \boldsymbol{z}; \boldsymbol{\gamma}) = -\frac{\partial S(w, \boldsymbol{x}, \boldsymbol{z}; \boldsymbol{\gamma})}{\partial w}$.

4.3 Estimation of parameters and standard errors

We implement EM algorithm to estimate $(\boldsymbol{\alpha}', \boldsymbol{\beta}', \boldsymbol{\gamma}')'$ while ϕ is estimated using profile likelihood method. The missing data are introduced by defining indicator I_i which takes 0 if the i-th individual is cured or 1 otherwise. Note that, $I_i = 1$ for $i \in \Delta_1$, however, I_i is unobserved for $i \in \Delta_0$; $\Delta_1 = \{i : \delta_i = 1\}$ and $\Delta_0 = \{i : \delta_i = 0\}$. The complete data are denoted by $\{(t_i, \delta_i, \boldsymbol{x}_i, \boldsymbol{z}_i, I_i)'; i = 1, \ldots, n\}$. The complete data likelihood function is expressed as

$$\begin{aligned} &L_c(\boldsymbol{\theta}; \boldsymbol{t}, \boldsymbol{x}, \boldsymbol{z}, \boldsymbol{\delta}, \boldsymbol{I}) \\ &\propto \prod_{i \in \Delta_1} f_p(t_i, \boldsymbol{x}_i, \boldsymbol{z}_i; \boldsymbol{\theta}) \prod_{i \in \Delta_0} q_0(\boldsymbol{\alpha}, \boldsymbol{\beta}, \boldsymbol{x}_i, \boldsymbol{z}_i)^{1-I_i} \{(1 - q_0(\boldsymbol{\alpha}, \boldsymbol{\beta}, \boldsymbol{x}_i, \boldsymbol{z}_i)) S_u(t_i, \boldsymbol{x}_i, \boldsymbol{z}_i; \boldsymbol{\theta})\}^{I_i} \end{aligned}$$

and the complete data log-likelihood function is given by

$$\begin{aligned} l_c(\boldsymbol{\theta};\boldsymbol{t},\boldsymbol{x},\boldsymbol{z},\boldsymbol{\delta},\boldsymbol{I}) = \;& \text{constant} + \sum_{i\in\Delta_1}\log f_p(t_i,\boldsymbol{x}_i,\boldsymbol{z}_i;\boldsymbol{\theta}) + \sum_{i\in\Delta_0}(1-I_i)\log q_0(\boldsymbol{\alpha},\boldsymbol{\beta},\boldsymbol{x}_i,\boldsymbol{z}_i) \\ & + \sum_{i\in\Delta_0} I_i \log(1-q_0(\boldsymbol{\alpha},\boldsymbol{\beta},\boldsymbol{x}_i,\boldsymbol{z}_i)) + \sum_{i\in\Delta_0} I_i \log S_u(t_i,\boldsymbol{x}_i,\boldsymbol{z}_i;\boldsymbol{\theta}), \end{aligned} \tag{4.3.1}$$

where $\boldsymbol{I} = (I_1,\ldots,I_n)'$ and $S_u(t_i,\boldsymbol{x}_i,\boldsymbol{z}_i;\boldsymbol{\theta}) = \frac{S_p(t_i,\boldsymbol{x}_i,\boldsymbol{z}_i;\boldsymbol{\theta})-q_0(\boldsymbol{\alpha},\boldsymbol{\beta},\boldsymbol{x}_i,\boldsymbol{z}_i)}{1-q_0(\boldsymbol{\alpha},\boldsymbol{\beta},\boldsymbol{x}_i,\boldsymbol{z}_i)}$.

E-step: For a fixed value ϕ_0 of ϕ and $(a+1)$-th iteration of EM algorithm, we compute the expected value of $l_c(\boldsymbol{\theta};\boldsymbol{t},\boldsymbol{x},\boldsymbol{\delta},\boldsymbol{I})$, given the observed data $\boldsymbol{O} = \{(t_i,\delta_i,\boldsymbol{x}_i,\boldsymbol{z}_i,I_{i'}) : i = 1,\ldots,n; i' \in \Delta_1\}$ and the current parameter estimates $\boldsymbol{\theta}^{*(a)}$ obtained from the a-th iteration, where $\boldsymbol{\theta}^* = (\boldsymbol{\alpha}',\boldsymbol{\beta}',\boldsymbol{\gamma}')'$. Therefore, from Equation (4.3.1) we have

$$\begin{aligned} & \mathbb{E}(l_c(\boldsymbol{\theta};\boldsymbol{t},\boldsymbol{x},\boldsymbol{z},\boldsymbol{\delta},\boldsymbol{I})|\boldsymbol{\theta}^{*(a)},\boldsymbol{O}) \\ = \;& \text{constant} + \sum_{i\in\Delta_1}\log f_p(t_i,\boldsymbol{x}_i,\boldsymbol{z}_i;\boldsymbol{\theta}) + \sum_{i\in\Delta_0}(1-\pi_i^{(a)})\log q_0(\boldsymbol{\alpha},\boldsymbol{\beta},\boldsymbol{x}_i,\boldsymbol{z}_i) \\ & + \sum_{i\in\Delta_0}\pi_i^{(a)}\log(1-q_0(\boldsymbol{\alpha},\boldsymbol{\beta},\boldsymbol{x}_i,\boldsymbol{z}_i)) + \sum_{i\in\Delta_0}\pi_i^{(a)}\log S_u(t_i,\boldsymbol{x}_i,\boldsymbol{z}_i;\boldsymbol{\theta}), \end{aligned} \tag{4.3.2}$$

where

$$\pi_i^{(a)} = \mathbb{E}[I_i|\boldsymbol{O},\boldsymbol{\theta}^{*(a)}] = \left.\frac{(1-q_0(\boldsymbol{\alpha},\boldsymbol{\beta},\boldsymbol{x}_i,\boldsymbol{z}_i))S_u(t_i,\boldsymbol{x}_i,\boldsymbol{z}_i;\boldsymbol{\theta})}{S_p(t_i,\boldsymbol{x}_i,\boldsymbol{z}_i;\boldsymbol{\theta})}\right|_{\boldsymbol{\theta}^*=\boldsymbol{\theta}^{*(a)}}.$$

We define $Q(\boldsymbol{\theta}^*,\boldsymbol{\pi}^{(a)}) = \mathbb{E}(l_c(\boldsymbol{\theta};\boldsymbol{t},\boldsymbol{x},\boldsymbol{z},\boldsymbol{\delta},\boldsymbol{I})|\boldsymbol{\theta}^{*(a)},\boldsymbol{O})$ where $\boldsymbol{\pi}^{(a)} = (\pi_i^{(a)} : i \in \Delta_0)$.

M-step: In the maximization step, we maximize $Q(\boldsymbol{\theta}^*,\boldsymbol{\pi}^{(a)})$ with respect to $\boldsymbol{\theta}^*$ to find the estimate $\boldsymbol{\theta}^{*(a+1)}$ of $\boldsymbol{\theta}^*$. The numerical maximization is carried out using Nelder-Mead or Quasi-Newton method for fixed ϕ_0. Explicit expressions for $Q(\boldsymbol{\theta}^*, \boldsymbol{\pi}^{(a)})$ and the first-order and second-order partial derivatives of $Q(\boldsymbol{\theta}^*, \boldsymbol{\pi}^{(a)})$ are presented in Appendix C.1, C.2 and C.3. The iteration process is considered to converge if $\max_{1\leq k'\leq p}\left|\frac{\hat{\theta^*_{k'}}-\theta^*_{k'}}{\theta^*_{k'}}\right| < \epsilon$, for some small ϵ and p denotes the number of parameters.

The estimation of ϕ is carried out using profile likelihood approach since the likelihood surface is quite flat w.r.t ϕ. The *E-step* and *M-step* are repeated for all $\phi \in \Phi$ where Φ denotes the admissible range of ϕ. The value of $\phi \in \Phi$ which provides the maximum value of the observed likelihood function is taken to be the ML estimate $\hat{\phi}$ of ϕ. For DEWP cure rate model, $\Phi = \{-2.0, -1.9, \ldots, 2.0\}$ while for DNB cure rate model, $\Phi = \{0.10, 0.15, \ldots, 7.00\}$.

The standard errors of the parameter estimates are obtained using Louis' method. The expression for calculating the observed information matrix is given by

$$\begin{aligned} I(\hat{\boldsymbol{\theta}^*}) = \quad & \mathbb{E}[B(\hat{\boldsymbol{\theta}^*}; \boldsymbol{t}, \boldsymbol{x}, \boldsymbol{z}, \boldsymbol{\delta}, \boldsymbol{I})] - \mathbb{E}[S(\hat{\boldsymbol{\theta}^*}; \boldsymbol{t}, \boldsymbol{x}, \boldsymbol{z}, \boldsymbol{\delta}, \boldsymbol{I}) S^T(\hat{\boldsymbol{\theta}^*}; \boldsymbol{t}, \boldsymbol{x}, \boldsymbol{z}, \boldsymbol{\delta}, \boldsymbol{I})] \\ & + \mathbb{E}[S(\hat{\boldsymbol{\theta}^*}; \boldsymbol{t}, \boldsymbol{x}, \boldsymbol{z}, \boldsymbol{\delta}, \boldsymbol{I})] \mathbb{E}[S^T(\hat{\boldsymbol{\theta}^*}; \boldsymbol{t}, \boldsymbol{x}, \boldsymbol{z}, \boldsymbol{\delta}, \boldsymbol{I})] \Big|_{\boldsymbol{\theta}^* = \hat{\boldsymbol{\theta}^*}}, \end{aligned} \tag{4.3.3}$$

where $B(\boldsymbol{\theta}^*; \boldsymbol{t}, \boldsymbol{x}, \boldsymbol{z}, \boldsymbol{\delta}, \boldsymbol{I}) = -\frac{\delta^2 l_c(\boldsymbol{\theta}; \boldsymbol{t}, \boldsymbol{x}, \boldsymbol{z}, \boldsymbol{\delta}, \boldsymbol{I})}{\delta \boldsymbol{\theta}^* \delta \boldsymbol{\theta}^{*'}}$ and $S(\boldsymbol{\theta}^*; \boldsymbol{t}, \boldsymbol{x}, \boldsymbol{x}, \boldsymbol{\delta}, \boldsymbol{I}) = \frac{\delta l_c(\boldsymbol{\theta}; \boldsymbol{t}, \boldsymbol{x}, \boldsymbol{z}, \boldsymbol{\delta}, \boldsymbol{I})}{\delta \boldsymbol{\theta}^*}$. The $100(1-\alpha)\%$ confidence interval (C.I.) of the parameters are obtained by using the asymptotic normality of ML estimators. The expressions for first-order and second-order derivatives of $l_c(\boldsymbol{\theta}; \boldsymbol{t}, \boldsymbol{x}, \boldsymbol{z}, \boldsymbol{\delta}, \boldsymbol{I})$ required for calculating the observed information matrix are not presented separately and can be obtained from Appendices C.1 and C.2.

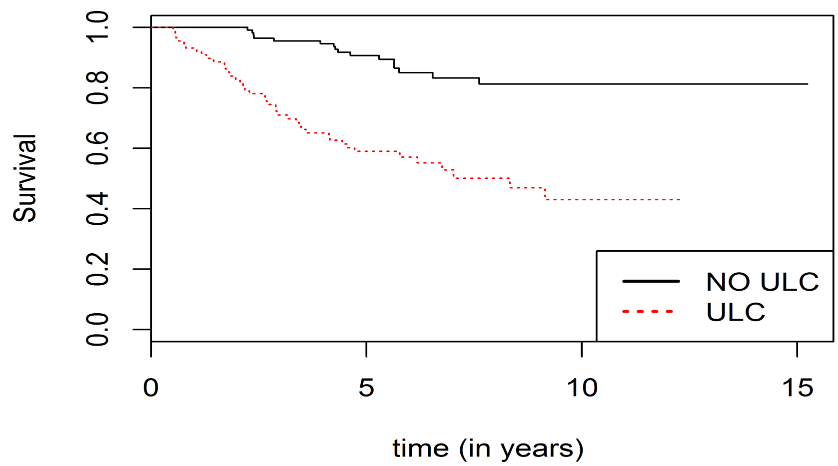

Figure 4.1: K-M plot categorized by ulceration status.

4.4 Analysis of cutaneous melanoma data

The observed time (in years) refers to the time since operation till patient's death or censoring time with mean and standard deviation (s.d.) to be 5.89 and 3.07 years, respectively. For our analysis, ulceration status (absent: $n = 115$; present: $n = 90$) and tumor thickness (in mm) were selected as covariates for the study. 44% of the patients have ulceration status as present. For this group, mean and s.d. of the tumor thickness were found to be 4.34 mm and 3.22 mm. For the group with ulceration status as absent, the mean and s.d. are 1.81 mm and 2.19 mm. The histograms of the tumor thickness for both the groups show positively skewed distributions. Figure 4.1 represents the Kaplan-Meier (KM) plot categorized based on ulceration status. It clearly indicates the presence of cured proportion in the data. We fitted destructive exponentially weighted Poisson, destructive length-biased Poisson and destructive negative binomial cure rate models to the melanoma data, respectively, under proportional hazards assumption of the lifetime of the susceptible. A Weibull baseline hazard function is considered since it provides a great degree of flexibility to the lifetime of the susceptible i.e. increasing, constant and decreasing hazard rate depending on the shape parameter (γ_0) greater than, equal to or less than 1. As mentioned before, we applied EM algorithm to estimate all the parameters except ϕ which was estimated using profile likelihood.

Table 4.1 presents the number of parameters fitted (k), maximized log-likelihood values, Akaike's Information Criterion (AIC) and Bayesian Information Criterion (BIC) values for all the fitted models. Apart from the main three models, the information values for all the sub-models are also presented. It is to be noted that, in case of DEWP, taking $\phi = 0$ reduces the model to destructive Poisson (DP) cure rate model. Again, we get exponentially weighted Poisson (EWP) and Poisson cure rate models by setting $p = 1$ and $(p = 1, \phi = 0)$, respectively. Similarly, in case of DNB, we get the reduced models *viz.*, destructive geometric (DG), negative binomial (NB) and geometric cure rate models by considering $\phi = 1$, $p = 1$ and $(\phi = 1, p = 1)$, respectively. $p = 1$ represents the cases where no destructive mechanism of the malignant cells is considered. When $p = 1$, we linked both the covariates to η using log-linear link function $\eta = \exp(\beta_0 + \beta_1 x + \alpha z)$. It is observed from Table 4.1 that DNB cure rate model provides best fit to the data with highest maximized log-likelihood (-199.108) and minimum AIC (414.216) values with $\hat{\phi} = 5.2$. The estimate, standard error (s.e.), lower confidence limit (LCL) and upper confidence limit (UCL) of the parameters for the three main models are presented in Table 4.2. For validating the heterogeneity among the lifetime of the susceptible , we tested $H_0 : \gamma_2 = \gamma_3 = 0$ for the DNB model. The p-value was found to be 0.061 with log-likelihood value as -201.908, thereby not rejecting H_0 at 5 % level of significance. Again, on testing $H_0 : \phi = 0$ for the full DNB model, we found the corresponding p-value to be 0.027 which provides sufficient evidence of using the DNB model over the DG model.

It is observed from Table 4.1 that incorporating destructive mechanisms to the cure rate models resulted in better log-likelihood, AIC and BIC values, thereby, justifying the practicality of destructive cure rate model over ordinary cure rate model. Table 4.3 shows the effect of using different link functions (e.g., L1-L4) on maximized log-likelihood value for the main three destructive cure rate models. Considering all four possible combinations, we found link L1 that we have used for our analysis (refer Section 4.2) provided with the higher maximized log-likelihood value consistently except in some cases of the DEWP model. However, since the DNB provides the best fit for the data with link L1 among all other links, we can argue that link L1 justifies the appropriateness of using it. Next, we considered representative values for tumor thickness, *viz.*, 0.320, 1.940 and 8.320 mm which are values corresponding to the 5-th, 50-th and 95-th percentiles. For these tumor thicknesses, we plotted the corresponding long-term survival function values, stratified by ulceration status (see Figure 4.2a-4.2c). The estimated survival function values were found to be higher for the group with ulceration status as absent and smaller tumor thicknesses. Figure 4.3 shows the estimated cure rates against tumor thickness stratified by ulceration status. A non-parametric test of difference suggests significant difference (p-value $< 2.2 \times 10^{-16}$) between cure rates of the two ulcer groups.

4.5 Simulation study

This Section demonstrates the performance of our suggested method of estimation and inference based on extensive Monte Carlo simulation study. We generate data set in a way that it mimics the real data on cutaneous melanoma as discussed in Section

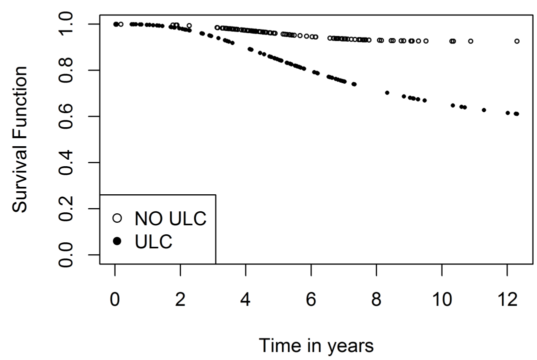

(a) Survival plots stratified by ulceration status with tumor thickness = 0.320 mm.

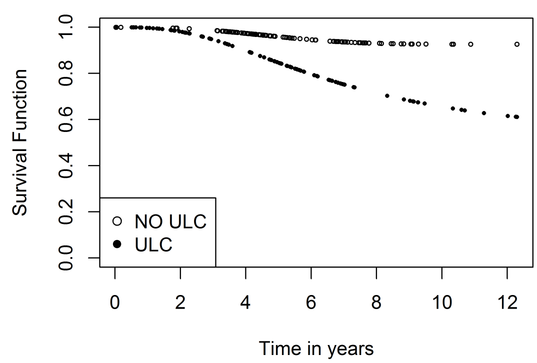

(b) Survival plots stratified by ulceration status with tumor thickness = 1.940 mm.

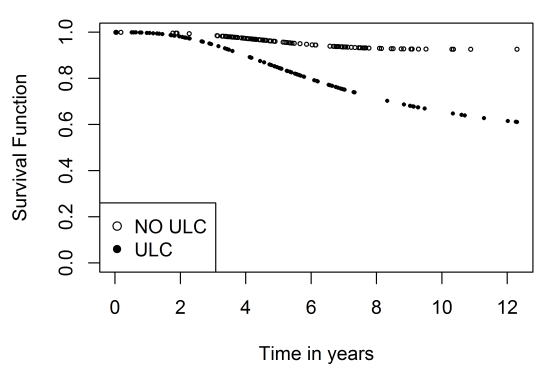

(c) Survival plots stratified by ulceration status with tumor thickness = 8.320 mm.

Figure 4.2: Survival plots stratified by ulceration status.

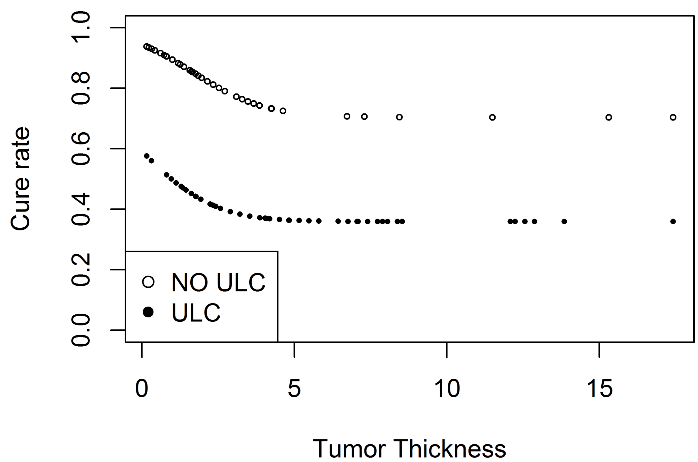

Figure 4.3: Cure rate vs. tumor thickness stratified by ulceration status.

Table 4.1: Maximized log-likelihood, AIC and BIC values for some destructive cure rate models.

Fitted Model	$\boldsymbol{k}$	$\hat{\boldsymbol{l}}$	**AIC**	**BIC**
DEWP ($\hat{\phi} = -0.7$)	8	-202.253	420.506	447.090
DP	7	-203.433	420.865	444.126
EWP ($\hat{\phi} = -1.5$)	8	-205.054	426.108	452.693
Poisson	7	-205.054	424.108	447.370
DLBP	7	-204.979	423.959	447.220
DNB ($\hat{\phi} = 5.2$)	8	**-199.108**	**414.216**	440.800
DG	7	-201.536	417.073	**440.334**
NB ($\hat{\phi} = 6.9$)	8	-199.973	415.946	442.531
Geometric	7	-204.027	422.053	445.314

4.4. For this purpose, we define a random variable (r.v.) U where $U \sim$ Uniform $(0, 1)$. If $U \leq 0.44$, we assign a r.v. $Z = 1$; otherwise $Z = 0$, where Z denotes the ulceration status for each subject. For simulating the tumor thickness data, we plot histograms of tumor thickness (X) from the cutaneous melanoma study. The histograms reveal positively skewed curves for both the ulceration statuses; the means and the standard deviations of which are presented in Section 4.4. Thus, for $Z = 1$, we assume X to follow a Weibull (α_1, α_2) since a Weibull distribution provides flexibility to model any non-negative continuous r.v. In this case, α_1 & α_2 are the shape and scale parameters respectively and are estimated by method of moments, i.e., equating $\alpha_2\Gamma(1 + 1/\alpha_1)$ to 4.34 and $\alpha_2^2\left[\Gamma\left(1+\frac{2}{\alpha_1}\right) - \left(\Gamma\left(1+\frac{1}{\alpha_1}\right)\right)^2\right]$ to $(3.22)^2$. Thus, we generate X using the estimated values of α_1 and α_2. A similar approach is taken to generate X for $Z = 0$ where we assume X from a Weibull (α_3, α_4) where α_3 and α_4 are estimated from $\alpha_4\Gamma(1+1/\alpha_3) = 1.81$ and $\alpha_4^2\left[\Gamma\left(1+\frac{2}{\alpha_3}\right) - \left(\Gamma\left(1+\frac{1}{\alpha_3}\right)\right)^2\right] = (2.19)^2$. As mentioned before, we linked η to z using $\eta = e^{\alpha z}$ and p to x using $p = \frac{e^{\beta_0+\beta_1 x}}{1+e^{\beta_0+\beta_1 x}}$, where an intercept term is not taken for linking η to z in order to avoid non-identifiability. Note that, $\eta = 1$ whenever $z = 0$. Also, a higher value of η signifies greater number of initial competing causes (M). Thus, we can safely assume η to be more than 1 for $z = 1$ since patients with ulceration status: present are likely to have greater value of M. Following the work of Pal and Balakrishnan (2017), we assume $\eta = 3$ for $z = 1$; thereby, we get the true value of $\alpha = 1.099$. In order to determine true values of β_0 and β_1, we turn our attention to $x_{\min} = \min\{x\} = 0.1$ mm and $x_{\max} = \max\{x\} = 17.42$ mm. Note that, the link $p = \frac{e^{\beta_0+\beta_1 x}}{1+e^{\beta_0+\beta_1 x}}$ is a monotonically increasing in x. So, we choose $p_{\min} = \min\{p\}$ and $p_{\max} = \max\{p\}$ and link them to $x_{\min}$ and $x_{\max}$ respectively. Two such choices of ($p_{\min}$, $p_{\max}$) are considered, *viz.*, (0.2, 0.6) and (0.3, 0.9), representing two scenarios of lower and higher proportions of active competing causes. The true values of β_0 and β_1 change depending on the generated values of x for each simulation.

M is generated with weighted Poisson distribution with η. For exponentially weighted Poisson cure rate model, we take true $\phi = -0.5$ and $\phi = 0.2$ and for negative binomial cure rate model, $\phi = 0.5, 0.75$ and 5.2 are taken. These values of ϕ are chosen to relate closely to the estimates of ϕ as obtained from the real data. For length- biased Poisson, M is generated from Poisson (η) + 1 distribution. Given $M = m > 0$, the number of undamaged competing causes D is generated from a binomial distribution with success probability p and m number of trials. If $M = 0$, we put $D = 0$. The true values of the lifetime parameters $(\gamma_0, \gamma_1, \gamma_2, \gamma_3)'$ are considered to be $(1.657, 3.764, -0.005, 0.023)'$ which are parameter estimates as obtained from the real data. If $D > 0$, then we generate $W_1, \ldots, W_D$ where each $W_j; j = 1, \ldots, D$ is simulated from a Weibull distribution with shape parameter γ_0 and scale parameter $\gamma_1 \exp\left(-\frac{\gamma_2 x}{\gamma_0} - \frac{\gamma_3 z}{\gamma_0}\right)$. We define lifetime $Y = \min\{W_1, \ldots, W_D\}$ and the censoring time C is assumed to be distributed exponentially with rate parameter λ. Hence, the observed time T is defined as $T = \min\{Y, C\}$. Again, if $D = 0$, we assign $T = C$. To assess the effect of censoring on the developed methodology, we study three different scenarios: $\lambda = 0.05, 0.15$ and 0.25 representing low, medium and high censoring. On examining $\lambda \in \{0.01, 0.02, \ldots, 1.50\}$ and comparing the proportion of censoring (i.e. no. of times $Y > C$) in 1000 replication, we find $\lambda = 0.05, 0.15$ and 0.25 corresponds to 52%, 64% and 72% of censoring percentages respectively. λ as low as 0.01 gives 45% of censoring whereas $\lambda = 1.50$ results in 95% of censored observations. To further investigate the robustness of the inferential technique, we consider two sample sizes $n = 300$ and $n = 400$ representing moderate and large samples respectively.

As mentioned in Section 4.2, we estimate all the parameters using EM algorithm except ϕ which is estimated using profile likelihood approach. The admissible ranges for ϕ are taken to be $\{-2.00, -1.90, \ldots, 2.00\}$ for DEWP cure rate model and $\{0.10, 0.15, \ldots, 2.00\}$ for DNB cure rate model when true $\phi = 0.5$ or 0.75 and

$\{3.0, 3.1, \ldots, 7.0\}$ when true $\phi = 5.2$. Apart from ϕ, initial parameter value is chosen uniformly from the interval $(0.85\theta_r,\ 1.15\theta_r)$ where θ_r denotes true value of the parameter. In table 4.4 - 4.12, we display the results of our simulation study. More specifically, table 4.4 - 4.6 present the simulation results corresponding to DEWP cure rate model, table 4.7 - 4.8 show results from DLBP cure rate model and table 4.9 - 4.12 depict the simulation results from DNB cure rate model. The accuracy and robustness of our proposed method of estimation are established through average estimated value (Est.), standard error (s.e.), bias, root mean squared error (RMSE), 95 % Confidence Interval (C.I.) and coverage probability (C.P.) under different simulation settings. CPs are obtained by assuming the asymptotic normality of the maximum likelihood (ML) estimators and a nominal level of 95% is used. The results are based on 500 replications of simulated data for each scenario and all calculations are done in R-3.1.3.

From table 4.4 - 4.12, we observe the estimates are quite close to the true parameter values, and the biases are small signifying the accuracy of the estimation technique. Profile likelihood method seems to perform relatively well in terms of accuracy, when data are generated from DEWP ($\phi = -0.5$) and DEWP ($\phi = 0.2$) cure rate models. However, when the true model is DNB, biases are found to be high for the estimates of ϕ. It can be attributed to the fact that the likelihood function is quite flat with respect to ϕ. An under-coverage for β_0 and γ_0 are observed for DEWP and DNB cure rate models respectively. To explain this under-coverage, we take one such setting where data are generated for DEWP model with $\phi = 0.2$ having large sample size $(n = 400)$, $(p_{\min}, p_{\max}) = (0.2, 0.6)$ and low censoring $(\lambda = 0.05)$. We fit DEWP cure rate model to the data and compare effect of estimating ϕ against taking fixed ϕ on coverage probability based on 100 replication. The result is presented in table 4.6. We observe that the coverage probability of β_0 is reaching the nominal level of 95% when ϕ is not estimated. This immediately points toward the imprecision in estimating ϕ (most likely due to flatness of the likelihood surface) which leads to the under-coverage of β_0. The s.e. and RMSE are found to decrease with an increase in sample size and decrease in censoring. Tables corresponding to DEWP with $\phi = -0.5$ and DNB with $\phi = 0.75$ are not presented to avoid repetition, however, can be retrieved from the author on request.

4.6 Model discrimination

To assess the impact of model mis-specification on estimate of cure rate, a model discrimination is performed based on specified selection criteria, e.g., Akaike Information Criterion (AIC) and Bayesian Information Criterion (BIC) values. This allows us to observe the frequency with which models other than the true model get selected through our method of estimation. For this, we generate 1000 samples each from five true models, *viz.*, DEWP ($\phi = -0.5$), DEWP ($\phi = 0.2$), DLBP, DNB ($\phi = 0.5$) and DNB ($\phi = 0.75$) with $(p_{\min}, p_{\max}) = (0.3, 0.9)$, $\eta = 3$ for $Z = 1$ and $\lambda = 0.15$ (i.e. medium censoring). The lifetime parameters are taken as $\boldsymbol{\gamma} = (\gamma_0, \gamma_1, \gamma_2, \gamma_3)' = (1.657, 3.764, -0.005, 0.023)'$ (see Section 4.5). Under these specifications, samples are generated with moderate ($n = 300$) and large ($n = 400$) sample sizes and denoted by Setting 1 and Setting 2 respectively.

We fit three candidate models, i.e., DEWP, DLBP and DNB cure rate models to these samples with our proposed method of estimation. The model with the least AIC or BIC value is selected to provide the best fit to the generated data. For a model, AIC and BIC are defined as:

$$AIC = -2\hat{l} + 2p; \quad BIC = -2\hat{l} + p\log(n),$$

where $\hat{l}$ is the maximized log-likelihood value corresponding to the model and p denotes number of parameters estimated. The selection rates based on AIC, BIC and $\hat{l}$ are presented in Table 4.13. AIC and BIC values are found to be quite low for the true models when the data are generated from DEWP and DNB cure rate models. The reason is attributed to the closeness of the values of log-likelihood function for all the fitted cure rate models. Due to this, AIC and BIC values are getting more penalized for having one extra parameter for DEWP and DNB models. When the log-likelihood value is used to select models, the results indicate more selection for the true models. Table 4.16 shows that when ϕ is not estimated, it results in much better selection rates for the true models.

To establish the importance of a model discrimination, we study the bias and MSE involved in the estimation of cure rate of patients under model mis-specification. For each model, we compute the total relative bias (TRB) as

$$TRB = \sum_{i=1}^{n} \frac{|\hat{q}_{0,i} - q_{0,i}|}{q_{0,i}}$$

where $q_{0,i}$ and $\hat{q}_{0,i}$ denote true and estimated cure rate for an individual $i; i = 1, \ldots, n$. Similarly, we define total mean squared error (TMSE) for a model as

$$TMSE = \frac{1}{n-1} \sum_{i=1}^{n} (\hat{q}_{0,i} - q_{0,i})^2.$$

Then, for two candidate models M1 and M2, total relative efficiency (TRE) of M2 with respect to M1 is defined as $TRE = \frac{TMSE_{M2}}{TMSE_{M1}}$ where $TMSE_{M1}$ and $TMSE_{M2}$ denote TMSE corresponding to M1 and M2 respectively. Thus, with these measures we compare the three candidate models. Table 4.14 presents TRB (in %), TMSE and TRE for the candidate models under Setting 1 and Setting 2, when the data are generated from one of the five true models as described earlier.

The model $M1$ is always chosen to be the true model. It is observed that in cases where data are generated from DLBP cure rate model, model mis-specification may lead to large bias and MSE. It is because higher TRB and lower TRE are observed on fitting candidate models when compared to the true DLBP model. For the other true models, TRB values are relatively closer to each other, thereby signifies not much precision is lost under model mis-specification. DNB cure rate model provides lesser TRB and higher TRE in most of the scenarios. On increasing sample size, TMSE and TRE are found to decrease but TRB increases. Table 4.15 shows TRB and TRE values when using AIC and estimated log-likelihood value ($\hat{l}$) as the model selection criteria. The output suggests that by allowing AIC or $\hat{l}$ to select a working model out of a set of candidate models may lead to lesser relative bias. The TRE values are greater than one is most cases, which implies that estimating the cured proportion on fitting the working model as selected by AIC or $\hat{l}$ results in higher efficiency.

Table 4.2: Estimate, s.e., 95% LCL and 95% UCL for DEWP, DLBP and DNB cure rate models on analyzing cutaneous melanoma data.

Fitted Model	Measure	α	β_0	β_1	γ_0	γ_1	γ_2	γ_3	ϕ
DEWP	Est.	0.761	-1.985	1.265	1.845	7.423	0.112	0.305	-0.700
	s.e.	0.218	0.909	0.646	0.219	1.904	0.043	0.492	-
	LCL	0.333	-3.768	-0.002	1.414	3.689	0.027	-0.660	-
	UCL	1.188	-0.202	2.532	2.276	11.156	0.196	1.270	-
DLBP	Est.	1.527	-2.119	0.081	1.822	8.011	0.115	0.433	-
	s.e.	0.529	0.454	0.053	0.224	2.723	0.046	0.611	-
	LCL	0.489	-3.009	-0.023	1.382	2.672	0.024	-0.765	-
	UCL	2.565	-1.229	0.186	2.263	13.349	0.207	1.633	-
DNB	Est.	3.670	-2.602	1.081	2.845	7.282	0.192	-1.596	5.200
	s.e.	1.205	0.925	0.537	0.328	1.342	0.071	1.236	-
	LCL	1.306	-4.416	0.027	2.201	4.650	0.052	-4.019	-
	UCL	6.033	-0.788	2.136	3.489	9.913	0.332	0.826	-

Table 4.3: Maximized log-likelihood values for destructive cure rate models with other link functions.

Link Function	Model	$\hat{\phi}$	$\hat{l}$
$\eta = e^{\alpha z}, \frac{e^{\beta_0+\beta_1 x}}{1+e^{\beta_0+\beta_1 x}}$ ** (L1)	DEWP	-0.7	-205.253
	DLBP	-	-204.979
	DNB	5.2	-199.108
$\eta = e^{\alpha x}, \frac{e^{\beta_0+\beta_1 z}}{1+e^{\beta_0+\beta_1 z}}$ (L2)	DEWP	-0.4	-205.055
	DLBP	-	-208.289
	DNB	6.9	-199.962
$\eta = e^{\alpha_0+\alpha_1 z}, \frac{e^{\beta x}}{1+e^{\beta x}}$ (L3)	DEWP	-1.0	-203.994
	DLBP	-	-206.786
	DNB	7.2	-201.085
$\eta = e^{\alpha_0+\alpha_1 x}, \frac{e^{\beta z}}{1+e^{\beta z}}$ (L4)	DEWP	-0.2	-205.302
	DLBP	-	-206.667
	DNB	6.4	-200.313

** This link is used for all analysis.

Table 4.4: Estimate, s.e., bias, RMSE, 95% CI and C.P. for destructive exponentially weighted Poisson cure rate model with $\phi = 0.2$ for moderate sample size.

n	$(p_{\min}, p_{\max})$	λ	θ	True Value	Est.	s.e.	bias	RMSE	95% C.I.	C.P.
300	(0.2, 0.6)	0.05	α	1.099	1.076	0.238	-0.023	0.333	(0.609, 1.543)	0.928
			β_0	-1.386	-1.470	0.258	-0.084	0.592	(-1.975, -0.965)	0.472
			β_1	0.142	0.144	0.087	0.037	0.122	(-0.027, 0.315)	0.949
			γ_0	1.658	1.810	0.138	0.153	0.231	(1.539, 2.082)	0.825
			γ_1	3.765	3.863	0.453	0.098	0.625	(2.975, 4.750)	0.940
			γ_2	-0.005	-0.029	0.042	-0.023	0.060	(-0.111, 0.054)	0.924
			γ_3	0.024	-0.167	0.270	-0.191	0.403	(-0.697, 0.363)	0.882
			ϕ	0.200	0.250	-	-	-	-	-
300	(0.3, 0.9)	0.05	α	1.099	1.074	0.201	-0.025	0.278	(0.680, 1.469)	0.934
			β_0	-0.848	-0.999	0.283	-0.151	0.610	(-1.553, -0.445)	0.504
			β_1	0.161	0.305	0.173	0.123	0.262	(-0.033, 0.644)	0.923
			γ_0	1.658	1.842	0.122	0.184	0.236	(1.602, 2.081)	0.702
			γ_1	3.765	3.926	0.386	0.162	0.550	(3.170, 4.683)	0.923
			γ_2	-0.005	-0.043	0.039	-0.038	0.064	(-0.119, 0.033)	0.815
			γ_3	0.024	-0.304	0.245	-0.328	0.447	(-0.785, 0.176)	0.746
			ϕ	0.200	0.289	-	-	-	-	-
300	(0.2, 0.6)	0.15	α	1.099	1.099	0.300	0.000	0.407	(0.511, 1.687)	0.941
			β_0	-1.386	-1.539	0.315	-0.153	0.596	(-2.158, -0.921)	0.693
			β_1	0.097	0.150	0.105	0.042	0.151	(-0.055, 0.355)	0.941
			γ_0	1.658	1.808	0.165	0.150	0.260	(1.484, 2.132)	0.869
			γ_1	3.765	3.809	0.618	0.045	0.836	(2.598, 5.021)	0.932
			γ_2	-0.005	-0.032	0.058	-0.027	0.083	(-0.146, 0.083)	0.925
			γ_3	0.024	-0.212	0.377	-0.236	0.556	(-0.952, 0.527)	0.894
			ϕ	0.200	0.296	-	-	-	-	-
300	(0.3, 0.9)	0.15	α	1.099	1.102	0.271	0.003	0.368	(0.571, 1.633)	0.946
			β_0	-0.848	-1.034	0.360	-0.186	0.668	(-1.739, -0.329)	0.664
			β_1	0.176	0.405	0.268	0.223	0.416	(-0.119, 0.930)	0.909
			γ_0	1.658	1.820	0.145	0.162	0.243	(1.535, 2.104)	0.824
			γ_1	3.765	3.915	0.543	0.150	0.742	(2.850, 4.979)	0.946
			γ_2	-0.005	-0.043	0.052	-0.038	0.080	(-0.144, 0.058)	0.854
			γ_3	0.024	-0.364	0.352	-0.388	0.581	(-1.053, 0.325)	0.821
			ϕ	0.200	0.294	-	-	-	-	-
300	(0.2, 0.6)	0.25	α	1.099	1.101	0.398	0.002	0.522	(0.321, 1.882)	0.953
			β_0	-1.387	-1.526	0.406	-0.139	0.647	(-2.323, -0.728)	0.839
			β_1	0.111	0.174	0.147	0.067	0.210	(-0.114, 0.463)	0.942
			γ_0	1.658	1.817	0.194	0.160	0.296	(1.436, 2.198)	0.900
			γ_1	3.765	3.843	0.870	0.079	1.156	(2.137, 5.550)	0.922
			γ_2	-0.005	-0.030	0.078	-0.024	0.107	(-0.182, 0.122)	0.912
			γ_3	0.024	-0.227	0.524	-0.251	0.723	(-1.254, 0.800)	0.930
			ϕ	0.200	0.286	-	-	-	-	-
300	(0.3, 0.9)	0.25	α	1.099	1.120	0.382	0.021	0.491	(0.372, 1.869)	0.967
			β_0	-0.847	-1.019	0.463	-0.171	0.765	(-1.925, -0.112)	0.812
			β_1	0.142	0.374	0.287	0.190	0.421	(-0.188, 0.936)	0.918
			γ_0	1.658	1.819	0.170	0.162	0.271	(1.486, 2.153)	0.866
			γ_1	3.765	3.950	0.777	0.185	1.014	(2.427, 5.472)	0.960
			γ_2	-0.005	-0.042	0.065	-0.037	0.097	(-0.170, 0.086)	0.887
			γ_3	0.024	-0.395	0.497	-0.419	0.734	(-1.370, 0.580)	0.924
			ϕ	0.200	0.293	-	-	-	-	-

Table 4.5: Estimate, s.e., bias, RMSE, 95% CI and C.P. for destructive exponentially weighted Poisson cure rate model with $\phi = 0.2$ for large sample size.

n	$(p_{\min}, p_{\max})$	λ	θ	True Value	Est.	s.e.	bias	RMSE	95% C.I.	C.P.
400	(0.2, 0.6)	0.05	α	1.099	1.080	0.207	-0.019	0.288	(0.675, 1.485)	0.929
			β_0	-1.386	-1.419	0.222	-0.033	0.568	(-1.855, -0.983)	0.374
			β_1	0.086	0.135	0.072	0.033	0.100	(-0.006, 0.276)	0.948
			γ_0	1.658	1.797	0.119	0.139	0.204	(1.564, 2.030)	0.802
			γ_1	3.765	3.844	0.392	0.079	0.533	(3.076, 4.611)	0.952
			γ_2	-0.005	-0.029	0.036	-0.023	0.052	(-0.099, 0.041)	0.905
			γ_3	0.024	-0.163	0.232	-0.187	0.356	(-0.618, 0.291)	0.874
			ϕ	0.200	0.216	-	-	-	-	-
400	(0.3, 0.9)	0.05	α	1.099	1.081	0.176	-0.018	0.241	(0.736, 1.426)	0.932
			β_0	-0.847	-0.991	0.236	-0.143	0.565	(-1.454, -0.527)	0.448
			β_1	0.153	0.245	0.123	0.071	0.182	(0.005, 0.486)	0.918
			γ_0	1.658	1.832	0.105	0.174	0.213	(1.625, 2.038)	0.652
			γ_1	3.765	3.923	0.337	0.158	0.475	(3.263, 4.583)	0.937
			γ_2	-0.005	-0.043	0.033	-0.038	0.057	(-0.109, 0.023)	0.793
			γ_3	0.024	-0.292	0.211	-0.315	0.404	(-0.706, 0.123)	0.688
			ϕ	0.200	0.293	-	-	-	-	-
400	(0.2, 0.6)	0.15	α	1.099	1.102	0.261	0.003	0.355	(0.589, 1.614)	0.935
			β_0	-1.386	-1.495	0.271	-0.108	0.535	(-2.025, -0.964)	0.642
			β_1	0.120	0.130	0.086	0.027	0.122	(-0.039, 0.300)	0.947
			γ_0	1.658	1.801	0.142	0.143	0.231	(1.522, 2.080)	0.846
			γ_1	3.765	3.836	0.536	0.071	0.733	(2.785, 4.886)	0.943
			γ_2	-0.005	-0.029	0.051	-0.024	0.072	(-0.129, 0.070)	0.920
			γ_3	0.024	-0.193	0.324	-0.217	0.475	(-0.828, 0.443)	0.898
			ϕ	0.200	0.278	-	-	-	-	-
400	(0.3, 0.9)	0.15	α	1.099	1.091	0.233	-0.008	0.318	(0.635, 1.548)	0.931
			β_0	-0.848	-0.983	0.427	-0.136	0.733	(-1.820, -0.147)	0.582
			β_1	0.210	0.295	0.192	0.118	0.282	(-0.081, 0.670)	0.925
			γ_0	1.658	1.810	0.125	0.152	0.217	(1.565, 2.054)	0.789
			γ_1	3.765	3.920	0.470	0.156	0.643	(2.998, 4.842)	0.954
			γ_2	-0.005	-0.046	0.045	-0.041	0.071	(-0.133, 0.042)	0.838
			γ_3	0.024	-0.329	0.300	-0.353	0.511	(-0.917, 0.258)	0.796
			ϕ	0.200	0.313	-	-	-	-	-
400	(0.2, 0.6)	0.25	α	1.099	1.092	0.342	-0.007	0.455	(0.421, 1.763)	0.954
			β_0	-1.386	-1.519	0.347	-0.132	0.557	(-2.199, -0.838)	0.836
			β_1	0.114	0.146	0.112	0.043	0.160	(-0.073, 0.365)	0.940
			γ_0	1.658	1.797	0.167	0.139	0.254	(1.469, 2.124)	0.891
			γ_1	3.765	3.868	0.764	0.103	0.995	(2.371, 5.365)	0.951
			γ_2	-0.005	-0.028	0.067	-0.023	0.092	(-0.160, 0.103)	0.926
			γ_3	0.024	-0.198	0.447	-0.222	0.618	(-1.073, 0.678)	0.928
			ϕ	0.200	0.286	-	-	-	-	-
400	(0.3, 0.9)	0.25	α	1.099	1.105	0.319	0.006	0.413	(0.479, 1.731)	0.962
			β_0	-0.847	-1.008	0.379	-0.160	0.640	(-1.751, -0.265)	0.791
			β_1	0.223	0.350	0.244	0.175	0.362	(-0.129, 0.829)	0.934
			γ_0	1.658	1.799	0.145	0.141	0.232	(1.514, 2.083)	0.850
			γ_1	3.765	3.941	0.670	0.176	0.900	(2.627, 5.255)	0.958
			γ_2	-0.005	-0.045	0.056	-0.040	0.087	(-0.155, 0.066)	0.847
			γ_3	0.024	-0.356	0.416	-0.380	0.634	(-1.171, 0.460)	0.885
			ϕ	0.200	0.286	-	-	-	-	-

Table 4.6: Estimate, s.e., bias, RMSE, 95% CI and C.P. for destructive exponentially weighted Poisson cure rate model with $\phi = 0.2$ for large sample size with $(p_{\min}, p_{\max}) = (0.2, 0.6)$ and $\lambda = 0.05$.

	ϕ is estimated with $\hat{\phi} = 0.597$						
θ	True Value	Est.	s.e.	Bias	RMSE	95%	C.P.
α	1.099	1.064	0.187	-0.035	0.252	(0.698, 1.430)	0.929
β_0	-1.386	-1.809	0.333	-0.422	1.452	(-2.462, -1.156)	0.291
β_1	0.099	0.778	0.570	0.675	0.923	(-0.339, 1.894)	0.899
γ_0	1.658	1.816	0.120	0.158	0.215	(1.581, 2.050)	0.758
γ_1	3.765	3.953	0.391	0.188	0.555	(3.187, 4.718)	0.929
γ_2	-0.005	-0.022	0.035	-0.017	0.049	(-0.091, 0.047)	0.919
γ_3	0.024	-0.148	0.230	-0.172	0.357	(-0.598, 0.302)	0.848
	ϕ is not estimated and fixed at 0.200						
α	1.099	1.086	0.204	-0.013	0.264	(0.685, 1.486)	0.979
β_0	-1.386	-1.348	0.208	0.038	0.276	(-1.756, -0.941)	0.979
β_1	0.099	0.099	0.053	-0.004	0.069	(-0.005, 0.202)	0.989
γ_0	1.658	1.815	0.120	0.157	0.214	(1.581, 2.049)	0.778
γ_1	3.765	3.944	0.390	0.180	0.553	(3.179, 4.709)	0.959
γ_2	-0.005	-0.022	0.036	-0.016	0.050	(-0.092, 0.049)	0.939
γ_3	0.024	-0.154	0.230	-0.178	0.362	(-0.606, 0.297)	0.870

Table 4.7: Estimate, s.e., bias, RMSE, 95% C.I. and C.P. for destructive length-biased Poisson cure rate model for moderate sample size.

n	$(p_{\min}, p_{\max})$	λ	θ	True Value	Est.	s.e.	Bias	RMSE	95% C.I.	C.P.
300	(0.2, 0.6)	0.05	α	1.099	1.083	0.290	-0.016	0.393	(0.515, 1.651)	0.958
			β_0	-1.387	-1.400	0.189	-0.013	0.254	(-1.770, -1.030)	0.957
			β_1	0.108	0.110	0.051	0.003	0.069	(0.010, 0.210)	0.957
			γ_0	1.658	1.799	0.123	0.141	0.208	(1.558, 2.040)	0.813
			γ_1	3.765	3.935	0.378	0.170	0.533	(3.194, 4.676)	0.937
			γ_2	-0.005	-0.027	0.038	-0.022	0.055	(-0.102, 0.047)	0.907
			γ_3	0.024	-0.144	0.240	-0.168	0.356	(-0.616, 0.327)	0.898
300	(0.3, 0.9)	0.05	α	1.099	1.064	0.287	-0.035	0.383	(0.501, 1.627)	0.966
			β_0	-0.847	-0.851	0.195	-0.003	0.262	(-1.233, -0.469)	0.949
			β_1	0.177	0.191	0.074	0.008	0.099	(0.045, 0.337)	0.946
			γ_0	1.658	1.830	0.109	0.173	0.214	(1.617, 2.044)	0.684
			γ_1	3.765	4.005	0.329	0.240	0.491	(3.361, 4.649)	0.901
			γ_2	-0.005	-0.046	0.035	-0.041	0.060	(-0.114, 0.022)	0.787
			γ_3	0.024	-0.281	0.236	-0.305	0.418	(-0.744, 0.182)	0.770
300	(0.2, 0.6)	0.15	α	1.099	1.077	0.387	-0.022	0.505	(0.318, 1.836)	0.982
			β_0	-1.387	-1.404	0.241	-0.018	0.315	(-1.876, -0.932)	0.968
			β_1	0.144	0.110	0.070	0.002	0.092	(-0.027, 0.247)	0.960
			γ_0	1.658	1.799	0.147	0.141	0.233	(1.511, 2.087)	0.868
			γ_1	3.765	3.893	0.515	0.129	0.691	(2.883, 4.903)	0.952
			γ_2	-0.005	-0.028	0.053	-0.023	0.074	(-0.132, 0.075)	0.936
			γ_3	0.024	-0.165	0.340	-0.189	0.480	(-0.832, 0.502)	0.929
300	(0.3, 0.9)	0.15	α	1.099	1.062	0.419	-0.037	0.540	(0.240, 1.884)	0.984
			β_0	-0.848	-0.845	0.253	0.003	0.332	(-1.340, -0.350)	0.970
			β_1	0.132	0.190	0.100	0.007	0.130	(-0.007, 0.386)	0.952
			γ_0	1.658	1.819	0.129	0.162	0.226	(1.567, 2.072)	0.762
			γ_1	3.765	3.972	0.452	0.207	0.620	(3.087, 4.857)	0.956
			γ_2	-0.005	-0.044	0.047	-0.039	0.072	(-0.136, 0.047)	0.850
			γ_3	0.024	-0.323	0.355	-0.347	0.552	(-1.018, 0.372)	0.877
300	(0.2, 0.6)	0.25	α	1.099	1.031	0.546	-0.068	0.679	(-0.038 , 2.100)	0.989
			β_0	-1.387	-1.424	0.314	-0.037	0.403	(-2.039, -0.808)	0.976
			β_1	0.144	0.117	0.094	0.009	0.121	(-0.066, 0.301)	0.953
			γ_0	1.658	1.806	0.172	0.149	0.267	(1.469, 2.143)	0.876
			γ_1	3.765	3.852	0.704	0.087	0.921	(2.471, 5.232)	0.952
			γ_2	-0.005	-0.029	0.070	-0.024	0.097	(-0.168, 0.109)	0.925
			γ_3	0.024	-0.167	0.472	-0.191	0.633	(-1.092, 0.757)	0.955
300	(0.3, 0.9)	0.25	α	1.099	1.020	0.692	-0.079	0.830	(-0.335, 2.375)	0.991
			β_0	-0.847	-0.852	0.330	-0.004	0.424	(-1.499, -0.205)	0.966
			β_1	0.160	0.185	0.124	0.003	0.161	(-0.058, 0.429)	0.943
			γ_0	1.658	1.808	0.149	0.150	0.237	(1.516, 2.099)	0.869
			γ_1	3.765	3.986	0.637	0.221	0.835	(2.736, 5.235)	0.974
			γ_2	-0.005	-0.043	0.058	-0.038	0.085	(-0.157, 0.071)	0.889
			γ_3	0.024	-0.292	0.496	-0.316	0.677	(-1.264, 0.679)	0.955

Table 4.8: Estimate, s.e., bias, RMSE, 95% C.I. and C.P. for destructive length-biased Poisson cure rate model for large sample size.

n	$(p_{\min}, p_{\max})$	λ	θ	True Value	Est.	s.e.	bias	RMSE	95% C.I.	C.P.
400	(0.2, 0.6)	0.05	α	1.099	1.060	0.252	-0.039	0.341	(0.567, 1.553)	0.952
			β_0	-1.386	-1.392	0.163	-0.005	0.220	(-1.711, -1.072)	0.957
			β_1	0.085	0.108	0.044	0.005	0.059	(0.022, 0.194)	0.954
			γ_0	1.658	1.792	0.106	0.135	0.186	(1.584, 2.000)	0.774
			γ_1	3.765	3.922	0.326	0.157	0.466	(3.284, 4.560)	0.926
			γ_2	-0.005	-0.028	0.033	-0.023	0.048	(-0.092, 0.036)	0.892
			γ_3	0.024	-0.139	0.207	-0.163	0.316	(-0.544, 0.266)	0.874
400	(0.3, 0.9)	0.05	α	1.099	1.052	0.247	-0.047	0.333	(0.568, 1.536)	0.961
			β_0	-0.847	-0.852	0.168	-0.004	0.233	(-1.181, -0.522)	0.942
			β_1	0.205	0.186	0.064	0.012	0.087	(0.062, 0.311)	0.942
			γ_0	1.658	1.811	0.093	0.153	0.187	(1.627, 1.994)	0.653
			γ_1	3.765	3.995	0.287	0.231	0.438	(3.433, 4.558)	0.904
			γ_2	-0.005	-0.048	0.03	-0.043	0.056	(-0.108, 0.011)	0.711
			γ_3	0.024	-0.254	0.203	-0.278	0.371	(-0.652, 0.143)	0.736
400	(0.2, 0.6)	0.15	α	1.099	1.062	0.333	-0.037	0.435	(0.409, 1.714)	0.975
			β_0	-1.386	-1.399	0.208	-0.013	0.273	(-1.807, -0.992)	0.964
			β_1	0.097	0.109	0.060	0.006	0.078	(-0.009, 0.227)	0.966
			γ_0	1.658	1.784	0.126	0.126	0.203	(1.537, 2.031)	0.848
			γ_1	3.765	3.895	0.448	0.130	0.599	(3.017, 4.773)	0.963
			γ_2	-0.005	-0.027	0.046	-0.022	0.064	(-0.116, 0.062)	0.920
			γ_3	0.024	-0.165	0.291	-0.189	0.422	(-0.736, 0.407)	0.894
400	(0.3, 0.9)	0.15	α	1.099	1.045	0.346	-0.054	0.447	(0.367, 1.724)	0.980
			β_0	-0.849	-0.852	0.216	-0.004	0.286	(-1.276, -0.428)	0.956
			β_1	0.165	0.180	0.084	0.004	0.110	(0.016, 0.344)	0.939
			γ_0	1.658	1.806	0.111	0.148	0.200	(1.589, 2.023)	0.748
			γ_1	3.765	3.965	0.391	0.200	0.537	(3.198, 4.732)	0.957
			γ_2	-0.005	-0.045	0.040	-0.040	0.065	(-0.124, 0.034)	0.827
			γ_3	0.024	-0.283	0.295	-0.307	0.475	(-0.861, 0.294)	0.856
400	(0.2, 0.6)	0.25	α	1.099	1.055	0.455	-0.044	0.566	(0.163, 1.947)	0.986
			β_0	-1.387	-1.406	0.270	-0.02	0.341	(-1.936, -0.876)	0.981
			β_1	0.093	0.108	0.081	0.005	0.102	(-0.050, 0.266)	0.962
			γ_0	1.658	1.784	0.147	0.127	0.225	(1.496, 2.072)	0.892
			γ_1	3.765	3.892	0.612	0.127	0.791	(2.692, 5.091)	0.973
			γ_2	-0.005	-0.029	0.062	-0.023	0.082	(-0.150, 0.092)	0.950
			γ_3	0.024	-0.150	0.408	-0.174	0.539	(-0.949, 0.649)	0.961
400	(0.3, 0.9)	0.25	α	1.099	1.031	0.553	-0.068	0.659	(-0.053, 2.115)	0.993
			β_0	-0.847	-0.839	0.284	0.009	0.356	(-1.396, -0.282)	0.979
			β_1	0.165	0.176	0.108	0.000	0.138	(-0.037, 0.388)	0.947
			γ_0	1.658	1.799	0.128	0.141	0.212	(1.548, 2.050)	0.830
			γ_1	3.765	3.995	0.547	0.230	0.716	(2.923, 5.067)	0.978
			γ_2	-0.005	-0.042	0.052	-0.037	0.076	(-0.143, 0.059)	0.885
			γ_3	0.024	-0.292	0.421	-0.316	0.593	(-1.117, 0.534)	0.939

Table 4.9: Estimate, s.e., bias, RMSE, 95% C.I. and C.P. for destructive negative binomial ($\phi = 0.5$) cure rate model for moderate sample size.

n	$(p_{\min}, p_{\max})$	λ	θ	True Value	Est.	s.e.	bias	RMSE	95% C.I.	C.P.
300	(0.2, 0.6)	0.05	α	1.099	1.078	0.286	-0.021	0.391	(0.518, 1.639)	0.942
			β_0	-1.387	-1.435	0.290	-0.048	0.393	(-2.004, -0.866)	0.955
			β_1	0.094	0.125	0.085	0.017	0.119	(-0.042, 0.292)	0.946
			γ_0	1.658	1.847	0.158	0.190	0.274	(1.537, 2.158)	0.795
			γ_1	3.765	3.926	0.511	0.161	0.721	(2.925, 4.927)	0.929
			γ_2	-0.005	-0.023	0.047	-0.018	0.065	(-0.115, 0.069)	0.945
			γ_3	0.024	-0.150	0.304	-0.174	0.445	(-0.746, 0.447)	0.899
			ϕ	0.500	0.415	-	-	-	-	-
300	(0.3, 0.9)	0.05	α	1.099	1.022	0.244	-0.077	0.355	(0.544, 1.500)	0.903
			β_0	-0.848	-0.904	0.299	-0.056	0.409	(-1.490, -0.317)	0.943
			β_1	0.168	0.207	0.129	0.024	0.190	(-0.047, 0.461)	0.876
			γ_0	1.658	1.852	0.137	0.195	0.257	(1.584, 2.121)	0.727
			γ_1	3.765	3.932	0.432	0.168	0.613	(3.085, 4.780)	0.944
			γ_2	-0.005	-0.031	0.043	-0.026	0.062	(-0.115, 0.052)	0.896
			γ_3	0.024	-0.233	0.268	-0.256	0.434	(-0.758, 0.293)	0.834
			ϕ	0.500	0.280	-	-	-	-	-
300	(0.2, 0.6)	0.15	α	1.099	1.095	0.358	-0.004	0.491	(0.393, 1.797)	0.939
			β_0	-1.387	-1.465	0.362	-0.078	0.488	(-2.175, -0.754)	0.953
			β_1	0.117	0.135	0.111	0.027	0.155	(-0.082, 0.352)	0.940
			γ_0	1.658	1.848	0.190	0.190	0.310	(1.476, 2.219)	0.842
			γ_1	3.765	3.838	0.690	0.073	0.953	(2.485, 5.191)	0.925
			γ_2	-0.005	-0.024	0.067	-0.018	0.093	(-0.155, 0.108)	0.940
			γ_3	0.024	-0.210	0.429	-0.234	0.621	(-1.051, 0.631)	0.909
			ϕ	0.500	0.414	-	-	-	-	-
300	(0.3, 0.9)	0.15	α	1.099	1.031	0.313	-0.068	0.442	(0.417, 1.645)	0.916
			β_0	-0.847	-0.954	0.383	-0.106	0.522	(-1.705, -0.202)	0.957
			β_1	0.187	0.263	0.183	0.081	0.273	(-0.097, 0.622)	0.891
			γ_0	1.658	1.856	0.165	0.199	0.284	(1.533, 2.179)	0.804
			γ_1	3.765	3.949	0.606	0.184	0.851	(2.761, 5.137)	0.931
			γ_2	-0.005	-0.032	0.057	-0.027	0.082	(-0.145, 0.08)	0.912
			γ_3	0.024	-0.250	0.381	-0.274	0.578	(-0.998, 0.497)	0.875
			ϕ	0.500	0.323	-	-	-	-	-
300	(0.2, 0.6)	0.25	α	1.099	1.088	0.472	-0.011	0.636	(0.162, 2.013)	0.943
			β_0	-1.386	-1.462	0.466	-0.075	0.618	(-2.375, -0.549)	0.962
			β_1	0.124	0.151	0.152	0.043	0.211	(-0.147, 0.449)	0.945
			γ_0	1.658	1.864	0.223	0.207	0.357	(1.427, 2.302)	0.866
			γ_1	3.765	3.797	0.943	0.032	1.270	(1.949, 5.645)	0.905
			γ_2	-0.005	-0.020	0.091	-0.015	0.124	(-0.199, 0.160)	0.931
			γ_3	0.024	-0.252	0.588	-0.276	0.829	(-1.404, 0.901)	0.925
			ϕ	0.500	0.416	-	-	-	-	-
300	(0.3, 0.9)	0.25	α	1.099	1.071	0.424	-0.028	0.565	(0.239, 1.903)	0.953
			β_0	-0.849	-0.949	0.499	-0.101	0.660	(-1.928, 0.030)	0.957
			β_1	0.205	0.312	0.281	0.130	0.394	(-0.238, 0.863)	0.900
			γ_0	1.658	1.850	0.192	0.193	0.311	(1.475, 2.226)	0.844
			γ_1	3.765	3.969	0.854	0.205	1.136	(2.296, 5.643)	0.954
			γ_2	-0.005	-0.029	0.076	-0.024	0.107	(-0.177, 0.120)	0.922
			γ_3	0.024	-0.312	0.536	-0.336	0.755	(-1.362, 0.738)	0.936
			ϕ	0.500	0.349	-	-	-	-	-

Table 4.10: Estimate, s.e., bias, RMSE, 95% C.I. and C.P. for destructive negative binomial ($\phi = 0.5$) cure rate model for large sample size.

n	$(p_{\min}, p_{\max})$	λ	θ	True Value	Est.	s.e.	bias	RMSE	95% C.I.	C.P.
400	(0.2, 0.6)	0.05	α	1.099	1.061	0.246	-0.038	0.352	(0.580, 1.543)	0.916
			β_0	-1.386	-1.432	0.248	-0.045	0.337	(-1.918, -0.946)	0.949
			β_1	0.115	0.116	0.071	0.013	0.101	(-0.022, 0.255)	0.928
			γ_0	1.658	1.827	0.136	0.169	0.241	(1.561, 2.093)	0.786
			γ_1	3.765	3.917	0.441	0.153	0.620	(3.052, 4.782)	0.925
			γ_2	-0.005	-0.023	0.040	-0.018	0.057	(-0.102, 0.056)	0.933
			γ_3	0.024	-0.131	0.262	-0.155	0.383	(-0.645, 0.382)	0.897
			ϕ	0.500	0.369	-	-	-	-	-
400	(0.3, 0.9)	0.05	α	1.099	1.012	0.212	-0.087	0.310	(0.597, 1.426)	0.894
			β_0	-0.847	-0.905	0.255	-0.057	0.349	(-1.404, -0.405)	0.944
			β_1	0.159	0.194	0.107	0.017	0.159	(-0.016, 0.403)	0.869
			γ_0	1.658	1.837	0.117	0.180	0.229	(1.607, 2.068)	0.683
			γ_1	3.765	3.968	0.379	0.203	0.551	(3.225, 4.710)	0.924
			γ_2	-0.005	-0.028	0.036	-0.023	0.053	(-0.100, 0.043)	0.916
			γ_3	0.024	-0.215	0.231	-0.239	0.382	(-0.667, 0.238)	0.806
			ϕ	0.500	0.265	-	-	-	-	-
400	(0.2, 0.6)	0.15	α	1.099	1.059	0.310	-0.040	0.430	(0.452, 1.667)	0.931
			β_0	-1.387	-1.450	0.312	-0.063	0.417	(-2.062, -0.838)	0.959
			β_1	0.098	0.128	0.097	0.024	0.135	(-0.062, 0.318)	0.931
			γ_0	1.658	1.816	0.162	0.158	0.264	(1.498, 2.133)	0.855
			γ_1	3.765	3.873	0.615	0.109	0.833	(2.669, 5.078)	0.959
			γ_2	-0.005	-0.024	0.057	-0.019	0.079	(-0.136, 0.088)	0.935
			γ_3	0.024	-0.166	0.367	-0.190	0.531	(-0.886, 0.554)	0.910
			ϕ	0.500	0.381	-	-	-	-	-
400	(0.3, 0.9)	0.15	α	1.099	1.048	0.271	-0.051	0.381	(0.517, 1.579)	0.928
			β_0	-0.847	-0.936	0.323	-0.088	0.442	(-1.568, -0.304)	0.941
			β_1	0.213	0.222	0.145	0.045	0.217	(-0.062, 0.505)	0.885
			γ_0	1.658	1.831	0.141	0.174	0.246	(1.556, 2.107)	0.774
			γ_1	3.765	3.936	0.526	0.171	0.724	(2.905, 4.966)	0.946
			γ_2	-0.005	-0.031	0.050	-0.025	0.073	(-0.129, 0.068)	0.906
			γ_3	0.024	-0.259	0.326	-0.283	0.502	(-0.898, 0.381)	0.871
			ϕ	0.5	0.303	-	-	-	-	-
400	(0.2, 0.6)	0.25	α	1.099	1.074	0.400	-0.025	0.537	(0.290, 1.857)	0.946
			β_0	-1.387	-1.454	0.398	-0.067	0.529	(-2.234, -0.674)	0.957
			β_1	0.094	0.131	0.119	0.027	0.164	(-0.103, 0.365)	0.945
			γ_0	1.658	1.826	0.190	0.169	0.297	(1.454, 2.199)	0.882
			γ_1	3.765	3.856	0.841	0.092	1.140	(2.208, 5.504)	0.922
			γ_2	-0.005	-0.027	0.077	-0.022	0.105	(-0.177, 0.123)	0.933
			γ_3	0.024	-0.194	0.503	-0.218	0.695	(-1.180, 0.792)	0.935
			ϕ	0.500	0.399	-	-	-	-	-
400	(0.3, 0.9)	0.25	α	1.099	1.068	0.361	-0.031	0.492	(0.361 , 1.775)	0.936
			β_0	-0.847	-0.944	0.413	-0.096	0.553	(-1.754, -0.133)	0.944
			β_1	0.204	0.240	0.186	0.064	0.267	(-0.124, 0.604)	0.895
			γ_0	1.658	1.824	0.164	0.166	0.266	(1.502, 2.146)	0.856
			γ_1	3.765	3.935	0.733	0.170	0.976	(2.498, 5.372)	0.951
			γ_2	-0.005	-0.029	0.065	-0.024	0.092	(-0.156, 0.097)	0.912
			γ_3	0.024	-0.302	0.453	-0.326	0.660	(-1.191, 0.587)	0.916
			ϕ	0.500	0.327	-	-	-	-	-

Table 4.11: Estimate, s.e., bias, RMSE, 95% C.I. and C.P. for destructive negative binomial ($\phi = 5.2$) cure rate model for moderate sample size.

n	$(p_{\min}, p_{\max})$	λ	θ	True Value	Est.	s.e.	bias	RMSE	95% C.I.	C.P.
300	(0.2, 0.6)	0.05	α	1.099	0.963	0.486	-0.136	0.685	(0.010, 1.915)	0.906
			β_0	-1.387	-0.592	0.479	0.795	1.671	(-1.530, 0.346)	0.914
			β_1	0.095	0.088	0.216	-0.020	0.463	(-0.335, 0.510)	0.908
			γ_0	1.658	2.028	0.224	0.370	0.458	(1.588, 2.467)	0.650
			γ_1	3.765	4.275	0.676	0.510	1.022	(2.950, 5.599)	0.898
			γ_2	-0.005	-0.016	0.074	-0.010	0.100	(-0.160, 0.129)	0.942
			γ_3	0.024	-0.189	0.442	-0.213	0.629	(-1.056, 0.677)	0.908
			ϕ	5.200	4.149	-	-	-	-	-
300	(0.3, 0.9)	0.05	α	1.099	0.860	0.452	-0.239	0.681	(-0.025, 1.745)	0.871
			β_0	-0.848	-0.677	0.665	0.171	1.330	(-1.980, 0.626)	0.867
			β_1	0.138	0.470	0.466	0.289	0.753	(-0.443, 1.383)	0.863
			γ_0	1.658	2.033	0.201	0.376	0.442	(1.640, 2.426)	0.590
			γ_1	3.765	4.405	0.631	0.640	1.051	(3.167, 5.642)	0.829
			γ_2	-0.005	-0.020	0.067	-0.015	0.092	(-0.152, 0.111)	0.940
			γ_3	0.024	-0.227	0.407	-0.251	0.594	(-1.024, 0.570)	0.904
			ϕ	5.200	3.893	-	-	-	-	-
300	(0.2, 0.6)	0.15	α	1.099	1.006	0.625	-0.093	0.892	(-0.219, 2.230)	0.918
			β_0	-1.387	-0.960	0.590	0.427	1.469	(-2.116, 0.196)	0.922
			β_1	0.092	0.089	0.225	-0.019	0.422	(-0.352, 0.530)	0.944
			γ_0	1.658	2.048	0.273	0.390	0.517	(1.512, 2.584)	0.729
			γ_1	3.765	4.154	0.961	0.389	1.322	(2.271, 6.037)	0.944
			γ_2	-0.005	-0.021	0.108	-0.016	0.152	(-0.233, 0.192)	0.926
			γ_3	0.024	-0.275	0.657	-0.299	0.958	(-1.564, 1.013)	0.912
			ϕ	5.200	4.177	-	-	-	-	-
300	(0.3, 0.9)	0.15	α	1.099	0.976	0.597	-0.123	0.846	(-0.195, 2.147)	0.911
			β_0	-0.847	1.715	0.886	2.563	3.939	(-0.022, 3.452)	0.901
			β_1	0.136	0.212	0.494	0.030	1.030	(-0.756, 1.179)	0.866
			γ_0	1.658	2.040	0.243	0.382	0.481	(1.564, 2.516)	0.694
			γ_1	3.765	4.315	0.905	0.550	1.267	(2.541, 6.089)	0.949
			γ_2	-0.005	-0.023	0.098	-0.018	0.138	(-0.216, 0.170)	0.935
			γ_3	0.024	-0.328	0.624	-0.352	0.894	(-1.550, 0.894)	0.927
			ϕ	5.200	4.070	-	-	-	-	-
300	(0.2, 0.6)	0.25	α	1.099	1.029	0.847	-0.070	1.159	(-0.631, 2.690)	0.914
			β_0	-1.386	-1.539	1.042	-0.152	1.390	(-3.582, 0.504)	0.931
			β_1	0.061	0.284	0.380	0.176	0.548	(-0.462, 1.029)	0.937
			γ_0	1.658	2.047	0.320	0.390	0.560	(1.419, 2.675)	0.800
			γ_1	3.765	4.238	1.493	0.474	1.990	(1.312, 7.164)	0.904
			γ_2	-0.005	-0.009	0.145	-0.004	0.210	(-0.293, 0.274)	0.890
			γ_3	0.024	-0.381	0.955	-0.405	1.337	(-2.253, 1.490)	0.921
			ϕ	5.200	4.225	-	-	-	-	-
300	(0.3, 0.9)	0.25	α	1.099	1.075	0.843	-0.024	1.161	(-0.577, 2.727)	0.892
			β_0	-0.848	-0.989	1.042	-0.141	1.499	(-3.031, 1.053)	0.917
			β_1	0.211	0.501	0.638	0.316	0.919	(-0.750, 1.751)	0.865
			γ_0	1.658	2.044	0.284	0.387	0.522	(1.487, 2.602)	0.771
			γ_1	3.765	4.358	1.309	0.594	1.789	(1.794, 6.923)	0.942
			γ_2	-0.005	-0.004	0.136	0.001	0.193	(-0.270, 0.262)	0.917
			γ_3	0.024	-0.507	0.939	-0.531	1.352	(-2.347, 1.334)	0.909
			ϕ	5.200	3.933	-	-	-	-	-

Table 4.12: Estimate, s.e., bias, RMSE, 95% C.I. and C.P. for destructive negative binomial ($\phi = 5.2$) cure rate model for large sample size.

n	$(p_{\min}, p_{\max})$	λ	θ	True Value	Est.	s.e.	bias	RMSE	95% C.I.	C.P.
400	(0.2, 0.6)	0.05	α	1.099	0.986	0.417	-0.113	0.599	(0.168, 1.804)	0.924
			β_0	-1.386	-1.548	0.383	-0.161	0.540	(-2.298, -0.798)	0.934
			β_1	0.134	0.127	0.138	0.024	0.201	(-0.145, 0.398)	0.910
			γ_0	1.658	1.968	0.188	0.310	0.386	(1.598, 2.337)	0.658
			γ_1	3.765	4.182	0.579	0.417	0.857	(3.047, 5.316)	0.932
			γ_2	-0.005	-0.021	0.062	-0.016	0.084	(-0.142, 0.100)	0.954
			γ_3	0.024	-0.204	0.375	-0.228	0.549	(-0.939, 0.531)	0.916
			ϕ	5.200	3.880	-	-	-	-	-
400	(0.3, 0.9)	0.05	α	1.099	0.861	0.395	-0.238	0.607	(0.087, 1.635)	0.851
			β_0	-0.847	-0.377	0.456	0.471	1.443	(-1.271, 0.517)	0.876
			β_1	0.184	0.272	0.323	0.096	0.558	(-0.362, 0.905)	0.847
			γ_0	1.658	2.004	0.171	0.346	0.397	(1.668, 2.339)	0.514
			γ_1	3.765	4.351	0.541	0.586	0.913	(3.291, 5.411)	0.845
			γ_2	-0.005	-0.025	0.058	-0.019	0.081	(-0.139, 0.089)	0.922
			γ_3	0.024	-0.200	0.349	-0.224	0.524	(-0.885, 0.485)	0.900
			ϕ	5.200	3.770	-	-	-	-	-
400	(0.2, 0.6)	0.15	α	1.099	0.933	0.527	-0.166	0.758	(-0.100, 1.966)	0.896
			β_0	-1.386	-1.577	0.498	-0.190	0.708	(-2.552, -0.601)	0.948
			β_1	0.087	0.211	0.218	0.107	0.323	(-0.217, 0.639)	0.934
			γ_0	1.658	1.984	0.228	0.326	0.429	(1.536, 2.431)	0.733
			γ_1	3.765	4.223	0.834	0.458	1.179	(2.588, 5.857)	0.944
			γ_2	-0.005	-0.022	0.092	-0.017	0.128	(-0.202, 0.157)	0.900
			γ_3	0.024	-0.229	0.551	-0.253	0.764	(-1.309, 0.851)	0.932
			ϕ	5.200	4.043	-	-	-	-	-
400	(0.3, 0.9)	0.15	α	1.099	0.928	0.507	-0.171	0.732	(-0.066, 1.922)	0.909
			β_0	-0.847	-1.035	0.633	-0.187	0.927	(-2.277, 0.206)	0.913
			β_1	0.183	0.445	0.413	0.271	0.654	(-0.364, 1.254)	0.842
			γ_0	1.658	1.997	0.206	0.339	0.417	(1.594, 2.400)	0.645
			γ_1	3.765	4.379	0.792	0.614	1.206	(2.826, 5.932)	0.917
			γ_2	-0.005	-0.014	0.085	-0.009	0.116	(-0.180, 0.152)	0.941
			γ_3	0.024	-0.312	0.522	-0.336	0.761	(-1.335, 0.7110)	0.917
			ϕ	5.200	3.834	-	-	-	-	-
400	(0.2, 0.6)	0.25	α	1.099	1.006	0.722	-0.093	0.998	(-0.409, 2.421)	0.918
			β_0	-1.386	-1.544	0.707	-0.158	1.065	(-2.929, -0.159)	0.926
			β_1	0.106	0.229	0.290	0.126	0.435	(-0.340, 0.797)	0.922
			γ_0	1.658	1.968	0.268	0.311	0.461	(1.443, 2.493)	0.817
			γ_1	3.765	4.253	1.290	0.488	1.752	(1.725, 6.780)	0.920
			γ_2	-0.005	-0.018	0.125	-0.013	0.176	(-0.263, 0.227)	0.912
			γ_3	0.024	-0.284	0.813	-0.308	1.120	(-1.878, 1.309)	0.932
			ϕ	5.200	4.087	-	-	-	-	-
400	(0.3, 0.9)	0.25	α	1.099	0.969	0.676	-0.130	0.924	(-0.356, 2.293)	0.923
			β_0	-0.847	-0.009	0.955	0.839	2.304	(-1.880, 1.863)	0.905
			β_1	0.177	0.235	0.379	0.060	0.660	(-0.508, 0.979)	0.872
			γ_0	1.658	1.990	0.242	0.333	0.446	(1.517, 2.464)	0.736
			γ_1	3.765	4.440	1.206	0.676	1.648	(2.078, 6.803)	0.953
			γ_2	-0.005	-0.008	0.112	-0.003	0.151	(-0.227, 0.210)	0.925
			γ_3	0.024	-0.389	0.752	-0.413	1.034	(-1.863, 1.085)	0.947
			ϕ	5.200	3.827	-	-	-	-	-

Table 4.13: Selection rate based on AIC, BIC and maximized log-likelihood value.

	Fitted Models					
True Models	Setting 1($n = 300$)			Setting 2 ($n = 400$)		
	DEWP	DLB	DNB	DEWP	DLB	DNB
DEWP ($\phi = -0.5$)	$\hat{\phi} = -0.044$		$\hat{\phi} = 0.115$	$\hat{\phi} = -0.275$		$\hat{\phi} = 0.378$
AIC	0.159	0.799	0.042	0.179	0.768	0.053
BIC	0.021	0.963	0.016	0.037	0.944	0.019
log-lik	0.589	0.257	0.154	0.630	0.152	0.218
DEWP ($\phi = 0.2$)	$\hat{\phi} = 0.303$		$\hat{\phi} = 0.125$	$\hat{\phi} = 0.222$		$\hat{\phi} = 0.186$
AIC	0.112	0.878	0.010	0.125	0.843	0.032
BIC	0.026	0.961	0.013	0.063	0.919	0.018
log-lik	0.568	0.398	0.034	0.597	0.360	0.043
DLB	$\hat{\phi} = -0.293$		$\hat{\phi} = 0.319$	$\hat{\phi} = -0.077$		$\hat{\phi} = 0.347$
AIC	0.084	0.903	0.013	0.073	0.919	0.008
BIC	0.023	0.972	0.005	0.016	0.983	0.001
log-lik	0.436	0.548	0.016	0.427	0.559	0.014
DNB ($\phi = 0.5$)	$\hat{\phi} = -0.046$		$\hat{\phi} = 0.184$	$\hat{\phi} = 0.311$		$\hat{\phi} = 0.336$
AIC	0.172	0.759	0.069	0.163	0.762	0.075
BIC	0.033	0.966	0.001	0.003	0.969	0.028
log-lik	0.589	0.234	0.177	0.556	0.262	0.182
DNB ($\phi = 0.75$)	$\hat{\phi}$=-0.143		$\hat{\phi} = 0.176$	$\hat{\phi} = 0.545$		$\hat{\phi} = 0.346$
AIC	0.187	0.745	0.068	0.174	0.737	0.089
BIC	0.046	0.934	0.020	0.040	0.927	0.033
log-lik	0.624	0.228	0.148	0.599	0.242	0.159

Table 4.14: TRB (%) (TMSE, $\hat{\phi}$, TRE) in estimation of cured proportion for all candidate models.

Fitted Model	True Model				
	DEWP ($\phi = -0.5$)	DEWP ($\phi = 0.2$)	DLBP	DNB ($\phi = 0.5$)	DNB ($\phi = 0.75$)
	Setting 1 ($n = 300$)				
True Model	28.42 (0.004, - , 1.000)	56.493 (0.005, - , 1.000)	66.935 (0.003, - , 1.000)	32.563 (0.004, - , 1.000)	33.942 (0.005, - , 1.000)
DEWP	30.018 (0.004, -0.108, 0.902)	62.255 (0.005, 0.267, 0.961)	82.547 (0.004, 0.755, 0.987)	35.146 (0.005, -0.044, 0.904)	36.008 (0.006, -0.131, 0.957)
DLBP	30.898 (0.005, - , 1.033)	52.888 (0.004, - , 1.287)	66.935 (0.003, - , 1.000)	34.73 (0.004, - , 1.138)	35.446 (0.005, - , 1.092)
DNB	27.869 (0.004, 0.459, 1.048)	59.482 (0.005, 0.189, 1.126)	157.468 (0.007, 0.113, 0.475)	31.053 (0.004, 0.277, 1.115)	33.143 (0.005, 0.517, 1.111)
	Setting 2 ($n = 400$)				
True Model	35.3 (0.003, -, 1.000)	62.365 (0.003, - , 1.000)	86.617 (0.003, - , 1.000)	41.663 (0.004, - , 1.000)	37.1 (0.003, - , 1.000)
DEWP	37.015 (0.004, -0.199, 0.962)	66.532 (0.004, 0.239, 1.004)	107.147 (0.004, 0.708, 0.964)	42.593 (0.004, -0.079, 1.006)	39.126 (0.004, -0.259, 0.972)
DLBP	37.73 (0.004, 0, 1.383)	61.101 (0.003, - , 1.087)	86.617 (0.003, - , 1.000)	42.992 (0.004, - , 1.052)	40.846 (0.004, - , 1.047)
DNB	34.957 (0.003, 0.461, 1.045)	67.786 (0.003, 0.198, 1.094)	193.413 (0.006, 0.117, 0.455)	40.039 (0.004, 0.396, 1.123)	37.247 (0.003, 0.379, 1.030)

Table 4.15: TRB (%) and TRE when AIC and $\hat{l}$ are used as a model selection criterion.

True Model	Setting 1				Setting 2			
	AIC		$\hat{l}$		AIC		$\hat{l}$	
	TRB (%)	TRE	TRB (%)	TRE	TRB (%)	TRE	TRB (%)	TRE
DEWP ($\phi = -0.5$)	29.432	1.007	29.589	0.962	36.347	1.148	36.659	1.085
DEWP ($\phi = 0.2$)	55.174	1.134	58.484	1.066	62.321	1.040	63.832	1.032
DLB	67.872	0.999	75.178	0.989	88.259	0.997	94.829	0.986
DNB ($\phi = 0.5$)	33.909	1.068	34.144	1.003	42.461	1.030	42.408	1.027
DNB ($\phi = 0.75$)	35.015	1.050	35.450	1.008	39.347	1.023	39.104	0.998

Table 4.16: AIC values when true model is fitted.

Fitted Model	True Model			
	DEWP ($\phi = -0.5$)		DNB ($\phi = 0.5$)	
	Setting 1	Setting 2	Setting 1	Setting 2
True Model	0.530	0.540	0.330	0.350
DEWP	0.070	0.060	0.100	0.090
DLBP	0.370	0.390	0.530	0.550
DNB	0.030	0.010	0.040	0.010

Chapter 5

Summary and Conclusions

With significant improvements in bio-medical fields, more patients are getting cured even for certain cancers. Consequently, in many cases, the survival plots levels off well above zero even after following up for considerable amount of time. This indicates the increasing requirement of applying cure rate models for analyzing lifetime data. Cure rate acts as an important marker to measure the efficacy of a treatment or therapy and thus, estimating cure rate is often crucial. As such, generalizing this model through various possible extensions (e.g., proportional hazards lifetimes) and more realistic assumptions are desirable.

5.1 Summary of research

In this thesis, cure rate and destructive cure rate models under proportional hazards lifetime for the susceptible are mainly studied. Consideration of a proportional hazards lifetime generalizes the i.i.d lifetimes of the susceptible by linking covariates to the lifetimes. Additional degrees of flexibility are added to the model by assuming the COM-Poisson distribution for the initial number of competing causes in case of ordinary cure rate model and weighted Poisson distribution in case of destructive cure rate model under competing cause scenario. The baseline hazard function is modeled by a Weibull hazard function or approximated by piecewise linear function.

In Chapter 2, a flexible COM-Poisson cure rate model has been studied with a proportional hazard model for the lifetime distribution of susceptible with the baseline hazard function being that of a Weibull distribution. The estimation for the model parameters has been carried out by using the EM algorithm, a profile likelihood approach for estimating the dispersion parameter of the COM-Poisson distribution, and Louis' method for finding the observed information matrix. A number of different scenarios have been taken into account concerning the values of cure rates, sample sizes, censoring proportions and lifetime parameters, in order to carefully evaluate the properties of the model as well as the performance of the inferential methods developed here. The estimates of the regression coefficients, lifetime parameters and the cure rates are all seen to be quite accurate. Low censoring, low cure rates and large sample size seem to result in more precise estimation. Moreover, the proposed model and the method has been illustrated by analyzing a real life data set on cutaneous melanoma; geometric cure rate model is seen to provide the best fit to the data which does not significantly differentiate between the lifetime distributions across covariate groups meaning that the test for homogeneity among the groups is not rejected. However, as ϕ increases ($\phi > 1$), the assumption of equal lifetime distributions among groups does get rejected. Thus, the choice of a proportional hazard model for the lifetime of susceptible becomes better than a parametric Weibull lifetime model, especially when $\phi > 1$.

In Chapter 3, the model proposed in this paper for modeling lifetime data with a surviving fraction offers a great advantage in terms of flexibility and robustness. The number of competing causes is modeled using a COM-Poisson distribution. A COM-

Poisson distribution takes into account many well known discrete distributions e.g. geometric, Poisson, Bernoulli depending on the value of the dispersion parameter ϕ. A COM-Poisson distribution in general constitutes over-dispersed distributions when $\phi < 1$ and under-dispersed distributions when $\phi > 1$. More flexibility is included to the model by assuming the lifetime distributions of the non-cured individuals to be from a proportional hazards family. A proportional hazard lifetime can vary with respect to the covariate values leading to non-homogeneity (different lifetime distributions) among the individuals. Moreover, the baseline hazard function is estimated non-parametrically by estimating with piecewise linear function. This PLA approach takes into consideration choices of cut-points $\tau_0, \tau_1, \ldots, \tau_N$ which are at the discretion of the reader. Here, we have used quantile values of the observed and censored times, and also based on the curvature of the kernel based baseline hazard function (only for the real data). In both cases, we have approximated the baseline hazard function in $[\tau_N, \infty)$ with the line in $[\tau_{N-1}, \tau_N]$. A comparative study was made among models with $N = 1, \ldots, 5$ and the true parametric model. The estimation of the model parameters was carried out using EM algorithm and the standard error of the estimates was obtained employing Louis' method. A profile likelihood approach provided the MLE for ϕ since the likelihood surface is very flat with respect to ϕ. In most of the cases, the estimates were close to the true value while s.e.'s and RMSE's are very similar among the PLAs and the true parametric model. A simulation study with a single covariate and four different settings depending on censoring rate and sample size (section 3.4) established the accuracy of the estimates of the model parameters. An increase in sample size and decrease in the true censoring proportion lead to improved results reducing s.e. and RMSE. To study the difference between true and estimated survival times, a measure of RISE was applied, which was found to be have a trend similar to RMSE. It was also observed that on increasing number of lines to approximate the baseline hazard beyond 5 did not sufficiently increase (in some cases decrease) the log-likelihood value. The estimate of ψ_N (baseline hazard at τ_N) suffers from large bias since in most of the cases τ_N lies far away from τ_{N-1}, so the PLA does not provide a good approximation. The performance of the model was also assessed based on a power study and model discrimination using LRT and AIC/BIC, which showed consistent result when the sample size was increased. The study of the real data on cutaneous melanoma with one covariate of nodule category suggested that a geometric cure rate model was appropriate unanimously for all N. On taking 3 covariates, geometric cure rate model delivered the best approximations for $N = 1, 2, 3$ but Poisson and Bernoulli cure rate models for $N = 4$ and $N = 5$ respectively. On the basis of AIC and BIC, geometric cure rate model with $N = 2$ provided the minimum values.

In Chapter 4, a destructive cure rate model is studied where the initial competing causes undergo a destructive mechanism under a competing risk scenario and examined under proportional hazards lifetime assumption for the susceptible. The model generalizes earlier works (see Pal and Balakrishnan, 2017, Pal and Balakrishnan, 2016) on destructive cure rate model by assuming non i.i.d lifetimes for susceptible. This is accomplished by linking covariates to the lifetimes through proportional hazards assumption. The parameter estimates are found to be quite accurate with small bias and RMSE. A relatively large bias is observed while estimating ϕ, especially when data are generated from DNB ($\phi = 0.75$) cure rate model. The estimates are observed to be more precise for low censoring ($\lambda = 0.05$), higher proportion of undamaged competing causes, i.e.,$(p_{\min}, p_{\min}) = (0.3, 0.9)$ and large sample size. A model discrimination is also carried out using information criteria. The importance of proper model selection is discussed by comparing TRB, TMSE and TRE across models. A well known real life example on cutaneous melanoma is considered for the purpose of illustration of our model. A Kaplan-Meier survival curve is plotted categorized by ulceration status and it indicates the presence of cured individuals. DNB cure rate model with $\hat{\phi} = 5.2$ provides best fit to the data based on AIC (414.216) and maximized log-likelihood (-199.108) values. Few nested sub-models are also fitted on the data and the DG cure rate model is found to have the lowest BIC value among all other models. The assumption of i.i.d. lifetimes among the susceptible could not be rejected at 5 % level of significance. Several link functions are considered for associating p and η to the covariates, however, the link L1 (defined in Section 4.6) is found to produce the highest log-likelihood value.

5.2 Future works

A wide spectrum of future works can be explored using this model. A more generalized COM-Poisson cure rate model with proportional hazards lifetime for the susceptible using a generalized gamma baseline hazard can be of interest since this may enable us with a two-way model discrimination (Balakrishnan and Pal, 2014). The use of an informative censoring or interval censoring in data instead of right censoring can be investigated. Future works on cure models under a destructive set-up may proceed by assuming a Conway-Maxwell (COM) Poisson distribution as the initial number of competing causes. A more generalized model can be obtained by utilizing the flexibility of a COM Poisson distribution along with a destructive mechanism with parametric i.i.d lifetime for the susceptible. An extension to destructive cure rate models can be implemented with PLA. Further, this can be complemented with a proportional hazard lifetime distribution as well. Another possible extension to the destructive cure rate model under proportional hazards assumption can be with respect to the estimation technique. Instead of maximizing the expected value $\mathbb{E}(I \mid \boldsymbol{\theta}^{\hat{(j)}}, \boldsymbol{O})$ while implementing EM-algorithm, we can maximize $\mathbb{E}(D, M \mid \boldsymbol{\theta}^{\hat{(j)}}, \boldsymbol{O})$,where $\boldsymbol{\theta}^{\hat{(j)}}$ is an estimate of the parameter $\boldsymbol{\theta}$ at j-th step of the iteration and $\boldsymbol{O}$ is the observed data (Gallardo et al., 2016).

A natural extension under the proportional hazard set-up is to include frailty through latent covariates. In real life scenario, there are many frailty factors which affect the lifetime of an individual. Among them, many are not observable but would be meaningful to contain them in the model. This can be done by including the frailties through some latent covariates. For this, we form clusters of individuals such that the k-th cluster is affected by the frailty X_k. Under proportional hazards model, we can consider the hazard function of the susceptible to be $h(t|x_k) = h_0(t)e^{\boldsymbol{\gamma}'\boldsymbol{x}_k}$ for the k-th cluster. On considering X_k to be random, the distribution of lifetime T is given by

$$f(t) = \int_{\mathbb{X}_k} h_0(t)e^{\boldsymbol{\gamma}'\boldsymbol{x}_k} \left\{ e^{-\int_0^t h_0(z)dz} \right\}^{e^{\boldsymbol{\gamma}'\boldsymbol{x}_k}} g(\boldsymbol{x}_k|\boldsymbol{\zeta}_k)d\boldsymbol{x}_k,$$

where $g(.|\boldsymbol{\zeta}_k)$ is a p.d.f. characterized by the parameter $\boldsymbol{\zeta}_k$. By assuming various distributions for the frailty variables, we can carry out simulation under competing risk and cure rate model (Balakrishnan and Peng, 2006).

Appendix A

Appendix corresponding to Chapter 2

A.1 The Q-functions

A.1.1 Bernoulli cure rate model

$$Q(\boldsymbol{\theta}^*, \boldsymbol{\pi}^{(k)}) = Q_1(\boldsymbol{\beta}, \boldsymbol{\pi}^{(k)}) + Q_2(\boldsymbol{\gamma}, \boldsymbol{\pi}^{(k)}),$$

where

$$Q_1(\boldsymbol{\beta}, \boldsymbol{\pi}^{(k)}) = \sum_{i\in\Delta_1} \boldsymbol{x}_i'\boldsymbol{\beta} + \sum_{i\in\Delta_0} \pi_i^{(k)} \boldsymbol{x}_i'\boldsymbol{\beta} - \sum_{i\in\Delta_0} \log(1 + e^{\boldsymbol{x}_i'\boldsymbol{\beta}})$$

and

$$\begin{aligned} Q_2(\boldsymbol{\gamma}, \boldsymbol{\pi}^{(k)}) = n_1 \log\gamma_0 - n_1\gamma_0\log\gamma_1 + (\gamma_0 - 1)\sum_{i\in\Delta_1}\log t_i + \sum_{i\in\Delta_1} \boldsymbol{x}_i'\boldsymbol{\gamma}_2 \\ - \sum_{i\in\Delta_1}\left(\frac{t_i}{\gamma_1}\right)^{\gamma_0} e^{\boldsymbol{x}_i'\boldsymbol{\gamma}_2} - \sum_{\Delta_0}\pi_i^{(k)}\left(\frac{t_i}{\gamma_1}\right)^{\gamma_0} e^{\boldsymbol{x}_i'\boldsymbol{\gamma}_2}, \end{aligned}$$

with

$$\pi_i^{(k)} = \left.\frac{\exp\left[\boldsymbol{x}_i'\boldsymbol{\beta} - \left(\frac{t_i}{\gamma_1}\right)^{\gamma_0} e^{\boldsymbol{x}_i'\boldsymbol{\gamma}_2}\right]}{1 + \exp\left[\boldsymbol{x}_i'\boldsymbol{\beta} - \left(\frac{t_i}{\gamma_1}\right)^{\gamma_0} e^{\boldsymbol{x}_i'\boldsymbol{\gamma}_2}\right]}\right|_{\boldsymbol{\theta}=\boldsymbol{\theta}^{*(k)}} \tag{A.1.1}$$

for $i \in \Delta_0$.

A.1.2 Poisson cure rate model

$$\begin{aligned} Q(\boldsymbol{\theta}^*, \boldsymbol{\pi}^{(k)}) = \quad & n_1 \log \gamma_0 - n_1 \gamma_0 \log \gamma_1 + (\gamma_0 - 1) \sum_{i \in \Delta_1} \log t_i \\ & + \sum_{i \in \Delta_1} \boldsymbol{x}_i' \boldsymbol{\gamma}_2 - \sum_{i \in \Delta_1} \left(\frac{t_i}{\gamma_1} \right)^{\gamma_0} e^{\boldsymbol{x}_i' \boldsymbol{\gamma}_2} \\ & + \sum_{i \in \Delta_1} \log(\log(1 + e^{\boldsymbol{x}_i' \boldsymbol{\beta}})) - \sum_{\Delta^*} \log(1 + e^{\boldsymbol{x}_i' \boldsymbol{\beta}}) + \sum_{i \in \Delta_1} A(t_i, \boldsymbol{x}_i; \boldsymbol{\beta}, \boldsymbol{\gamma}) \\ & - \sum_{i \in \Delta_0} \pi_i^{(k)} \log(A(t_i, \boldsymbol{x}_i; \boldsymbol{\beta}, \boldsymbol{\gamma}) - 1), \end{aligned}$$

where

$$A(t_i, \boldsymbol{x}_i; \boldsymbol{\beta}, \boldsymbol{\gamma}) = \exp\left[-\left(\frac{t_i}{\gamma_1} \right)^{\gamma_0} e^{\boldsymbol{x}_i' \boldsymbol{\gamma}_2} \right] \log(1 + e^{\boldsymbol{x}_i' \boldsymbol{\beta}})$$

for $i \in \Delta^*$, with

$$\pi_i^{(k)} = \left. \frac{e^{A(t_i, \boldsymbol{x}_i; \boldsymbol{\beta}, \boldsymbol{\gamma})} - 1}{e^{A(t_i, \boldsymbol{x}_i; \boldsymbol{\beta}, \boldsymbol{\gamma})}} \right|_{\boldsymbol{\theta} = \boldsymbol{\theta}^{*(k)}} \tag{A.1.2}$$

for $i \in \Delta_0$.

A.1.3 Geometric cure rate model

$$\begin{aligned} Q(\boldsymbol{\theta}^*, \boldsymbol{\pi}^{(k)}) &= n_1 \log \gamma_0 - n_1 \gamma_0 \log \gamma_1 + (\gamma_0 - 1) \sum_{i \in \Delta_1} \log t_i + \sum_{i \in \Delta_1} \boldsymbol{x}_i' \boldsymbol{\gamma}_2 \\ & + \sum_{i \in \Delta_1} B(t_i, \boldsymbol{x}_i; \boldsymbol{\beta}, \boldsymbol{\gamma}) \\ & - 2 \sum_{i \in \Delta_1} \log(1 + C(t_i, \boldsymbol{x}_i; \boldsymbol{\beta}, \boldsymbol{\gamma})) + \sum_{i \in \Delta_0} \pi_i^{(k)} B(t_i, \boldsymbol{x}_i; \boldsymbol{\beta}, \boldsymbol{\gamma}) \\ & - \sum_{i \in \Delta_0} \pi_i^{(k)} \log(1 + C(t_i, \boldsymbol{x}_i; \boldsymbol{\beta}, \boldsymbol{\gamma})) - \sum_{i \in \Delta_0} \log(1 + e^{\boldsymbol{x}_i' \boldsymbol{\beta}}), \end{aligned}$$

where

$$B(t_i, \boldsymbol{x}_i; \boldsymbol{\beta}, \boldsymbol{\gamma}) = \boldsymbol{x}_i' \boldsymbol{\beta} - \left(\frac{t_i}{\gamma_1} \right)^{\gamma_0} e^{\boldsymbol{x}_i' \boldsymbol{\gamma}_2}$$

and

$$C(t_i, \boldsymbol{x}_i; \boldsymbol{\beta}, \boldsymbol{\gamma}) = e^{\boldsymbol{x}_i'\boldsymbol{\beta}} \left[1 - \exp\left(-\left(\frac{t_i}{\gamma_1}\right)^{\gamma_0} e^{\boldsymbol{x}_i'\boldsymbol{\gamma}_2}\right)\right]$$

for $i \in \Delta^*$, with

$$\pi_i^{(k)} = \left.\frac{e^{B(t_i, \boldsymbol{x}_i; \boldsymbol{\beta}, \boldsymbol{\gamma})}}{1 + e^{\boldsymbol{x}_i'\boldsymbol{\beta}}}\right|_{\boldsymbol{\theta} = \boldsymbol{\theta}^{*(k)}} \tag{A.1.3}$$

for $i \in \Delta_0$.

A.1.4 COM-Poisson cure rate model

$$\begin{aligned} Q(\boldsymbol{\theta}^*, \boldsymbol{\pi}^{(k)}) =& n_1 \log \gamma_0 - n_1 \gamma_0 \log \gamma_1 + (\gamma_0 - 1) \sum_{i \in \Delta_1} \log t_i \\ &+ \sum_{i \in \Delta_1} \boldsymbol{x}_i' \boldsymbol{\gamma}_2 - \sum_{i \in \Delta^*} \log(1 + e^{\boldsymbol{x}_i'\boldsymbol{\beta}}) \\ &+ \sum_{i \in \Delta_1} \log z_{2i} + \sum_{i \in \Delta_0} \pi_i^{(k)} \log z_{1i} \end{aligned}$$

where

$$z_1 = z_1(\boldsymbol{\theta}; \boldsymbol{x}, t) = \sum_{j=1}^{\infty} \frac{\{\eta S(t; \boldsymbol{\gamma})\}^j}{(j!)^\phi}, z_2 = z_2(\boldsymbol{\theta}; \boldsymbol{x}, t) = \sum_{j=1}^{\infty} \frac{\{j\eta S(t; \boldsymbol{\gamma})\}^j}{(j!)^\phi},$$

$$\eta = \eta(\boldsymbol{\beta}; \boldsymbol{x}) = H_\phi^{-1}(1 + e^{\boldsymbol{x}_i'\boldsymbol{\beta}}) \text{ and } S(t; \boldsymbol{\gamma}) = \exp\left[-\left(\frac{t}{\gamma_1}\right)^{\gamma_0} e^{\boldsymbol{x}_i'\boldsymbol{\gamma}_2}\right],$$

with

$$\pi_i^{(k)} = \left.\frac{z_1(\boldsymbol{\theta}; \boldsymbol{x}_i, t_i)}{1 + z_1(\boldsymbol{\theta}; \boldsymbol{x}_i, t_i)}\right|_{\boldsymbol{\theta} = \boldsymbol{\theta}^{*(k)}} \tag{A.1.4}$$

for $i \in \Delta_0$.

Using the invariance property of MLEs, we can then easily find estimate of the cure rate as

$$\hat{p}_0 = \frac{1}{1 + e^{\boldsymbol{x}'\hat{\boldsymbol{\beta}}}},$$

where $\hat{\boldsymbol{\beta}}$ is the MLE of $\boldsymbol{\beta}$.

A.2 First- and second-order derivatives of the Q-function

A.2.1 Bernoulli cure rate model

The first- and second-order partial derivatives of $Q_1(\boldsymbol{\beta}, \boldsymbol{\pi}^{(k)})$ with respect to $\boldsymbol{\beta}$ and of $Q_2(\boldsymbol{\gamma}, \boldsymbol{\pi}^{(k)})$ function with respect to $\boldsymbol{\gamma}$ are as follows:

$$\frac{\partial Q_1}{\partial \beta_l} = \sum_{i\in\Delta_1} x_{il} - \sum_{i\in\Delta^*} x_{il} \frac{e^{\boldsymbol{x}_i'\boldsymbol{\beta}}}{1+e^{\boldsymbol{x}_i'\boldsymbol{\beta}}} + \sum_{i\in\Delta_0} \pi_i^{(k)} x_{il},$$

$$\begin{aligned}\frac{\partial Q_2}{\partial \gamma_0} =& \frac{n_1}{\gamma_0} - n_1 \ \log\gamma_1 + \sum_{i\in\Delta_1} \log t_i - \sum_{i\in\Delta_1} \left(\frac{t_i}{\gamma_1}\right)^{\gamma_0} \log\left(\frac{t_i}{\gamma_1}\right) e^{\boldsymbol{x}_{ic}'\boldsymbol{\gamma}_2} \\ & - \sum_{i\in\Delta_0} \pi_i^{(k)} \left(\frac{t_i}{\gamma_1}\right)^{\gamma_0} \log\left(\frac{t_i}{\gamma_1}\right) e^{\boldsymbol{x}_{ic}'\boldsymbol{\gamma}_2},\end{aligned}$$

$$\frac{\partial Q_2}{\partial \gamma_1} = -\frac{n_1\gamma_0}{\gamma_1} + \sum_{i\in\Delta_1} \frac{\gamma_0}{\gamma_1} \left(\frac{t_i}{\gamma_1}\right)^{\gamma_0} e^{\boldsymbol{x}_{ic}'\boldsymbol{\gamma}_2} + \sum_{i\in\Delta_0} \pi_i^{(k)} \frac{\gamma_0}{\gamma_1} \left(\frac{t_i}{\gamma_1}\right)^{\gamma_0} e^{\boldsymbol{x}_{ic}'\boldsymbol{\gamma}_2},$$

$$\frac{\partial Q_2}{\partial \gamma_{2h}} = \sum_{i\in\Delta_1} x_{ih} - \sum_{i\in\Delta_1} x_{ih} \left(\frac{t_i}{\gamma_1}\right)^{\gamma_0} e^{\boldsymbol{x}_{ic}'\boldsymbol{\gamma}_2} - \sum_{i\in\Delta_0} \pi_i^{(k)} x_{ih} \left(\frac{t_i}{\gamma_1}\right)^{\gamma_0} e^{\boldsymbol{x}_{ic}'\boldsymbol{\gamma}_2},$$

$$\frac{\partial^2 Q_1}{\partial \beta_l \partial \beta_{l'}} = -\sum_{i\in\Delta^*} x_{il} x_{il'} \frac{e^{\boldsymbol{x}_i'\boldsymbol{\beta}}}{(1+e^{\boldsymbol{x}_i'\boldsymbol{\beta}})^2},$$

$$\frac{\partial^2 Q_2}{\partial \gamma_0^2} = -\frac{n_1}{\gamma_0^2} - \sum_{i\in\Delta_1}\left(\frac{t_i}{\gamma_1}\right)^{\gamma_0}\left[\log\left(\frac{t_i}{\gamma_1}\right)\right]^2 e^{\boldsymbol{x}_{ic}'\boldsymbol{\gamma}_2}$$
$$-\sum_{i\in\Delta_0}\pi_i^{(k)}\left(\frac{t_i}{\gamma_1}\right)^{\gamma_0}\left[\log\left(\frac{t_i}{\gamma_1}\right)\right]^2 e^{\boldsymbol{x}_{ic}'\boldsymbol{\gamma}_2},$$

$$\frac{\partial^2 Q_2}{\partial \gamma_0 \partial \gamma_1} = -\frac{n_1}{\gamma_1} + \sum_{i\in\Delta_1}\left(\frac{t_i}{\gamma_1}\right)^{\gamma_0}\left[\frac{1+\gamma_0\log\left(\frac{t_i}{\gamma_1}\right)}{\gamma_1}\right] e^{\boldsymbol{x}_{ic}'\boldsymbol{\gamma}_2}$$
$$+\sum_{i\in\Delta_0}\pi_i^{(k)}\left(\frac{t_i}{\gamma_1}\right)^{\gamma_0}\left[\frac{1+\gamma_0\log\left(\frac{t_i}{\gamma_1}\right)}{\gamma_1}\right] e^{\boldsymbol{x}_{ic}'\boldsymbol{\gamma}_2},$$

$$\frac{\partial^2 Q_2}{\partial \gamma_0 \partial \gamma_{2h}} = -\sum_{i\in\Delta_1} x_{ih}\left(\frac{t_i}{\gamma_1}\right)^{\gamma_0}\log\left(\frac{t_i}{\gamma_1}\right) e^{\boldsymbol{x}_{ic}'\boldsymbol{\gamma}_2}$$
$$-\sum_{i\in\Delta_0}\pi_i^{(k)} x_{ih}\left(\frac{t_i}{\gamma_1}\right)^{\gamma_0}\log\left(\frac{t_i}{\gamma_1}\right) e^{\boldsymbol{x}_{ic}'\boldsymbol{\gamma}_2},$$

$$\frac{\partial^2 Q_2}{\partial \gamma_1^2} = \frac{n_1\gamma_0}{\gamma_1^2} - \sum_{i\in\Delta_1}\left(\frac{t_i}{\gamma_1}\right)^{\gamma_0}\left[\frac{\gamma_0(1+\gamma_0)}{\gamma_1^2}\right] e^{\boldsymbol{x}_{ic}'\boldsymbol{\gamma}_2}$$
$$-\sum_{i\in\Delta_0}\pi_i^{(k)}\left(\frac{t_i}{\gamma_1}\right)^{\gamma_0}\left[\frac{\gamma_0(1+\gamma_0)}{\gamma_1^2}\right] e^{\boldsymbol{x}_{ic}'\boldsymbol{\gamma}_2},$$

$$\frac{\partial^2 Q_2}{\partial \gamma_1 \partial \gamma_{2h}} = \sum_{i\in\Delta_1} x_{ih}\frac{\gamma_0}{\gamma_1}\left(\frac{t_i}{\gamma_1}\right)^{\gamma_0} e^{\boldsymbol{x}_{ic}'\boldsymbol{\gamma}_2} + \sum_{i\in\Delta_0}\pi_i^{(k)} x_{ih}\frac{\gamma_0}{\gamma_1}\left(\frac{t_i}{\gamma_1}\right)^{\gamma_0} e^{\boldsymbol{x}_{ic}'\boldsymbol{\gamma}_2},$$

$$\frac{\partial Q_2}{\partial \gamma_{2h}\partial \gamma_{2h'}} = -\sum_{i\in\Delta_1} x_{ih}x_{ih'}\left(\frac{t_i}{\gamma_1}\right)^{\gamma_0} e^{\boldsymbol{x}_{ic}'\boldsymbol{\gamma}_2} - \sum_{i\in\Delta_0}\pi_i^{(k)} x_{ih}x_{ih'}\left(\frac{t_i}{\gamma_1}\right)^{\gamma_0} e^{\boldsymbol{x}_{ic}'\boldsymbol{\gamma}_2},$$

where

$$\pi_i^{(k)} = \frac{e^{\boldsymbol{x}_i'\boldsymbol{\beta} - \left(\frac{t_i}{\gamma_1}\right)^{\gamma_0} e^{\boldsymbol{x}_{ic}'\boldsymbol{\gamma}_2}}}{1 + e^{\boldsymbol{x}_i'\boldsymbol{\beta} - \left(\frac{t_i}{\gamma_1}\right)^{\gamma_0} e^{\boldsymbol{x}_{ic}'\boldsymbol{\gamma}_2}}} \Bigg|_{\boldsymbol{\theta}=\boldsymbol{\theta}^{(k)}}$$

for l,l' =0,$\ldots$, p, x_{i0}= 1, h, h'=1, $\ldots$, p, and i=1, $\ldots$, n.

A.2.2 Poisson cure rate model

The first- and second-order partial derivatives of $Q(\boldsymbol{\theta}, \boldsymbol{\pi}^{(k)})$ with respect to $\boldsymbol{\beta}$ and $\boldsymbol{\gamma}$ are as follows:

$$\begin{aligned}
\frac{\partial Q}{\partial \beta_l} &= \sum_{i\in\Delta_1} x_{il} \frac{e^{\boldsymbol{x}_i'\boldsymbol{\beta}}}{(1+e^{\boldsymbol{x}_i'\boldsymbol{\beta}})\log(1+e^{\boldsymbol{x}_i'\boldsymbol{\beta}})} + \sum_{i\in\Delta_1} x_{il} \frac{e^{\boldsymbol{x}_i'\boldsymbol{\beta}} S(t_i;\boldsymbol{\gamma})}{(1+e^{\boldsymbol{x}_i'\boldsymbol{\beta}})} - \sum_{i\in\Delta^*} x_{il} \frac{e^{\boldsymbol{x}_i'\boldsymbol{\beta}}}{(1+e^{\boldsymbol{x}_i'\boldsymbol{\beta}})} \\
&+ \sum_{i\in\Delta_0} \pi_i^{(k)} x_{il} \frac{e^{\boldsymbol{x}_i'\boldsymbol{\beta}} P(t_i, \boldsymbol{x}_i; \boldsymbol{\beta}, \boldsymbol{\gamma}) S(t_i;\boldsymbol{\gamma})}{(1+e^{\boldsymbol{x}_i'\boldsymbol{\beta}})},
\end{aligned}$$

$$\begin{aligned}
\frac{\partial Q}{\partial \gamma_0} &= n_1 \left[\frac{1}{\gamma_0} - \log \gamma_1\right] + \sum_{i\in\Delta_1} \left[\log t_i - \left(\frac{t_i}{\gamma_1}\right)^{\gamma_0} \log\left(\frac{t_i}{\gamma_1}\right) e^{\boldsymbol{x}_{ic}'\boldsymbol{\gamma}_2}\right] \\
&+ \sum_{i\in\Delta_1} \log\left(\frac{t_i}{\gamma_1}\right) \log(1+e^{\boldsymbol{x}_i'\boldsymbol{\beta}}) S(t_i;\boldsymbol{\gamma}) \log S(t_i;\boldsymbol{\gamma}) \\
&+ \sum_{i\in\Delta_0} \pi_i^{(k)} P(t_i, \boldsymbol{x}_i; \boldsymbol{\beta}, \boldsymbol{\gamma}) \log\left(\frac{t_i}{\gamma_1}\right) \log(1+e^{\boldsymbol{x}_i'\boldsymbol{\beta}}) S(t_i;\boldsymbol{\gamma}) \log S(t_i;\boldsymbol{\gamma}),
\end{aligned}$$

$$\begin{aligned}
\frac{\partial Q}{\partial \gamma_1} &= -\frac{\gamma_0}{\gamma_1} \left[n_1 + \sum_{i\in\Delta_1} \log S(t_i;\boldsymbol{\gamma}) \left(1 + \log(1+e^{\boldsymbol{x}_i'\boldsymbol{\beta}}) S(t_i;\boldsymbol{\gamma})\right)\right] \\
&- \frac{\gamma_0}{\gamma_1} \left[\sum_{i\in\Delta_0} \pi_i^{(k)} P(t_i, \boldsymbol{x}_i; \boldsymbol{\beta}, \boldsymbol{\gamma}) \log(1+e^{\boldsymbol{x}_i'\boldsymbol{\beta}}) S(t_i;\boldsymbol{\gamma}) \log S(t_i;\boldsymbol{\gamma})\right],
\end{aligned}$$

$$\frac{\partial Q}{\partial \gamma_{2h}} = \sum_{i\in\Delta_1} x_{ih}\left[1+\log S(t_i;\boldsymbol{\gamma})\left(1+S(t_i;\boldsymbol{\gamma})\log(1+e^{\boldsymbol{x}_i'\boldsymbol{\beta}})\right)\right]$$
$$+\sum_{i\in\Delta_0}\pi_i^{(k)}x_{ih}P(t_i,\boldsymbol{x}_i;\boldsymbol{\beta},\boldsymbol{\gamma})\log(1+e^{\boldsymbol{x}_i'\boldsymbol{\beta}})S(t_i;\boldsymbol{\gamma})\log S(t_i;\boldsymbol{\gamma}),$$

$$\frac{\partial^2 Q}{\partial \beta_l \partial \beta_l'} = \sum_{i\in\Delta_1} x_{il}x_{il'}\left[\frac{e^{\boldsymbol{x}_i'\boldsymbol{\beta}}}{(1+e^{\boldsymbol{x}_i'\boldsymbol{\beta}})^2}\left(\frac{1}{\log(1+e^{\boldsymbol{x}_i'\boldsymbol{\beta}})}\left[1-\frac{e^{\boldsymbol{x}_i'\boldsymbol{\beta}}}{\log(1+e^{\boldsymbol{x}_i'\boldsymbol{\beta}})}\right]+S(t_i;\boldsymbol{\gamma})\right)\right]$$
$$-\sum_{i\in\Delta^*} x_{il}x_{il'}\frac{e^{\boldsymbol{x}_i'\boldsymbol{\beta}}}{(1+e^{\boldsymbol{x}_i'\boldsymbol{\beta}})^2}$$
$$+\sum_{i\in\Delta_0}\pi_i^{(k)}x_{il}x_{il'}P(t_i,\boldsymbol{x}_i;\boldsymbol{\beta},\boldsymbol{\gamma})S(t_i;\boldsymbol{\gamma})\frac{e^{\boldsymbol{x}_i'\boldsymbol{\beta}}}{(1+e^{\boldsymbol{x}_i'\boldsymbol{\beta}})^2}\left[1-\frac{e^{\boldsymbol{x}_i'\boldsymbol{\beta}}}{e^{A(t_i,\boldsymbol{x}_i;\boldsymbol{\beta},\boldsymbol{\gamma})}-1}\right],$$

$$\frac{\partial^2 Q}{\partial \beta_l \partial \gamma_0} = \sum_{i\in\Delta_1} x_{il}\frac{e^{\boldsymbol{x}_i'\boldsymbol{\beta}}}{(1+e^{\boldsymbol{x}_i'\boldsymbol{\beta}})}S(t_i;\boldsymbol{\gamma})\log S(t_i;\boldsymbol{\gamma})\log\left(\frac{t_i}{\gamma_1}\right)$$
$$+\sum_{i\in\Delta_0}\pi_i^{(k)}x_{il}P(t_i,\boldsymbol{x}_i;\boldsymbol{\beta},\boldsymbol{\gamma})\frac{e^{\boldsymbol{x}_i'\boldsymbol{\beta}}}{(1+e^{\boldsymbol{x}_i'\boldsymbol{\beta}})}S(t_i;\boldsymbol{\gamma})\log S(t_i;\boldsymbol{\gamma})\log\left(\frac{t_i}{\gamma_1}\right)$$
$$\times\left[1-\frac{S(t_i;\boldsymbol{\gamma})\log(1+e^{\boldsymbol{x}_i'\boldsymbol{\beta}})}{e^{A(t_i,\boldsymbol{x}_i;\boldsymbol{\beta},\boldsymbol{\gamma})}-1}\right],$$

$$\frac{\partial^2 Q}{\partial \beta_l \partial \gamma_1} = -\sum_{i\in\Delta_1} x_{il}\frac{\gamma_0}{\gamma_1}\frac{e^{\boldsymbol{x}_i'\boldsymbol{\beta}}}{(1+e^{\boldsymbol{x}_i'\boldsymbol{\beta}})}S(t_i;\boldsymbol{\gamma})\log S(t_i;\boldsymbol{\gamma})$$
$$-\sum_{i\in\Delta_0}\pi_i^{(k)}x_{il}\frac{\gamma_0}{\gamma_1}P(t_i,\boldsymbol{x}_i;\boldsymbol{\beta},\boldsymbol{\gamma})\frac{e^{\boldsymbol{x}_i'\boldsymbol{\beta}}}{(1+e^{\boldsymbol{x}_i'\boldsymbol{\beta}})}S(t_i;\boldsymbol{\gamma})\log S(t_i;\boldsymbol{\gamma})$$
$$\times\left[1-\frac{S(t_i;\boldsymbol{\gamma})\log(1+e^{\boldsymbol{x}_i'\boldsymbol{\beta}})}{e^{A(t_i,\boldsymbol{x}_i;\boldsymbol{\beta},\boldsymbol{\gamma})}-1}\right],$$

$$\begin{aligned}\frac{\partial^2 Q}{\partial \beta_l \partial \gamma_{2h}} =& \sum_{i\in\Delta_1} x_{il}x_{ih}\frac{e^{\boldsymbol{x}_i'\boldsymbol{\beta}}}{(1+e^{\boldsymbol{x}_i'\boldsymbol{\beta}})}S(t_i;\boldsymbol{\gamma})\log S(t_i;\boldsymbol{\gamma})\\ &+\sum_{i\in\Delta_0}\pi_i^{(k)}x_{il}x_{ih}P(t_i,\boldsymbol{x}_i;\boldsymbol{\beta},\boldsymbol{\gamma})\frac{e^{\boldsymbol{x}_i'\boldsymbol{\beta}}}{(1+e^{\boldsymbol{x}_i'\boldsymbol{\beta}})}S(t_i;\boldsymbol{\gamma})\log S(t_i;\boldsymbol{\gamma})\\ &\times\left[1-\frac{S(t_i;\boldsymbol{\gamma})\log(1+e^{\boldsymbol{x}_i'\boldsymbol{\beta}})}{e^{A(t_i,\boldsymbol{x}_i;\boldsymbol{\beta},\boldsymbol{\gamma})}-1}\right],\end{aligned}$$

$$\begin{aligned}\frac{\partial^2 Q}{\partial \gamma_0^2} =& -\frac{n_1}{\gamma_0^2}+\sum_{i\in\Delta_1}\left[\log\left(\frac{t_i}{\gamma_1}\right)\right]^2\log S(t_i;\boldsymbol{\gamma})\left[1+\log(1+e^{\boldsymbol{x}_i'\boldsymbol{\beta}})S(t_i;\boldsymbol{\gamma})(1+\log S(t_i;\boldsymbol{\gamma}))\right]\\ &+\sum_{i\in\Delta_0}\pi_i^{(k)}P(t_i,\boldsymbol{x}_i;\boldsymbol{\beta},\boldsymbol{\gamma})\left[\log\left(\frac{t_i}{\gamma_1}\right)\right]^2\log(1+e^{\boldsymbol{x}_i'\boldsymbol{\beta}})S(t_i;\boldsymbol{\gamma})\log S(t_i;\boldsymbol{\gamma})\\ &\times\left[1+\log S(t_i;\boldsymbol{\gamma})-\frac{S(t_i;\boldsymbol{\gamma})\log S(t_i;\boldsymbol{\gamma})\log(1+e^{\boldsymbol{x}_i'\boldsymbol{\beta}})}{e^{A(t_i,\boldsymbol{x}_i;\boldsymbol{\beta},\boldsymbol{\gamma})}-1}\right],\end{aligned}$$

$$\begin{aligned}\frac{\partial^2 Q}{\partial \gamma_0 \partial \gamma_1} =& -\frac{n_1}{\gamma_1}-\sum_{i\in\Delta_1}\frac{\log S(t_i;\boldsymbol{\gamma})}{\gamma_1}\left[1+\gamma_0\log\left(\frac{t_i}{\gamma_1}\right)\right]\\ &-\sum_{i\in\Delta_1}\left[1+\gamma_0\log\left(\frac{t_i}{\gamma_1}\right)(1+\log S(t_i;\boldsymbol{\gamma}))\right]\frac{S(t_i;\boldsymbol{\gamma})\log S(t_i;\boldsymbol{\gamma})\log(1+e^{\boldsymbol{x}_i'\boldsymbol{\beta}})}{\gamma_1}\\ &-\sum_{i\in\Delta_0}\pi_i^{(k)}P(t_i,\boldsymbol{x}_i;\boldsymbol{\beta},\boldsymbol{\gamma})\frac{S(t_i;\boldsymbol{\gamma})\log S(t_i;\boldsymbol{\gamma})\log(1+e^{\boldsymbol{x}_i'\boldsymbol{\beta}})}{\gamma_1}\\ &\times\left[1+\gamma_0\log\left(\frac{t_i}{\gamma_1}\right)(1+\log S(t_i;\boldsymbol{\gamma}))\right.\\ &\left.-\frac{\gamma_0 S(t_i;\boldsymbol{\gamma})\log S(t_i;\boldsymbol{\gamma})\log\left(\frac{t_i}{\gamma_1}\right)\log(1+e^{\boldsymbol{x}_i'\boldsymbol{\beta}})}{e^{A(t_i,\boldsymbol{x}_i;\boldsymbol{\beta},\boldsymbol{\gamma})}-1}\right],\end{aligned}$$

$$
\begin{aligned}
\frac{\partial^2 Q}{\partial\gamma_0\partial\gamma_{2h}} =& \sum_{i\in\Delta_1} x_{ih}\log\left(\frac{t_i}{\gamma_1}\right)\log S(t_i;\boldsymbol{\gamma})\left[1+\log(1+e^{\boldsymbol{x}_i'\boldsymbol{\beta}})S(t_i;\boldsymbol{\gamma})(1+\log S(t_i;\boldsymbol{\gamma}))\right]\\
&+\sum_{i\in\Delta_0}\pi_i^{(k)}x_{ih}P(t_i,\boldsymbol{x}_i;\boldsymbol{\beta},\boldsymbol{\gamma})\log\left(\frac{t_i}{\gamma_1}\right)S(t_i;\boldsymbol{\gamma})\log S(t_i;\boldsymbol{\gamma})\log(1+e^{\boldsymbol{x}_i'\boldsymbol{\beta}})\\
&\times\left[(1+\log S(t_i;\boldsymbol{\gamma}))-\frac{\log(1+e^{\boldsymbol{x}_i'\boldsymbol{\beta}})S(t_i;\boldsymbol{\gamma})\log S(t_i;\boldsymbol{\gamma})}{e^{A(t_i,\boldsymbol{x}_i;\boldsymbol{\beta},\boldsymbol{\gamma})}-1}\right],
\end{aligned}
$$

$$
\begin{aligned}
\frac{\partial^2 Q}{\partial\gamma_1^2} =& \frac{n_1\gamma_0}{\gamma_1^2}-\sum_{i\in\Delta_1}\frac{\gamma_0(1+\gamma_0)}{\gamma_1^2}\log S(t_i;\boldsymbol{\gamma})\\
&+\sum_{i\in\Delta_1}\frac{\gamma_0}{\gamma_1^2}\log(1+e^{\boldsymbol{x}_i'\boldsymbol{\beta}})S(t_i;\boldsymbol{\gamma})\left[1+\gamma_0(1+\log S(t_i;\boldsymbol{\gamma}))\right]\\
&+\sum_{i\in\Delta_0}\pi_i^{(k)}\frac{\gamma_0}{\gamma_1^2}P(t_i,\boldsymbol{x}_i;\boldsymbol{\beta},\boldsymbol{\gamma})S(t_i;\boldsymbol{\gamma})\log S(t_i;\boldsymbol{\gamma})\log(1+e^{\boldsymbol{x}_i'\boldsymbol{\beta}})\\
&\times\left[1+\gamma_0(1+\log S(t_i;\boldsymbol{\gamma}))-\frac{\gamma_0 S(t_i;\boldsymbol{\gamma})\log S(t_i;\boldsymbol{\gamma})\log(1+e^{\boldsymbol{x}_i'\boldsymbol{\beta}})}{e^{A(t_i,\boldsymbol{x}_i;\boldsymbol{\beta},\boldsymbol{\gamma})}-1}\right],
\end{aligned}
$$

$$
\begin{aligned}
\frac{\partial^2 Q}{\partial\gamma_1\partial\gamma_{2h}} =& -\sum_{i\in\Delta_1} x_{ih}\frac{\gamma_0}{\gamma_1}\log S(t_i;\boldsymbol{\gamma})\left[1+S(t_i;\boldsymbol{\gamma})(1+\log S(t_i;\boldsymbol{\gamma}))\log(1+e^{\boldsymbol{x}_i'\boldsymbol{\beta}})\right]\\
&-\sum_{i\in\Delta_0}\pi_i^{(k)}x_{ih}\frac{\gamma_0}{\gamma_1}P(t_i,\boldsymbol{x}_i;\boldsymbol{\beta},\boldsymbol{\gamma})S(t_i;\boldsymbol{\gamma})\log S(t_i;\boldsymbol{\gamma})\log(1+e^{\boldsymbol{x}_i'\boldsymbol{\beta}})\\
&\times\left[(1+\log S(t_i;\boldsymbol{\gamma}))-\frac{S(t_i;\boldsymbol{\gamma})\log S(t_i;\boldsymbol{\gamma})\log(1+e^{\boldsymbol{x}_i'\boldsymbol{\beta}})}{e^{A(t_i,\boldsymbol{x}_i;\boldsymbol{\beta},\boldsymbol{\gamma})}-1}\right],
\end{aligned}
$$

$$
\begin{aligned}
\frac{\partial^2 Q}{\partial\gamma_{2h}\partial\gamma_{2h'}} =& \sum_{i\in\Delta_1} x_{ih}x_{ih'}\log S(t_i;\boldsymbol{\gamma})\left[1+S(t_i;\boldsymbol{\gamma})(1+\log S(t_i;\boldsymbol{\gamma}))\log(1+e^{\boldsymbol{x}_i'\boldsymbol{\beta}})\right]\\
&+\sum_{i\in\Delta_0}\pi_i^{(k)}x_{ih}x_{ih'}P(t_i,\boldsymbol{x}_i;\boldsymbol{\beta},\boldsymbol{\gamma})\\
&\times\left[(1+\log S(t_i;\boldsymbol{\gamma}))-\frac{S(t_i;\boldsymbol{\gamma})\log S(t_i;\boldsymbol{\gamma})\log(1+e^{\boldsymbol{x}_i'\boldsymbol{\beta}})}{e^{A(t_i,\boldsymbol{x}_i;\boldsymbol{\beta},\boldsymbol{\gamma})}-1}\right],
\end{aligned}
$$

where

$$\pi_i^{(k)} = \left.\frac{e^{A(t_i,\boldsymbol{x}_i;\boldsymbol{\beta},\boldsymbol{\gamma})}-1}{e^{A(t_i,\boldsymbol{x}_i;\boldsymbol{\beta},\boldsymbol{\gamma})}}\right|_{\boldsymbol{\theta}=\boldsymbol{\theta}^{(k)}},$$

$$A(t_i,\boldsymbol{x}_i;\boldsymbol{\beta},\boldsymbol{\gamma}) = \log S(t_i;\boldsymbol{\gamma})\log(1+e^{\boldsymbol{x}_i'\boldsymbol{\beta}}),$$

$$P(t_i,\boldsymbol{x}_i;\boldsymbol{\beta},\boldsymbol{\gamma}) = \frac{e^{A(t_i,\boldsymbol{x}_i;\boldsymbol{\beta},\boldsymbol{\gamma})}}{e^{A(t_i,\boldsymbol{x}_i;\boldsymbol{\beta},\boldsymbol{\gamma})}-1}$$

and

$$S(t_i;\boldsymbol{\gamma}) = \exp\left[-\left(\frac{t_i}{\gamma_1}\right)^{\gamma_0} e^{\boldsymbol{x}_{ic}'\boldsymbol{\gamma}_2}\right]$$

for l,l' =0, $\ldots$, p, x_{i0}= 1, h, h'=1, $\ldots$, p, and i=1, $\ldots$, n.

A.2.3 Geometric cure rate model

The first- and second-order partial derivatives of $Q(\boldsymbol{\theta},\boldsymbol{\pi}^{(k)})$ with respect to $\boldsymbol{\beta}$ and $\boldsymbol{\gamma}$ are as follows:

$$\begin{aligned}\frac{\partial Q}{\partial \beta_l} =& \sum_{i\in\Delta_1} x_{il} - 2\sum_{i\in\Delta_1} x_{il}\frac{B(t_i,\boldsymbol{x}_i;\boldsymbol{\beta},\boldsymbol{\gamma})-1}{B(t_i,\boldsymbol{x}_i;\boldsymbol{\beta},\boldsymbol{\gamma})} \\ &+ \sum_{i\in\Delta_0} x_{il}\left(\pi_i^{(k)} - \frac{e^{\boldsymbol{x}_i'\boldsymbol{\beta}}}{1+e^{\boldsymbol{x}_i'\boldsymbol{\beta}}}\right) - \sum_{i\in\Delta_0}\pi^{(k)}x_{il}\frac{B(t_i,\boldsymbol{x}_i;\boldsymbol{\beta},\boldsymbol{\gamma})-1}{B(t_i,\boldsymbol{x}_i;\boldsymbol{\beta},\boldsymbol{\gamma})},\end{aligned}$$

$$\begin{aligned}\frac{\partial Q}{\partial \gamma_0} =& \frac{n_1}{\gamma_0} - n_1\log(\gamma_1) + \sum_{i\in\Delta_1}\log t_i + \sum_{i\in\Delta_1}\log\left(\frac{t_i}{\gamma_1}\right)\log S(t_i;\boldsymbol{\gamma}) \\ &+ \sum_{i\in\Delta_0}\pi_i^{(k)}\log\left(\frac{t_i}{\gamma_1}\right)\log S(t_i;\boldsymbol{\gamma}) \\ &+ 2\sum_{i\in\Delta_1}\frac{e^{\boldsymbol{x}_i'\boldsymbol{\beta}}\log\left(\frac{t_i}{\gamma_1}\right)S(t_i;\boldsymbol{\gamma})\log S(t_i;\boldsymbol{\gamma})}{B(t_i,\boldsymbol{x}_i;\boldsymbol{\beta},\boldsymbol{\gamma})} \\ &+ \sum_{i\in\Delta_0}\pi_i^{(k)}\frac{e^{\boldsymbol{x}_i'\boldsymbol{\beta}}\log\left(\frac{t_i}{\gamma_1}\right)S(t_i;\boldsymbol{\gamma})\log S(t_i;\boldsymbol{\gamma})}{B(t_i,\boldsymbol{x}_i;\boldsymbol{\beta},\boldsymbol{\gamma})},\end{aligned}$$

$$\begin{aligned}\frac{\partial Q}{\partial \gamma_1} =&- \frac{n_1\gamma_0}{\gamma_1} - \sum_{i\in\Delta_1} \log\left(\frac{\gamma_0}{\gamma_1}\right)\log S(t_i;\boldsymbol{\gamma}) - \sum_{i\in\Delta_0} \pi_i^{(k)} \log\left(\frac{\gamma_0}{\gamma_1}\right)\log S(t_i;\boldsymbol{\gamma})\\ &- 2\sum_{i\in\Delta_1} \frac{e^{\boldsymbol{x}_i'\boldsymbol{\beta}}\log\left(\frac{\gamma_0}{\gamma_1}\right) S(t_i;\boldsymbol{\gamma})\log S(t_i;\boldsymbol{\gamma})}{B(t_i,\boldsymbol{x}_i;\boldsymbol{\beta},\boldsymbol{\gamma})}\\ &- \sum_{i\in\Delta_0} \pi_i^{(k)} \frac{e^{\boldsymbol{x}_i'\boldsymbol{\beta}}\log\left(\frac{\gamma_0}{\gamma_1}\right) S(t_i;\boldsymbol{\gamma})\log S(t_i;\boldsymbol{\gamma})}{B(t_i,\boldsymbol{x}_i;\boldsymbol{\beta},\boldsymbol{\gamma})},\end{aligned}$$

$$\begin{aligned}\frac{\partial Q}{\partial \gamma_{2h}} =&\sum_{I1} x_{ih}\left(1+\log S(t_i;\boldsymbol{\gamma})\right) + 2\sum_{i\in\Delta_1} \frac{x_{ih}e^{\boldsymbol{x}_i'\boldsymbol{\beta}} S(t_i;\boldsymbol{\gamma})\log S(t_i;\boldsymbol{\gamma})}{B(t_i,\boldsymbol{x}_i;\boldsymbol{\beta},\boldsymbol{\gamma})}\\ &+ \sum_{I0} \pi_i^{(k)} x_{ih}\log S(t_i;\boldsymbol{\gamma})\\ &+ \sum_{i\in\Delta_0} \pi_i^{(k)} \frac{x_{ih}e^{\boldsymbol{x}_i'\boldsymbol{\beta}} S(t_i;\boldsymbol{\gamma})\log S(t_i;\boldsymbol{\gamma})}{B(t_i,\boldsymbol{x}_i;\boldsymbol{\beta},\boldsymbol{\gamma})},\end{aligned}$$

$$\begin{aligned}\frac{\partial^2 Q}{\partial \beta_l \partial \beta_{l'}} =&- 2\sum_{i\in\Delta_1} x_{il}x_{il'} \frac{B(t_i,\boldsymbol{x}_i;\boldsymbol{\beta},\boldsymbol{\gamma})-1}{B(t_i,\boldsymbol{x}_i;\boldsymbol{\beta},\boldsymbol{\gamma})^2} - \sum_{i\in\Delta_0} \frac{x_{il}x_{il'}e^{\boldsymbol{x}_i'\boldsymbol{\beta}}}{(1+e^{\boldsymbol{x}_i'\boldsymbol{\beta}})^2}\\ &- \sum_{i\in\Delta_0} \pi_i^{(k)} x_{il}x_{il'} \frac{B(t_i,\boldsymbol{x}_i;\boldsymbol{\beta},\boldsymbol{\gamma})-1}{B(t_i,\boldsymbol{x}_i;\boldsymbol{\beta},\boldsymbol{\gamma})^2},\end{aligned}$$

$$\begin{aligned}\frac{\partial^2 Q}{\partial \beta_l \partial \gamma_0} =&2\sum_{i\in\Delta_1} \frac{x_{il}e^{\boldsymbol{x}_i'\boldsymbol{\beta}}\log\left(\frac{t_i}{\gamma_1}\right) S(t_i;\boldsymbol{\gamma})\log S(t_i;\boldsymbol{\gamma})}{B(t_i,\boldsymbol{x}_i;\boldsymbol{\beta},\boldsymbol{\gamma})^2}\\ &+ \sum_{i\in\Delta_0} \pi_i^{(k)} \frac{x_{il}e^{\boldsymbol{x}_i'\boldsymbol{\beta}}\log\left(\frac{t_i}{\gamma_1}\right) S(t_i;\boldsymbol{\gamma})\log S(t_i;\boldsymbol{\gamma})}{B(t_i,\boldsymbol{x}_i;\boldsymbol{\beta},\boldsymbol{\gamma})^2},\end{aligned}$$

$$\begin{aligned}\frac{\partial^2 Q}{\partial \beta_l \partial \gamma_1} =& -2\sum_{i\in\Delta_1} \frac{x_{il} e^{\boldsymbol{x}_i'\boldsymbol{\beta}} \left(\frac{\gamma_0}{\gamma_1}\right) S(t_i;\boldsymbol{\gamma}) \log S(t_i;\boldsymbol{\gamma})}{B(t_i,\boldsymbol{x}_i;\boldsymbol{\beta},\boldsymbol{\gamma})^2} \\ & - \sum_{i\in\Delta_0} \pi_i^{(k)} \frac{x_{il} e^{\boldsymbol{x}_i'\boldsymbol{\beta}} \left(\frac{\gamma_0}{\gamma_1}\right) S(t_i;\boldsymbol{\gamma}) \log S(t_i;\boldsymbol{\gamma})}{B(t_i,\boldsymbol{x}_i;\boldsymbol{\beta},\boldsymbol{\gamma})^2},\end{aligned}$$

$$\begin{aligned}\frac{\partial^2 Q}{\partial \beta_l \partial \gamma_{2h}} =& 2\sum_{i\in\Delta_1} \frac{x_{il} x_{ih} e^{\boldsymbol{x}_i'\boldsymbol{\beta}} S(t_i;\boldsymbol{\gamma}) \log S(t_i;\boldsymbol{\gamma})}{B(t_i,\boldsymbol{x}_i;\boldsymbol{\beta},\boldsymbol{\gamma})^2} \\ & + \sum_{i\in\Delta_0} \pi_i^{(k)} \frac{x_{il} x_{ih} e^{\boldsymbol{x}_i'\boldsymbol{\beta}} S(t_i;\boldsymbol{\gamma}) \log S(t_i;\boldsymbol{\gamma})}{B(t_i,\boldsymbol{x}_i;\boldsymbol{\beta},\boldsymbol{\gamma})^2},\end{aligned}$$

$$\begin{aligned}\frac{\partial^2 Q}{\partial \gamma_0^2} =& -\frac{n_1}{\gamma_0^2} + \sum_{i\in\Delta_1} \left[\log\left(\frac{t_i}{\gamma_1}\right)\right]^2 \log S(t_i;\boldsymbol{\gamma}) + \sum_{i\in\Delta_0} \pi_i^{(k)} \left[\log\left(\frac{t_i}{\gamma_1}\right)\right]^2 \log S(t_i;\boldsymbol{\gamma}) \\ & + 2\sum_{i\in\Delta_1} \frac{e^{\boldsymbol{x}_i'\boldsymbol{\beta}} \left[\log\left(\frac{t_i}{\gamma_1}\right)\right]^2 S(t_i;\boldsymbol{\gamma}) \log S(t_i;\boldsymbol{\gamma}) C_1(t_i,\boldsymbol{x}_i;\boldsymbol{\beta},\boldsymbol{\gamma})}{B(t_i,\boldsymbol{x}_i;\boldsymbol{\beta},\boldsymbol{\gamma})^2} \\ & + \sum_{i\in\Delta_0} \pi_i^{(k)} \frac{e^{\boldsymbol{x}_i'\boldsymbol{\beta}} \left[\log\left(\frac{t_i}{\gamma_1}\right)\right]^2 S(t_i;\boldsymbol{\gamma}) \log S(t_i;\boldsymbol{\gamma}) C_1(t_i,\boldsymbol{x}_i;\boldsymbol{\beta},\boldsymbol{\gamma})}{B(t_i,\boldsymbol{x}_i;\boldsymbol{\beta},\boldsymbol{\gamma})^2},\end{aligned}$$

$$\begin{aligned}\frac{\partial^2 Q}{\partial \gamma_0 \gamma_1} =& -\frac{n_1}{\gamma_1} - \sum_{i\in\Delta_1} \frac{\log S(t_i;\boldsymbol{\gamma})}{\gamma_1} \left[1 + \gamma_0 \log\left(\frac{t_i}{\gamma_1}\right)\right] \\ & - \sum_{i\in\Delta_0} \pi_i^{(k)} \frac{\log S(t_i;\boldsymbol{\gamma})}{\gamma_1} \left[1 + \gamma_0 \log\left(\frac{t_i}{\gamma_1}\right)\right] \\ & - 2\sum_{i\in\Delta_1} \frac{e^{\boldsymbol{x}_i'\boldsymbol{\beta}} S(t_i;\boldsymbol{\gamma}) \log S(t_i;\boldsymbol{\gamma}) \left[B(t_i,\boldsymbol{x}_i;\boldsymbol{\beta},\boldsymbol{\gamma}) + \gamma_0 \log\left(\frac{t_i}{\gamma_1}\right) C_1(t_i,\boldsymbol{x}_i;\boldsymbol{\beta},\boldsymbol{\gamma})\right]}{\gamma_1 B(t_i,\boldsymbol{x}_i;\boldsymbol{\beta},\boldsymbol{\gamma})^2} \\ & - \sum_{i\in\Delta_0} \pi_i^{(k)} \frac{e^{\boldsymbol{x}_i'\boldsymbol{\beta}} S(t_i;\boldsymbol{\gamma}) \log S(t_i;\boldsymbol{\gamma}) \left[B(t_i,\boldsymbol{x}_i;\boldsymbol{\beta},\boldsymbol{\gamma}) + \gamma_0 \log\left(\frac{t_i}{\gamma_1}\right) C_1(t_i,\boldsymbol{x}_i;\boldsymbol{\beta},\boldsymbol{\gamma})\right]}{\gamma_1 B(t_i,\boldsymbol{x}_i;\boldsymbol{\beta},\boldsymbol{\gamma})^2},\end{aligned}$$

$$
\begin{aligned}
\frac{\partial^2 Q}{\partial\gamma_0\gamma_{2h}} = &\sum_{i\in\Delta_1} x_{ih}\log\left(\frac{t_i}{\gamma_1}\right)\log S(t_i;\boldsymbol{\gamma}) + \sum_{i\in\Delta_0}\pi_i^{(k)} x_{ih}\log\left(\frac{t_i}{\gamma_1}\right)\log S(t_i;\boldsymbol{\gamma}) \\
&+ 2\sum_{i\in\Delta_1}\frac{x_{ih}e^{\boldsymbol{x}_i'\boldsymbol{\beta}}S(t_i;\boldsymbol{\gamma})\log S(t_i;\boldsymbol{\gamma})\log\left(\frac{t_i}{\gamma_1}\right)C_1(t_i,\boldsymbol{x}_i;\boldsymbol{\beta},\boldsymbol{\gamma})}{B(t_i,\boldsymbol{x}_i;\boldsymbol{\beta},\boldsymbol{\gamma})^2} \\
&+ \sum_{i\in\Delta_0}\pi_i^{(k)}\frac{x_{ih}e^{\boldsymbol{x}_i'\boldsymbol{\beta}}S(t_i;\boldsymbol{\gamma})\log S(t_i;\boldsymbol{\gamma})\log\left(\frac{t_i}{\gamma_1}\right)C_1(t_i,\boldsymbol{x}_i;\boldsymbol{\beta},\boldsymbol{\gamma})}{B(t_i,\boldsymbol{x}_i;\boldsymbol{\beta},\boldsymbol{\gamma})^2},
\end{aligned}
$$

$$
\begin{aligned}
\frac{\partial^2 Q}{\partial\gamma_1^2} &= \frac{n_1\gamma_0}{\gamma_1^2} + \sum_{i\in\Delta_1}\frac{\gamma_0(1+\gamma_0)}{\gamma_1^2}\log S(t_i;\boldsymbol{\gamma}) + \sum_{i\in\Delta_0}\pi_i^{(k)}\frac{\gamma_0(1+\gamma_0)}{\gamma_1^2}\log S(t_i;\boldsymbol{\gamma}) \\
&+ 2\sum_{i\in\Delta_1}\frac{e^{\boldsymbol{x}_i'\boldsymbol{\beta}}\left(\frac{\gamma_0}{\gamma_1}\right)S(t_i;\boldsymbol{\gamma})\log S(t_i;\boldsymbol{\gamma})\left[B(t_i,\boldsymbol{x}_i;\boldsymbol{\beta},\boldsymbol{\gamma})+\gamma_0C_1(t_i,\boldsymbol{x}_i;\boldsymbol{\beta},\boldsymbol{\gamma})\right]}{\gamma_1B(t_i,\boldsymbol{x}_i;\boldsymbol{\beta},\boldsymbol{\gamma})^2} \\
&+ \sum_{i\in\Delta_0}\pi_i^{(k)}\frac{e^{\boldsymbol{x}_i'\boldsymbol{\beta}}\left(\frac{\gamma_0}{\gamma_1}\right)S(t_i;\boldsymbol{\gamma})\log S(t_i;\boldsymbol{\gamma})\left[B(t_i,\boldsymbol{x}_i;\boldsymbol{\beta},\boldsymbol{\gamma})+\gamma_0C_1(t_i,\boldsymbol{x}_i;\boldsymbol{\beta},\boldsymbol{\gamma})\right]}{\gamma_1B(t_i,\boldsymbol{x}_i;\boldsymbol{\beta},\boldsymbol{\gamma})^2},
\end{aligned}
$$

$$
\begin{aligned}
\frac{\partial^2 Q}{\partial\gamma_1\gamma_{2h}} = &-\sum_{i\in\Delta_1} x_{ih}\frac{\gamma_0}{\gamma_1}\log S(t_i;\boldsymbol{\gamma}) \\
&- 2\sum_{i\in\Delta_1} x_{ih}\frac{e^{\boldsymbol{x}_i'\boldsymbol{\beta}}\left(\frac{\gamma_0}{\gamma_1}\right)S(t_i;\boldsymbol{\gamma})\log S(t_i;\boldsymbol{\gamma})C_1(t_i,\boldsymbol{x}_i;\boldsymbol{\beta},\boldsymbol{\gamma})}{B(t_i,\boldsymbol{x}_i;\boldsymbol{\beta},\boldsymbol{\gamma})^2} \\
&- \sum_{i\in\Delta_0}\pi_i^{(k)}x_{ih}\frac{\gamma_0}{\gamma_1}\log S(t_i;\boldsymbol{\gamma}) \\
&- \sum_{i\in\Delta_0}\pi_i^{(k)}x_{ih}\frac{e^{\boldsymbol{x}_i'\boldsymbol{\beta}}\left(\frac{\gamma_0}{\gamma_1}\right)S(t_i;\boldsymbol{\gamma})\log S(t_i;\boldsymbol{\gamma})C_1(t_i,\boldsymbol{x}_i;\boldsymbol{\beta},\boldsymbol{\gamma})}{B(t_i,\boldsymbol{x}_i;\boldsymbol{\beta},\boldsymbol{\gamma})^2},
\end{aligned}
$$

$$\begin{aligned}\frac{\partial^2 Q}{\partial\gamma_{2h}\gamma_{2h'}} = &\sum_{i\in\Delta_1} x_{ih}x_{ih'}\log S(t_i;\boldsymbol{\gamma})\\ &+2\sum_{i\in\Delta_1} x_{ih}x_{ih'}\frac{e^{\boldsymbol{x}_i'\boldsymbol{\beta}}S(t_i;\boldsymbol{\gamma})\log S(t_i;\boldsymbol{\gamma})C_1(t_i,\boldsymbol{x}_i;\boldsymbol{\beta},\boldsymbol{\gamma})}{B(t_i,\boldsymbol{x}_i;\boldsymbol{\beta},\boldsymbol{\gamma})^2}\\ &+\sum_{i\in\Delta_0}\pi_i^{(k)}x_{ih}x_{ih'}\log S(t_i;\boldsymbol{\gamma})\\ &+\sum_{i\in\Delta_0}\pi_i^{(k)}x_{ih}x_{ih'}\frac{e^{\boldsymbol{x}_i'\boldsymbol{\beta}}S(t_i;\boldsymbol{\gamma})\log S(t_i;\boldsymbol{\gamma})C_1(t_i,\boldsymbol{x}_i;\boldsymbol{\beta},\boldsymbol{\gamma})}{B(t_i,\boldsymbol{x}_i;\boldsymbol{\beta},\boldsymbol{\gamma})^2},\end{aligned}$$

where

$$\pi_i^{(k)} = \left.\frac{e^{\boldsymbol{x}_i'\boldsymbol{\beta}}S(t_i;\boldsymbol{\gamma})}{1+e^{\boldsymbol{x}_i'\boldsymbol{\beta}}}\right|_{\boldsymbol{\theta}=\boldsymbol{\theta}^{(k)}},$$

$$B(t_i,\boldsymbol{x}_i;\boldsymbol{\beta},\boldsymbol{\gamma}) = 1+e^{\boldsymbol{x}_i'\boldsymbol{\beta}}[1-S(t_i;\boldsymbol{\gamma})],$$

$$C_1(t_i,\boldsymbol{x}_i;\boldsymbol{\beta},\boldsymbol{\gamma}) = B(t_i,\boldsymbol{x}_i;\boldsymbol{\beta},\boldsymbol{\gamma})+(1+e^{\boldsymbol{x}_i'\boldsymbol{\beta}})\log S(t_i;\boldsymbol{\gamma})$$

and

$$S(t_i;\boldsymbol{\gamma}) = \exp\left[-\left(\frac{t_i}{\gamma_1}\right)^{\gamma_0} e^{\boldsymbol{x}_{ic}'\boldsymbol{\gamma}_2}\right]$$

for l,l' =0, $\ldots$, p, x_{i0}= 1, h, h'=1, $\ldots$, p, and i=1, $\ldots$, n.

A.2.4 COM-Poisson cure rate model

The first- and second-order partial derivatives of $Q(\boldsymbol{\theta}, \boldsymbol{\pi}^{(k)})$ with respect to $\boldsymbol{\beta}$ and $\boldsymbol{\gamma}$, for a fixed value of the dispersion parameter ϕ, are as follows:

$$\frac{\partial Q}{\partial\beta_l} = -\sum_{i\in\Delta^*} x_{il}\frac{e^{\boldsymbol{x}_i'\boldsymbol{\beta}}}{1+e^{\boldsymbol{x}_i'\boldsymbol{\beta}}}+\sum_{i\in\Delta_1} x_{il}\frac{e^{\boldsymbol{x}_i'\boldsymbol{\beta}}z_{21,i}}{z_{2,i}z_{01,i}}+\sum_{i\in\Delta_0}\pi_i^{(k)}x_{il}\frac{e^{\boldsymbol{x}_i'\boldsymbol{\beta}}z_{2,i}}{z_{1,i}z_{01,i}},$$

$$\frac{\partial Q}{\partial\gamma_h} = \frac{\partial R(t_i,\boldsymbol{x}_i;\boldsymbol{\gamma})}{\partial\gamma_h}+\sum_{i\in\Delta_1}\left[\frac{\partial\log S(t_i;\boldsymbol{\gamma})}{\partial\gamma_h}\right]\frac{z_{21,i}}{z_{2,i}}+\sum_{i\in\Delta_0}\pi_i^{(k)}\left[\frac{\partial\log S(t_i;\boldsymbol{\gamma})}{\partial\gamma_h}\right]\frac{z_{2,i}}{z_{1,i}},$$

$$
\begin{aligned}
\frac{\partial^2 Q}{\partial\beta_l\beta_{l'}} &= -\sum_{i\in\Delta^*} x_{il}x_{il'}\frac{e^{\boldsymbol{x}_i'\boldsymbol{\beta}}}{(1+e^{\boldsymbol{x}_i'\boldsymbol{\beta}})^2} \\
&+ \sum_{I1} x_{il}x_{il'}e^{\boldsymbol{x}_i'\boldsymbol{\beta}}\left[\frac{z_{21,i}}{z_{01,i}z_{2,i}} - e^{\boldsymbol{x}_i'\boldsymbol{\beta}}\left(\frac{z_{01,i}z_{21,i}^2 + z_{02,i}z_{2,i}z_{21,i} - z_{01,i}z_{2,i}z_{31,i}}{z_{2,i}^2 z_{01,i}^3}\right)\right] \\
&+ \sum_{I0} \pi_i^{(k)} x_{il}x_{il'}e^{\boldsymbol{x}_i'\boldsymbol{\beta}}\left[\frac{z_{2,i}}{z_{01,i}z_{1,i}} - e^{\boldsymbol{x}_i'\boldsymbol{\beta}}\left(\frac{z_{01,i}z_{2,i}^2 + z_{02,i}z_{1,i}z_{2,i} - z_{01,i}z_{1,i}z_{21,i}}{z_{1,i}^2 z_{01,i}^3}\right)\right],
\end{aligned}
$$

$$
\begin{aligned}
\frac{\partial^2 Q}{\partial\beta_l\gamma_h} &= \sum_{i\in\Delta_1} x_{il}e^{\boldsymbol{x}_i'\boldsymbol{\beta}}\left[\frac{\partial\log S(t_i;\boldsymbol{\gamma})}{\partial\gamma_h}\right]\frac{z_{2,i}z_{31,i} - z_{21,i}^2}{z_{01,i}z_{2,i}^2} \\
&+ \sum_{i\in\Delta_0} \pi_i^{(k)} x_{il}e^{\boldsymbol{x}_i'\boldsymbol{\beta}}\left[\frac{\partial\log S(t_i;\boldsymbol{\gamma})}{\partial\gamma_h}\right]\frac{z_{1,i}z_{21,i} - z_{2,i}^2}{z_{01,i}z_{1,i}^2},
\end{aligned}
$$

$$
\begin{aligned}
\frac{\partial^2 Q}{\partial\gamma_h\gamma_{h'}} &= \frac{\partial^2 R(t_i,\boldsymbol{x}_i;\boldsymbol{\gamma})}{\partial\gamma_h\partial\gamma_{h'}} \\
&+ \sum_{i\in\Delta_1}\left[\left(\frac{\partial^2\log S(t_i;\boldsymbol{\gamma})}{\partial\gamma_h\partial\gamma_{h'}}\right)\frac{z_{21,i}}{z_{2,i}} - \left(\frac{\partial\log S(t_i;\boldsymbol{\gamma})}{\partial\gamma_h}\right)\left(\frac{\partial\log S(t_i;\boldsymbol{\gamma})}{\partial\gamma_{h'}}\right)\frac{z_{21,i}^2 - z_{2,i}z_{31,i}}{z_{2,i}^2}\right] \\
&+ \sum_{i\in\Delta_0}\pi_i^{(k)} \\
&\times\left[\left(\frac{\partial^2\log S(t_i;\boldsymbol{\gamma})}{\partial\gamma_h\partial\gamma_{h'}}\right)\frac{z_{2,i}}{z_{1,i}} - \left(\frac{\partial\log S(t_i;\boldsymbol{\gamma})}{\partial\gamma_h}\right)\left(\frac{\partial\log S(t_i;\boldsymbol{\gamma})}{\partial\gamma_{h'}}\right)\frac{z_{2,i}^2 - z_{1,i}z_{21,i}}{z_{1,i}^2}\right],
\end{aligned}
$$

where

$$
\pi_i^{(k)} = \left.\frac{z_{1,i}}{1+z_{1,i}}\right|_{\boldsymbol{\theta}=\boldsymbol{\theta}^{(k)}},
$$

$$
z_1 = z_1(\boldsymbol{\theta};\boldsymbol{x},t) = \sum_{j=1}^{\infty}\frac{\{\eta S(t_i;\boldsymbol{\gamma})\}^j}{(j!)^\phi}, z_2 = z_2(\boldsymbol{\theta};\boldsymbol{x},t) = \sum_{j=1}^{\infty}\frac{j\{\eta S(t_i;\boldsymbol{\gamma})\}^j}{(j!)^\phi},
$$

$$
z_{21} = z_{21}(\boldsymbol{\theta};\boldsymbol{x},t) = \sum_{j=1}^{\infty}\frac{j^2\{\eta S(t_i;\boldsymbol{\gamma})\}^j}{(j!)^\phi}, z_{31} = z_{31}(\boldsymbol{\theta};\boldsymbol{x},t) = \sum_{j=1}^{\infty}\frac{j^3\{\eta S(t_i;\boldsymbol{\gamma})\}^j}{(j!)^\phi},
$$

$$z_{01} = z_{01}(\boldsymbol{\theta}; \boldsymbol{x}, t) = \sum_{j=1}^{\infty} \frac{j\eta^j}{(j!)^{\phi}}, z_{02} = z_{02}(\boldsymbol{\theta}; \boldsymbol{x}, t) = \sum_{j=1}^{\infty} \frac{j^2\eta^j}{(j!)^{\phi}},$$

$$\eta = \eta(\boldsymbol{\beta}; \boldsymbol{x}) = H_{\phi}^{-1}(1 + e^{\boldsymbol{x}_i'\boldsymbol{\beta}}),$$

$$S(t_i; \boldsymbol{\gamma}) = \exp\left[-\left(\frac{t_i}{\gamma_1}\right)^{\gamma_0} e^{\boldsymbol{x}_{ic}'\boldsymbol{\gamma}_2}\right]$$

and

$$R = R(t_i, \boldsymbol{x}_i; \boldsymbol{\gamma}) = n_1 \log\gamma_0 + (\gamma_0 - 1)\sum_{i\in\Delta_1} \log t_i - n_1\gamma_0 \log\gamma_1 + \sum_{i\in\Delta_1} \boldsymbol{x}_{ic}'\boldsymbol{\gamma}_2$$

for l,l' =0, …, p, x_{i0}= 1, h, h'=0, 1,$j*$, where $j*$=21, 22, …, 2p, and i=1, …, n.

The derivatives of $R(t_i, \boldsymbol{x}_i; \boldsymbol{\gamma})$ and $S(t; \boldsymbol{\gamma})$ are as follows:

$$\frac{\partial R}{\partial\gamma_0} = \frac{n_1}{\gamma_0} + \sum_{i\in\Delta_1} \log t_i - n_1 \log(\gamma_1), \quad \frac{\partial R}{\partial\gamma_1} = -\frac{n_1\gamma_0}{\gamma_1}, \quad \frac{\partial R}{\partial\gamma_{2h}} = \sum_{i\in\Delta_1} x_{ih},$$
$$\frac{\partial^2 R}{\partial\gamma_0^2} = -\frac{n_1}{\gamma_0^2}, \quad \frac{\partial^2 R}{\partial\gamma_0\partial\gamma_1} = -\frac{n_1}{\gamma_1^2}, \quad \frac{\partial^2 R}{\partial\gamma_0\partial\gamma_{2h}} = 0,$$
$$\frac{\partial^2 R}{\partial\gamma_1^2} = \frac{n_1\gamma_0}{\gamma_1^2}, \quad \frac{\partial^2 R}{\partial\gamma_1\partial\gamma_{2h}} = 0, \quad \frac{\partial^2 R}{\partial\gamma_{2h}\partial\gamma_{2h'}} = 0.$$

$$\frac{\partial \log S(t;\boldsymbol{\gamma})}{\partial \gamma_0} = \log S(t;\boldsymbol{\gamma}) \log\left(\frac{t}{\gamma_1}\right), \ \frac{\partial \log S(t;\boldsymbol{\gamma})}{\partial \gamma_1} = \log S(t;\boldsymbol{\gamma}) \left(\frac{-\gamma_0}{\gamma_1}\right),$$
$$\frac{\partial \log S(t;\boldsymbol{\gamma})}{\partial \gamma_{2h}} = x_h \log S(t;\boldsymbol{\gamma}), \ \frac{\partial^2 \log S(t;\boldsymbol{\gamma})}{\partial \gamma_0^2} = \log S(t;\boldsymbol{\gamma}) \left[\log\left(\frac{t}{\gamma_1}\right)\right]^2,$$
$$\frac{\partial^2 \log S(t;\boldsymbol{\gamma})}{\partial \gamma_0 \partial \gamma_1} = \log S(t;\boldsymbol{\gamma}) \left[\frac{-1-\gamma_0 \log\left(\frac{t}{\gamma_1}\right)}{\gamma_1}\right],$$
$$\frac{\partial^2 \log S(t;\boldsymbol{\gamma})}{\partial \gamma_0 \partial \gamma_{2h}} = x_h \log S(t;\boldsymbol{\gamma}) \log\left(\frac{t}{\gamma_1}\right),$$
$$\frac{\partial^2 \log S(t;\boldsymbol{\gamma})}{\partial \gamma_1^2} = \log S(t;\boldsymbol{\gamma}) \left[\frac{\gamma_0(1+\gamma_0)}{\gamma_1^2}\right],$$
$$\frac{\partial^2 \log S(t;\boldsymbol{\gamma})}{\partial \gamma_1 \partial \gamma_{2h}} = x_h \log S(t;\boldsymbol{\gamma}) \left(\frac{-\gamma_0}{\gamma_1}\right), \quad \frac{\partial^2 \log S(t;\boldsymbol{\gamma})}{\partial \gamma_{2h} \partial \gamma_{2h'}} = x_h x_{h'} \log S(t;\boldsymbol{\gamma}),$$

for l,l' =0, $\ldots$, p, x_{i0}= 1, h, h'=1, $\ldots$, p, and i=1, $\ldots$, n.

Appendix B

Appendix corresponding to Chapter 3

B.1 The Q-functions

B.1.1 Bernoulli cure rate model

$$Q(\boldsymbol{\theta}, \boldsymbol{\pi}^{(k)}) = Q_1(\boldsymbol{\beta}, \boldsymbol{\pi}^{(k)}) + Q_2(\boldsymbol{\psi}, \boldsymbol{\gamma}, \boldsymbol{\pi}^{(k)})$$

where

$$Q_1(\boldsymbol{\beta}, \boldsymbol{\pi}^{(k)}) = \sum_{i \in \Delta_1} \boldsymbol{\beta}' \boldsymbol{x}_i^* + \sum_{i \in \Delta_0} \pi_i^{(k)} \boldsymbol{\beta}' \boldsymbol{x}_i^* - \sum_{i \in \Delta^*} \log(1 + e^{\boldsymbol{\beta}' \boldsymbol{x}_i^*})$$

and

$$Q_2(\boldsymbol{\psi}, \boldsymbol{\gamma}, \boldsymbol{\pi}^{(k)}) = \sum_{i \in \Delta_1} \log h_0(t_i; \boldsymbol{\psi}) + \sum_{i \in \Delta_1} \boldsymbol{\gamma}' \boldsymbol{x}_i - \sum_{i \in \Delta_1} H_0(t_i; \boldsymbol{\psi}) e^{\boldsymbol{\gamma}' \boldsymbol{x}_i} - \sum_{i \in \Delta_0} \pi_i^{(k)} H_0(t_i; \boldsymbol{\psi}) e^{\boldsymbol{\gamma}' \boldsymbol{x}_i}$$

with

$$\pi_i^{(k)} = \left. \frac{\exp\left[\boldsymbol{\beta}' \boldsymbol{x}_i^* - H_0(t_i; \boldsymbol{\psi}) e^{\boldsymbol{\gamma}' \boldsymbol{x}_i}\right]}{1 + \exp\left[\boldsymbol{\beta}' \boldsymbol{x}_i^* - H_0(t_i; \boldsymbol{\psi}) e^{\boldsymbol{\gamma}' \boldsymbol{x}_i}\right]} \right|_{\boldsymbol{\theta} = \boldsymbol{\theta}^{(k)}} \tag{B.1.1}$$

for $i \in \Delta_0$ and $\Delta^* = \Delta_1 \cup \Delta_0$.

B.1.2 Poisson cure rate model

$$\begin{aligned} Q(\boldsymbol{\theta}, \boldsymbol{\pi}^{(k)}) = & \sum_{i\in\Delta_1} \log h_0(t_i;\boldsymbol{\psi}) + \sum_{i\in\Delta_1} \boldsymbol{\gamma}'\boldsymbol{x}_i + \sum_{i\in\Delta_1} \log(\log(1+e^{\boldsymbol{\beta}'\boldsymbol{x}_i^*})) - \sum_{i\in\Delta_1} H_0(t_i;\boldsymbol{\psi})e^{\boldsymbol{\gamma}'\boldsymbol{x}_i} \\ & - \sum_{\Delta^*} \log(1+e^{\boldsymbol{\beta}'\boldsymbol{x}_i^*}) + \sum_{i\in\Delta_1} A(t_i,\boldsymbol{x}_i;\boldsymbol{\beta},\boldsymbol{\psi},\boldsymbol{\gamma}) \\ & - \sum_{i\in\Delta_0} \pi_i^{(k)} \log(A(t_i,\boldsymbol{x}_i;\boldsymbol{\beta},\boldsymbol{\psi},\boldsymbol{\gamma})-1) \end{aligned}$$

where

$$A(t_i,\boldsymbol{x}_i;\boldsymbol{\beta},\boldsymbol{\psi},\boldsymbol{\gamma}) = \exp[-H_0(t_i;\boldsymbol{\psi})e^{\boldsymbol{\gamma}'\boldsymbol{x}_i}]\log(1+e^{\boldsymbol{\beta}'\boldsymbol{x}_i^*})$$

for $i \in \Delta^*$ and

$$\pi_i^{(k)} = \left.\frac{e^{A(t_i,\boldsymbol{x}_i;\boldsymbol{\beta},\boldsymbol{\psi},\boldsymbol{\gamma})}-1}{e^{A(t_i,\boldsymbol{x}_i;\boldsymbol{\beta},\boldsymbol{\psi},\boldsymbol{\gamma})}}\right|_{\boldsymbol{\theta}=\boldsymbol{\theta}^{(k)}} \tag{B.1.2}$$

for $i \in \Delta_0$.

B.1.3 Geometric cure rate model

$$\begin{aligned} Q(\boldsymbol{\theta}, \boldsymbol{\pi}^{(k)}) = & \sum_{i\in\Delta_1} \boldsymbol{\beta}'\boldsymbol{x}_i^* + \sum_{i\in\Delta_1} \log h_0(t_i;\boldsymbol{\psi}) + \sum_{i\in\Delta_1} \boldsymbol{\gamma}'\boldsymbol{x}_i - \sum_{i\in\Delta_1} H_0(t_i;\boldsymbol{\psi})e^{\boldsymbol{\gamma}'\boldsymbol{x}_i} \\ & - 2\sum_{i\in\Delta_1} \log(1+C(t_i,\boldsymbol{x}_i;\boldsymbol{\beta},\boldsymbol{\psi},\boldsymbol{\gamma})) + \sum_{i\in\Delta_0} \pi_i^{(k)} \left[\boldsymbol{\beta}'\boldsymbol{x}_i^* - H_0(t_i;\boldsymbol{\psi})e^{\boldsymbol{\gamma}'\boldsymbol{x}_i}\right] \\ & - \sum_{i\in\Delta_0} \pi_i^{(k)} \log(1+C(t_i,\boldsymbol{x}_i;\boldsymbol{\beta},\boldsymbol{\psi},\boldsymbol{\gamma})) - \sum_{i\in\Delta_0} \log(1+e^{\boldsymbol{\beta}'\boldsymbol{x}_i^*}) \end{aligned}$$

where

$$C(t_i,\boldsymbol{x}_i;\boldsymbol{\beta},\boldsymbol{\psi},\boldsymbol{\gamma}) = e^{\boldsymbol{\beta}'\boldsymbol{x}_i^*}\left\{1-\exp\left[-H_0(t_i;\boldsymbol{\psi})e^{\boldsymbol{\gamma}'\boldsymbol{x}_i}\right]\right\}$$

for $i \in \Delta^*$ and

$$\pi_i^{(k)} = \left.\frac{e^{\left[\boldsymbol{\beta}'\boldsymbol{x}_i^* - H_0(t_i;\boldsymbol{\psi})e^{\boldsymbol{\gamma}'\boldsymbol{x}_i}\right]}}{1+e^{\boldsymbol{\beta}'\boldsymbol{x}_i^*}}\right|_{\boldsymbol{\theta}=\boldsymbol{\theta}^{(k)}} \tag{B.1.3}$$

for $i \in \Delta_0$.

B.1.4 COM-Poisson cure rate model

$$Q(\boldsymbol{\theta}, \boldsymbol{\pi}^{(k)}) = \sum_{i\in\Delta_1} \log h_0(t_i;\boldsymbol{\psi}) + \sum_{i\in\Delta_1} \boldsymbol{\gamma}'\boldsymbol{x}_i - \sum_{i\in\Delta^*} \log(1+e^{\boldsymbol{\beta}'\boldsymbol{x}_i^*})$$
$$+ \sum_{i\in\Delta_1} \log z_{2i} + \sum_{i\in\Delta_0} \pi_i^{(k)} \log z_{1i}$$

where

$$z_{1i} = z_1(\boldsymbol{\theta};\boldsymbol{x}_i,t_i) = \sum_{j=1}^{\infty} \frac{\{\eta_i S(t_i,\boldsymbol{x}_i;\boldsymbol{\psi},\boldsymbol{\gamma})\}^j}{(j!)^\phi}, z_{2i} = z_2(\boldsymbol{\theta};\boldsymbol{x}_i,t_i) = \sum_{j=1}^{\infty} \frac{j\{\eta_i S(t_i,\boldsymbol{x}_i;\boldsymbol{\psi},\boldsymbol{\gamma})\}^j}{(j!)^\phi},$$

$$\eta_i = \eta(\boldsymbol{\beta};\boldsymbol{x}_i) = H_\phi^{*-1}(1+e^{\boldsymbol{\beta}'\boldsymbol{x}_i^*}) \text{ and } S(t_i,\boldsymbol{x}_i;\boldsymbol{\psi},\boldsymbol{\gamma}) = \exp\left[-H_0(t_i;\boldsymbol{\psi})e^{\boldsymbol{\gamma}'\boldsymbol{x}_i}\right].$$

with

$$\pi_i^{(k)} = \left.\frac{z_1(\boldsymbol{\theta};\boldsymbol{x}_i,t_i)}{1+z_1(\boldsymbol{\theta};\boldsymbol{x}_i,t_i)}\right|_{\boldsymbol{\theta}=\boldsymbol{\theta}^{(k)}} \tag{B.1.4}$$

for $i \in \Delta_0$,

where $\Delta^* = \Delta_1 \cup \Delta_0$ and $n_1 = |\Delta_1|$ (i.e. n_1 is the cardinality of Δ_1). The expressions for $h_0(t_i;\boldsymbol{\psi})$ and $H_0(t_i;\boldsymbol{\psi})$ are provided in (**??**) and (**??**) respectively.

B.2 First- and second-order derivatives of the Q-function

B.2.1 Bernoulli cure rate model

The first- and the second-order partial derivatives of the $Q_1(\boldsymbol{\beta}, \boldsymbol{\pi}^{(k)})$ function with respect to $\boldsymbol{\beta}$ and of the $Q_2(\boldsymbol{\psi}, \boldsymbol{\gamma}, \boldsymbol{\pi}^{(k)})$ function with respect to $\boldsymbol{\psi}$ and $\boldsymbol{\gamma}$ are as follows:

$$\frac{\partial Q_1}{\partial \beta_d} = \sum_{i\in\Delta_1} x_{id} - \sum_{i\in\Delta^*} x_{id}\frac{e^{\boldsymbol{\beta}'\boldsymbol{x}_i^*}}{1+e^{\boldsymbol{\beta}'\boldsymbol{x}_i^*}} + \sum_{i\in\Delta_0} \pi_i^{(k)} x_{id},$$

$$\frac{\partial Q_2}{\partial \psi_l} = \sum_{i\in\Delta_1} \frac{\frac{\partial h_0(t_i;\boldsymbol{\psi})}{\partial \psi_l}}{h_0(t_i;\boldsymbol{\psi})} - \sum_{i\in\Delta_1} \frac{\partial H_0(t_i;\boldsymbol{\psi})}{\partial \psi_l} e^{\boldsymbol{\gamma}'\boldsymbol{x}_i} - \sum_{i\in\Delta_0} \pi_i^{(k)} \frac{\partial H_0(t_i;\boldsymbol{\psi})}{\partial \psi_l} e^{\boldsymbol{\gamma}'\boldsymbol{x}_i},$$

$$\frac{\partial Q_2}{\partial \gamma_r} = \sum_{i\in\Delta_1} x_{ir} - \sum_{i\in\Delta_1} x_{ir} H_0(t_i;\boldsymbol{\psi}) e^{\boldsymbol{\gamma}'\boldsymbol{x}_i} - \sum_{i\in\Delta_0} \pi_i^{(k)} x_{ir} H_0(t_i;\boldsymbol{\psi}) e^{\boldsymbol{\gamma}'\boldsymbol{x}_i},$$

$$\frac{\partial^2 Q_1}{\partial \beta_d \partial \beta_{d'}} = -\sum_{i\in\Delta^*} x_{id} x_{id'} \frac{e^{\boldsymbol{\beta}'\boldsymbol{x}_i^*}}{(1+e^{\boldsymbol{\beta}'\boldsymbol{x}_i^*})^2},$$

$$\frac{\partial^2 Q_2}{\partial \psi_l \partial \psi_{l'}} = -\sum_{i\in\Delta_1} \frac{\left(\frac{\partial h_0(t_i;\boldsymbol{\psi})}{\partial \psi_l}\right)\left(\frac{\partial h_0(t_i;\boldsymbol{\psi})}{\partial \psi_{l'}}\right)}{h_0^2(t_i;\boldsymbol{\psi})} - \sum_{i\in\Delta_1} \frac{\partial^2 H_0(t_i;\boldsymbol{\psi})}{\partial \psi_l \partial \psi_{l'}} e^{\boldsymbol{\gamma}'\boldsymbol{x}_i} - \sum_{i\in\Delta_0} \pi_i^{(k)} \frac{\partial^2 H_0(t_i;\boldsymbol{\psi})}{\partial \psi_l \partial \psi_{l'}} e^{\boldsymbol{\gamma}'\boldsymbol{x}_i},$$

$$\frac{\partial^2 Q_2}{\partial \psi_l \partial \gamma_r} = -\sum_{i\in\Delta_1} x_{ir} \frac{\partial H_0(t_i;\boldsymbol{\psi})}{\partial \psi_l} e^{\boldsymbol{\gamma}'\boldsymbol{x}_i} - \sum_{i\in\Delta_0} \pi_i^{(k)} x_{ir} \frac{\partial H_0(t_i;\boldsymbol{\psi})}{\partial \psi_l} e^{\boldsymbol{\gamma}'\boldsymbol{x}_i},$$

$$\frac{\partial^2 Q_2}{\partial \gamma_r \partial \gamma_{r'}} = -\sum_{i\in\Delta_1} x_{ir} x_{ir'} H_0(t_i;\boldsymbol{\psi}) e^{\boldsymbol{\gamma}'\boldsymbol{x}_i} - \sum_{i\in\Delta_0} \pi_i^{(k)} x_{ir} x_{ir'} H_0(t_i;\boldsymbol{\psi}) e^{\boldsymbol{\gamma}'\boldsymbol{x}_i};$$

for $d, d' = 0, 1, \ldots, p$ with $x_{i0} = 1$; $r, r' = 1, 2, \ldots, p$ and $l = 0, 1, \ldots, N$.

B.2.2 Poisson cure rate model

The first- and the second-order partial derivatives of the $Q(\boldsymbol{\theta}, \boldsymbol{\pi}^{(k)})$ function with respect to $\boldsymbol{\beta}$, $\boldsymbol{\psi}$ and $\boldsymbol{\gamma}$ are as follows:

$$\begin{aligned}\frac{\partial Q}{\partial \beta_d} &= \sum_{i \in \Delta_1} x_{id} \frac{e^{\boldsymbol{\beta}' \boldsymbol{x}_i^*}}{(1 + e^{\boldsymbol{\beta}' \boldsymbol{x}_i^*}) \log(1 + e^{\boldsymbol{\beta}' \boldsymbol{x}_i^*})} + \sum_{i \in \Delta_1} x_{id} \frac{e^{\boldsymbol{\beta}' \boldsymbol{x}_i^*} S(t_i, \boldsymbol{x}_i; \boldsymbol{\psi}, \boldsymbol{\gamma})}{(1 + e^{\boldsymbol{\beta}' \boldsymbol{x}_i^*})} - \sum_{i \in \Delta^*} x_{id} \frac{e^{\boldsymbol{\beta}' \boldsymbol{x}_i^*}}{(1 + e^{\boldsymbol{\beta}' \boldsymbol{x}_i^*})} \\ &\quad + \sum_{i \in \Delta_0} \pi_i^{(k)} x_{id} \frac{e^{\boldsymbol{\beta}' \boldsymbol{x}_i^*} P(t_i, \boldsymbol{x}_i; \boldsymbol{\beta}, \boldsymbol{\psi}, \boldsymbol{\gamma}) S(t_i, \boldsymbol{x}_i; \boldsymbol{\psi}, \boldsymbol{\gamma})}{(1 + e^{\boldsymbol{\beta}' \boldsymbol{x}_i^*})},\end{aligned}$$

$$\begin{aligned}\frac{\partial Q}{\partial \psi_l} &= \sum_{i \in \Delta_1} \frac{\frac{\partial h_0(t_i; \boldsymbol{\psi})}{\partial \psi_l}}{h_0(t_i; \boldsymbol{\psi})} - \sum_{i \in \Delta_1} \frac{\partial H_0(t_i; \boldsymbol{\psi})}{\partial \psi_l} e^{\boldsymbol{\gamma}' \boldsymbol{x}_i} \{A(t_i, \boldsymbol{x}_i; \boldsymbol{\beta}, \boldsymbol{\psi}, \boldsymbol{\gamma}) + 1\} \\ &\quad + \sum_{i \in \Delta_0} \pi_i^{(k)} \frac{\partial H_0(t_i; \boldsymbol{\psi})}{\partial \psi_l} e^{\boldsymbol{\gamma}' \boldsymbol{x}_i} P(t_i, \boldsymbol{x}_i; \boldsymbol{\beta}, \boldsymbol{\psi}, \boldsymbol{\gamma}),\end{aligned}$$

$$\begin{aligned}\frac{\partial Q}{\partial \gamma_r} &= \sum_{i \in \Delta_1} x_{ir} - \sum_{i \in \Delta_1} x_{ir} H_0(t_i; \boldsymbol{\psi}) e^{\boldsymbol{\gamma}' \boldsymbol{x}_i} \{A(t_i, \boldsymbol{x}_i; \boldsymbol{\beta}, \boldsymbol{\psi}, \boldsymbol{\gamma}) + 1\} \\ &\quad + \sum_{i \in \Delta_0} \pi_i^{(k)} x_{ir} H_0(t_i; \boldsymbol{\psi}) e^{\boldsymbol{\gamma}' \boldsymbol{x}_i} P(t_i, \boldsymbol{x}_i; \boldsymbol{\beta}, \boldsymbol{\psi}, \boldsymbol{\gamma}),\end{aligned}$$

$$\frac{\partial^2 Q}{\partial \beta_d \partial \beta_{d'}} = \sum_{i\in\Delta_1} x_{id}x_{id'} \left\{ \frac{e^{\boldsymbol{\beta}'\boldsymbol{x}_i^*}}{(1+e^{\boldsymbol{\beta}'\boldsymbol{x}_i^*})^2} \left(\frac{1}{\log(1+e^{\boldsymbol{\beta}'\boldsymbol{x}_i^*})} \left[1 - \frac{e^{\boldsymbol{\beta}'\boldsymbol{x}_i^*}}{\log(1+e^{\boldsymbol{\beta}'\boldsymbol{x}_i^*})} \right] + S(t_i, \boldsymbol{x}_i; \boldsymbol{\psi}, \boldsymbol{\gamma}) \right) \right\}$$
$$- \sum_{i\in\Delta^*} x_{id}x_{id'} \frac{e^{\boldsymbol{\beta}'\boldsymbol{x}_i^*}}{(1+e^{\boldsymbol{\beta}'\boldsymbol{x}_i^*})^2}$$
$$+ \sum_{i\in\Delta_0} \pi_i^{(k)} x_{id}x_{id'} P(t_i, \boldsymbol{x}_i; \boldsymbol{\beta}, \boldsymbol{\psi}, \boldsymbol{\gamma}) S(t_i, \boldsymbol{x}_i; \boldsymbol{\psi}, \boldsymbol{\gamma}) \frac{e^{\boldsymbol{\beta}'\boldsymbol{x}_i^*}}{(1+e^{\boldsymbol{\beta}'\boldsymbol{x}_i^*})^2} \left[1 - \frac{e^{\boldsymbol{\beta}'\boldsymbol{x}_i^*}}{e^{A(t_i, \boldsymbol{x}_i; \boldsymbol{\beta}, \boldsymbol{\psi}, \boldsymbol{\gamma})} - 1} \right],$$

$$\frac{\partial^2 Q}{\partial \beta_d \partial \psi_l} = - \sum_{i\in\Delta_1} x_{id} \frac{e^{\boldsymbol{\beta}'\boldsymbol{x}_i^*}}{(1+e^{\boldsymbol{\beta}'\boldsymbol{x}_i^*})} S(t_i, \boldsymbol{x}_i; \boldsymbol{\psi}, \boldsymbol{\gamma}) \frac{\partial H_0(t_i; \boldsymbol{\psi})}{\partial \psi_l} e^{\boldsymbol{\gamma}'\boldsymbol{x}_i}$$
$$- \sum_{i\in\Delta_0} \pi_i^{(k)} x_{id} \frac{e^{\boldsymbol{\beta}'\boldsymbol{x}_i^*}}{(1+e^{\boldsymbol{\beta}'\boldsymbol{x}_i^*})} P(t_i, \boldsymbol{x}_i; \boldsymbol{\beta}, \boldsymbol{\psi}, \boldsymbol{\gamma}) S(t_i, \boldsymbol{x}_i; \boldsymbol{\psi}, \boldsymbol{\gamma}) \frac{\partial H_0(t_i; \boldsymbol{\psi})}{\partial \psi_l} e^{\boldsymbol{\gamma}'\boldsymbol{x}_i}$$
$$\times \left[1 - \frac{S(t_i, \boldsymbol{x}_i; \boldsymbol{\psi}, \boldsymbol{\gamma}) \log(1+e^{\boldsymbol{\beta}'\boldsymbol{x}_i^*})}{e^{A(t_i, \boldsymbol{x}_i; \boldsymbol{\beta}, \boldsymbol{\psi}, \boldsymbol{\gamma})} - 1} \right],$$

$$\frac{\partial^2 Q}{\partial \beta_d \partial \gamma_r} = - \sum_{i\in\Delta_1} x_{id}x_{ir} \frac{e^{\boldsymbol{\beta}'\boldsymbol{x}_i^*}}{(1+e^{\boldsymbol{\beta}'\boldsymbol{x}_i^*})} S(t_i, \boldsymbol{x}_i; \boldsymbol{\psi}, \boldsymbol{\gamma}) H_0(t_i; \boldsymbol{\psi}) e^{\boldsymbol{\gamma}'\boldsymbol{x}_i}$$
$$- \sum_{i\in\Delta_0} \pi_i^{(k)} x_{id}x_{ir} \frac{e^{\boldsymbol{\beta}'\boldsymbol{x}_i^*}}{(1+e^{\boldsymbol{\beta}'\boldsymbol{x}_i^*})} P(t_i, \boldsymbol{x}_i; \boldsymbol{\beta}, \boldsymbol{\psi}, \boldsymbol{\gamma}) S(t_i, \boldsymbol{x}_i; \boldsymbol{\psi}, \boldsymbol{\gamma}) H_0(t_i; \boldsymbol{\psi}) e^{\boldsymbol{\gamma}'\boldsymbol{x}_i}$$
$$\times \left[1 - \frac{S(t_i, \boldsymbol{x}_i; \boldsymbol{\psi}, \boldsymbol{\gamma}) \log(1+e^{\boldsymbol{\beta}'\boldsymbol{x}_i^*})}{e^{A(t_i, \boldsymbol{x}_i; \boldsymbol{\beta}, \boldsymbol{\psi}, \boldsymbol{\gamma})} - 1} \right],$$

$$
\begin{aligned}
\frac{\partial^2 Q}{\partial \psi_l \partial \psi_{l'}} &= -\sum_{i\in\Delta_1} \frac{\left(\frac{\partial h_0(t_i;\boldsymbol{\psi})}{\partial \psi_l}\right)\left(\frac{\partial h_0(t_i;\boldsymbol{\psi})}{\partial \psi_{l'}}\right)}{h_0^2(t_i;\boldsymbol{\psi})} - \sum_{i\in\Delta_1} \frac{\partial^2 H_0(t_i;\boldsymbol{\psi})}{\partial \psi_l \partial \psi_{l'}} e^{\boldsymbol{\gamma}'\boldsymbol{x}_i} \\
&\quad - \sum_{i\in\Delta_1} A(t_i,\boldsymbol{x}_i;\boldsymbol{\beta},\boldsymbol{\psi},\boldsymbol{\gamma}) e^{\boldsymbol{\gamma}'\boldsymbol{x}_i} \left[\frac{\partial^2 H_0(t_i;\boldsymbol{\psi})}{\partial \psi_l \partial \psi_{l'}} - \left(\frac{\partial H_0(t_i;\boldsymbol{\psi})}{\partial \psi_l}\right)\left(\frac{\partial H_0(t_i;\boldsymbol{\psi})}{\partial \psi_{l'}}\right) e^{\boldsymbol{\gamma}'\boldsymbol{x}_i}\right] \\
&\quad + \sum_{i\in\Delta_0} \pi_i^{(k)} P(t_i,\boldsymbol{x}_i;\boldsymbol{\beta},\boldsymbol{\psi},\boldsymbol{\gamma}) e^{\boldsymbol{\gamma}'\boldsymbol{x}_i} \\
&\quad \times \left[\frac{\partial^2 H_0(t_i;\boldsymbol{\psi})}{\partial \psi_l \partial \psi_{l'}} + \left(\frac{\partial H_0(t_i;\boldsymbol{\psi})}{\partial \psi_l}\right)\left(\frac{\partial H_0(t_i;\boldsymbol{\psi})}{\partial \psi_{l'}}\right) \frac{A(t_i,\boldsymbol{x}_i;\boldsymbol{\beta},\boldsymbol{\psi},\boldsymbol{\gamma}) e^{\boldsymbol{\gamma}'\boldsymbol{x}_i}}{e^{A(t_i,\boldsymbol{x}_i;\boldsymbol{\beta},\boldsymbol{\psi},\boldsymbol{\gamma})}-1}\right],
\end{aligned}
$$

$$
\begin{aligned}
\frac{\partial^2 Q}{\partial \psi_l \partial \gamma_r} &= -\sum_{i\in\Delta_1} x_{ir} \frac{\partial H_0(t_i;\boldsymbol{\psi})}{\partial \psi_l} e^{\boldsymbol{\gamma}'\boldsymbol{x}_i} \\
&\quad - \sum_{i\in\Delta_1} x_{ir} A(t_i,\boldsymbol{x}_i;\boldsymbol{\beta},\boldsymbol{\psi},\boldsymbol{\gamma}) \frac{\partial H_0(t_i;\boldsymbol{\psi})}{\partial \psi_l} e^{\boldsymbol{\gamma}'\boldsymbol{x}_i} (1 - H_0(t_i;\boldsymbol{\psi}) e^{\boldsymbol{\gamma}'\boldsymbol{x}_i}) \\
&\quad + \sum_{i\in\Delta_0} \pi_i^{(k)} x_{ir} P(t_i,\boldsymbol{x}_i;\boldsymbol{\beta},\boldsymbol{\psi},\boldsymbol{\gamma}) \frac{\partial H_0(t_i;\boldsymbol{\psi})}{\partial \psi_l} e^{\boldsymbol{\gamma}'\boldsymbol{x}_i} \left[1 + \frac{H_0(t_i;\boldsymbol{\psi}) A(t_i,\boldsymbol{x}_i;\boldsymbol{\beta},\boldsymbol{\psi},\boldsymbol{\gamma}) e^{\boldsymbol{\gamma}'\boldsymbol{x}_i}}{e^{A(t_i,\boldsymbol{x}_i;\boldsymbol{\beta},\boldsymbol{\psi},\boldsymbol{\gamma})}-1}\right],
\end{aligned}
$$

$$
\begin{aligned}
\frac{\partial^2 Q}{\partial \gamma_r \partial \gamma_{r'}} &= -\sum_{i\in\Delta_1} x_{ir} x_{ir'} H_0(t_i;\boldsymbol{\psi}) e^{\boldsymbol{\gamma}'\boldsymbol{x}_i} \\
&\quad - \sum_{i\in\Delta_1} x_{ir} x_{ir'} A(t_i,\boldsymbol{x}_i;\boldsymbol{\beta},\boldsymbol{\psi},\boldsymbol{\gamma}) H_0(t_i;\boldsymbol{\psi}) e^{\boldsymbol{\gamma}'\boldsymbol{x}_i} (1 - H_0(t_i;\boldsymbol{\psi}) e^{\boldsymbol{\gamma}'\boldsymbol{x}_i}) \\
&\quad + \sum_{i\in\Delta_0} \pi_i^{(k)} x_{ir} x_{ir'} P(t_i,\boldsymbol{x}_i;\boldsymbol{\beta},\boldsymbol{\psi},\boldsymbol{\gamma}) H_0(t_i;\boldsymbol{\psi}) e^{\boldsymbol{\gamma}'\boldsymbol{x}_i} \left[1 + \frac{H_0(t_i;\boldsymbol{\psi}) A(t_i,\boldsymbol{x}_i;\boldsymbol{\beta},\boldsymbol{\psi},\boldsymbol{\gamma}) e^{\boldsymbol{\gamma}'\boldsymbol{x}_i}}{e^{A(t_i,\boldsymbol{x}_i;\boldsymbol{\beta},\boldsymbol{\psi},\boldsymbol{\gamma})}-1}\right];
\end{aligned}
$$

where

$$A(t_i,\boldsymbol{x}_i;\boldsymbol{\beta},\boldsymbol{\psi},\boldsymbol{\gamma}) = S(t_i,\boldsymbol{x}_i;\boldsymbol{\psi},\boldsymbol{\gamma}) \log(1 + e^{\boldsymbol{\beta}'\boldsymbol{x}_i^*}),$$

$$P(t_i,\boldsymbol{x}_i;\boldsymbol{\beta},\boldsymbol{\psi},\boldsymbol{\gamma}) = \frac{e^{A(t_i,\boldsymbol{x}_i;\boldsymbol{\beta},\boldsymbol{\psi},\boldsymbol{\gamma})}}{e^{A(t_i,\boldsymbol{x}_i;\boldsymbol{\beta},\boldsymbol{\psi},\boldsymbol{\gamma})}-1}$$

and

$$S(t_i, \boldsymbol{x}_i; \boldsymbol{\psi}, \boldsymbol{\gamma}) = \exp\left[-H_0(t_i; \boldsymbol{\psi}) e^{\boldsymbol{x}_i' \boldsymbol{\gamma}}\right];$$

for $d, d' = 0, 1, \ldots, p$ with x_{i0}= 1; $r, r' = 1, 2, \ldots, p$ and $l = 0, 1, \ldots, N$.

B.2.3 Geometric cure rate model

The first- and the second-order partial derivatives of the $Q(\boldsymbol{\theta}, \boldsymbol{\pi}^{(k)})$ function with respect to $\boldsymbol{\beta}$, $\boldsymbol{\psi}$ and $\boldsymbol{\gamma}$ are as follows:

$$\begin{aligned}\frac{\partial Q}{\partial \beta_d} &= \sum_{i \in \Delta_1} x_{id} - 2 \sum_{i \in \Delta_1} x_{id} \frac{C(t_i, \boldsymbol{x}_i; \boldsymbol{\beta}, \boldsymbol{\psi}, \boldsymbol{\gamma})}{1 + C(t_i, \boldsymbol{x}_i; \boldsymbol{\beta}, \boldsymbol{\psi}, \boldsymbol{\gamma})} - \sum_{i \in \Delta_0} x_{id} \frac{e^{\boldsymbol{x}_i^{*\prime} \boldsymbol{\beta}}}{1 + e^{\boldsymbol{x}_i^{*\prime} \boldsymbol{\beta}}} \\ &+ \sum_{i \in \Delta_0} \pi_i^{(k)} x_{id} - \sum_{i \in \Delta_0} \pi_i^{(k)} x_{id} \frac{C(t_i, \boldsymbol{x}_i; \boldsymbol{\beta}, \boldsymbol{\psi}, \boldsymbol{\gamma})}{1 + C(t_i, \boldsymbol{x}_i; \boldsymbol{\beta}, \boldsymbol{\psi}, \boldsymbol{\gamma})},\end{aligned}$$

$$\begin{aligned}\frac{\partial Q}{\partial \psi_l} &= \sum_{i \in \Delta_1} \frac{\frac{\partial h_0(t_i; \boldsymbol{\psi})}{\partial \psi_l}}{h_0(t_i; \boldsymbol{\psi})} - \sum_{i \in \Delta_1} \frac{\partial H_0(t_i; \boldsymbol{\psi})}{\partial \psi_l} e^{\boldsymbol{\gamma}' \boldsymbol{x}_i} - 2 \sum_{i \in \Delta_1} \frac{\partial H_0(t_i; \boldsymbol{\psi})}{\partial \psi_l} e^{\boldsymbol{x}_i^{*\prime} \boldsymbol{\beta} + \boldsymbol{\gamma}' \boldsymbol{x}_i} \frac{S(t_i, \boldsymbol{x}_i; \boldsymbol{\psi}, \boldsymbol{\gamma})}{1 + C(t_i, \boldsymbol{x}_i; \boldsymbol{\beta}, \boldsymbol{\psi}, \boldsymbol{\gamma})} \\ &- \sum_{i \in \Delta_0} \pi_i^{(k)} \frac{\partial H_0(t_i; \boldsymbol{\psi})}{\partial \psi_l} e^{\boldsymbol{\gamma}' \boldsymbol{x}_i} - \sum_{i \in \Delta_0} \pi_i^{(k)} \frac{\partial H_0(t_i; \boldsymbol{\psi})}{\partial \psi_l} e^{\boldsymbol{x}_i^{*\prime} \boldsymbol{\beta} + \boldsymbol{\gamma}' \boldsymbol{x}_i} \frac{S(t_i, \boldsymbol{x}_i; \boldsymbol{\psi}, \boldsymbol{\gamma})}{1 + C(t_i, \boldsymbol{x}_i; \boldsymbol{\beta}, \boldsymbol{\psi}, \boldsymbol{\gamma})},\end{aligned}$$

$$\begin{aligned}\frac{\partial Q}{\partial \gamma_r} &= \sum_{i \in \Delta_1} x_{ir} - \sum_{i \in \Delta_1} x_{ir} H_0(t_i; \boldsymbol{\psi}) e^{\boldsymbol{\gamma}' \boldsymbol{x}_i} - 2 \sum_{i \in \Delta_1} x_{ir} H_0(t_i; \boldsymbol{\psi}) e^{\boldsymbol{x}_i^{*\prime} \boldsymbol{\beta} + \boldsymbol{\gamma}' \boldsymbol{x}_i} \frac{S(t_i, \boldsymbol{x}_i; \boldsymbol{\psi}, \boldsymbol{\gamma})}{1 + C(t_i, \boldsymbol{x}_i; \boldsymbol{\beta}, \boldsymbol{\psi}, \boldsymbol{\gamma})} \\ &- \sum_{i \in \Delta_0} \pi_i^{(k)} x_{ir} H_0(t_i; \boldsymbol{\psi}) e^{\boldsymbol{\gamma}' \boldsymbol{x}_i} - \sum_{i \in \Delta_0} \pi_i^{(k)} x_{ir} H_0(t_i; \boldsymbol{\psi}) e^{\boldsymbol{x}_i^{*\prime} \boldsymbol{\beta} + \boldsymbol{\gamma}' \boldsymbol{x}_i} \frac{S(t_i, \boldsymbol{x}_i; \boldsymbol{\psi}, \boldsymbol{\gamma})}{1 + C(t_i, \boldsymbol{x}_i; \boldsymbol{\beta}, \boldsymbol{\psi}, \boldsymbol{\gamma})},\end{aligned}$$

$$\frac{\partial^2 Q}{\partial \beta_d \partial \beta_{d'}} = -2 \sum_{i \in \Delta_1} x_{id} x_{id'} \frac{C(t_i, \boldsymbol{x}_i; \boldsymbol{\beta}, \boldsymbol{\psi}, \boldsymbol{\gamma})}{(1 + C(t_i, \boldsymbol{x}_i; \boldsymbol{\beta}, \boldsymbol{\psi}, \boldsymbol{\gamma}))^2} - \sum_{i \in \Delta_0} x_{id} x_{id'} \frac{e^{\boldsymbol{x}_i^{*'} \boldsymbol{\beta}}}{(1 + e^{\boldsymbol{x}_i^{*'} \boldsymbol{\beta}})^2}$$
$$- \sum_{i \in \Delta_0} \pi_i^{(k)} x_{id} x_{id'} \frac{C(t_i, \boldsymbol{x}_i; \boldsymbol{\beta}, \boldsymbol{\psi}, \boldsymbol{\gamma})}{(1 + C(t_i, \boldsymbol{x}_i; \boldsymbol{\beta}, \boldsymbol{\psi}, \boldsymbol{\gamma}))^2},$$

$$\frac{\partial^2 Q}{\partial \beta_d \partial \psi_l} = -2 \sum_{i \in \Delta_1} x_{id} \frac{\partial H_0(t_i; \boldsymbol{\psi})}{\partial \psi_l} \frac{S(t_i, \boldsymbol{x}_i; \boldsymbol{\psi}, \boldsymbol{\gamma}) e^{\boldsymbol{x}_i^{*'} \boldsymbol{\beta} + \boldsymbol{\gamma}' \boldsymbol{x}_i}}{(1 + C(t_i, \boldsymbol{x}_i; \boldsymbol{\beta}, \boldsymbol{\psi}, \boldsymbol{\gamma}))^2}$$
$$- \sum_{i \in \Delta_0} \pi_i^{(k)} x_{id} \frac{\partial H_0(t_i; \boldsymbol{\psi})}{\partial \psi_l} \frac{S(t_i, \boldsymbol{x}_i; \boldsymbol{\psi}, \boldsymbol{\gamma}) e^{\boldsymbol{x}_i^{*'} \boldsymbol{\beta} + \boldsymbol{\gamma}' \boldsymbol{x}_i}}{(1 + C(t_i, \boldsymbol{x}_i; \boldsymbol{\beta}, \boldsymbol{\psi}, \boldsymbol{\gamma}))^2},$$

$$\frac{\partial^2 Q}{\partial \beta_d \partial \gamma_r} = -2 \sum_{i \in \Delta_1} x_{id} x_{ir} H_0(t_i; \boldsymbol{\psi}) \frac{S(t_i, \boldsymbol{x}_i; \boldsymbol{\psi}, \boldsymbol{\gamma}) e^{\boldsymbol{x}_i^{*'} \boldsymbol{\beta} + \boldsymbol{\gamma}' \boldsymbol{x}_i}}{(1 + C(t_i, \boldsymbol{x}_i; \boldsymbol{\beta}, \boldsymbol{\psi}, \boldsymbol{\gamma}))^2}$$
$$- \sum_{i \in \Delta_0} \pi_i^{(k)} x_{id} x_{ir} H_0(t_i; \boldsymbol{\psi}) \frac{S(t_i, \boldsymbol{x}_i; \boldsymbol{\psi}, \boldsymbol{\gamma}) e^{\boldsymbol{x}_i^{*'} \boldsymbol{\beta} + \boldsymbol{\gamma}' \boldsymbol{x}_i}}{(1 + C(t_i, \boldsymbol{x}_i; \boldsymbol{\beta}, \boldsymbol{\psi}, \boldsymbol{\gamma}))^2},$$

$$\frac{\partial^2 Q}{\partial \psi_l \partial \psi_{l'}} = - \sum_{i \in \Delta_1} \frac{\left(\frac{\partial h_0(t_i; \boldsymbol{\psi})}{\partial \psi_l}\right)\left(\frac{\partial h_0(t_i; \boldsymbol{\psi})}{\partial \psi_{l'}}\right)}{h_0^2(t_i; \boldsymbol{\psi})} - \sum_{i \in \Delta_1} \frac{\partial^2 H_0(t_i; \boldsymbol{\psi})}{\partial \psi_l \partial \psi_{l'}} e^{\boldsymbol{\gamma}' \boldsymbol{x}_i} - 2 \sum_{i \in \Delta_1} \frac{S(t_i, \boldsymbol{x}_i; \boldsymbol{\psi}, \boldsymbol{\gamma}) e^{\boldsymbol{x}_i^{*'} \boldsymbol{\beta} + \boldsymbol{\gamma}' \boldsymbol{x}_i}}{1 + C(t_i, \boldsymbol{x}_i; \boldsymbol{\beta}, \boldsymbol{\psi}, \boldsymbol{\gamma})}$$
$$\times \left[\frac{\partial^2 H_0(t_i; \boldsymbol{\psi})}{\partial \psi_l \partial \psi_{l'}} - \left(\frac{\partial H_0(t_i; \boldsymbol{\psi})}{\partial \psi_l}\right)\left(\frac{\partial H_0(t_i; \boldsymbol{\psi})}{\partial \psi_{l'}}\right) e^{\boldsymbol{\gamma}' \boldsymbol{x}_i} \left\{ 1 + \frac{e^{\boldsymbol{x}_i^{*'} \boldsymbol{\beta}} S(t_i, \boldsymbol{x}_i; \boldsymbol{\psi}, \boldsymbol{\gamma})}{1 + C(t_i, \boldsymbol{x}_i; \boldsymbol{\beta}, \boldsymbol{\psi}, \boldsymbol{\gamma})} \right\} \right]$$
$$- \sum_{i \in \Delta_0} \pi_i^{(k)} \frac{\partial^2 H_0(t_i; \boldsymbol{\psi})}{\partial \psi_l \partial \psi_{l'}} e^{\boldsymbol{\gamma}' \boldsymbol{x}_i} - \sum_{i \in \Delta_0} \pi_i^{(k)} \frac{S(t_i, \boldsymbol{x}_i; \boldsymbol{\psi}, \boldsymbol{\gamma}) e^{\boldsymbol{x}_i^{*'} \boldsymbol{\beta} + \boldsymbol{\gamma}' \boldsymbol{x}_i}}{1 + C(t_i, \boldsymbol{x}_i; \boldsymbol{\beta}, \boldsymbol{\psi}, \boldsymbol{\gamma})}$$
$$\times \left[\frac{\partial^2 H_0(t_i; \boldsymbol{\psi})}{\partial \psi_l \partial \psi_{l'}} - \left(\frac{\partial H_0(t_i; \boldsymbol{\psi})}{\partial \psi_l}\right)\left(\frac{\partial H_0(t_i; \boldsymbol{\psi})}{\partial \psi_{l'}}\right) e^{\boldsymbol{\gamma}' \boldsymbol{x}_i} \left\{ 1 + \frac{e^{\boldsymbol{x}_i^{*'} \boldsymbol{\beta}} S(t_i, \boldsymbol{x}_i; \boldsymbol{\psi}, \boldsymbol{\gamma})}{1 + C(t_i, \boldsymbol{x}_i; \boldsymbol{\beta}, \boldsymbol{\psi}, \boldsymbol{\gamma})} \right\} \right],$$

$$
\begin{aligned}
\frac{\partial^2 Q}{\partial \psi_l \partial \gamma_r} = & - \sum_{i \in \Delta_1} x_{ir} \frac{\partial H_0(t_i; \boldsymbol{\psi})}{\partial \psi_l} e^{\boldsymbol{\gamma}' \boldsymbol{x}_i} - 2 \sum_{i \in \Delta_1} x_{ir} \frac{\partial H_0(t_i; \boldsymbol{\psi})}{\partial \psi_l} \frac{S(t_i, \boldsymbol{x}_i; \boldsymbol{\psi}, \boldsymbol{\gamma}) e^{\boldsymbol{x}_i^{*'} \boldsymbol{\beta} + \boldsymbol{\gamma}' \boldsymbol{x}_i}}{1 + C(t_i, \boldsymbol{x}_i; \boldsymbol{\beta}, \boldsymbol{\psi}, \boldsymbol{\gamma})} \\
& \times \left[1 - H_0(t_i; \boldsymbol{\psi}) e^{\boldsymbol{\gamma}' \boldsymbol{x}_i} \left\{ 1 + \frac{e^{\boldsymbol{x}_i^{*'} \boldsymbol{\beta}} S(t_i, \boldsymbol{x}_i; \boldsymbol{\psi}, \boldsymbol{\gamma})}{1 + C(t_i, \boldsymbol{x}_i; \boldsymbol{\beta}, \boldsymbol{\psi}, \boldsymbol{\gamma})} \right\} \right] \\
& - \sum_{i \in \Delta_0} \pi_i^{(k)} x_{ir} \frac{\partial H_0(t_i; \boldsymbol{\psi})}{\partial \psi_l} e^{\boldsymbol{\gamma}' \boldsymbol{x}_i} - \sum_{i \in \Delta_0} \pi_i^{(k)} x_{ir} \frac{\partial H_0(t_i; \boldsymbol{\psi})}{\partial \psi_l} \frac{S(t_i, \boldsymbol{x}_i; \boldsymbol{\psi}, \boldsymbol{\gamma}) e^{\boldsymbol{x}_i^{*'} \boldsymbol{\beta} + \boldsymbol{\gamma}' \boldsymbol{x}_i}}{1 + C(t_i, \boldsymbol{x}_i; \boldsymbol{\beta}, \boldsymbol{\psi}, \boldsymbol{\gamma})} \\
& \times \left[1 - H_0(t_i; \boldsymbol{\psi}) e^{\boldsymbol{\gamma}' \boldsymbol{x}_i} \left\{ 1 + \frac{e^{\boldsymbol{x}_i^{*'} \boldsymbol{\beta}} S(t_i, \boldsymbol{x}_i; \boldsymbol{\psi}, \boldsymbol{\gamma})}{1 + C(t_i, \boldsymbol{x}_i; \boldsymbol{\beta}, \boldsymbol{\psi}, \boldsymbol{\gamma})} \right\} \right],
\end{aligned}
$$

$$
\begin{aligned}
\frac{\partial^2 Q}{\partial \gamma_r \partial \gamma_{r'}} = & - \sum_{i \in \Delta_1} x_{ir} x_{ir'} H_0(t_i; \boldsymbol{\psi}) e^{\boldsymbol{\gamma}' \boldsymbol{x}_i} - 2 \sum_{i \in \Delta_1} x_{ir} x_{ir'} H_0(t_i; \boldsymbol{\psi}) \frac{S(t_i, \boldsymbol{x}_i; \boldsymbol{\psi}, \boldsymbol{\gamma}) e^{\boldsymbol{x}_i^{*'} \boldsymbol{\beta} + \boldsymbol{\gamma}' \boldsymbol{x}_i}}{1 + C(t_i, \boldsymbol{x}_i; \boldsymbol{\beta}, \boldsymbol{\psi}, \boldsymbol{\gamma})} \\
& \times \left[1 - H_0(t_i; \boldsymbol{\psi}) e^{\boldsymbol{\gamma}' \boldsymbol{x}_i} \left\{ 1 + \frac{e^{\boldsymbol{x}_i^{*'} \boldsymbol{\beta}} S(t_i, \boldsymbol{x}_i; \boldsymbol{\psi}, \boldsymbol{\gamma})}{1 + C(t_i, \boldsymbol{x}_i; \boldsymbol{\beta}, \boldsymbol{\psi}, \boldsymbol{\gamma})} \right\} \right] \\
& - \sum_{i \in \Delta_0} \pi_i^{(k)} x_{ir} x_{ir'} H_0(t_i; \boldsymbol{\psi}) e^{\boldsymbol{\gamma}' \boldsymbol{x}_i} - \sum_{i \in \Delta_0} \pi_i^{(k)} x_{ir} x_{ir'} H_0(t_i; \boldsymbol{\psi}) \frac{S(t_i, \boldsymbol{x}_i; \boldsymbol{\psi}, \boldsymbol{\gamma}) e^{\boldsymbol{x}_i^{*'} \boldsymbol{\beta} + \boldsymbol{\gamma}' \boldsymbol{x}_i}}{1 + C(t_i, \boldsymbol{x}_i; \boldsymbol{\beta}, \boldsymbol{\psi}, \boldsymbol{\gamma})} \\
& \times \left[1 - H_0(t_i; \boldsymbol{\psi}) e^{\boldsymbol{\gamma}' \boldsymbol{x}_i} \left\{ 1 + \frac{e^{\boldsymbol{x}_i^{*'} \boldsymbol{\beta}} S(t_i, \boldsymbol{x}_i; \boldsymbol{\psi}, \boldsymbol{\gamma})}{1 + C(t_i, \boldsymbol{x}_i; \boldsymbol{\beta}, \boldsymbol{\psi}, \boldsymbol{\gamma})} \right\} \right],
\end{aligned}
$$

where

$$C(t_i, \boldsymbol{x}_i; \boldsymbol{\beta}, \boldsymbol{\psi}, \boldsymbol{\gamma}) = e^{\boldsymbol{\beta}' \boldsymbol{x}_i^*} \left\{ 1 - \exp \left[-H_0(t_i; \boldsymbol{\psi}) e^{\boldsymbol{\gamma}' \boldsymbol{x}_i} \right] \right\}$$

and

$$S(t_i, \boldsymbol{x}_i; \boldsymbol{\psi}, \boldsymbol{\gamma}) = \exp \left[-H_0(t_i; \boldsymbol{\psi}) e^{\boldsymbol{\gamma}' \boldsymbol{x}_i} \right];$$

for $d, d' = 0, 1, \ldots, p$ with x_{i0}= 1; $r, r' = 1, 2, \ldots, p$ and $l = 0, 1, \ldots, N$.

B.2.4 COM-Poisson cure rate model

The first- and the second-order partial derivatives of the $Q(\boldsymbol{\theta}, \boldsymbol{\pi}^{(k)})$ function with respect to $\boldsymbol{\beta}$, $\boldsymbol{\psi}$, and $\boldsymbol{\gamma}$, for a fixed value of ϕ, are as follows:

$$\frac{\partial Q}{\partial \beta_d} = -\sum_{i\in\Delta^*} x_{id}\frac{e^{\boldsymbol{\beta}'\boldsymbol{x}_i^*}}{1+e^{\boldsymbol{\beta}'\boldsymbol{x}_i^*}} + \sum_{i\in\Delta_1} x_{id}\frac{e^{\boldsymbol{\beta}'\boldsymbol{x}_i^*} z_{21,i}}{z_{2,i}z_{01,i}} + \sum_{i\in\Delta_0} \pi_i^{(k)} x_{id}\frac{e^{\boldsymbol{\beta}'\boldsymbol{x}_i^*} z_{2,i}}{z_{1,i}z_{01,i}},$$

$$\frac{\partial Q}{\partial \psi_l} = \sum_{i\in\Delta_1} \frac{\frac{\partial h_0(t_i;\boldsymbol{\psi})}{\partial \psi_l}}{h_0(t_i;\boldsymbol{\psi})} - \sum_{i\in\Delta_1} \frac{\partial H_0(t_i;\boldsymbol{\psi})}{\partial \psi_l}\frac{z_{21,i}}{z_{2,i}} e^{\boldsymbol{\gamma}'\boldsymbol{x}_i} - \sum_{i\in\Delta_0} \pi_i^{(k)} \frac{\partial H_0(t_i;\boldsymbol{\psi})}{\partial \psi_l}\frac{z_{2,i}}{z_{1,i}} e^{\boldsymbol{\gamma}'\boldsymbol{x}_i},$$

$$\frac{\partial Q}{\partial \gamma_r} = \sum_{i\in\Delta_1} x_{ir} - \sum_{i\in\Delta_1} x_{ir} H_0(t_i;\boldsymbol{\psi})\frac{z_{21,i}}{z_{2,i}} e^{\boldsymbol{\gamma}'\boldsymbol{x}_i} - \sum_{i\in\Delta_0} \pi_i^{(k)} x_{ir} H_0(t_i;\boldsymbol{\psi})\frac{z_{2,i}}{z_{1,i}} e^{\boldsymbol{\gamma}'\boldsymbol{x}_i},$$

$$\begin{aligned}\frac{\partial^2 Q}{\partial \beta_d \partial \beta_{d'}} &= -\sum_{i\in\Delta^*} x_{id}x_{id'}\frac{e^{\boldsymbol{\beta}'\boldsymbol{x}_i^*}}{(1+e^{\boldsymbol{\beta}'\boldsymbol{x}_i^*})^2} \\ &\quad + \sum_{i\in\Delta_1} x_{id}x_{id'} e^{\boldsymbol{\beta}'\boldsymbol{x}_i^*}\left[\frac{z_{21,i}}{z_{01,i}z_{2,i}} - e^{\boldsymbol{\beta}'\boldsymbol{x}_i^*}\left(\frac{z_{01,i}z_{21,i}^2 + z_{02,i}z_{2,i}z_{21,i} - z_{01,i}z_{2,i}z_{31,i}}{z_{2,i}^2 z_{01,i}^3}\right)\right] \\ &\quad + \sum_{i\in\Delta_0} \pi_i^{(k)} x_{id}x_{id'} e^{\boldsymbol{\beta}'\boldsymbol{x}_i^*}\left[\frac{z_{2,i}}{z_{01,i}z_{1,i}} - e^{\boldsymbol{\beta}'\boldsymbol{x}_i^*}\left(\frac{z_{01,i}z_{2,i}^2 + z_{02,i}z_{1,i}z_{2,i} - z_{01,i}z_{1,i}z_{21,i}}{z_{1,i}^2 z_{01,i}^3}\right)\right],\end{aligned}$$

$$\frac{\partial^2 Q}{\partial \beta_d \partial \psi_l} = -\sum_{i\in\Delta_1} x_{id} e^{\boldsymbol{\beta}'\boldsymbol{x}_i^* + \boldsymbol{\gamma}'\boldsymbol{x}_i} \frac{\partial H_0(t_i;\boldsymbol{\psi})}{\partial \psi_l} \left[\frac{z_{2,i} z_{31,i} - z_{21,i}^2}{z_{01,i} z_{2,i}^2}\right]$$
$$- \sum_{i\in\Delta_0} \pi_i^{(k)} x_{id} e^{\boldsymbol{\beta}'\boldsymbol{x}_i^* + \boldsymbol{\gamma}'\boldsymbol{x}_i} \frac{\partial H_0(t_i;\boldsymbol{\psi})}{\partial \psi_l} \left[\frac{z_{1,i} z_{21,i} - z_{2,i}^2}{z_{01,i} z_{1,i}^2}\right],$$

$$\frac{\partial^2 Q}{\partial \beta_d \partial \gamma_r} = -\sum_{i\in\Delta_1} x_{id} x_{ir} e^{\boldsymbol{\beta}'\boldsymbol{x}_i^* + \boldsymbol{\gamma}'\boldsymbol{x}_i} H_0(t_i;\boldsymbol{\psi}) \left[\frac{z_{2,i} z_{31,i} - z_{21,i}^2}{z_{01,i} z_{2,i}^2}\right]$$
$$- \sum_{i\in\Delta_0} \pi_i^{(k)} x_{id} x_{ir} e^{\boldsymbol{\beta}'\boldsymbol{x}_i^* + \boldsymbol{\gamma}'\boldsymbol{x}_i} H_0(t_i;\boldsymbol{\psi}) \left[\frac{z_{1,i} z_{21,i} - z_{2,i}^2}{z_{01,i} z_{1,i}^2}\right],$$

$$\frac{\partial^2 Q}{\partial \psi_l \partial \psi_{l'}} = -\sum_{i\in\Delta_1} \frac{\left(\frac{\partial h_0(t_i;\boldsymbol{\psi})}{\partial \psi_l}\right)\left(\frac{\partial h_0(t_i;\boldsymbol{\psi})}{\partial \psi_{l'}}\right)}{h_0^2(t_i;\boldsymbol{\psi})}$$
$$+ \sum_{i\in\Delta_1} \left(\frac{\partial H_0(t_i;\boldsymbol{\psi})}{\partial \psi_l}\right)\left(\frac{\partial H_0(t_i;\boldsymbol{\psi})}{\partial \psi_{l'}}\right) \left[\frac{z_{2,i} z_{31,i} - z_{21,i}^2}{z_{01,i} z_{2,i}^2}\right] e^{2\boldsymbol{\gamma}'\boldsymbol{x}_i}$$
$$+ \sum_{i\in\Delta_0} \pi_i^{(k)} \left(\frac{\partial H_0(t_i;\boldsymbol{\psi})}{\partial \psi_l}\right)\left(\frac{\partial H_0(t_i;\boldsymbol{\psi})}{\partial \psi_{l'}}\right) \left[\frac{z_{1,i} z_{21,i} - z_{2,i}^2}{z_{01,i} z_{1,i}^2}\right] e^{2\boldsymbol{\gamma}'\boldsymbol{x}_i},$$

$$\frac{\partial^2 Q}{\partial \psi_l \partial \gamma_r} = \sum_{i\in\Delta_1} x_{ir} H_0(t_i;\boldsymbol{\psi}) \left(\frac{\partial H_0(t_i;\boldsymbol{\psi})}{\partial \psi_l}\right) \left[\frac{z_{2,i} z_{31,i} - z_{21,i}^2}{z_{01,i} z_{2,i}^2}\right] e^{2\boldsymbol{\gamma}'\boldsymbol{x}_i}$$
$$+ \sum_{i\in\Delta_0} \pi_i^{(k)} x_{ir} H_0(t_i;\boldsymbol{\psi}) \left(\frac{\partial H_0(t_i;\boldsymbol{\psi})}{\partial \psi_l}\right) \left[\frac{z_{1,i} z_{21,i} - z_{2,i}^2}{z_{01,i} z_{1,i}^2}\right] e^{2\boldsymbol{\gamma}'\boldsymbol{x}_i},$$

$$\frac{\partial^2 Q}{\partial \gamma_r \partial \gamma_{r'}} = \sum_{i \in \Delta_1} x_{ir} x_{ir'} H_0^2(t_i; \boldsymbol{\psi}) \left[\frac{z_{2,i} z_{31,i} - z_{21,i}^2}{z_{01,i} z_{2,i}^2} \right] e^{2\boldsymbol{\gamma}' \boldsymbol{x}_i}$$
$$+ \sum_{i \in \Delta_0} \pi_i^{(k)} x_{ir} x_{ir'} H_0^2(t_i; \boldsymbol{\psi}) \left[\frac{z_{1,i} z_{21,i} - z_{2,i}^2}{z_{01,i} z_{1,i}^2} \right] e^{2\boldsymbol{\gamma}' \boldsymbol{x}_i}$$

where

$$z_{1,i} = z_1(\boldsymbol{\theta}; \boldsymbol{x}_i, t_i) = \sum_{j=1}^{\infty} \frac{\{\eta_i S(t_i, \boldsymbol{x}_i; \boldsymbol{\psi}, \boldsymbol{\gamma})\}^j}{(j!)^{\phi}}, z_{2,i} = z_2(\boldsymbol{\theta}; \boldsymbol{x}_i, t_i) = \sum_{j=1}^{\infty} \frac{j\{\eta_i S(t_i, \boldsymbol{x}_i; \boldsymbol{\psi}, \boldsymbol{\gamma})\}^j}{(j!)^{\phi}},$$

$$z_{21,i} = z_{21}(\boldsymbol{\theta}; \boldsymbol{x}_i, t_i) = \sum_{j=1}^{\infty} \frac{j^2\{\eta_i S(t_i, \boldsymbol{x}_i; \boldsymbol{\psi}, \boldsymbol{\gamma})\}^j}{(j!)^{\phi}}, z_{31,i} = z_{31}(\boldsymbol{\theta}; \boldsymbol{x}_i, t_i) = \sum_{j=1}^{\infty} \frac{j^3\{\eta_i S(t_i, \boldsymbol{x}_i; \boldsymbol{\psi}, \boldsymbol{\gamma})\}^j}{(j!)^{\phi}},$$

$$z_{01,i} = z_{01}(\boldsymbol{\theta}; \boldsymbol{x}_i, t_i) = \sum_{j=1}^{\infty} \frac{j\eta_i^j}{(j!)^{\phi}}, z_{02,i} = z_{02}(\boldsymbol{\theta}; \boldsymbol{x}_i, t_i) = \sum_{j=1}^{\infty} \frac{j^2\eta_i^j}{(j!)^{\phi}},$$

$$\eta_i = \eta(\boldsymbol{\beta}; \boldsymbol{x}_i) = H_{\phi}^{*-1}(1 + e^{\boldsymbol{\beta}' \boldsymbol{x}_i^*}),$$

and

$$S(t_i, \boldsymbol{x}_i; \boldsymbol{\psi}, \boldsymbol{\gamma}) = \exp\left[-H_0(t_i; \boldsymbol{\psi}) e^{\boldsymbol{\gamma}' \boldsymbol{x}_i} \right];$$

for $d, d' = 0, 1, \ldots, p$ with x_{i0}= 1; $r, r' = 1, 2, \ldots, p$ and $l = 0, 1, \ldots, N$.

The expressions for $h_0(t_i; \boldsymbol{\psi})$ and $H_0(t_i; \boldsymbol{\psi})$ are provided in (**??**) and (**??**), while that for $\frac{\partial h_0(t_i;\boldsymbol{\psi})}{\partial \psi_l}$, $\frac{\partial H_0(t_i;\boldsymbol{\psi})}{\partial \psi_l}$, $\frac{\partial^2 h_0(t_i;\boldsymbol{\psi})}{\partial \psi_l \partial \psi_{l'}}$ and $\frac{\partial^2 H_0(t_i;\boldsymbol{\psi})}{\partial \psi_l \partial \psi_{l'}}$ are provided in Appendix **??**. The expressions for $\pi_i^{(k)}$ can be found in Appendix **??**.

B.3 First- and second-order derivatives of the baseline hazard and baseline cumulative hazard function

$$\frac{\partial h_0(t_i;\boldsymbol{\psi})}{\partial \psi_l} = \left(1 - \frac{\tau_l - t_i}{\tau_l - \tau_{l-1}}\right) I_{[\tau_{l-1},\tau_l]}(t_i) + \left(\frac{\tau_{l+1} - t_i}{\tau_{l+1} - \tau_l}\right) I_{[\tau_l,\tau_{l+1}]}(t_i)$$

with

$$\frac{\partial h_0(t_i;\boldsymbol{\psi})}{\partial \psi_0} = \left(\frac{\tau_1 - t_i}{\tau_1 - \tau_0}\right) I_{[\tau_0,\tau_1]}(t_i)$$

for $l = 1, 2, \ldots, N$ and

$$\frac{\partial^2 h_0(t_i;\boldsymbol{\psi})}{\partial \psi_l \partial \psi_{l'}} = 0$$

for $l, l' = 0, 1, \ldots, N$.

$$\begin{aligned}\frac{\partial H_0(t_i;\boldsymbol{\psi})}{\partial \psi_l} = &\left[\left(1 - \frac{\tau_l}{\tau_l - \tau_{l-1}}\right)(\min(\tau_l, t_i) - \tau_{l-1}) + \frac{(\min^2(\tau_l, t_i) - \tau_{l-1}^2)}{2(\tau_l - \tau_{l-1})}\right] I_{[\tau_{l-1},\infty)}(t_i)\\ &+ \left[\left(\frac{\tau_{l+1}}{\tau_{l+1} - \tau_l}\right)(\min(\tau_{l+1}, t_i) - \tau_l) - \frac{(\min^2(\tau_{l+1}, t_i) - \tau_l^2)}{2(\tau_{l+1} - \tau_l)}\right] I_{[\tau_l,\infty)}(t_i)\end{aligned}$$

with

$$\frac{\partial H_0(t_i;\boldsymbol{\psi})}{\partial \psi_0} = \left[\left(\frac{\tau_1}{\tau_1 - \tau_0}\right)(\min(\tau_1, t_i) - \tau_0) - \frac{(\min^2(\tau_1, t_i) - \tau_0^2)}{2(\tau_1 - \tau_0)}\right] I_{[\tau_0,\infty)}(t_i)$$

for $l = 1, 2, \ldots, N$ and

$$\frac{\partial^2 H_0(t_i;\boldsymbol{\psi})}{\partial \psi_l \partial \psi_{l'}} = 0$$

for $l, l' = 0, 1, \ldots, N$.

Appendix C

Appendix corresponding to Chapter 4

C.1 The Q-function - destructive weighted Poisson cure rate model

We define:

$$\eta_i = e^{\boldsymbol{\alpha}'\boldsymbol{z}_i}, p_i = \frac{e^{\boldsymbol{\beta}'\boldsymbol{x}_i}}{1+e^{\boldsymbol{\beta}'\boldsymbol{x}_i}},$$

$$f_i = f(t_i;\boldsymbol{\gamma}) = \frac{\gamma_0}{\gamma_1}\left(\frac{t_i}{\gamma_1}\right)^{\gamma_0-1} e^{\boldsymbol{\gamma}_2'\boldsymbol{x}_i+\boldsymbol{\gamma}_3'\boldsymbol{z}_i} e^{-\left(\frac{t_i}{\gamma_1}\right)^{\gamma_0-1} e^{\boldsymbol{\gamma}_2'\boldsymbol{x}_i+\boldsymbol{\gamma}_3'\boldsymbol{z}_i}},$$

$$S_i = S(t_i;\boldsymbol{\gamma}) = e^{-\left(\frac{t_i}{\gamma_1}\right)^{\gamma_0-1} e^{\boldsymbol{\gamma}_2'\boldsymbol{x}_i+\boldsymbol{\gamma}_3'\boldsymbol{z}_i}},$$

$$F_i = F(t_i;\boldsymbol{\gamma}) = 1 - e^{-\left(\frac{t_i}{\gamma_1}\right)^{\gamma_0-1} e^{\boldsymbol{\gamma}_2'\boldsymbol{x}_i+\boldsymbol{\gamma}_3'\boldsymbol{z}_i}},$$

and

$$h_i = h(t_i;\boldsymbol{\gamma}) = \frac{\gamma_0}{\gamma_1}\left(\frac{t_i}{\gamma_0}\right)^{\gamma_0-1} e^{\boldsymbol{\gamma}_2'\boldsymbol{x}+\boldsymbol{\gamma}_3'\boldsymbol{z}}$$

C.1.1 Destructive exponentially weighted Poisson cure rate model

$$Q(\boldsymbol{\theta}^*,\boldsymbol{\pi}^{(a)}) = \sum_{\Delta_1}\log M_i - \sum_{\Delta^*} M_i + \sum_{\Delta_1} M_i S_i + \sum_{\Delta_1}\log f_i + \sum_{\Delta_0}\pi_i^{(a)}\log(e^{M_i S_i}-1),$$

where

$$\pi_i^{(a)} = 1 - e^{-\eta_i e^{\phi} p_i S_i}\Big|_{\boldsymbol{\theta}^*=\boldsymbol{\theta}^{*(a)}},$$

and

$$M_i = M(\boldsymbol{\theta}; t_i, \boldsymbol{x}_i, \boldsymbol{z}_i) = \eta_i e^{\phi} p_i,$$

C.1.2 Destructive length-biased Poisson cure rate model

$$\begin{aligned} Q(\boldsymbol{\theta}^*,\boldsymbol{\pi}^{(a)}) = & \sum_{\Delta_1}\log\eta_i + \sum_{\Delta_1}\log p_i + \sum_{\Delta_1}\log f_i - \sum_{\Delta_1} A_i + \sum_{\Delta_1} B_i \\ & - \sum_{\Delta_0}\eta_i p_i + \sum_{\Delta_0}\log(1-p_i) + \sum_{\Delta_0}\pi_i^{(a)}\log(C_i D_i - 1), \end{aligned}$$

where

$$\pi_i^{(a)} = 1 - e^{-\eta_i p_i S_i}\left(\frac{1-p_i}{1-p_i F_i}\right)\Bigg|_{\boldsymbol{\theta}^*=\boldsymbol{\theta}^{*(a)}},$$

$$A_i = A(\boldsymbol{\theta};\boldsymbol{t}_i,\boldsymbol{x}_i,\boldsymbol{z}_i) = \eta_i p_i F_i, B_i = B(\boldsymbol{\theta};\boldsymbol{t}_i,\boldsymbol{x}_i,\boldsymbol{z}_i) = \log\left[1 - p_i F_i - \frac{p_i f_i}{\eta_i}\right],$$

$$C_i = C(\boldsymbol{\theta};\boldsymbol{t}_i,\boldsymbol{x}_i,\boldsymbol{z}_i) = e^{\eta_i p_i(1-F_i)},$$

and

$$D_i = D(\boldsymbol{\theta}; \boldsymbol{t}_i, \boldsymbol{x}_i, \boldsymbol{z}_i) = \frac{1 - p_i F_i}{1 - p_i}.$$

C.1.3 Destructive negative binomial cure rate model

$$Q(\boldsymbol{\theta}^*, \boldsymbol{\pi}^{(a)}) = \sum_{\Delta_1} \log \eta_i p_i - \left(\frac{1}{\phi} + 1\right) \sum_{\Delta_1} \log(1 + E_i F_i) + \sum_{\Delta_1} \log f_i$$
$$- \frac{1}{\phi} \sum_{\Delta_0} \log(1 + E_i) + \sum_{\Delta_0} \pi_i^{(a)} \log\left(G_i^{-1/\phi} - 1\right)$$

where

$$\pi_i^{(a)} = 1 - G_i\Big|_{\boldsymbol{\theta}^* = \boldsymbol{\theta}^{*(a)}},$$

$$E_i = E(\boldsymbol{\theta}; t_i, \boldsymbol{x}_i, \boldsymbol{z}_i) = \phi \eta_i p_i,$$

and

$$G_i = G(\boldsymbol{\theta}; t_i, \boldsymbol{x}_i, \boldsymbol{z}_i) = \frac{1 + E_i F_i}{1 + E_i}.$$

C.2 First- and second-order derivatives of the Q-function for destructive weighted Poisson cure rate model:

C.2.1 Destructive exponentially weighted Poisson cure rate model

$$\frac{\partial Q(\boldsymbol{\theta}^*, \boldsymbol{\pi}^{(a)})}{\partial \alpha_j} = \sum_{\Delta_1} z_{ij} - \sum_{\Delta^*} z_{ij} M_i + \sum_{\Delta_1} z_{ij} M_i S_i + \sum_{\Delta_0} \pi_i^{(a)} z_{ij} D_i^* M_i S_i,$$

$$\frac{\partial Q(\boldsymbol{\theta}^*, \boldsymbol{\pi}^{(a)})}{\partial \beta_k} = \sum_{\Delta_1} x_{ik}(1-p_i) - \sum_{\Delta^*} x_{ik} M_i (1-p_i) + \sum_{\Delta_1} x_{ik} M_i S_i (1-p_i) + \sum_{\Delta_0} \pi_i^{(a)} x_{ik} D_i^* M_i S_i (1-p_i),$$

$$\frac{\partial Q(\boldsymbol{\theta}^*, \boldsymbol{\pi}^{(a)})}{\partial \gamma_0} = \sum_{\Delta_1} M_i S'_{i,0} + \sum_{\Delta_1} \left[\frac{1}{\gamma_0} + \log\left(\frac{t_i}{\gamma_1}\right) + \frac{S'_{i,0}}{S_i} \right] + \sum_{\Delta_0} \pi_i^{(a)} D_i^* M_i S'_{i,0},$$

$$\frac{\partial Q(\boldsymbol{\theta}^*, \boldsymbol{\pi}^{(a)})}{\partial \gamma_1} = \sum_{\Delta_1} M_i S'_{i,1} + \sum_{\Delta_1} \left[-\frac{\gamma_0}{\gamma_1} + \frac{S'_{i,1}}{S_i} \right] + \sum_{\Delta_0} \pi_i^{(a)} D_i^* M_i S'_{i,1},$$

$$\frac{\partial Q(\boldsymbol{\theta}^*, \boldsymbol{\pi}^{(a)})}{\partial \gamma_{2l}} = \sum_{\Delta_1} M_i S'_{i,2l} + \sum_{\Delta_1} \left[x_{il} + \frac{S'_{i,2l}}{S_i} \right] + \sum_{\Delta_0} \pi_i^{(a)} D_i^* M_i S'_{i,2l},$$

$$\frac{\partial Q(\boldsymbol{\theta}^*, \boldsymbol{\pi}^{(a)})}{\partial \gamma_{3m}} = \sum_{\Delta_1} M_i S'_{i,3m} + \sum_{\Delta_1} \left[z_{im} + \frac{S'_{i,3m}}{S_i} \right] + \sum_{\Delta_0} \pi_i^{(a)} D_i^* M_i S'_{i,3m},$$

$$\frac{\partial^2 Q(\boldsymbol{\theta}^*, \boldsymbol{\pi}^{(a)})}{\partial \alpha_j \partial \alpha_{j'}} = -\sum_{\Delta^*} z_{ij} z_{ij'} M_i + \sum_{\Delta_1} z_{ij} z_{ij'} M_i S_i + \sum_{\Delta_0} \pi_i^{(a)} z_{ij} z_{ij'} D_i^* M_i S_i \left[1 - \frac{M_i S_i}{e^{M_i S_i} - 1} \right],$$

$$\frac{\partial^2 Q(\boldsymbol{\theta}^*, \boldsymbol{\pi}^{(a)})}{\partial \alpha_j \partial \beta_k} = -\sum_{\Delta^*} x_{ij} z_{ik} M_i (1-p_i) + \sum_{\Delta_1} x_{ik} z_{ij} M_i S_i (1-p_i)$$
$$+ \sum_{\Delta_0} \pi_i^{(a)} x_{ik} z_{ij} D_i^* M_i S_i (1-p_i) \left[1 - \frac{M_i S_i}{e^{M_i S_i} - 1}\right],$$

$$\frac{\partial^2 Q(\boldsymbol{\theta}^*, \boldsymbol{\pi}^{(a)})}{\partial \beta_k \partial \beta_{k'}} = -\sum_{\Delta^*} x_{ik} x_{ik'} M_i (1-p_i)(1-2p_i) + \sum_{\Delta_1} x_{ik} x_{ik'} M_i S_i (1-p_i)(1-2p_i)$$
$$+ \sum_{\Delta_0} \pi_i^{(a)} x_{ik} x_{ik'} D_i^* M_i S_i (1-p_i)(1-2p_i) \left[1 - \frac{M_i S_i (1-p_i)}{(1-2p_i)(e^{M_i S_i} - 1)}\right],$$

$$\frac{\partial^2 Q(\boldsymbol{\theta}^*, \boldsymbol{\pi}^{(a)})}{\partial \alpha_j \partial \gamma_0} = \sum_{\Delta_1} z_{ij} M_i S'_{i,0} + \sum_{\Delta_0} \pi_i^{(a)} z_{ij} D_i^* M_i S'_{i,0} \left[1 - \frac{M_i S_i}{e^{M_i S_i} - 1}\right],$$

$$\frac{\partial^2 Q(\boldsymbol{\theta}^*, \boldsymbol{\pi}^{(a)})}{\partial \alpha_j \partial \gamma_1} = \sum_{\Delta_1} z_{ij} M_i S'_{i,1} + \sum_{\Delta_0} \pi_i^{(a)} z_{ij} D_i^* M_i S'_{i,1} \left[1 - \frac{M_i S_i}{e^{M_i S_i} - 1}\right],$$

$$\frac{\partial^2 Q(\boldsymbol{\theta}^*, \boldsymbol{\pi}^{(a)})}{\partial \alpha_j \partial \gamma_{2l}} = \sum_{\Delta_1} z_{ij} M_i S'_{i,2l} + \sum_{\Delta_0} \pi_i^{(a)} z_{ij} D_i^* M_i S'_{i,2l} \left[1 - \frac{M_i S_i}{e^{M_i S_i} - 1}\right],$$

$$\frac{\partial^2 Q(\boldsymbol{\theta}^*, \boldsymbol{\pi}^{(a)})}{\partial \alpha_j \partial \gamma_{3m}} = \sum_{\Delta_1} z_{ij} M_i S'_{i,3m} + \sum_{\Delta_0} \pi_i^{(a)} z_{ij} D_i^* M_i S'_{i,3m} \left[1 - \frac{M_i S_i}{e^{M_i S_i} - 1}\right],$$

$$\frac{\partial^2 Q(\boldsymbol{\theta}^*, \boldsymbol{\pi}^{(a)})}{\partial\beta_k\partial\gamma_0} = \sum_{\Delta_1} x_{ik}(1-p_i)M_iS'_{i,0} + \sum_{\Delta_0} \pi_i^{(a)} x_{ik}(1-p_i)D_i^* M_i S'_{i,0}\left[1-\frac{M_iS_i}{e^{M_iS_i}-1}\right],$$

$$\frac{\partial^2 Q(\boldsymbol{\theta}^*, \boldsymbol{\pi}^{(a)})}{\partial\beta_k\partial\gamma_1} = \sum_{\Delta_1} x_{ik}(1-p_i)M_iS'_{i,1} + \sum_{\Delta_0} \pi_i^{(a)} x_{ik}(1-p_i)D_i^* M_i S'_{i,1}\left[1-\frac{M_iS_i}{e^{M_iS_i}-1}\right],$$

$$\frac{\partial^2 Q(\boldsymbol{\theta}^*, \boldsymbol{\pi}^{(a)})}{\partial\beta_k\partial\gamma_{2l}} = \sum_{\Delta_1} x_{ik}(1-p_i)M_iS'_{i,2l} + \sum_{\Delta_0} \pi_i^{(a)} x_{ik}(1-p_i)D_i^* M_i S'_{i,2l}\left[1-\frac{M_iS_i}{e^{M_iS_i}-1}\right],$$

$$\frac{\partial^2 Q(\boldsymbol{\theta}^*, \boldsymbol{\pi}^{(a)})}{\partial\beta_k\partial\gamma_{3m}} = \sum_{\Delta_1} x_{ik}(1-p_i)M_iS'_{i,3m} + \sum_{\Delta_0} \pi_i^{(a)} x_{ik}(1-p_i)D_i^* M_i S'_{i,3m}\left[1-\frac{M_iS_i}{e^{M_iS_i}-1}\right],$$

$$\begin{aligned}\frac{\partial^2 Q(\boldsymbol{\theta}^*, \boldsymbol{\pi}^{(a)})}{\partial\gamma_0^2} &= \sum_{\Delta_1} M_iS''_{i,00} + \sum_{\Delta_1}\left[-\frac{1}{\gamma_0^2} + \frac{S_iS''_{i,00}-(S'_{i,0})^2}{S_i^2}\right] \\ &\quad + \sum_{\Delta_0} \pi_i^{(a)} D_i^* M_i \left[S''_{i,00} - \frac{M_i(S'_{i,0})^2}{e^{M_iS_i}-1}\right],\end{aligned}$$

$$\begin{aligned}\frac{\partial^2 Q(\boldsymbol{\theta}^*, \boldsymbol{\pi}^{(a)})}{\partial\gamma_0\partial\gamma_1} &= \sum_{\Delta_1} M_iS''_{i,01} + \sum_{\Delta_1}\left[-\frac{1}{\gamma_1} + \frac{S_iS''_{i,01}-S'_{i,0}S'_{i,1}}{S_i^2}\right] \\ &\quad + \sum_{\Delta_0} \pi_i^{(a)} D_i^* M_i \left[S''_{i,01} - \frac{M_iS'_{i,0}S'_{i,1}}{e^{M_iS_i}-1}\right],\end{aligned}$$

$$\frac{\partial^2 Q(\boldsymbol{\theta}^*, \boldsymbol{\pi}^{(a)})}{\partial\gamma_0 \partial\gamma_{2l}} = \sum_{\Delta_1} M_i S''_{i,0(2l)} + \sum_{\Delta_1} \left[\frac{S_i S''_{i,0(2l)} - S'_{i,0} S'_{i,2l}}{S_i^2} \right] + \sum_{\Delta_0} \pi_i^{(a)} D_i^* M_i \left[S''_{i,0(2l)} - \frac{M_i S'_{i,0} S'_{i,2l}}{e^{M_i S_i} - 1} \right],$$

$$\frac{\partial^2 Q(\boldsymbol{\theta}^*, \boldsymbol{\pi}^{(a)})}{\partial\gamma_0 \partial\gamma_{3m}} = \sum_{\Delta_1} M_i S''_{i,0(3m)} + \sum_{\Delta_1} \left[\frac{S_i S''_{i,0(3m)} - S'_{i,0} S'_{i,3m}}{S_i^2} \right] + \sum_{\Delta_0} \pi_i^{(a)} D_i^* M_i \left[S''_{i,0(3m)} - \frac{M_i S'_{i,0} S'_{i,3m}}{e^{M_i S_i} - 1} \right],$$

$$\frac{\partial^2 Q(\boldsymbol{\theta}^*, \boldsymbol{\pi}^{(a)})}{\partial\gamma_1^2} = \sum_{\Delta_1} M_i S''_{i,11} + \sum_{\Delta_1} \left[\frac{\gamma_0}{\gamma_1^2} + \frac{S_i S''_{i,11} - (S'_{i,1})^2}{S_i^2} \right] + \sum_{\Delta_0} \pi_i^{(a)} D_i^* M_i \left[S''_{i,11} - \frac{M_i (S'_{i,1})^2}{e^{M_i S_i} - 1} \right],$$

$$\frac{\partial^2 Q(\boldsymbol{\theta}^*, \boldsymbol{\pi}^{(a)})}{\partial\gamma_1 \partial\gamma_{2l}} = \sum_{\Delta_1} M_i S''_{i,1(2l)} + \sum_{\Delta_1} \left[\frac{S_i S''_{i,1(2l)} - S'_{i,1} S'_{i,2l}}{S_i^2} \right] + \sum_{\Delta_0} \pi_i^{(a)} D_i^* M_i \left[S''_{i,1(2l)} - \frac{M_i S'_{i,1} S'_{i,2l}}{e^{M_i S_i} - 1} \right],$$

$$\frac{\partial^2 Q(\boldsymbol{\theta}^*, \boldsymbol{\pi}^{(a)})}{\partial\gamma_1\partial\gamma_{3m}} = \sum_{\Delta_1} M_i S''_{i,1(3m)} + \sum_{\Delta_1}\left[\frac{S_i S''_{i,1(3m)} - S'_{i,1}S'_{i,3m}}{S_i^2}\right] + \sum_{\Delta_0}\pi_i^{(a)} D_i^* M_i \left[S''_{i,1(3m)} - \frac{M_i S'_{i,1}S'_{i,3m}}{e^{M_i S_i}-1}\right],$$

$$\frac{\partial^2 Q(\boldsymbol{\theta}^*, \boldsymbol{\pi}^{(a)})}{\partial\gamma_{2l}\partial\gamma_{2l'}} = \sum_{\Delta_1} M_i S''_{i,(2l)(2l')} + \sum_{\Delta_1}\left[\frac{S_i S''_{i,(2l)(2l')} - S'_{i,2l}S'_{i,2l'}}{S_i^2}\right] + \sum_{\Delta_0}\pi_i^{(a)} D_i^* M_i \left[S''_{i,(2l)(2l')} - \frac{M_i S'_{i,2l}S'_{i,2l'}}{e^{M_i S_i}-1}\right],$$

$$\frac{\partial^2 Q(\boldsymbol{\theta}^*, \boldsymbol{\pi}^{(a)})}{\partial\gamma_{2l}\partial\gamma_{3m}} = \sum_{\Delta_1} M_i S''_{i,(2l)(3m)} + \sum_{\Delta_1}\left[\frac{S_i S''_{i,(2l)(3m)} - S'_{i,2l}S'_{i,3m}}{S_i^2}\right] + \sum_{\Delta_0}\pi_i^{(a)} D_i^* M_i \left[S''_{i,(2l)(3m)} - \frac{M_i S'_{i,2l}S'_{i,3m}}{e^{M_i S_i}-1}\right],$$

$$\frac{\partial^2 Q(\boldsymbol{\theta}^*, \boldsymbol{\pi}^{(a)})}{\partial\gamma_{3m}\partial\gamma_{3m'}} = \sum_{\Delta_1} M_i S''_{i,(3m)(3m')} + \sum_{\Delta_1}\left[\frac{S_i S''_{i,(3m)(3m')} - S'_{i,3m}S'_{i,3m'}}{S_i^2}\right] + \sum_{\Delta_0}\pi_i^{(a)} D_i^* M_i \left[S''_{i,(3m)(3m')} - \frac{M_i S'_{i,3m}S'_{i,3m'}}{e^{M_i S_i}-1}\right],$$

where

$$D_i^* = \frac{e^{M_i S_i}}{e^{M_i S_i}-1}.$$

Here, $i = 1, \ldots, n$, $j, j' = 1, \ldots, q_1$, $k, k' = 0, 1, \ldots, q_2$, $r, r' = 0, 1, 20, 21, \ldots, 2q_2, 31, 32, \ldots, 3q_1,$

$l, l' = 0, 1, \ldots, q_2$, $m, m' = 1, \ldots, q_1$ and $x_{i0} \equiv 1$.

C.2.2 Destructive length-biased Poisson cure rate model

$$\frac{\partial Q(\boldsymbol{\theta}^*, \boldsymbol{\pi}^{(a)})}{\partial \alpha_j} = \sum_{\Delta_1} z_{ij} - \sum_{\Delta_1} A'_{i,j} + \sum_{\Delta_1} B'_{i,j} - \sum_{\Delta_0} z_{ij}\eta_i p_i + \sum_{\Delta_0} \pi_i^{(a)} \frac{C'_{i,j} D_i}{C_i D_i - 1},$$

$$\frac{\partial Q(\boldsymbol{\theta}^*, \boldsymbol{\pi}^{(a)})}{\partial \beta_k} = \sum_{\Delta_1} x_{ik}(1 - p_i) - \sum_{\Delta_1} A'_{i,k} + \sum_{\Delta_1} B'_{i,k} - \sum_{\Delta_0} x_{ik}\eta_i p_i(1 - p_i) + \sum_{\Delta_0} x_{ik} p_i + \sum_{\Delta_0} \pi_i^{(a)} \frac{C'_{i,k} D_i + D'_{i,k} C_i}{C_i D_i - 1},$$

$$\frac{\partial Q(\boldsymbol{\theta}^*, \boldsymbol{\pi}^{(a)})}{\partial \gamma_r} = \sum_{\Delta_1} \frac{\partial \log f_i}{\partial \gamma_r} - \sum_{\Delta_1} A'_{i,r} + \sum_{\Delta_1} B'_{i,r} + \sum_{\Delta_0} \pi_i^{(a)} \frac{C'_{i,r} D_i + D'_{i,r} C_i}{C_i D_i - 1},$$

$$\frac{\partial^2 Q(\boldsymbol{\theta}^*, \boldsymbol{\pi}^{(a)})}{\partial \alpha_j \partial \alpha'_j} = -\sum_{\Delta_1} A''_{i,jj'} + \sum_{\Delta_1} B''_{i,jj'} - \sum_{\Delta_0} z_{ij} z_{ij'} \eta_i p_i + \sum_{\Delta_0} \pi_i^{(a)} D_i \left[\frac{D_i (C_i C''_{i,jj'} - C'_j C'_{j'}) - C''_{i,jj'}}{(C_i D_i - 1)^2} \right],$$

$$\frac{\partial^2 Q(\boldsymbol{\theta}^*, \boldsymbol{\pi}^{(a)})}{\partial \alpha_j \partial \beta_k} = -\sum_{\Delta_1} A''_{i,jk} + \sum_{\Delta_1} B''_{i,jk} + \sum_{\Delta_0} \pi_i^{(a)} D_i \left[\frac{D_i (C_i C''_{i,jk} - C'_j C'_k) - C''_{i,jk}}{(C_i D_i - 1)^2} \right],$$

$$\frac{\partial^2 Q(\boldsymbol{\theta}^*, \boldsymbol{\pi}^{(a)})}{\partial \alpha_j \partial \gamma_r} = -\sum_{\Delta_1} A''_{i,jr} + \sum_{\Delta_1} B''_{i,jr} + \sum_{\Delta_0} \pi_i^{(a)} D_i \left[\frac{D_i (C_i C''_{i,jr} - C'_j C'_r) - C''_{i,jr}}{(C_i D_i - 1)^2} \right],$$

$$\begin{aligned}
\frac{\partial^2 Q(\boldsymbol{\theta}^*, \boldsymbol{\pi}^{(a)})}{\partial \beta_k \partial \beta_{k'}} = & -\sum_{\Delta_1} x_{ik} x_{ik'} p_i (1 - p_i) - \sum_{\Delta_1} A''_{i,kk'} + \sum_{\Delta_1} B''_{i,kk'} + \sum_{\Delta_0} x_{ik} x_{ik'} p_i (1 - p_i) \\
& - \sum_{\Delta_1} x_{ik} x_{ik'} \eta_i p_i (1 - p_i)(1 - 2p_i) \\
& + \sum_{\Delta_0} \pi_i^{(a)} \left[\frac{D_i^2 \{ C_i C''_{i,kk'} - C'_{i,k} C'_{i,k'} \} + C_i^2 \{ D_i D''_{i,kk'} - D'_{i,k} D'_{i,k'} \}}{(C_i D_i - 1)^2} \right] \\
& - \sum_{\Delta_0} \pi_i^{(a)} \left[\frac{\{ C_i D''_{i,kk'} + D_i C''_{i,kk'} + C'_{i,k} D'_{i,k'} + C'_{i,k'} D'_{i,k} \}}{(C_i D_i - 1)^2} \right],
\end{aligned}$$

$$\begin{aligned}
\frac{\partial^2 Q(\boldsymbol{\theta}^*, \boldsymbol{\pi}^{(a)})}{\partial \beta_k \partial \gamma_k} = & -\sum_{\Delta_1} (A''_{i,kr} - B''_{i,kr}) \\
& + \sum_{\Delta_0} \pi_i^{(a)} \left[\frac{D_i^2 \{ C_i C''_{i,kr} - C'_{i,k} C'_{i,r} \} + C_i^2 \{ D_i D''_{i,kr} - D'_{i,k} D'_{i,r} \}}{(C_i D_i - 1)^2} \right] \\
& - \sum_{\Delta_0} \pi_i^{(a)} \left[\frac{\{ C_i D''_{i,kr} + D_i C''_{i,kr} + C'_{i,k} D'_{i,r} + C'_{i,r} D'_{i,k} \}}{(C_i D_i - 1)^2} \right],
\end{aligned}$$

$$\begin{aligned}
\frac{\partial^2 Q(\boldsymbol{\theta}^*, \boldsymbol{\pi}^{(a)})}{\partial \gamma_r \partial \gamma_{r'}} = & \sum_{\Delta_1} \frac{\partial^2 \log f_i}{\partial \gamma_r \partial \gamma_{r'}} - \sum_{\Delta_1} A''_{i,rr'} + \sum_{\Delta_1} B''_{i,rr'} \\
& + \sum_{\Delta_0} \pi_i^{(a)} \left[\frac{D_i^2 \{ C_i C''_{i,rr'} - C'_{i,r} C'_{i,r'} \} + C_i^2 \{ D_i D''_{i,rr'} - D'_{i,r} D'_{i,r'} \}}{(C_i D_i - 1)^2} \right] \\
& - \sum_{\Delta_0} \pi_i^{(a)} \left[\frac{\{ C_i D''_{i,rr'} + D_i C''_{i,rr'} + C'_{i,r} D'_{i,r'} + C'_{i,r'} D'_{i,r} \}}{(C_i D_i - 1)^2} \right],
\end{aligned}$$

where

$$A'_{i,j} = \frac{\partial A_i}{\partial \alpha_j} = z_{ij}\eta_i p_i F_i, A'_{i,k} = \frac{\partial A_i}{\partial \beta_k} = x_{ik}\eta_i p_i(1-p_i)F_i,$$

$$A'_{i,r} = \frac{\partial A_i}{\partial \gamma_r} = \eta_i p_i F'_{i,r},$$

$$A''_{i,jj'} = \frac{\partial^2 A_i}{\partial \alpha_j \partial \alpha_{j'}} = z_{ij}z_{ij'}\eta_i p_i F_i, A''_{i,jk} = \frac{\partial^2 A_i}{\partial \alpha_j \partial \beta_j} = x_{ik}z_{ij}\eta_i p_i(1-p_i)F_i,$$

$$A''_{i,kk'} = \frac{\partial^2 A_i}{\partial \beta_k \partial \beta_{k'}} = x_{ik}x_{ik'}\eta_i p_i(1-p_i)(1-2p_i)F_i, A''_{i,jr} = \frac{\partial^2 A_i}{\partial \alpha_j \partial \gamma_r} = z_{ij}\eta_i p_i F'_{i,r},$$

$$A''_{i,kr} = \frac{\partial^2 A_i}{\partial \beta_j \partial \gamma_r} = x_{ik}\eta_i p_i(1-p_i)F'_{i,r}, A''_{i,rr'} = \frac{\partial^2 A_i}{\partial \gamma_r \partial \gamma_{r'}} = \eta_i p_i F''_{i,rr'};$$

$$B'_{i,j} = \frac{\partial B_i}{\partial \alpha_j} = \frac{z_{ij}p_i F_i}{\eta_i e^{B_i}}, B'_{i,k} = \frac{\partial B_i}{\partial \beta_k} = -\frac{x_{ik}p_i(1-p_i)}{e^{B_i}}\left[F_i + \frac{f_i}{\eta_i}\right],$$

$$B'_{i,r} = \frac{\partial B_i}{\partial \gamma_r} = -e^{-B_i}\left[p_i F'_{i,r} + \frac{p_i}{\eta_i}f'_{i,r}\right], B''_{i,jj'} = \frac{\partial^2 B_i}{\partial \alpha_j \partial \alpha_{j'}} = -z_{ij}z_{ij'}\frac{p_i f_i(1-p_iF_i)}{\eta_i e^{2B_i}},$$

$$B''_{i,jk} = \frac{\partial^2 B_i}{\partial \alpha_j \partial \beta_j} = x_{ik}z_{ij}\frac{p_i(1-p_i)f_i}{\eta_i e^{2B_i}},$$

$$B''_{i,kk'} = \frac{\partial^2 B_i}{\partial \beta_k \partial \beta_{k'}} = -x_{ik}x_{ik'}\frac{p_i(1-p_i)}{e^{2B_i}}\left[F_i + \frac{f_i}{\eta_i}\right]\left[1-p_i-e^{B_i}\right],$$

$$B''_{i,jr} = \frac{\partial^2 B_i}{\partial \alpha_j \partial \gamma_r} = \frac{p_i z_{ij} f'_{i,r}}{\eta_i e^{B_i}} + \frac{p_i z_{ij} f_i \left[p_i F'_{i,r} + \frac{p_i f'_{i,r}}{\eta_i}\right]}{\eta_i e^{B_i}},$$

$$B''_{i,kr} = \frac{\partial^2 B_i}{\partial \beta_j \partial \gamma_r} = -\frac{x_{ik}p_i(1-p_i)\left[F'_{i,r} + \frac{f'_{i,r}}{\eta_i}\right]}{e^{B_i}} - \frac{x_{ik}p_i(1-p_i)\left[F_i + \frac{f_i}{\eta_i}\right]\left[p_i F'_{i,r} + \frac{p_i f'_{i,r}}{\eta_i}\right]}{e^{2B_i}},$$

$$B''_{i,rr'} = \frac{\partial^2 B_i}{\partial \gamma_r \partial \gamma_{r'}} = -\frac{p_i\left[F''_{i,rr'} + \frac{f''_{i,rr'}}{\eta_i}\right]}{e^{B_i}} - \frac{p_i^2\left[F'_{i,r} + \frac{f'_{i,r}}{\eta_i}\right]\left[F'_{i,r'} + \frac{f'_{i,r'}}{\eta_i}\right]}{e^{2B_i}};$$

$$C'_{i,j} = \frac{\partial C_i}{\partial \alpha_j} = z_{ij}\eta_i p_i(1-F_i)e^{\eta_i p_i(1-F_i)}, C'_{i,k} = \frac{\partial C_i}{\partial \beta_k} = x_{ik}\eta_i p_i(1-p_i)(1-F_i)e^{\eta_i p_i(1-F_i)},$$

$$C'_{i,r} = \frac{\partial C_i}{\partial \gamma_r} = -\eta_i p_i F'_{i,r} e^{\eta_i p_i(1-F_i)},$$

$$C''_{i,jj'} = \frac{\partial^2 C_i}{\partial \alpha_j \partial \alpha_{j'}} = z_{ij} z_{ij'} \eta_i p_i (1-F_i) e^{\eta_i p_i(1-F_i)}[1+\eta_i p_i(1-F_i)],$$

$$C''_{i,jk} = \frac{\partial^2 C_i}{\partial \alpha_j \partial \beta_j} = x_{ik} z_{ij} \eta_i p_i (1-p_i)(1-F_i) e^{\eta_i p_i(1-F_i)}[1+\eta_i p_i(1-F_i)],$$

$$C''_{i,kk'} = \frac{\partial^2 C_i}{\partial \beta_k \partial \beta_{k'}} = x_{ik} x_{ik'} \eta_i p_i (1-p_i)(1-F_i) e^{\eta_i p_i(1-F_i)}[1-2p_i+\eta_i p_i(1-p_i)(1-F_i)],$$

$$C''_{i,jr} = \frac{\partial^2 C_i}{\partial \alpha_j \partial \gamma_r} = -z_{ij} \eta_i p_i F'_{i,r} e^{\eta_i p_i(1-F_i)}[1+\eta_i p_i(1-F_i)],$$

$$C''_{i,kr} = \frac{\partial^2 C_i}{\partial \beta_j \partial \gamma_r} = -x_{ik} \eta_i p_i (1-p_i) F'_{i,r} e^{\eta_i p_i(1-F_i)}[1+\eta_i p_i(1-F_i)],$$

$$C''_{i,rr'} = \frac{\partial^2 C_i}{\partial \gamma_r \partial \gamma_{r'}} = -\eta_i p_i e^{\eta_i p_i(1-F_i)} \left(F''_{i,rr'} - \eta_i p_i F'_{i,r} F'_{i,r'}\right);$$

$$D'_{i,j} = \frac{\partial D_i}{\partial \alpha_j} = 0, D'_{i,k} = \frac{\partial D_i}{\partial \beta_k} = \frac{x_{ik} p_i (1-F_i)}{1-p_i}, D'_{i,r} = \frac{\partial D_i}{\partial \gamma_r} = -\frac{p_i F'_{i,r}}{1-p_i},$$

$$D''_{i,jj'} = \frac{\partial^2 D_i}{\partial \alpha_j \partial \alpha_{j'}} = 0, D''_{i,jk} = \frac{\partial^2 D_i}{\partial \alpha_j \partial \beta_j} = 0, D''_{i,kk'} = \frac{\partial^2 D_i}{\partial \beta_k \partial \beta_{k'}} = 0,$$

$$D''_{i,jr} = \frac{\partial^2 D_i}{\partial \alpha_j \partial \gamma_r} = \frac{x_{ik} x_{ik'} p_i (1-F_i)}{1-p_i},$$

$$D''_{i,kr} = \frac{\partial^2 D_i}{\partial \beta_j \partial \gamma_r} = -\frac{x_{ik} p_i F'_{i,r}}{1-p_i}, D''_{i,rr'} = \frac{\partial^2 D_i}{\partial \gamma_r \partial \gamma_{r'}} = -\frac{p_i F''_{i,rr'}}{1-p_i}.$$

Here, $i = 1, \ldots, n$, $j, j' = 1, \ldots, q_1$, $k, k' = 0, 1, \ldots, q_2$, $r, r' = 0, 1, 20, 21, \ldots, 2q_2, 31, 32, \ldots, 3q_1$, $l, l' = 0, 1, \ldots, q_2$, $m, m' = 1, \ldots, q_1$ and $x_{i0} \equiv 1$.

C.2.3 Destructive negative binomial cure rate model

$$\frac{\partial Q(\boldsymbol{\theta}^*, \boldsymbol{\pi}^{(a)})}{\partial \alpha_j} = \sum_{\Delta_1} z_{ij} - \left(\frac{1}{\phi}+1\right) \sum_{\Delta_1} z_{ij} \frac{E_i F_i}{1+E_i F_i} - \frac{1}{\phi} \sum_{\Delta_0} z_{ij} \frac{E_i}{1+E_i} + \sum_{\Delta_0} \pi_i^{(a)} \frac{G'_{i,j}}{\phi G_i (G_i^{1/\phi}-1)},$$

$$\frac{\partial Q(\boldsymbol{\theta}^*, \boldsymbol{\pi}^{(a)})}{\partial \beta_k} = \sum_{\Delta_1} x_{ik}(1-p_i) - \left(\frac{1}{\phi}+1\right) \sum_{\Delta_1} x_{ik} \frac{E_i F_i (1-p_i)}{1+E_i F_i} - \frac{1}{\phi} \sum_{\Delta_0} x_{ik} \frac{E_i(1-p_i)}{1+E_i} + \sum_{\Delta_0} \pi_i^{(a)} \frac{G'_{i,k}}{\phi G_i (G_i^{1/\phi}-1)},$$

$$\frac{\partial Q(\boldsymbol{\theta}^*, \boldsymbol{\pi}^{(a)})}{\partial \gamma_r} = -\left(\frac{1}{\phi}+1\right) \sum_{\Delta_1} \frac{E_i F'_{i,r}}{1+E_i F_i} + \sum_{\Delta_1} \frac{\partial \log f_i}{\partial \gamma_r} + \sum_{\Delta_0} \pi_i^{(a)} \frac{G'_{i,r}}{\phi G_i (G_i^{1/\phi}-1)},$$

$$\frac{\partial^2 Q(\boldsymbol{\theta}^*, \boldsymbol{\pi}^{(a)})}{\partial \alpha_j \partial \alpha_{j'}} = -\left(\frac{1}{\phi}+1\right) \sum_{\Delta_1} \frac{z_{ij} z_{ij'} E_i F_i}{(1+E_i F_i)^2} - \frac{1}{\phi} \sum_{\Delta_0} \frac{z_{ij} z_{ij'} E_i}{(1+E_i)^2} + \sum_{\Delta_0} \pi_i^{(a)} \left[\frac{G''_{i,jj'} G_i (G_i^{1/\phi}-1) - G'_{i,j} G'_{i,j'} \{(1/\phi+1) G_i^{1/\phi} - 1\}}{\phi \left(G_i^{1/\phi+1}-1\right)^2} \right],$$

$$\frac{\partial^2 Q(\boldsymbol{\theta}^*, \boldsymbol{\pi}^{(a)})}{\partial \alpha_j \partial \beta_k} = -\left(\frac{1}{\phi}+1\right)\sum_{\Delta_1}\frac{z_{ij}x_{ik}E_iF_i(1-p_i)}{(1+E_iF_i)^2} - \frac{1}{\phi}\sum_{\Delta_0}\frac{z_{ij}x_{ik}(1-p_i)E_i}{(1+E_i)^2}$$
$$+\sum_{\Delta_0}\pi_i^{(a)}\left[\frac{G''_{i,jk}G_i(G_i^{1/\phi}-1) - G'_{i,j}G'_{i,k}\{(1/\phi+1)G_i^{1/\phi}-1\}}{\phi\left(G_i^{1/\phi+1}-1\right)^2}\right],$$

$$\frac{\partial^2 Q(\boldsymbol{\theta}^*, \boldsymbol{\pi}^{(a)})}{\partial \beta_k \partial \beta_{k'}} = -\left(\frac{1}{\phi}+1\right)\sum_{\Delta_1}\frac{x_{ik}x_{ik'}E_iF_i(1-p_i)(1-2p_i-E_iF_ip_i)}{(1+E_iF_i)^2}$$
$$-\frac{1}{\phi}\sum_{\Delta_0}\frac{x_{ik}x_{ik'}(1-p_i)^2E_i}{(1+E_i)^2}$$
$$+\sum_{\Delta_0}\pi_i^{(a)}\left[\frac{G''_{i,kk'}G_i(G_i^{1/\phi}-1) - G'_{i,k}G'_{i,k'}\{(1/\phi+1)G_i^{1/\phi}-1\}}{\phi\left(G_i^{1/\phi+1}-1\right)^2}\right],$$

$$\frac{\partial^2 Q(\boldsymbol{\theta}^*, \boldsymbol{\pi}^{(a)})}{\partial \alpha_j \partial \gamma_r} = -\left(\frac{1}{\phi}+1\right)\sum_{\Delta_1}\frac{z_{ij}E_iF'_{i,r}}{(1+E_iF_i)^2}$$
$$+\sum_{\Delta_0}\pi_i^{(a)}\left[\frac{G''_{i,jr}G_i(G_i^{1/\phi}-1) - G'_{i,j}G'_{i,r}\{(1/\phi+1)G_i^{1/\phi}-1\}}{\phi\left(G_i^{1/\phi+1}-1\right)^2}\right],$$

$$\frac{\partial^2 Q(\boldsymbol{\theta}^*, \boldsymbol{\pi}^{(a)})}{\partial \beta_k \partial \gamma_r} = -\left(\frac{1}{\phi}+1\right)\sum_{\Delta_1}\frac{x_{ik}(1-p_i)E_iF'_{i,r}}{(1+E_iF_i)^2}$$
$$+\sum_{\Delta_0}\pi_i^{(a)}\left[\frac{G''_{i,kr}G_i(G_i^{1/\phi}-1) - G'_{i,k}G'_{i,r}\{(1/\phi+1)G_i^{1/\phi}-1\}}{\phi\left(G_i^{1/\phi+1}-1\right)^2}\right],$$

$$\frac{\partial^2 Q(\boldsymbol{\theta}^*, \boldsymbol{\pi}^{(a)})}{\partial\gamma_r\partial\gamma_{r'}} = -\left(\frac{1}{\phi}+1\right)\sum_{\Delta_1}\left[\frac{E_iF''_{i,rr'} + E_i^2\{F_iF''_{i,rr'} - F'_{i,r}F'_{i,r'}\}}{(1+E_iF_i)^2}\right]$$
$$+\sum_{\Delta_1}\frac{\partial^2 \log f_i}{\partial\gamma_r\partial\gamma_{r'}} + \sum_{\Delta_0}\pi_i^{(a)}\left[\frac{G''_{i,rr'}G_i(G_i^{1/\phi}-1) - G'_{i,r}G'_{i,r'}\{(1/\phi+1)G_i^{1/\phi}-1\}}{\phi\left(G_i^{1/\phi+1}-1\right)^2}\right],$$

where

$$G'_{i,j} = \frac{\partial G_i}{\partial \alpha_j} = \frac{z_{ij}E_i(F_i-1)}{(1+E_i)^2}, G'_{i,k} = \frac{\partial G_i}{\partial \beta_k} = \frac{x_{ik}E_i(1-p_i)(F_i-1)}{(1+E_i)^2}, G'_{i,r} = \frac{\partial G_i}{\partial \gamma_r} = \frac{E_iF'_{i,r}}{(1+E_i)},$$

$$G''_{i,jj'} = \frac{\partial^2 G_i}{\partial\alpha_j\partial\alpha_{j'}} = \frac{z_{ij}z_{ij'}E_i(1-E_i)(F_i-1)}{(1+E_i)^3},$$

$$G''_{i,jk} = \frac{\partial^2 G_i}{\partial\alpha_j\partial\beta_k} = \frac{z_{ij}x_{ik}E_i(1-p_i)(1-E_i)(F_i-1)}{(1+E_i)^3},$$

$$G''_{i,kk'} = \frac{\partial^2 G_i}{\partial\beta_k\partial\beta_{k'}} = \frac{x_{ik}x_{ik'}E_i(1-p_i)^2(1-E_i)(F_i-1)}{(1+E_i)^3},$$

$$G''_{i,jr} = \frac{\partial^2 G_i}{\partial\alpha_j\partial\gamma_r} = \frac{z_{ij}E_iF'_{i,r}}{(1+E_i)^2}, G''_{i,kr} = \frac{\partial^2 G_i}{\partial\beta_k\partial\gamma_r} = \frac{x_{ik}E_i(1-p_i)F'_{i,r}}{(1+E_i)^2},$$

$$G''_{i,rr'} = \frac{\partial^2 G_i}{\partial\gamma_r\partial\gamma_{r'}} = \frac{E_i}{(1+E_i)}F''_{i,rr'}.$$

Here, $i = 1, \ldots, n$, $j, j' = 1, \ldots, q_1$, $k, k' = 0, 1, \ldots, q_2$, $r, r' = 0, 1, 20, 21, \ldots, 2q_2, 31, 32, \ldots, 3q_1$, $l, l' = 0, 1, \ldots, q_2$, $m, m' = 1, \ldots, q_1$ and $x_{i0} \equiv 1$.

C.3 First- and second-order derivatives of the density, cumulative distribution and survival functions

C.3.1 The density and log-density functions

$$f'_{i,0} = \frac{\partial f_i}{\partial \gamma_0} = \left\{ -F'_{i,0} + S_i \left[\frac{1}{\gamma_0} + \log\left(\frac{t_i}{\gamma_1}\right) \right] \right\} h_i, f'_{i,1} = \frac{\partial f_i}{\gamma_1} = -\left\{ F'_{i,1} + S_i \left(\frac{\gamma_0}{\gamma_1}\right) \right\} h_i,$$

$$f'_{i,2l} = \frac{\partial f_i}{\partial \gamma_{2l}} = \left\{ -F'_{i,2l} + S_i x_{il} \right\} h_i, f'_{i,3m} = \frac{\partial f_i}{\partial \gamma_{3m}} = \left\{ -F'_{i,3m} + S_i z_{im} \right\} h_i,$$

$$f''_{i,00} = \frac{\partial^2 f_i}{\partial \gamma_0^2} = \left\{ -F''_{i,00} + S_i \log\left(\frac{t_i}{\gamma_1}\right) \left[\frac{2}{\gamma_0} + \log\left(\frac{t_i}{\gamma_1}\right) \right] - 2\left[\frac{1}{\gamma_0} + \log\left(\frac{t_i}{\gamma_1}\right) \right] F'_{i,0} \right\} h_i,$$

$$f''_{i,01} = \frac{\partial^2 f_i}{\partial \gamma_0 \partial \gamma_1} = \left\{ -F''_{i,01} - S_i \frac{\gamma_0}{\gamma_1} \left[\frac{2}{\gamma_0} + \log\left(\frac{t_i}{\gamma_1}\right) \right] - \left[\frac{1}{\gamma_0} + \log\left(\frac{t_i}{\gamma_1}\right) \right] F'_{i,1} + \frac{\gamma_0}{\gamma_1} F'_{i,0} \right\} h_i,$$

$$f''_{i,11} = \frac{\partial^2 f_i}{\partial \gamma_1^2} = \left\{ -F''_{i,11} + S_i \frac{\gamma_0(\gamma_0+1)}{\gamma_1^2} + 2\frac{\gamma_0}{\gamma_1} F'_{i,1} \right\} h_i,$$

$$f''_{i,0(2l)} = \frac{\partial^2 f_i}{\partial \gamma_0 \partial \gamma_{2l}} = \left\{ -F''_{i,0(2l)} + (S_i x_{il} - F'_{i,2l}) \left[\frac{1}{\gamma_0} + \log\left(\frac{t_i}{\gamma_1}\right) \right] - x_{il} F'_{i,0} \right\} h_i,$$

$$f''_{i,0(3m)} = \frac{\partial^2 f_i}{\partial \gamma_0 \partial \gamma_{3m}} = \left\{ -F''_{i,0(3m)} + (S_i z_{im} - F'_{i,3m}) \left[\frac{1}{\gamma_0} + \log\left(\frac{t_i}{\gamma_1}\right) \right] - z_{im} F'_{i,0} \right\} h_i,$$

$$f''_{i,1(2l)} = \frac{\partial^2 f_i}{\partial \gamma_1 \partial \gamma_{2l}} = \left\{ -F''_{i,1(2l)} - (S_i x_{il} - F'_{i,2l}) \frac{\gamma_0}{\gamma_1} - x_{il} F'_{i,1} \right\} h_i,$$

$$f''_{i,1(3m)} = \frac{\partial^2 f_i}{\partial \gamma_1 \partial \gamma_{3m}} = \left\{ -F''_{i,1(3m)} - (S_i z_{im} - F'_{i,3m}) \frac{\gamma_0}{\gamma_1} - z_{im} F'_{i,1} \right\} h_i,$$

$$f''_{i,(2l)(2l')} = \frac{\partial^2 f_i}{\partial \gamma_{2l} \partial \gamma_{2l'}} = \left\{ -F''_{i,(2l)(2l')} + S_i x_{il} x_{il'} - F'_{i,2l} x_{il'} - x_{il} F'_{i,2l'} \right\} h_i,$$

$$f''_{i,(2l)(3m)} = \frac{\partial^2 f_i}{\partial \gamma_{2l} \partial \gamma_{3m}} = \left\{ -F''_{i,(2l)(3m)} + S_i x_{il} z_{im} - F'_{i,2l} z_{im} - x_{il} F'_{i,3m} \right\} h_i,$$

$$f''_{i,(3m)(3m')} = \frac{\partial^2 f_i}{\partial \gamma_{3m} \partial \gamma_{3m'}} = \left\{ -F''_{i,(3m)(3m')} + S_i z_{im} z_{im'} - F'_{i,3m} z_{im'} - z_{im} F'_{i,3m'} \right\} h_i;$$

$$\frac{\partial \log f_i}{\partial \gamma_r} = \frac{f'_{i,r}}{f_i}, \frac{\partial^2 \log f_i}{\partial \gamma_r \partial \gamma_{r'}} = \frac{f_i f''_{i,rr'} - f'_{i,r} f'_{i,r'}}{f_i^2}$$

where $i = 1, \ldots, n$, $j, j' = 1, \ldots, q_1$, $k, k' = 0, 1, \ldots, q_2$, $r, r' = 0, 1, 20, 21, \ldots, 2q_2, 31, 32, \ldots, 3q_1$, $l, l' = 0, 1, \ldots, q_2$, $m, m' = 1, \ldots, q_1$ and $x_{i0} \equiv 1$.

C.3.2 The cumulative distribution function

$$F'_{i,0} = \frac{\partial F_i}{\partial \gamma_0} = -S_i \log S_i \log\left(\frac{t_i}{\gamma_1}\right), F'_{i,1} = \frac{\partial F_i}{\gamma_1} = S_i \log S_i \log\left(\frac{\gamma_0}{\gamma_1}\right),$$

$$F'_{i,2l} = \frac{\partial F_i}{\partial \gamma_{2l}} = -x_{il} S_i \log S_i, F'_{i,3m} = \frac{\partial F_i}{\gamma_{3m}} = -z_{im} S_i \log S_i,$$

$$F''_{i,00} = \frac{\partial^2 F_i}{\partial \gamma_0^2} = -\left[\log\left(\frac{t_i}{\gamma_0}\right)\right]^2 S_i \log S_i (1 + \log S_i),$$

$$F''_{i,01} = \frac{\partial^2 F_i}{\partial \gamma_0 \partial \gamma_1} = \frac{S_i \log S_i}{\gamma_1}\left[1 + \gamma_0 \log\left(\frac{t_i}{\gamma_1}\right)(1 + \log S_i)\right],$$

$$F''_{i,11} = \frac{\partial^2 F_i}{\partial \gamma_1^2} = -\frac{\gamma_0}{\gamma_1^2} S_i \log S_i \left[1 + \gamma_0 \log\left(\frac{t_i}{\gamma_1}\right)\right],$$

$$F''_{i,0(2l)} = \frac{\partial^2 F_i}{\partial \gamma_0 \partial \gamma_{2l}} = -x_{il} \log\left(\frac{t_i}{\gamma_1}\right) S_i \log S_i (1 + \log S_i),$$

$$F''_{i,0(3m)} = \frac{\partial^2 F_i}{\partial \gamma_0 \partial \gamma_{3m}} = -z_{im} \log\left(\frac{t_i}{\gamma_1}\right) S_i \log S_i (1 + \log S_i),$$

$$F''_{i,1(2l)} = \frac{\partial^2 F_i}{\partial \gamma_1 \partial \gamma_{2l}} = x_{il}\left(\frac{\gamma_0}{\gamma_1}\right) S_i \log S_i (1 + \log S_i),$$

$$F''_{i,1(3m)} = \frac{\partial^2 F_i}{\partial \gamma_1 \partial \gamma_{3m}} = z_{im}\left(\frac{\gamma_0}{\gamma_1}\right) S_i \log S_i (1 + \log S_i),$$

$$F''_{i,(2l)(2l')} = \frac{\partial^2 F_i}{\partial \gamma_{2l} \partial \gamma_{2l'}} = -x_{il} x_{il'} S_i \log S_i (1 + \log S_i),$$

$$F''_{i,(2l)(3m)} = \frac{\partial^2 F_i}{\partial\gamma_{2l}\partial\gamma_{3m}} = -x_{il}z_{im}S_i \log S_i(1+\log S_i),$$

$$F''_{i,(3m)(3m')} = \frac{\partial^2 F_i}{\partial\gamma_{3m}\partial\gamma_{3m'}} = -z_{im}z_{im'}S_i \log S_i(1+\log S_i),$$

where $i = 1, \ldots, n$, $j, j' = 1, \ldots, q_1$, $k, k' = 0, 1, \ldots, q_2$, $r, r' = 0, 1, 20, 21, \ldots, 2q_2, 31, 32, \ldots, 3q_1$, $l, l' = 0, 1, \ldots, q_2$, $m, m' = 1, \ldots, q_1$ and $x_{i0} \equiv 1$.

C.3.3 The survival function

$$S'_{i,0} = -F'_{i,0}, S'_{i,1} = -F'_{i,1}, S'_{i,2l} = -F'_{i,2l}, S'_{i,3m} = -F'_{i,3m},$$

$$S''_{i,00} = -F''_{i,00}, S''_{i,01} = -F''_{i,01}, S''_{i,0(2l)} = -F''_{i,0(2l)}, S''_{i,0(3m)} = -F''_{i,0(3m)},$$

$$S''_{i,11} = -F''_{i,11}, S''_{i,1(2l)} = -F''_{i,1(2l)}, S''_{i,1(3m)} = -F''_{i,1(3m)},$$

$$S''_{i,(2l)(2l')} = -F''_{i,(2l)(2l')}, S''_{i,(2l)(3m)} = -F''_{i,(2l)(3m)}, S''_{i,(3m)(3m')} = -F''_{i,(3m)(3m')}.$$

where $i = 1, \ldots, n$, $j, j' = 1, \ldots, q_1$, $k, k' = 0, 1, \ldots, q_2$, $r, r' = 0, 1, 20, 21, \ldots, 2q_2, 31, 32, \ldots, 3q_1$, $l, l' = 0, 1, \ldots, q_2$, $m, m' = 1, \ldots, q_1$ and $x_{i0} \equiv 1$.

Bibliography

Andersen, P. K., Borgan, O., Gill, R. D., and Keiding, N. (2012). *Statistical Models based on Counting Processes*. Springer, Berlin.

Balakrishnan, N., Koutras, M., Milienos, F., and Pal, S. (2015). Piecewise linear approximations for cure rate models and associated inferential issues. *Methodology and Computing in Applied Probability*, pages 1–30.

Balakrishnan, N. and Pal, S. (2012). EM algorithm-based likelihood estimation for some cure rate models. *Journal of Statistical Theory and Practice*, 6:698–724.

Balakrishnan, N. and Pal, S. (2013a). COM-Poisson cure rate models and associated likelihood-based inference with exponential and Weibull lifetimes. In Frenkel, I. B., Karagrigoriou, A., Lisnianski, A., and Kleyner, A., editors, *Applied Reliability Engineering and Risk Analysis*, chapter 22, page doi: 10.1002/9781118701881. John Wiley & Sons, Chichester, UK.

Balakrishnan, N. and Pal, S. (2013b). Lognormal lifetimes and likelihood-based inference for flexible cure rate models based on COM-Poisson family. *Computational Statistics & Data Analysis*, 67:41–67.

Balakrishnan, N. and Pal, S. (2014). An EM algorithm for the estimation of parameters of a flexible cure rate model with generalized gamma lifetime and model discrimination using likelihood- and information-based methods. *Computational Statistics*, 30:151–189.

Balakrishnan, N. and Peng, Y. (2006). Generalized gamma frailty model. *Statistics in Medicine*, 25(16):2797–2816.

Berkson, J. and Gage, R. P. (1952). Survival curve for cancer patients following treatment. *Journal of the American Statistical Association*, 47:501–515.

Boag, J. W. (1949). Maximum likelihood estimates of the proportion of patients cured by cancer therapy. *Journal of the Royal Statistical Society, Series B*, 11:15–53.

Borges, P., Rodrigues, J., and Balakrishnan, N. (2012). Correlated destructive generalized power series cure rate models and associated inference with an application to a cutaneous melanoma data. *Computational Statistics & Data Analysis*, 56(6):1703–1713.

Cancho, V. G., Bandyopadhyay, D., Louzada, F., and Yiqi, B. (2013). The destructive negative binomial cure rate model with a latent activation scheme. *Statistical methodology*, 13:48–68.

Chen, M.-H., Ibrahim, J. G., and Sinha, D. (1999). A new Bayesian model for survival data with a surviving fraction. *Journal of the American Statistical Association*, 94:909–919.

Conway, R. and Maxwell, W. (1961). A queuing model with state dependent services rates. *Journal of Industrial Engineering*, 12:132–136.

Cox, D. R. and Oakes, D. (1984). *Analysis of Survival Data*, volume 21. CRC Press, London–New York.

Dempster, A. P., Laird, N. M., and Rubin, D. B. (1977). Maximum likelihood from incomplete data via the EM algorithm. *Journal of the royal statistical society. Series B (methodological)*, pages 1–38.

Fang, H.-B., Li, G., and Sun, J. (2005). Maximum likelihood estimation in a semiparametric logistic/proportional-hazards mixture model. *Scandinavian Journal of Statistics*, 32:59–75.

Farewell, V. T. (1982). The use of mixture models for the analysis of survival data with long-term survivors. *Biometrics*, 38:1041–1046.

Gallardo, D. I., Bolfarine, H., and Pedroso-de Lima, A. C. (2016). An EM algorithm for estimating the destructive weighted Poisson cure rate model. *Journal of Statistical Computation and Simulation*, 86(8):1497–1515.

Haybittle, J. (1965). A two-parameter model for the survival curve of treated cancer patients. *Journal of the American Statistical Association*, 60(309):16–26.

Ibrahim, J. G., Chen, M.-H., and Sinha, D. (2001). Bayesian semiparametric models for survival data with a cure fraction. *Biometrics*, 57:383–388.

Ibrahim, J. G., Chen, M.-H., and Sinha, D. (2005). *Bayesian Survival Analysis*. John Wiley & Sons., Hoboken, New Jersey.

Kadane, J. B., Shmueli, G., Minka, T. P., Borle, S., and Boatwright, P. (2006). Conjugate analysis of the Conway-Maxwell-Poisson distribution. *Bayesian Analysis*, 1:363–374.

Kuk, A. Y. and Chen, C.-H. (1992). A mixture model combining logistic regression with proportional hazards regression. *Biometrika*, 79:531–541.

Lambert, P. C., Thompson, J. R., Weston, C. L., and Dickman, P. W. (2007). Estimating and modeling the cure fraction in population-based cancer survival analysis. *Biostatistics*, 8(3):576.

Larson, M. G. and Dinse, G. E. (1985). A mixture model for the regression analysis of competing risks data. *Applied Statistics*, 34:201–211.

Li, C.-S., Taylor, J. M., and Sy, J. P. (2001). Identifiability of cure models. *Statistics & Probability*

Letters, 54:389–395.

Liu, M., Lu, W., and Shao, Y. (2006). Interval mapping of quantitative trait loci for time-to-event data with the proportional hazards mixture cure model. *Biometrics*, 62:1053–1061.

Liu, M., Lu, W., and Shao, Y. (2006). Mixture cure model with an application to interval mapping of quantitative trait loci. *Lifetime Data Analysis*, 12:421–440.

Lo, Y.-C., Taylor, J. M., McBride, W. H., and Withers, H. R. (1993). The effect of fractionated doses of radiation on mouse spinal cord. *International Journal of Radiation Oncology* Biology* Physics*, 27:309–317.

Louis, T. A. (1982). Finding the observed information matrix when using the EM algorithm. *Journal of the Royal Statistical Society, Series B*, 44:226–233.

Lu, W. (2008). Maximum likelihood estimation in the proportional hazards cure model. *Annals of the Institute of Statistical Mathematics*, 60:545–574.

Maller, R. A. and Zhou, X. (1996). *Survival Analysis with Long-term Survivors*. John Wiley & Sons., New York.

McLachlan, G. and Krishnan, T. (2007). *The EM Algorithm and Extensions*. John Wiley & Sons., Second edition, Hoboken, New Jersey.

Pal, S. and Balakrishnan, N. (2015). Likelihood inference based on EM algorithm for the destructive length-biased Poisson cure rate model with Weibull lifetime. *Communications in Statistics-Simulation and Computation*, (to appear).

Pal, S. and Balakrishnan, N. (2016). Destructive negative binomial cure rate model and EM-based likelihood inference under Weibull lifetime. *Statistics & Probability Letters*, 116:9–20.

Pal, S. and Balakrishnan, N. (2017). Likelihood inference for the destructive exponentially weighted poisson cure rate model with weibull lifetime and an application to melanoma data. *Computational Statistics*, 32(2):429–449.

Peng, Y. and Dear, K. B. (2000). A nonparametric mixture model for cure rate estimation. *Biometrics*, 56:237–243.

Rodrigues, J., Cancho, V. G., de Castro, M., and Balakrishnan, N. (2012). A Bayesian destructive weighted Poisson cure rate model and an application to a cutaneous melanoma data. *Statistical methods in medical research*, 21(6):585–597.

Rodrigues, J., de Castro, M., Balakrishnan, N., and Cancho, V. G. (2011). Destructive weighted Poisson cure rate models. *Lifetime data analysis*, 17(3):333–346.

Rodrigues, J., de Castro, M., Cancho, V. G., and Balakrishnan, N. (2009). COM-Poisson cure rate survival models and an application to a cutaneous melanoma data. *Journal of Statistical Planning and Inference*, 139:3605–3611.

Self, S. G. and Liang, K.-Y. (1987). Asymptotic properties of maximum likelihood estimators and likelihood ratio tests under nonstandard conditions. *Journal of the American Statistical Association*, 82:605–610.

Shmueli, G., Minka, T. P., Kadane, J. B., Borle, S., and Boatwright, P. (2005). A useful distribution for fitting discrete data: revival of the Conway-Maxwell-Poisson distribution. *Journal of the Royal Statistical Society, Series C*, 54:127–142.

Sy, J. P. and Taylor, J. M. (2000). Estimation in a Cox proportional hazards cure model. *Biometrics*, 56:227–236.

Sy, J. P. and Taylor, J. M. (2001). Standard errors for the Cox proportional hazards cure model. *Mathematical and Computer Modelling*, 33:1237–1251.

Tsodikov, A., Ibrahim, J., and Yakovlev, A. (2003). Estimating cure rates from survival data. *Journal of the American Statistical Association*, 98:1063–1078.

Yakovlev, A. Y. and Tsodikov, A. D. (1996). *Stochastic Models of Tumor Latency and their Biostatistical Applications*. OECD Publishing, Vol.1, World Scientific, Singapore.

Yang, G. L. and Chen, C. W. (1991). A stochastic two-stage carcinogenesis model: a new approach to computing the probability of observing tumor in animal bioassays. *Mathematical biosciences*, 104(2):247–258.

Zeng, D., Yin, G., and Ibrahim, J. G. (2006). Semiparametric transformation models for survival data with a cure fraction. *Journal of the American Statistical Association*, 101:670–684.

Zhao, L., Feng, D., Bellile, E. L., and Taylor, J. M. (2014). Bayesian random threshold estimation in a Cox proportional hazards cure model. *Statistics in Medicine*, 33:650–661.